NUMERICAL MODELING OF EXPANSIVE SOILS USING UNCOUPLED APPROACH

by

YOUSSEF GOMAA YOUSSEF MORSI

M.Sc., Civil Engineering, Cairo University, Fayoum Branch

A Thesis Submitted to The Faculty of Engineering,
Cairo University
in Partial Fulfillment
of the Requirements for the Degree of
DOCTOR OF PHILOSOPHY

in

PUBLIC WORKS DEPARTEMENT

FACULTY OF ENGINEERING
CAIRO UNIVERSITY
2010

NUMERICAL MODELING OF EXPANSIVE SOILS USING UNCOUPLED APPROACH

by

YOUSSEF GOMAA YOUSSEF MORSI

M.Sc., Civil Engineering, Cairo University, Fayoum Branch

A Thesis Submitted to The Faculty of Engineering,
Cairo University,
in Partial Fulfillment of the Requirements for the Degree of
DOCTOR OF PHILOSOPHY

in

PUBLIC WORKS DEPARTEMENT

Under the Supervision of

Professor: Ahmed Amr Darrag
Civil Engineering Department
Faculty of Engineering
Cairo University

Assistant Prof.: Tamer Yehia Elkady
Civil Engineering Department
Faculty of Engineering
Cairo University

FACULTY OF ENGINEERING,
CAIRO UNIVERSITY
EGYPT
2010

NUMERICAL MODELING OF EXPANSIVE SOILS USING UNCOUPLED APPROACH

by

YOUSSEF GOMAA YOUSSEF MORSI

M.Sc., Civil Engineering

A Thesis Submitted to The Faculty of Engineering,

Cairo University

in Partial Fulfillment of the Requirements for the Degree of

DOCTOR OF PHILOSOPHY

in

PUBLIC WORKS DEPARTEMENT

Approved by the

Examining Committee:

Professor Dr. Fathalla Mohamed El-Nahhas: …..... (Member)

Head of structural engineering department, (Ain Shams University)

Professor Dr. Mostafa El-Sayed Mossaad: …..... (Member)

Professor of soil mechanics and Foundation Engineering, (Cairo University)

Professor Dr. Ahmed Amr Darrag: ……..……..... (Supervisor)

Professor of soil mechanics and Foundation Engineering, (Cairo University)

FACULTY OF ENGINEERING,

CAIRO UNIVERSITY

EGYPT

2010

DEDICATION

TO MY PARENTS

ACKNOWLEDGEMENT

I wish to express my sincere thanks to Professor **Ahmed Amr Darrag** and Assistant Professor **Tamer Yehia Elkady** who supervised this thesis. They gave me support and guidance throughout this research.

Special thanks go to Associate Professor Omr Ezz-Eldin for sharing his experience in finite element programming and providing invaluable support and suggestions in the extension of the computer program used in my research study.

Also, I would like to thank all professors and engineers in the faculty of engineering, Cairo University and Fayoum University who contributed in their own way to the improvement the content of this thesis, in particular, the soil mechanics and foundation engineering staff in both faculties. I am also very grateful to all employees in these faculties especially in the soil mechanics laboratory.

I am indebted to my parents for their effort and constant encouragement to me. Finally, I took a tremendous pleasure in writing this thesis. I hope that all readers and researchers will enjoy and benefit from it. I wish that my research contributes to the progress and development of the research in civil engineering.

TABLE OF CONTENTS

LIST OF FIGURES

LIST OF TABLES

NOTATIONAL SYSTEM

Symbol	Term	Unit
$\frac{\partial H_t}{\partial L}$	Total Head Gradient	-
m_2^w	Slope of the storage curve (Soil Water Characteristic Curve)	-
m_1^s	Coefficient of volume change with respect to a change in net normal stress.	m^2/ KN
m_2^s	Coefficient of volume change with respect to a change in matric suction	m^2/ KN
m_1^w	Coefficient of volume change respect to a change in net normal stress	m^2/ KN
m_2^w	Coefficient of volume change with respect to a change in matric suction.	m^2/ KN
m_1^a	Coefficient of air volume change associated with change in net normal stress	m^2/ KN
m_2^a	Coefficient of air volume change associated with change in matric suction.	m^2/ KN
D_a^*	Coefficient of transmission for air phase	-
$\langle N_p \rangle$	Pore water pressure shape function	-
δ	Angle of Friction of Soil with The Wall	Degree
φ	Angle of Internal Friction	Degree
ν	Possion's Ratio of Soil	-
Ψ	Total Soil Suction	Degree
θ	Volumetric water content	-
σ'	Effective Normal Stress	kPa
$(\sigma - u_a)$	Net Normal Stress	kN/m^2
φ_b	Angle indicating the rate of increase in shear strength relative to the matric suction	Degree
γ_d	Dry unit weight of Soil	kN/m^3
τ_f	Shear Strength of Soil	kN/m^2

Symbol	Term	Unit
σ_{ij}	Components of the net total stress tensor	-
θr	Residual Volumetric Water Content	-
θs	Volumetric Water Content at Saturation	-
$(u_a - u_w)$	Matric Soil Suction	kN/m^2
ρ_w	Water Density	KN/m^3
θw	Volumetric Water Content	-
γ_w	Unit weight of water	kN/m^3
[D]	Drained constitutive matrix	-
$[K]$	Stiffness matrix	-
$[L_d]$	Coupling matrix	-
$\{\varepsilon\}$	Strain Vector	-
$\{m_H\}$	Isotropic suction Vector	-
A	Activity	%
a_f	Soil Parameter Related to the Air Entry of Soil	-
B	Footing Width	m
b_i	Components of the body force vector	-
C	Percentage of Clay Size (Clay Content)	%
c'	Effective Cohesion	-
C_m	Expansion index with respect to matric suction	-
C_s	Expansion index with respect effective stress (swelling index)	-
C_t	Expansion index with respect to net normal stress	-
D_L	Effective depth of Lawn	m
D_P	Depth of Leaked Pipe below Foundation Level	m
e	Natural Constant (2.718)	-

Symbol	Term	Unit
E	Elasticity parameter for the soil structure with respect to a change in the net normal stress	kN /m^2
E_a	Volumetric modulus associated with change in net normal stress	KN /m^2
E_w	Water volumetric modulus associated with a change in the net normal stress	KN /m^2
f	Function related to degree of saturation.	-
g	Gravitational Acceleration	m^2/sec
H	Elasticity Parameter for the Soil Structure with respect to a Change in Matric Suction	KN /m^2
H_a	Air volumetric modulus associated with change in matric suction	KN /m^2
H_r	Thickness of Replacement	m
H_t	Total Head (Hydraulic Head)	m
H_w	Water volumetric modulus associated with a change in matric suction.	KN /m^2
i	Gradient of fluid head or potential	-
J	Jacobian of the transformation	-
J_{ai}	Mass rate of air in i-direction	-
k	Coefficient of Permeability (Hydraulic Conductivity)	m/sec
k_x	Hydraulic conductivity in the x-direction	m/sec
k_y	Hydraulic conductivity in the y-direction	m/sec
L_L	Distance of Lawn from Footing Edge	m
L_p	Distance of Leaked Pipe from Footing Edge	m
n	Number of element nodes	-
n_f	Soil Parameter Related to the Rate of Desaturation	-
N_i:	Shape Function (Interpolation Function) for Node i	-
PI	Plasticity Index	%
P_s	Swelling pressure	kPa

Symbol	Term	Unit
q	Flux of Water per Unit Cross Sectional Area	m^3/sec
q	Specific discharge	m^3/sec
Q	Applied boundary flux	m^3/sec
q_L	Lawn intake from soil	m^3/sec
r_i, s_i	local co-ordinates of integration point *i*	m
S	Swelling Potential	%
S	Suction Change at Ground Surface due to Climate Effect	kPa
S	Degree of saturation	-
SL	Shrinkage Limit	%
t	Time	sec
u_a	Pore Air Pressure	kPa
u_i	Nodal displacement in local direction r for Node *i*	m
u_w	Pore Water Pressure	kPa
v_i	Nodal Displacement in local direction s for node *i*	m
v_w	Discharge velocity	m/sec
w_i	Weight for a given integration point *i*	-
y	Elevation Head	m
y	Elevation head	m
Z_a	Active Zone Depth	m
Δq	Footing Pressure	kN/m^2
χ	Bishop Parameter is a function of the degree of saturation	-

ABSTRACT

Expansive soils cause damages to structures due to swelling or shrinking as a response to change in soil moisture. Expansive soil is one of the most costly natural disasters in the world. Its destructive impact is manifested predominantly in structural damage and is not as catastrophic as other natural disasters such as earthquakes, tornadoes, and floods. Jones and Holtz (1973) reported that expansive soil is the second most likely natural disaster to cause economic loss. Changes in the pore-water pressure can occur as a result of variations in climate, change in depth to the water table, water uptake by vegetation, removal of vegetation or the excessive watering of a lawn.

This dissertation presents an investigation of engineering behavior of expansive soils. An analytical study was undertaken for the implementation of a unsaturated nonlinear elastic constitutive soil model in two-dimensional finite element computer program that performs a sequentially uncoupled flow-displacement analysis for the prediction of volume change in soils supporting various elements of civil infrastructure. This analytical tool for the prediction of heave is extremely valuable to geotechnical engineers. There has been little advancement in the development of such a tool for solving engineering problems.

A major problem in design foundations on expansive soils is to consider the expected different causes of water variations along the life of building. The research studies in detail the different caues of water variations and its effect on volume change of expansive soills. A paramteric study for causes of water variations such as climate conditions, lawn, pipe leakage and surface infiltration are conducted. The parametric analysis resulting from the program showed that using the new analytical technique provides a good and simple tool to asses the effect of different water variations causes on shallow foundation heave.

Furthermore, this research aims to advance the state of the art with respect to using sand cushion to avoid the danger of expansive soils heave on shallow foundation. Research investigate the effect of sand cushion depth, lateral extension and relative density on soil heave.

In summary, the proposed analysis methodology provides a practical and economical approach to estimate heave of shallow foundations on expansive soils.

CHAPTER (1)

INTRODUCTION

Expansive soils undergo appreciable changes in volume and strength following changes in moisture content. The changes in volume can cause extensive damage to infrastructure. Damage to lightly loaded structures founded on expansive soils has been widely reported throughout the world, which complicate construction activities around the world. Although, damage costs from expansive soil exceed damage costs from earthquakes and hurrcanies, expansive soils have not given the sufficient interest (Jones and Holtz, 1973). This is attributed to the slow process of foundation heave which damage the structure many years after construction. Damage due to expansive soils is usually a gradual process that starts with wall cracking at window or door openings and progressively worsens.

Expansive soils owe its behavior to the presence of swelling clay minerals. As they get wet, the clay minerals absorb water molecules and expand; conversely, as they dry they shrink, leaving large voids in the soil. Soils with smectite clay minerals, such as montmorillonite, exhibit the most profound swelling properties.

Expansive soils pose the greatest hazard in arid regions. Sources of water in developed areas are not limited to temporal weather cycles, but can be introduced by people. A frequent source of damage is the differential swelling caused by pockets of moist soil adjacent to dry soil. For example, lawn and garden watering creates a moist zone on the exterior of a building, whereas the interior zone of building is dry; this creates differential swelling pressure on foundation elements. Also, there is frequently a moisture differential between the soils beneath a house and those that are more directly exposed to changes in the weather. Leaky pipes and swimming pools are other common sources of water.

Many methods for the prediction of expansive soils volume change have been proposed. These methods may be classified as empirical methods, semi empirical methods, laboratory methods and theoretical methods. The laboratory methods of volume change prediction are based either on soil suction measurements (or estimations) or on one-dimensional oedometer tests. Inspite of difficulties associated with the unsaturated soil mechanics theoretical approach, it is still considered as a powerful tool for estimation of volume change of expansive soils.

Applying the unsaturated soil mechanics concepts for heave predication requires using numerical methods to overcome the difficulties of solving the non linear differential equations of water flow and soil deformation. The finite element method considered the most favorable method.

1.1 Research Objectives and Scope

The focus of this research is to apply the concepts of unsaturated soil mechanics for the quantification of volume change (heave) of expansive soil under different factors. The objectives of the research proposed herein are to:

(1) Provide an analytical tool for the deformation analysis of unsaturated expansive soils.

(2) Use uncoupled approach to model volume change problems associated with expansive soils in the finite element framework.

(3) Implement Fredlund's unsaturated soil model (Fredlund, 1993) in finite element framework and used it to quantify heave of expansive soils.

(4) Use the modified finite element program to simulate the effect of variation in soil suction from different sources, such as rainfall, lawn and garden watering and pipe leakage and to estimate heave due to change in soil suction and external stresses.

(5) Perform a parametric study of the factors affecting the swelling process, such as climate conditions, lawn effect, pipe leakage and infiltration on soil deformation.

(6) Perform a parametric study to investigate the effect of sand cushion parameters on decreasing the heave of foundation rested on expansive soils.

(7) Asses the effect of footing dimensions and pressures on the heave of expansive soils.

The scope of this thesis is limited to a theoretical study. Most practical geotechnical geometries can be reduced to a two-dimensional plane strain condition. Therefore, the models proposed herein are limited to two-dimensional conditions. The analysis of the flow and stress deformation mechanism is modeled using uncoupled approach.

1.2 Research Methodology

The research methodology established herein was designed in order to overcome difficulties associated with the application of unsaturated soil mechanics into engineering practice and give an analytical tool for analysis of deformation for unsaturated expansive soil. To achieve the aforementioned objectives, a number of methodological steps were performed as described below.

(i) Selection and preparation of finite element program: CRISP Program is used in this thesis. The program was rewritten with Fortran code in 6.1 power station version;

(ii) Verification of the program for saturated soil models: five examples from the manual were used for verifying the rewritten program with different soil models: Linear Elastic, Cam Clay and Modified Cam Clay;

(iii) Finite Element formulation of the Fredlund's unsaturated soil model: the constitutive model of Fredlund is used to model the stress deformation behaviour of unsaturated expansive soil. This model is formulated in the finite element form. The incremental suction effect was modeled as equivalent nodal forces;

(iv) Implementation of Fredlund's model in CRISP: the model is implemented with FORTRAN code in the CRISP program. The program is modified to fit the two stress variable model with the capability to read soil suction as an input file from commercial flow program (SEEP/W);

(v) Simulation of flow in unsaturated soil using commercial Program (SEEP/W): SEEP/W is used to estimate the suction field in the domain of the problem due to water infiltration from rainfall, lawn and pipe leakage. The output of the flow analysis is used as input for the stress deformation analysis;

(vi) Verification of program for unsaturated expansive soil: Analysis of one case history and three example problems are performed to verify the finite element implementation of the model. Case history for the heave of slab on floor in Regina site is used to verify the implemented model and comparison the theoretical analysis to field tests. Also, example problems which include simple heave example

introduced by Fredlund's, (1993) to simulate the effect of suction, lawn effect example and water infiltration example were used for verification.

(vii) Parametric study for the sources of water content variation affecting the swelling process: Analysis of the water content variation sources affecting the swelling such climate conditions, lawn effect, water infiltration effect and pipe leakage effect was performed. Also the effect of dimensions and parameters of sand cushion was investigated. The parametric study of these factors provides insight about the effect of each factor.

1.3 Thesis Outline

This thesis is organized in seven chapters. The present chapter introduces the unsaturated expansive soil problem. A description of the hazards of expansive soils was presented, along with an overview of water variation sources in developed areas. In addition, different methods for estimation of foundation heave in expansive soils were mentioned. Finally, the objectives and scope of the thesis were presented. The following paragraphs present a concise description of the contents of the remaining chapters.

Chapter 2 presents a literature review covering different aspects of expansive soil behaviour. A concise review of identification methods of expansive soils such as standard classification tests, mineralogical tests and cation exchange capacity tests is presented. A review of mechanical behavior of unsaturated soil included shear strength and volume change mechanisms is presented. A review of water and air flow properties is also summarized. The soil water characteristic curves (SWCC) and unsaturated soil property functions that relate hydraulic and mechanical properties to SWCC are introduced. Finally, heave prediction using empirical, theoretical and numerical methods are reviewed.

Chapter 3 presents the theoretical approaches as well as programs used in this research. First, Fredlund’s model (Fredlund, 1993) for unsaturated soil that relates the deformation to stress variables is introduced in detail. Next, an overall description of the CRISP (CRItical State soil mechanics Program) is provided, showing the soil elements, soil models incorporated in this program. In addition, SEEP/W program is presented with its soil elements and flow models of water and air through unsaturated soil. Also, finite

element formulation of unsaturated expansive soil model using uncoupled approach is presented. Finally, the evaluation of the elasticity parameter functions from volume change indices used in this research is provided.

Chapter 4 provides verification of the modified program in the light of past case histories and example problems for volume change of unsaturated expansive soils. First, simple heave example problem introduced by Fredlund, (1993) is modeled by the program to verify the incremental suction effect. Second, the heave of a floor slab on Regina clay is introduced to compare the field measurements with results of implemented model. Third, example problem for simulation the effect of lawn on soil deformation is modeled to verify the implemented model. Finally, example problem for simulation the effect of infiltration on soil volume changes is presented.

Chapter 5 presents the analysis of different sources of water content variation such as climate conditions, lawn effect, pipe leakage and surface infiltration on soil suction changes and soil volume changes. A parametric study for the effect of these conditions on the shallow foundation is investigated as well as footings dimensions and loading pressures.

Chapter 6 presents a study for the effect of sand cushion on the magnitude of heave under footings. The study includes effect of depth, lateral extension, modulus of elasticity of sand cushion on heave of footing.

Finally, the conclusions from this research and the recommendations for potential future studies are provided in Chapter 7.

CHAPTER (2)

LITERTURE REVIEW

2.1 Introduction

Expansive soils include clays and fine silts which swell as their moisture content increases and shrink as their moisture content decreases. These soils cause widespread problems for the structures especially light weight structures. The structures most commonly damaged are roadways, irrigation canals , pipelines and small buildings.

Damage to light structures caused by expansive soils has been recoreded over the world. Expansive soils have been called the hidden disaster because their damage cost is greater than the combined damage from natural disasters such as floods, earthquakes and hurrcanies (Jones and Holtz, 1973). The damages regarding expansive soils have caused $7 billion each year in the united state alone (Senthen, 1986) . In Canada, volume change for clay is considederd the most costly natural hazard to buildings on shallow foundations (Hamilton, 1977) . In Egypt, there is no official survey for damage from expanive soils. However, it is clear, for all geotechnical specialists that the costs of damage or over-design are extermally high.

The moisture in soils near the ground surface fluctuates due to variations in climate, watering of gardens and lawn, presence of trees and shurbs, change of water table, and leakage from water and drainage pipes. All sources of mositure changes may be controlled to some extent except the climatic variations.

Expansive soils are commonly unsaturated; therefore the the theory of unsaturated soil mechanics may be used for predicting the behviour of expansive soils. The mechanical behavior of unsaturated soils has become of special interest in recent years only. There were four international conferences on unsaturated soils from 1995 to 2006.

2.2 Identification of Expansive Soil

In engineering practice, identification is often based on standard classification tests such as liquid limit and plasticity index. However, other laboratory tests are used in identifying the swelling potential. These laboratory tests include the mineralogical methods, cation exchange capacity (CEC), free swell, California Bearing Ratio (CBR), coefficient of linear extensibility (COLE) and expansion index test. Details about the most popular methods are introduced in the following sections.

2.2.1 Standard Classification Tests

Atterberg limits are widely used for identification of swelling soil. The increase of the plasticity index is considered as an indicator of increase of sweling potential. Chen (1988) presented a classification of swelling soil based on plasticity index as shown in Table (2.1)

Table (2.1): Expansive Soil Classification Based on Plasticity Index

Plasticity Index	Swelling Potential
0 – 15	Low
10 – 35	Medium
35 – 55	High
55 and above	Very high

Classification based on shrinkage index is found to be unreliable to predict the swelling potential of soil. However, it may be used with the plasticity index for identification as shown in Table (2.2) (Raman, 1967).

Table (2.2): Expansive Soil Classification Based on Plasticity and Shrinkage Index

PI (%)	SI(%)	Degree of Expansion
<12	<15	Low
12 – 23	15 – 30	Medium
23 – 32	30 – 40	High
>32	>40	Very high

The colloidal sized particles have a significant effect on the swelling potential. The colloid size refers to the fraction finer than 0.002 mm which is determined by hydrometer analysis. The amount of swell increases with the increase of colloid content. Seed (1962) studied the influence of clay content on swelling potential and suggested that Atterberg limits and clay content can be combined into a single parameter called soil activity for

more reliable classification of expansive soils as shown in Figure (2.1). Soil activity may be defined as follows:

$$A = \frac{PI}{C} \tag{2.1}$$

Where:

A : Activity of soil.

PI : Plasticity index.

C : Percentage of clay size.

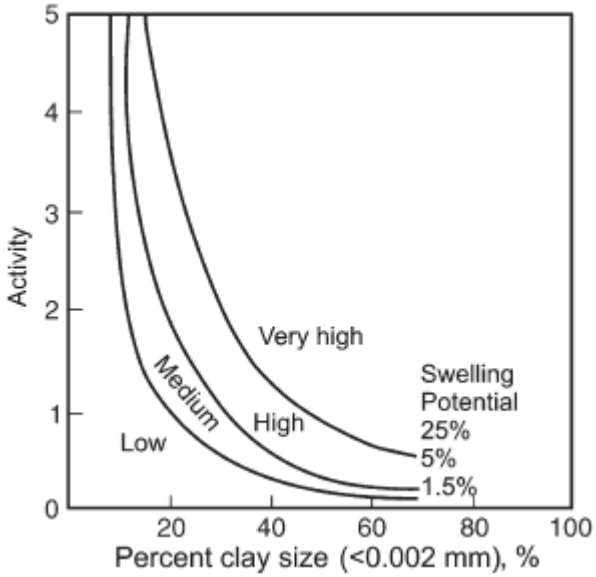

Figure (2.1): Classification of Expansive Soil with Activity (Seed, 1962)

Based on soil activity, Skempton (1953) suggested three classes of clay: inactive for activities less than 0.75; normal for activities between 0.75 and 1.25; and active for activities greater than 1.25. Typical values of activities for different clay minerals are as follows in Table (2.3).

Table (2.3): Typical Values of Activity for Clay Minerals

Mineral	Activity
Halloysite ($4H_2o$)	0.10
Halloysite ($2H_2o$)	0.50
Kaolinite	0.33 – 0.50
Ilitte	0.50 – 1.00
Attapulgite	0.50 – 1.20
Altophane	0.50 – 1.20
Montmorillonite (Ca)	1.50
Smectities	1.00 – 7.00
Montmorillonite (Na)	7.20

Holtz (1959) proposed a method for estimated the degree of expansion of expansive soils. This method involves the direct correlation of observed volume change with colloidal content, plastic index, and shrinkage limit. The degree of expansion and limits of correlated properties are shown in the following tabulation:

Table (2.4): Expansive Soil Classification Based on Colloid Content, Plasticity Index and Shrinkage Limit (Holtz, 1959)

Colloid Content % (-1μm)	PI %	SL %	Expansion %	Degree of Expansion
<15	<18	>15	<10	Low
13-23	15-28	10-16	10-20	Medium
20-31	25-41	7-12	20-30	High
>28	>35	<11	>30	Very high

Experience has shown that this method correlates reasonably well with expected behavior and provides a good indicator of potential volume change. The major criticisms of the method are that the colloidal content indicates amount but not the type of clay constituents and that the hydrometer test is not a routine test in many agency laboratories.

A comparison between the different classification procedures shows a considerable range of potential volume changes for a given plasticity index. This difference may be attributed to different soil types, different samples types (i.e. remolded or undisturbed) and different initial moisture content (i.e. air dried, compacted to optimum moisture content or natural).

2.2.2 Mineralogical Tests

Clay mineralogy is a fundamental factor controlling expansive soil behavior. There are different procedures for determination the clay minerals and its percentage in specific sample. These common methods include X- ray diffraction, differential thermal analysis and electron microscopy. Other mineralogical methods may be used for identification such as chemical analysis, infrared spectroscope, dye adsorption and radio electrical dispersion.

The most popular method is X – ray diffraction analyis which works on the principle that beams of X- rays diffracted from crystals are characteristic for each clay mineral group. The differential thermal analysis (DTA) consists of simultaneously heating a sample of clay with an inert substanc. The resulting thermograms are used to identify the minerals. Electron microscopes are used to observe the size and shape of particles.

2.2.3 Cation Exchange Capacity

Clay minerals have the property of adsorbing cations and retaining them in exchangable state. The adsorbed cations can be replaced by other cations which have stronger attraction. For example, Al^{3+} cations are more strongly attracted than Ca^{2+} cations. Thus Al^{3+} ions can replace Ca^{2+} ions. This process of replacement called "Cation Exchange" or "Base Exchange". Cation Exchange Capacity is expressed in terms of the total number of positive charges adsorbed per 100 gms of soil. It is measured in milliequivalent (meq), which is equal to $6x10^{20}$ electonic charges.

In general, swell potential increases as CEC increases because of the higher surface activity. Typical values of the CEC for different clay minerals are given in Table (2.5). The measurement of CEC is routinely performed in agriculture soils laboratories with low cost.

Table (2.5): Typical Values of CEC for Clay Minerals (Mitchell, 1976)

Mineral	Cation Exchange Capacity
Kaolinite	3 - 15
Ilitte	10 - 40
Montmorillonite	80 - 150

2.2.4 Free Swell

The free swell test is a very simple test used only as indicator. A 10 cm^3 dry sample passing through the sieve No. 40 is placed into a 100 cm^3 graduted cylinder filled with distilled water. The free swell is determined as the percentage ratio of the change in volume to the initial volume. Holtz and Gibbs (1956) stated that soils having a free swell value below 50% are considered to be non-considerable swelling while soils having values between 50% to 100% may exhibit considerable expansion in field.

2.2.5 Oedometer Tests

Several test procedures have been used in the indentifical and mechanical modelling of expansive soils using one-dimensional consolidation apparatus. Various loading sequences and applied surcharges pressures have been used to simulate in situ conditions. The main types of tests are the swelling-consolidation test, constant volume test and double oedometer test.

2.2.5.1 Swell-Consolidation Test (Free Swell oedometer Test)

In this test, the unsaturated sample is initially loaded to the overburden surcharge or the overbuden surcharge plus the structure load. Then, the sample is allowed to swell when water is added to it. After complete swelling. The sample is loaded and unloaded as the conventional manner in the standard consolidation test.

The swelling pressure is defined as the pressure required to recompress the fully swollen sample back to its initial volume. An idealized plot of swell-consolidation test data is shown in Figure (2.2).

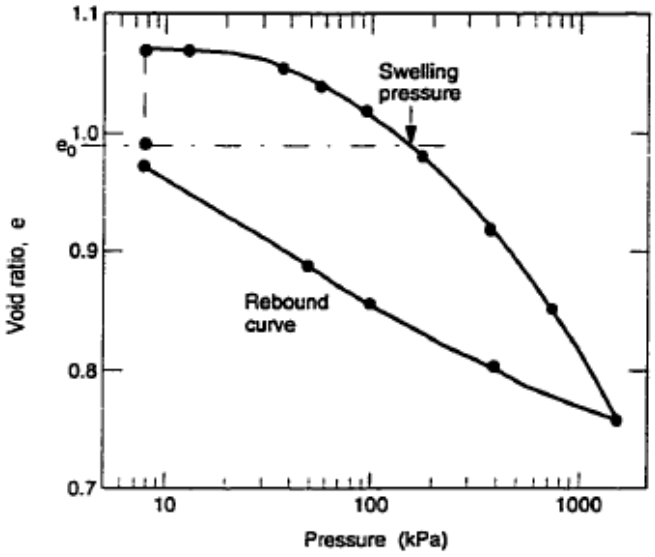

Figure (2.2) : Swell-Consolidation Test Data Plot

2.2.5.2 Constant Volume Test

The sample is inundated in the oedometer cell while preventing it from swelling. The swelling pressure in this test is defined as the maximum pressure required to maintain the sample at its initial volume. When the sample have no increase in volume after soaking, it may be loading and unloading in conventional manner in oedometer test. Figure (2.3) illustrates an idealized constant volume test.

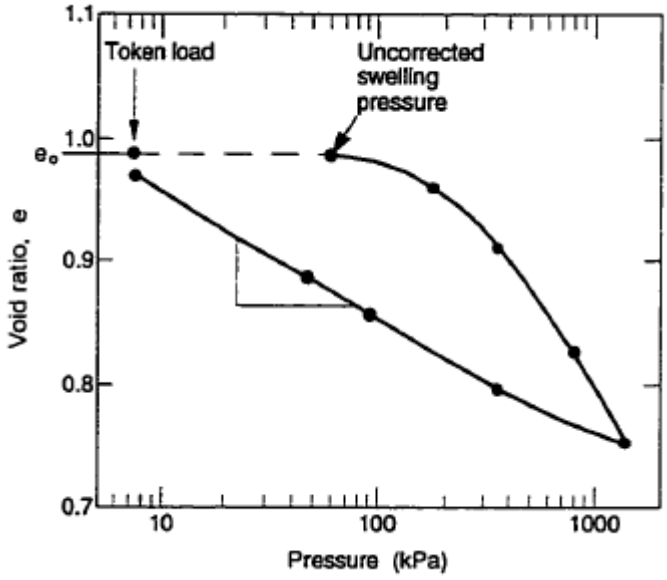

Figure (2.3) : Constant Volume Test Data Plot

2.2.5.3 Double Oedometer Test

The test involves two undistrubed samples. One loaded at its natural water content while the other is loaded under saturated condition. The two samples consolidation are plotted on the same graph. The curve of the initially dry sample is adjusted to match the curve for the saturated sample at high loads. This adjustement is made to consider the difference in the initial void ratios of the two tested samples. The initial void ratio is obtained from the initially dry sample curve at the initial stress and the final void ratio is obtained from the saturated sample curve at the final field stress including the structure loads as introduced in Figure (2.4).

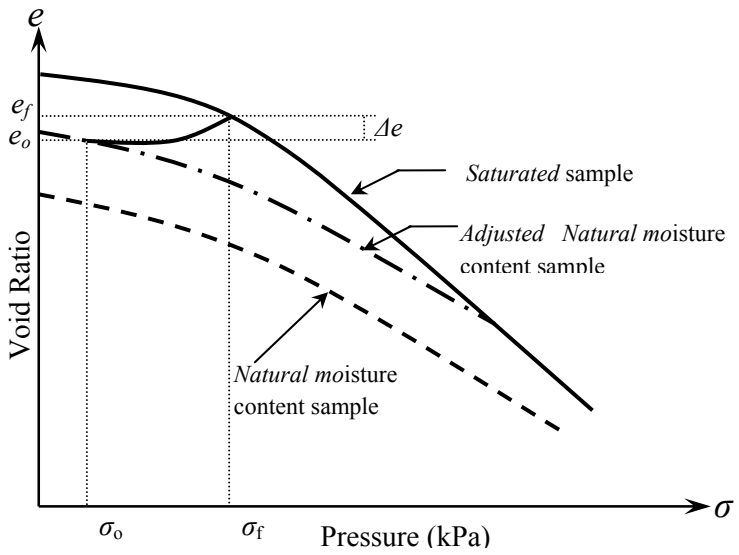

Figure (2.4) : Double Oedometer Swell Test (Jennings and Knight, 1957)

2. 2.5.4 Corrections for Oedomter Test Results

Sampling disturbance increases the compressibilty of the soil, and does not permit the laboratory specimen to return to its insitu stress state at its insitu void ratio. Sampling disturbance causes the conventionally determined swelling pressure, P_s, to fall below the true swelling pressure. Fredlund et al. (1980) proposed an emperical procedure to compensate for the effect of sampling disturbance. In this test procedure, a constant volume test is conducted. Once the uncorrected swelling pressure, P_s, is reached, the specimen is further loaded in compression up to a higher pressure and then unloaded. The void ratio, e, versus log pressure curve obtained is used to find a corrected swelling pressure, *Ps*, by using a modified Casagrande type of geometrical construction as shown in Figure (2.5). The corrected swelling pressure may be significantly greater than the magnitude of uncorrected swelling pressure.

In addition, the results of the oedometer test should be corrected to considering the compressibilty of the oedometer cell. The compressibity of the appartus is signifant due to the high incompressiblity of the expansive soil samples which have high preconsolidation pressure.

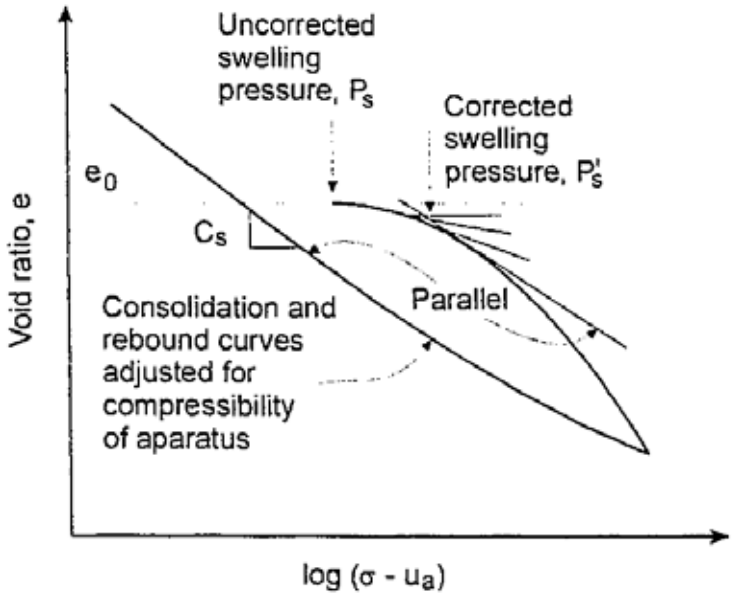

Figure (2.5): Constuction Procedure to Correct the Effect of Sampling Disturbance (Fredlund et al., 1980)

2.3 Prediction of Heave

Heave prediction of expansive soils can be conducted using different methods to various degrees of accuracy. These methods can be classified into three categories: theoretical, semi-empirical, empirical methods. Theoretical methods rely on testing procedures and analysis techniques and empirical methods usually based on test data from particular region in which they are developed.

2.3.1 Empirical Methods

Many empirical procedures have been developed to predict the swelling potential and swelling pressure. These methods are generally easy to use and do not required special tests. The major disadvantage of empirical methods that they are based on a limited amount of data from specific region. Therfore, the application of these methods should be used with caution because they considered only as indicator for heave.

2.3.1.1 Van Der Merwe's Method (1964)

This method provides an empirical relationship between the degree of expansion, the plasticity index, the percent of clay fraction and the surcharge pressure. The total heave at ground surface is found from:

$$\Delta H = \sum_{D=1}^{D=n} F * PE \qquad (2.2)$$

Where:

ΔH: total heave (inches)

F: reduction factor for surcharge pressure, $F = 10^{-Hs/20}$

PE: potential expansiveness in inch/foot of depth

Hs: depth of soil layer in increments of 1 foot

The potential Expansiveness, PE, is found by assumed values of PE = 0, 0.25, 0.50 and 1.0 inch/foot for low, medium, high, and very high levels of potential expansiveness; respectively. Levels of potential expansiveness are determined from Figure (2.6) as function of plasticity index and percentage of clay fraction. The potential expansiveness values are based on consolidometer swell test and field observations. This method does not consider initial soil conditions such as water content, suction or density.

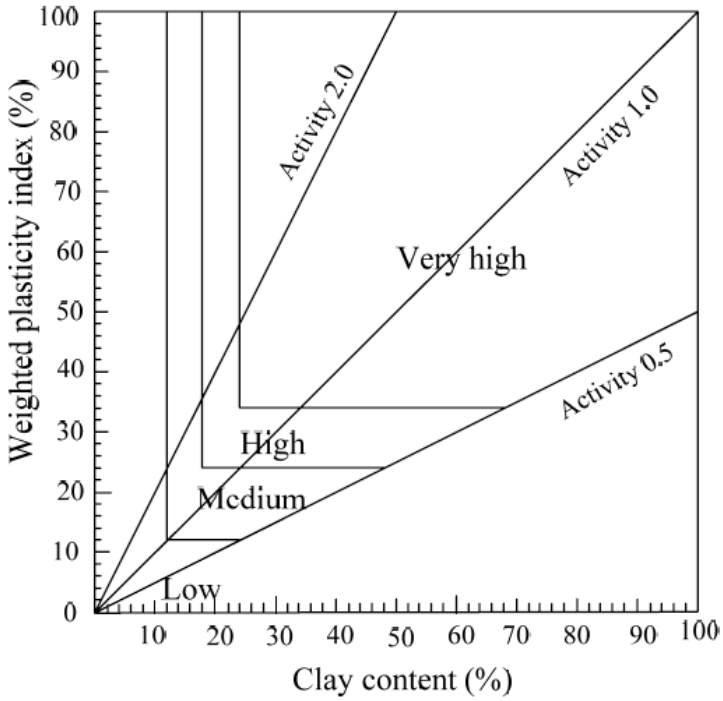

Figure (2.6): Potential Expansiveness of Volume Change (Van Der Merwe, 1964)

2.3.1.2 Vijayvergiya and Sullivan's Correlation (1973)

The swell ratio from initial water content to fully saturarion condtion under 0.1 tsf surcharge pressure may be estimated as follow:

$$Log\ S_p = 1/12\ (0.44LL - w_o + 5.5) \quad (2.3)$$

$$Log\ S_p = 1/19.5\ (6.242\gamma_d + 0.65LL - 130.5) \quad (2.4)$$

Where:

S_p: swell ratio ($\Delta H/Hs$)

LL: liquid limit

w_o: initial water content

γ_d: dry weight density in kN/m^3

2.3.1.3 Schneider and Poor's Correlation (1974)

The swell ratio under diffenent surcharge loads may be evlauated by correlations given in Table (2.6).

Table (2.6): Swell Ratio Correlations under Different Surcharge Loads (Schneider, 1974)

Surcharge (ft)	Log Sp
0	= 0.90 (PI/w_o) – 1.19
3	= 0.65 (PI/w_o) – 0.93
5	= 0.51 (PI/w_o) – 0.76
10	= 0.41 (PI/w_o) – 0.69
20	= 0.33 (PI/w_o) – 0.62

2.3.1.4 Nayak and Christensen's method (1974)

The method involves the development of two statistical relationships, one for swell percentage and the other for swelling pressure, in terms of plasticity index, percent clay content, and initial moisture content. The developed relationships are:

$$S_p(\%) = 0.0229(PI)^{1.45}\frac{C}{w_o} + 6.38 \qquad (2.5)$$

$$P_s = 0.035817(PI)^{1.12}\frac{C}{2} + 3.7912 \qquad (2.6)$$

Where:

S_P: predicted swell percentage

PI: plasticity index, percent

C : clay content, percent

w_o: initial moisture content

P_s: swelling pressure

2.4.1.5 Johnson's Correlation (1978)

The swell ratio from initial water content to fully saturarion condtion under 1 psi surcharge pressure may be estimated as follow:

$$Sp = 23.82 + 0.734PI - 0.1458Hs - 1.7\, w_o + 0.0025\, PI\, w_o - 0.00884\, PI\,(Hs) \qquad PI > 40 \qquad (2.7)$$

$$Sp = -9.18 + 1.5546\, PI + 0.08424\, Hs + 0.1\, w_o - 0.0432\, PI\, w_o - 0.01215\, PI(Hs) \qquad PI < 40 \qquad (2.8)$$

Where:

S_p: swell Ratio ($\Delta H/Hs$).

PI: plasticity Index.

w_o: initial water content in percent.

Hs : depth of soil in feet.

2.3.1.6 Weston's Model (1980)

Weston (1980) presented a method of calculating swell based on the liquid limit which can be determined more accurately than plastic index. This method is an improvement of Van der Merwe's method (1964) to take into account the moisture content.

$$S_p(\%) = 0.00041(W_{LW})^{4.17}(P)^{-0.386}(w_o)^{-2.33} \quad (2.9)$$

$$W_{LW} = (LL)\left(\frac{\% < 0.425mm}{100}\right) \quad (2.10)$$

Where:

S_p: swell Ratio ($\Delta H/Hs$)

ΔH : total heave

Hs: depth of soil

P: vertical pressure in kN/m^2 (kPa), under which swell takes place

w_o: initial moisture content (%)

LL: liquid limit

2.3.2 Semi-Empirical Methods

These methods are developed based on a extensive laboratory and field tests. In these methods, empirical equations are used to estimate the swelling and compression indexes which can not be easily obtained from conventional soil tests.

2.3.2.1 McKeen and Lytton's Correlation (1981)

Mckeen suggested a model to predict the volume change considering the initial and final soil suction. The model may be expressed as follow:

$$Sp = -100\ \gamma_h \log (\tau_f / \tau_o) \qquad (2.11)$$

Where:

γ_h : suction compression index.

τ_f : final in situ soil suction .

τ_o : initial in situ soil suction.

2.3.2.2 U.S. Army Corps of Engineers (WES) Method (Snethen et al. 1979)

The U.S. Army Corps of Engineers Waterways Experiment Station (WES) introduced the equation (2.12) for estimating the matric suction coefficient, C_m.

$$C_m = \alpha\ Gs/\ 100\ B \qquad (2.12)$$

Where:

α: compressibility factor
(slope of specific volume versus water content curve)

B: slope of suction versus water content curve

Gs: Specific gravity of soil

The compressibility factor, α, may be determined by a test or estimated from the empirical equations given by equation (2.13)

$$\begin{array}{ll} \alpha = 0 & PI < 5 \\ \alpha = 0.0275\ PI - 0.125 & 5 < PI < 40 \\ \alpha = 1 & PI > 40 \end{array} \qquad (2.13)$$

The soil suction versus water content relationship is used for the prediction of heave. The data are plotted on a pF scale and straight line approximation for the water content range of interest is represented as follows:

$$\log h_s^o = A - Bw \qquad (2.14)$$

Where:

h_s^o : soil suction without surcharge pressure

A,B: constants (intercept and slope, respectively)

The heave of an expansive soil profile is estimated using soil suction relationship as follows:

$$\frac{\Delta H}{H_s} = \frac{C_m}{1+e_o}\left[\left(A - Bw_o\right) - \log(h_s^f + \sigma_f)\right] \quad (2.15)$$

Where:

ΔH : total heave

Hs: depth of soil

e_o: initial void ratio

w_o: initial water content

h_s^f : final soil suction

σ_f : final applied pressure

2.3.2.3 McKeen's Model (1992)

Including a lateral restraint factor, the effects of changes in total suction and confining stress on heave prediction is considered in the following equation.

$$\frac{\Delta H}{H_s} = C_h \Delta h \, f \, s \quad (2.16)$$

Where:

ΔH : total heave.

Hs: depth of soil.

C_h: suction compression index.

Δh : total suction change.

f: lateral restraint factor($0.5<f<0.8$ for clays).

s: load effect coefficient (typically, s = 0.9).

McKeen, (1992) presented an empirical relationship for suction compression index, C_h, as follows:

$$C_h = -0.02673\left(\frac{\Delta h}{\Delta w}\right) - 0.388704 \quad (2.17)$$

Where:

Δw : change in soil water content

Perko et al. (2000) suggested the following relationship for the McKeen's suction compression index for the Denver area:

$$C_h = -\frac{10}{3} PL^2 \left(\frac{e+F}{e+1}\right) \quad (2.18)$$

Where:

PL: plastic limit

F: weight percent passing the No. 200 sieve

e: void ratio

2.3.2.4 Hafez's Model (1994)

Hafez proposed a model for predicting the swelling ratio of expansive soils. This model was based on laboratory oedometer tests for artificial samples with different percentages of clay content. The suction mearurement was performed using filter paper technique.

$$\frac{\Delta H}{H_s} = 0.022\left(\frac{\gamma_d}{\gamma_w}\right)^2 \log\left(\frac{h_s^o}{h_s^f}\right) \tag{2.19}$$

Where:

ΔH : total heave.

Hs: depth of soil.

γ_d: dry unit weight of soil.

γ_w: unit weight of water.

h_s^o : initial soil suction head.

h_s^f : final soil suction head.

2.3.3 Theoretical Methods

Theoretical methods are based on soil mechanics principles, these methods may be classified into analytical methods and numerical methods. The analytical methods are based on mechanical or suction models.

2.3.3.1 Heave Predicion Based on Constant Volume Oedometer Test

The heave of swelling soil may predicted from the rebound protion of the oedometer test according to the following equation:

$$\Delta H = \frac{H_s}{1+e_0}\left[C_s \Delta \log\left(\frac{\sigma_f^{'}}{\sigma_{sc}^{'}}\right)\right] \qquad (2.20)$$

Where:

H_s: depth of soil layer

e_o : initial void ratio

C_s : swelling index

$\sigma_f^{'}$: final effective stress

$\sigma_{sc}^{'}$: Corrected swelling pressure as indicated before

The final effective stress state should be considered the initial overburden pressure, $\sigma_0^{'}$, the increment of stress due to applied loads, $\Delta\sigma'$, and an equivalent stress due to the final suction, u_{wf} as follow:

$$\sigma_f' = \sigma_o' + \Delta\sigma' - u_{wf} \qquad (2.21)$$

2.3.3.2 Heave Prediction Based on Soil Suction Tests (Controlled Suction Oedometer Tests)

The total heave due to changes in both the net normal stress and the matric suction may be written as :

$$\Delta H = \frac{H_s}{1+e_0}\left[C_m \Delta \log\left(u_a - u_w\right) + C_t \Delta \log\left(\sigma - u_a\right)\right] \qquad (2.22)$$

Where:

C_m : volume change index with respect to soil suction.

C_t : volume change index with respect to net normal stress.

u_a-u_w : soil suction.

σ-u_a : net normal stress.

2.3.3.3 Numerical Methods

In order to obtain an exact theoretical solution the requirements of equilibrium, compatibility, material behaviour and boundary conditions must all be satisfied. While all the methods have their respective advantages and disadvantages, only numerical analysis satisfies all the required conditions and is therefore capable of approximating sufficiently the exact solution to any geotechnical problem (Potts and Zdravkovic, 1999).

One of the most widely used methods of numerical analysis is the finite element method. Finite element plays an important role in the prediction of the behavior of soils in geotechnical engineering. This method is based on constitutive models that are capable of describing the features of the soil. The constitutive models for expansive required theories and principles of unsaturated soil mechanics, which will be introduced in the following paragraphs.

2.4 Mechanical Behaviour of Unsaturated Soils

The understanding of mechanical behaviour of unsaturated soil is considered important for the analysis and design of several geotechnical projects resting on expansive soils such as light structures, pavements, embankments and on-grade slabs. The modeling of unsaturated soil is different from saturated soil due to the differences in behaviour. The behaviour of saturated soil is governed only by the interparticle forces. In unsaturated soils, the negative pore water pressure (soil suction), in addition to the inter-particle forces effect on the behavior of unsaturated soils.

2.4.1 Stress State Variables

Early attempts to describe the behaviour of unsaturated soils were based on the effective stress principle. One of the most known equations to define the state of stress was that proposed by Bishop (1959):

$$\sigma' = \sigma - u_a + \chi(u_a - u_w) \qquad (2.23)$$

Where:

σ': effective normal stress.

σ: total normal stress.

u_a: pore air pressure.

u_w: pore water pressure.

$(u_a - u_w)$: soil suction

χ: Bishop's parameter is a function of the degree of saturation.

Several other effective stress equations have been proposed for unsaturated soils. All equations incorporate a soil parameter in order to form a single-value stress variable (Aitchison, 1961; Jennings, 1961; Richards, 1967; Aitchison, 1973). In 1963, Bishop and Blight re-evaluated the proposed effective stress concept for unsaturated soils. It was noted that a variation in matric suction, (u_a-u_w), did not result in the same change in effective stress as did a change in the net normal stress, (σ-u_a). In addition, all equations included soil parameter, which is difficult to evaluate. Reexamination of the proposed effective stress equations has led many researches to suggest the use of two independent stress variables.

Fredlund and Hasan (1979) stated that there are three possible combinations of stress state variables for unsaturated soil as shown in Table (2.7). These combinations are obtained from equilibrium equations for soil structure. However, the most suitable combination for soil practice is the (σ-u_a) and (u_a-u_w) because that the pore air pressure is atmospheric for most practical engineering problems.

Table (2.7): Combinations of Stress State Variables for Unsaturated Soil (Fredlund and Hasan, 1979)

Reference Pressure	Stress State Variables
Air pressure, u_a	(σ - u_a) and ($u_a - u_w$)
Water Pressure,u_w	(σ - u_w) and ($u_a - u_w$)
Total stress,σ	(σ - u_a) and ($\sigma - u_w$)

2.4.2 Volume Change of Unsaturated Soils

Unsaturated soil is a four-phase continuum; solid, air, water, and contractile skin phases. The contractile skin phase may be defined as the air-water interface, where the surface tension acts. The volume change of unsaturated soil is the sum of the volume change of the four phases, which can expressed as follow:

$$\Delta V = \Delta V_s + \Delta V_a + \Delta V_w + \Delta V_c \qquad (2.24)$$

The volume changes associated with contractile skin can be neglected. In addition, the volume change of the solid particles can be neglected under loading conditions of geotechnical engineering practice. Therefore, under applied stresses, the volume change of unsaturated soil may be considered due to volume changes from the air and water phases only as follow:

$$\Delta V = \Delta V_v = \Delta V_a + \Delta V_w \qquad (2.25)$$

The above relationship showed that only the volume changes associated with two phases must be measured. In practice, the volume changes in void volume and water phase are usually measured, while the volume change of air phase can be estimated using the above equation.

The volume change of each phase can be predicted using the volume change constitutive relatioships (volume-mass constitutive models) which relating state variables to changes in stress state variables. Numerous volume change constititive models for

unsaturated soils have been proposed including elastic models and elasto-plastic models. The elastic models can be categorized into physical and empirical modeles. Physical models are based on the elastic theory with phsically meaningful soil paramters; modulus of elasticity and Poisson's ratio While, the empirical models are based on mathematical fitting for the laboratory tests results for obtaining mathematical expressions for state surfaces which representing the relationship between state variables and stress state variables. The surface-fitting paramters have no physical meaning. Figure (2.7) presents a brief review for volume change constitutive models.

Wheeler and Karube (1996) stated that elastic models have the advantage that it is relatively easy to implement them within numerical analysis and measure the relevant parameters. Fredlund (1979) proposed a nonlinear elastic model. It is originally suggested that the void ratio constitutive surface for unsaturated soil could be assumed to be linear over a wide range of logarithmic stress variables. The void ratio and water content under any set of stress conditions can be calculated as follows:

$$e = e_o - C_t \log\frac{(\sigma - u_a)}{(\sigma - u_a)_o} - C_m \log\frac{(u_a - u_w)}{(u_a - u_w)_o} \quad (2.26)$$

$$w = w_o - D_t \log\frac{(\sigma - u_a)}{(\sigma - u_a)_o} - D_m \log\frac{(u_a - u_w)}{(u_a - u_w)_o} \quad (2.27)$$

Where:

e_o: initial void ratio

C_t: volume change index with respect to net normal stress

C_m: volume change index with respect to matric suction

$(\sigma - u_a)_o$: initial net normal stress

$(u_a - u_w)_o$: initial matric suction

w_o: initial water content

D_t: water content index with respect to net normal stress

D_m: water content index with respect to matric suction

The parameters C_t, D_t are functions of soil suction, while parameters C_m, D_m are functions of net normal stress.

Fredlund and Rahardjo (1993) proposed an equation for the water phase constitutive relationship using a semi-empirical approach based on linear relationship between volumetric water content and stress variables. In an elasticity form, the constitutive equation can be written as follows:

$$\frac{dV_w}{V_o} = \frac{3}{E_w} d(\sigma_{mean} - u_a) + \frac{1}{H_w} d(u_a - u_w) \tag{2.28}$$

Where:

$\sigma_{mean} = \frac{\sigma_x + \sigma_y + \sigma_z}{3}$, mean total stress

E_w : water volumetric modulus associated with a change in the net normal stress.

H_w : water volumetric modulus associated with a change in matric suction.

One of the first elastoplastic constitutive models to be developed for unsaturated soils was the Barcelona Basic Model developed by Alonso et al. (1990) which, was based on the theoretical framework proposed by Alonso et al. (1987). This model was an extension of the Modified Cam-Clay model for fully saturated soils to unsaturated states through the introduction of the concept of the Loading-Collapse yield surface. There are two main categories of elastoplastic models; expansive and non-expansive models. Some of the existing models for expansive soils are the models by Gens and Alonso (1992), Alonso et al., (1994) and Alonso et al., (2000).

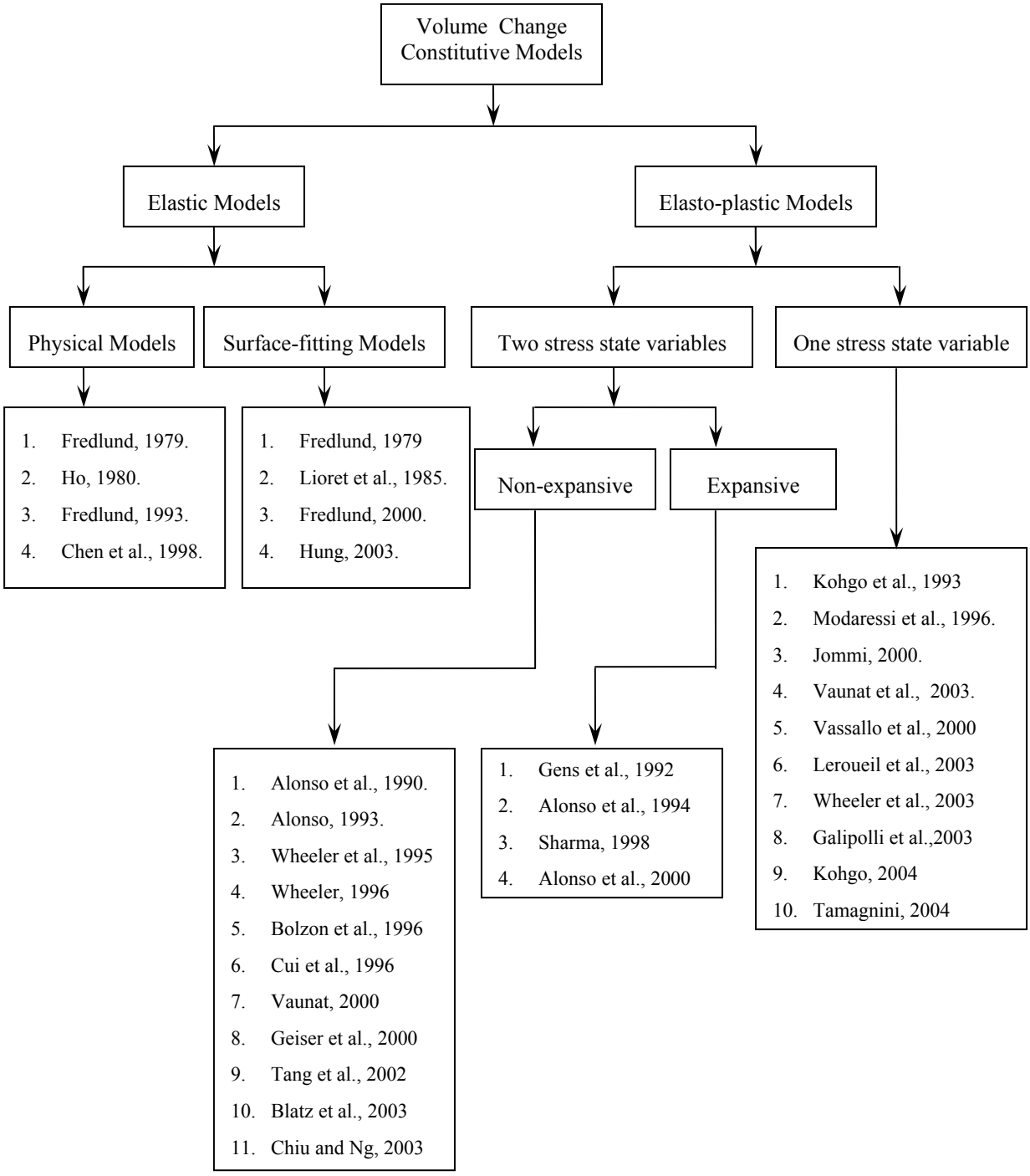

Figure (2.7): Volume Mass Constitutive Models for Unsaturated Soils

2.4.3 Shear Strength of Unsaturated Soils

Shear strength forms an important engineering property for the design of foundation, retaining structures, earth dams pavements, etc. Several procedures have been proposed in the recent years to predict shear strength of unsaturated soil. Bishop (1959) proposed shear strength equation for unsaturated soils by extending Terzaghi's principle of effective stress. Bishop's equation can be arranged as shown below.

$$\tau_f = c' + (\sigma - u_a)\tan\varphi' + (u_a - u_w)[\chi \tan\varphi'] \quad (2.29)$$

Where:

τ_f: shear strength of unsaturated soil.

c': effective cohesion.

φ': angle of internal friction.

$(\sigma\text{-}u_a)$: net normal stress.

$(u_a\text{-}u_w)$: matric suction.

χ: Bishop parameter is a function of the degree of saturation.

The shear strength of unsaturated soil can interpreted in terms of two stress variables at both drained and undrained conditions. Fredlund and el. (1978), proposed a three dimensional failure envelope for unsaturated soil as shown in Figure (2.8).

$$\tau_f = c' + (\sigma - u_a)\tan\varphi' + (u_a - u_w)\tan\varphi_b \quad (2.30)$$

Where:

φ_b: angle indicating the rate of increase in shear strength w.r.t. the matric suction.

Gan et al. (1988) and Escario et al. (1989) established that the shear strength for unsaturated soils is nonlinear when tested over a large range of suction. Bishop's and Fredlund's equations are valid for interpreting data for both linear and nonlinear shear strength envelopes. Those two formulas have rarely been adapted in engineering practice because of the difficulty in measuring suction and correlation parameters φ_b and χ

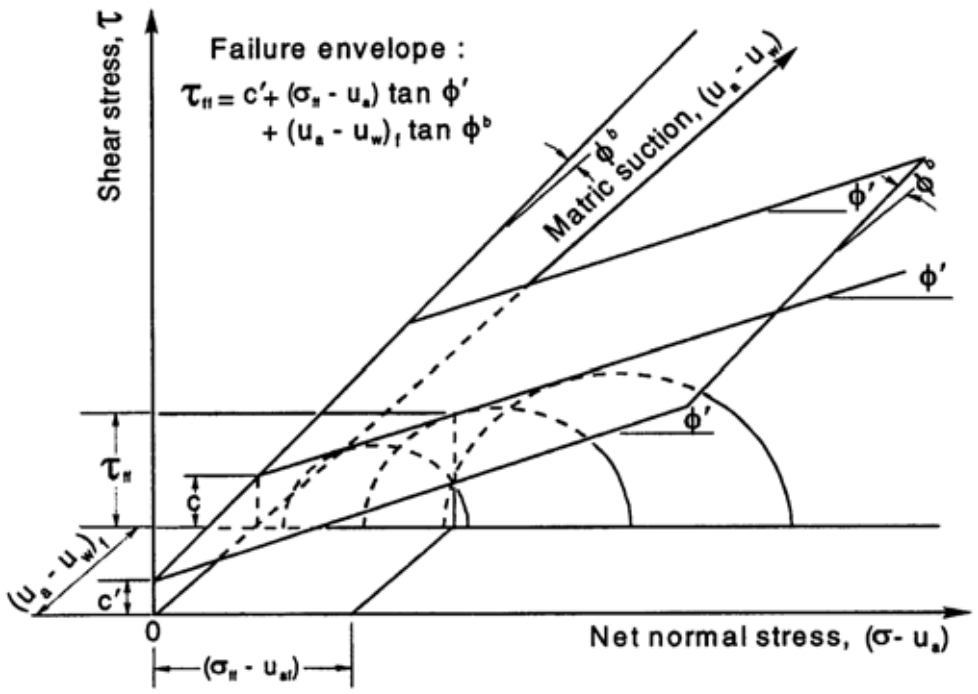

Figure (2.8): Failure Envelope for Unsaturated Soils after Fredlund (1978)

Karube (1988) performed triaxial tests on compacted kaolin. From the test results, he derived the following equation for the shear strength:

$$q_f = M\,(p - u_a) \tag{2.31}$$

Where:

$$M = M'\left(\frac{1}{\alpha}\right) + \left(-\frac{\Delta\nu}{\Delta\varepsilon}\right)_f$$

$$\left(\frac{1}{\alpha}\right) = \left[1 + \frac{f(s)}{p}\right]$$

q_f : deviator stress at failure.

p: mean total stress.

$(\Delta v/\Delta\varepsilon)$: dilatancy index.

ε: shear strain ($\varepsilon = 2(\varepsilon_1 - \varepsilon_3)/3$).

M': inclination of the failure lines.

$f(s)$: intercept of the failure lines on the (p - u_a) axis.

Toll (1990) presented a framework for the behaviour of partially saturated soils, which was supported by a number of triaxial test results on gravel. He proposed the following expression for the critical state shear strength

$$q = M_a(p - u_a) + M_w(u_a - u_w) \quad (2.32)$$

Where:

q : deviator stress.

p: mean total stress.

M_a: total stress ratio (soil parameter depend on the degree of saturation).

M_w: suction ratio (soil parameter depend on the degree of saturation).

2.5 Flow of Water and Air in Unsaturated Soils

Two phases of an unsaturated soil which flow under driving energy are water and air phase. Therefore, the analysis of flow problems in unsaturated soil is based on the laws which govern the flow of these phases.

The hydraulic head (total head) gradient is the driving potential for the water phase, where water flows from a point of high total head to a ponit of low total head. Some researchers stated another driving potential for water flow such as water content gradient, matric suction gradient, however, these potentials don't govern the flow in all condinditions. The total head can be expressed as the sum of elevation head, pressure head and velocity head. The velocity head in soil has a negligiable value thus the total are given by Equation (2.33).

$$H_t = \frac{u_w}{\rho_w g} + y \tag{2.33}$$

Where:

H_t: total head (Hydraulic head).

y : elevation head.

u_w: pore water presssure.

ρ_w: water density.

g : gravitational accelaration.

Above the water table, the pressure heads are negative whereas below the water table pressure heads are positive. In the field, piezometers are used to provide a measurement of hydraulic head in saturated material. In the unsaturated zone however, hydraulic head is determined indirectly through the measurement of the suction head or negative pore-water pressure using tensiometers and psychrometers.

Past experiments showed that Darcy's law is valid for predicting the flow in unsaturated soils as commonly used in saturated soils. Darcy (1586) proposed that the rate of water flow through soil is proportional to the total head gradient. Darcy's law can be written for water moves through soils according to Darcy's Law:

$$q = k \frac{\partial H_t}{\partial L} \tag{2.34}$$

Where:

q: flux of water per unit cross sectional area.

k: permeability or hydraulic conductivity.

$\frac{\partial H_t}{\partial L}$: total head gradient.

Under saturated conditions, the hydraulic conductivity is approximately constant. In unsaturated conditions, the hydraulic conductivity is a function of the water content as shown in Figure (2.9). Childs and Collis-George (1950) stated that the soil coefficient of permeability with respect to water for unsaturated soils is a function of the water content or soil suction. Lioret and Alonso (1980) and Fredlund (1981) reported that the soil permeability must be expressed as a function of volume-mass soil properties. Water flows through pores filled with water and therefore, under unsaturated condition, fewer pores are available for flow. As a result, lower water contents correspond to lower values of hydraulic conductivity. During the drainage of a saturated soil, air begins to enter the large pore spaces first and water flow is forced to move along the more tortuous path in the smaller pores. The hydraulic conductivity will decrease rapidly as the volume of pore space occupied by water decreases.

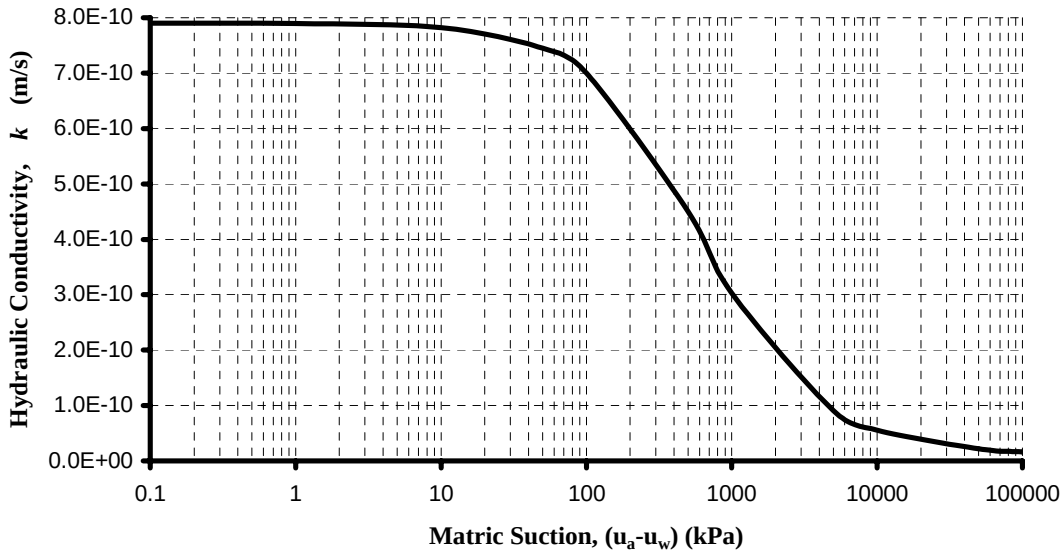

Figure (2.9): Variation of Hydraulic Conductivity with Soil Suction

2.6 Soil-Water Characteristic Curve (SWCC)

The soil-water characteristic defines the relationship between the soil suction and either the gravimetric water content, *w*, or the volumetric water content, θ, or the degree of saturation, *S*. The soil-water characteristic can be described as a measure of the water holding capacity (i.e. storage capacity) of the soil as the water content changes when subjected to various values of suction.

The soil-water characteristic is a conceptual and interpretative tool by which the behaviour of unsaturated soils can be understood. As the soil moves from a saturated state to drier conditions, the distribution of the soil, water, and air phases changes as the stress state changes. The relationships between these phases take different forms and influence the engineering behaviour of unsaturated soils.

The soil-water characteristic curve has three stages that describe the process of desaturation (i.e., for increasing suction) of a soil as shown in Figure (2.10). These are outlined below starting with saturation conditions in the soil.

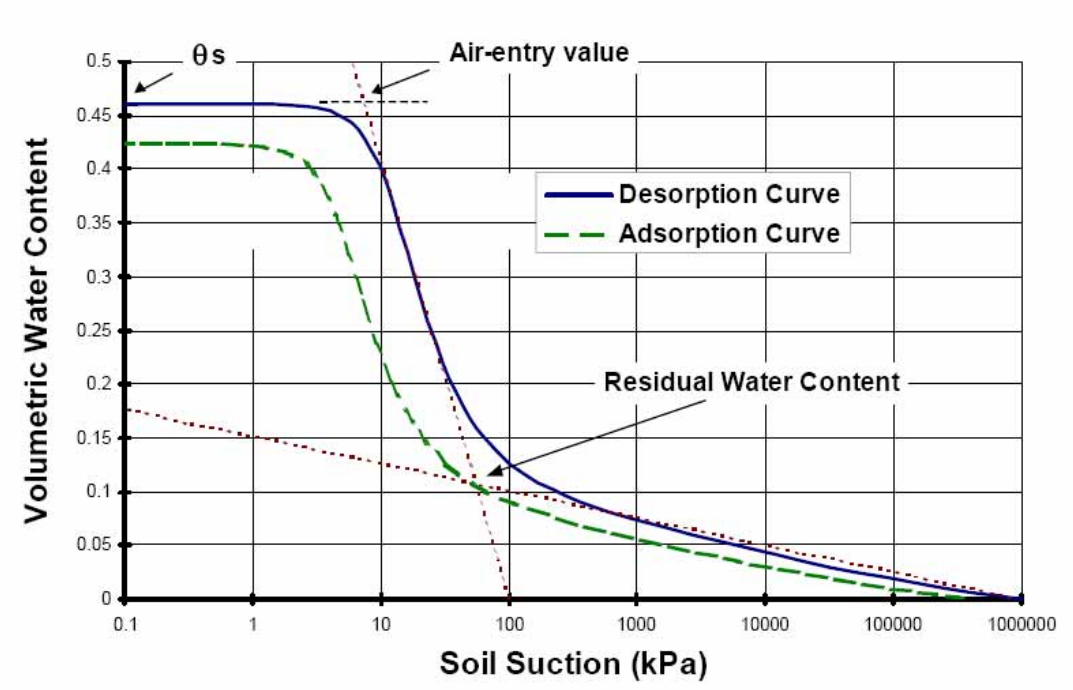

Figure (2.10): Definition of Variables Associated with the Soil-Water Characteristic Curve.

1. The Capillary *Saturation* Zone where the pore-water is in tension but the soil remains saturated. This stage ends at the air entry value, *AEV,* where the applied suction overcomes the capillary water forces in the largest pore in the soil.

2. The *Desaturation Zone* where water is displaced by air within the pores. Liquid water drains from the pores and is displaced by air. This stage ends at the residual water content, θ_r, where the pore-water becomes discontinuous and the coefficient of permeability is greatly reduced.

3. The Residual Saturation Zone where the water is tightly adsorbed on to the soil particles and flow occurs in the form of vapor. This stage is terminated at oven dryness. When the soil is heated to 105º C, the soil is defined to have zero water

content and the soil suction is approximately 1 x 10^6 kPa (Fredlund and Rahardjo, 1993)

Over the years, a number of equations have been suggested for soil water characteristic curve. A comprehensive comparison between commonly used curve-fitting equations for soil-water characteristic curve using a database of more than 200 soils has been conducted by Siller et al. (2001). It was found that the Fredlund and Xing (1994) equation was the best curve fitting equation in the sense that it provided the close fit to the data points. The equation proposed by Fredlund and Xing (1994) to empirically best-fit the soil-water characteristic curve is as follows:

$$\theta_w = C(\Psi)\left[\frac{1}{\ln\left(e+\left(\frac{\Psi}{a_f}\right)^{n_f}\right)}\right]^{m_f} \qquad (2.35)$$

Where:

θ_w: volumetric water content.

e: natural constant =2.718.

$\psi = (u_a - u_w)$: soil suction.

a_f : soil parameter related to the air entry of the soil.

n_f : soil parameter related to the rate of desaturation.

m_f : soil parameter related to residual water content conditions.

$C(\psi)$: correction factor to ensure that the function goes through 1,000,000 kPa of suction at zero water content.

While it is relatively easy to measure the soil-water characteristic curve in the laboratory, it is still quite costly and the test has not found its way into most conventional soils laboratories. For this reason, estimation of the soil-water characteristic using grain size distribution and volume-mass properties is beneficial. A theoretical curve could be fitted through the data from a grain size analysis. The theoretical grain size curve is then used for predicting the soil-water characteristic curve (Fredlund, 1999).

2.6.1 Factors Infleuncing Soil Water Characteristic Curve

Many factors have potentially significant effects on features of the SWCC such as soil structure, stress history, initial water content, void ratio, type of soil, mineralogy, and compaction method. Among these factors, initial void ratio, initial water content and stress history often have the greatest effect on soil structure, which in turn dominates the nature of the soil-water characteristic curve.

Kawai *et al*. (2000) studied the effect of initial void ratio on the SWCC. He stated that the smaller the initial void ratio (i.e. the denser the soil), the higher the air-entry value, and the higher the residual degree of saturation as well. The denser the soil, the higher the AEV, which implies that for soils with low void ratio values, small changes in degree of saturation can be assumed at low suctions, i.e. the soil can be treated as fully saturated.

The initial water content has considerable influence on the shape of SWCC curves. The higher the initial water content, the steeper the curve. The air-entry value also increases with initial water content. The resistance to de-saturation is relatively low in the dry of optimum specimens in comparison to optimum and wet of optimum specimens. So for soils of high initial water content the effect of de-saturation is more obvious, especially at low suction values. Curves with different initial water contents tend to converge at high suction values (Vanapalli *et al*., 1999).

Stress history seems not to affect significantly the shape of SWCC, although the AEV increases and the rate of change of the degree of saturation decreases with the increasing of net total stress (Ng and Pang, 2000).

2.7 Unsaturated Soil Property Functions

The term, unsaturated soil property functions**,** refers to such relationships as: coefficient of permeability versus soil suction, water storage variable versus soil suction, and shear strength versus soil suction.

Figure (2.11) presents some approaches that can be taken for the determination of unsaturated soil properties. Laboratory tests can be used as a direct measure of the required unsaturated soil property. For example, a (modified) direct shear test can be used to measure the relationship between matric suction and shear strength. These tests can be costly and the necessary equipment may not be available. Therefore, it may be sufficient to revert to an indirect laboratory test involving the measurement of the soil-water

characteristic curve for the soil. The soil-water characteristic curve can then be used in conjunction with the saturated shear strength properties of the soil, to predict the relationship between shear strength and matric suction. Some accuracy will likely be lost in reverting to this approach; however, the trade-off between accuracy and cost may be acceptable for many engineering projects.

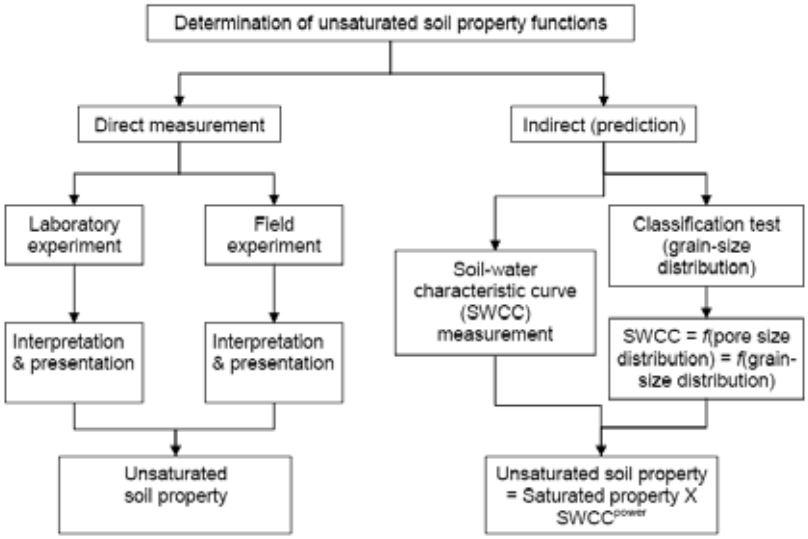

Figure (2.11): Approaches to Determine Unsaturated Soil Property Functions.

2.8 Uncoupled and Coupled Aproaches for Unsaturated Soils

The consolidation analysis of saturated soils may be conducted by two different approaches. One approach is based on the Biot's Theory, where a simultaneous solution for the pore water pressure and strains in soil structure is performed. This solution is called a "coupled approach". In the second approach, the solution is implemented with two steps. First, the pore water pressure distribution is obtained by solving the flow equation of water through soil. Second, the volume change of soil is obtained using one-dimensional consolidation theory. During solution of the flow equations, the soil structure is assumed to be rigid, i.e. constant stress state and displacements. This approach is called "uncoupled approach" because the flow equations and equilibrium equations are solved separately (Corapeioglou, 1984).

The solution of the unsaturated soil problems is more complex than saturated soils. The volume change of unsaturated soils involved several process: stress deformation, water flow, air flow, heat flow and chemical flow. In addition, soil properties associated with unsaturated soisl are non-linear. The volume change behaviour of unsaturated soil may be

conducted using coupled approach or uncoupled approach. The following sections provid a survey of research performed using both approaches.

2.8.1 Uncoupled Approach for Unsaturated Soils

In the uncoupled approach, the water phase continuity (i.e., seepage) equation is solved separately from the equilibrium (i.e., stress-deformation) equations. The pore-water pressure changes from seepage analysis are used as input in a deformation analysis. The involvement of dependent variables and a number of non-linear soil properties are separated into two analyses; namely, a seepage analysis and a stress-deformation analysis. For seepage analyses, the dependent variable is pore-water pressure (or hydraulic head). For a stress-deformation analysis, dependent variables are horizontal displacement, *u*, and vertical.

Rees and Thomas (1993) proposed an uncoupled model for the simulation of one-dimensional movement. It was assumed that soil was homogeneous and pore-air pressure was atmospheric. The method required the solution of the unsaturated seepage equation for obtaining variations of pore-water pressure. Then the variations of pore-water pressures were related to the volumetric deformation.

Hung (2000) presented an uncoupled solution of one and two-dimensional volume change problems associated with expansive soils. The proposed method is conducted using the finite element method. The formulation of the method was based on the general theory of volume change for an unsaturated soil. The seepage analysis and the stress-deformation analysis were performed independently using a general-purpose partial differential equation solver, called PDEase2D. Several typical examples and case histories were analyzed using the proposed model.

2.8.2 Coupled Approach for Unsaturated Soils

Biot (1941) proposed three-dimensional coupled equations to analyze the consolidation process for unsaturated soils. The soil was assumed to be an isotropic and linear elastic material. Two constitutive relationships were proposed in order to completely describe the deformation state of the soil. One constitutive relationship was formulated for the soil structure and the other was for the water phase. Two stress state variables were used in the formulations. Therefore, four volumatric deformation coefficeints were required to link the stress state variables and the deformation state variables.

Pereira (1996) developed a computer program, called COUPSO, to solve the coupled equations for the consolidation of unsaturated collapsing soils. The formulations were based on finte element solution for equilbrium equations and flow equations. The program was used to simulate the behavior of collapsing soil in an earth dam during saturation.

Wong et al. (1998) implemented coupled equations into finite element code, namely SEEP/W and SIGMA/W to allow two-dimensional analysis associated with consolidation and swell of unsaturated soils. However, the programs do not allow the description of the parameters as function of net normal stress. As well, the code has not been extensively verified.

CHAPTER (3)

THEORY OF MODEL AND PROGRAMS

3.1 Introduction

Heave prediction of expansive soils may be estimated using different analylatical methods. One of the most powerful methods is the finite elemenet analysis method. Finite element method is mainly depend on the constitutive relationship for soil. In this research, the finite element method is used to model the mechanical behaviour of unsaturated expansive soils. Uncoupled approach is used to solve the flow and equilibrium equations. The flow equations have been solved by the commercial program called SEEP/W (Seepage analysis Program). SEEP/W is a finite element software product that can be used to model the movement of water and pore-water pressure distribution within soil. SEEP/W is a general seepage analysis program that models both saturated and unsaturated flow. In SEEP/W, the field variables are the hydraulic heads at nodes. The output pressure head from SEEP/W is used as input for stress-deformation analysis.

The equilibrium equations have been implemented in CRISP (CRItical State soil mechanics Program). CRISP is a geotechnical finite element program incorporating the critical state soil mechanics theory (Britto and Gunn, 1987). It was developed by research workers at Cambridge University in 1975 onwards and was first released publicly in 1982. In CRISP, the field variables are the incremental displacements at nodes. CRISP is rewritten in fortran code with power station version 6. Then, CRISP is modified to model the mechanical behaviour of unsaturated soil. The modification is conducted by incorporating Fredlund's model in the open source version of CRISP. The implemented model was proposed by Fredlund, (1993). This model is nonlinear elastic analysis of unsaturated soil behaviour. Details about implemented model, CRISP and SEEP/W are presented herein. In addition, formulation of the implemented model in finite element equations form also introduced. Flow chart for steps of analysis of unsaturated expansive soils and required data for analysis are presented in Figure (3.1).

3.2 Fredlund's Model for Unsaturated Soil

Fredlund (1993) proposed a simple elastic nonlinear model for simulate the behaviour of unsaturated soil. This model characterize the soil behaviour with five soil parameters, elasticity parameter for the soil structure with respect to a change in the net normal stress, E, elasticity parameter for the soil structure with respect to a change in matric suction, H, water volumetric modulus associated with a change in the net normal stress, E_w, volumetric modulus associated with a change in matric suction, H_w, and Poisson's ratio, ν. Numerical modeling of behaviour of unsaturated soils required the constitutive equations of soil phases, flow equations for air and water phases and equilibrium equations. These different equations are presented in the following sections.

3.2.1 Constitutive Relationships of Unsaturated Soil

Constitutive relations for an unsaturated soil can be formulated by linking selected deformation state to appropriate stress state variables. The deformation state variables must satisfy the continuity requirements. Constitutive relationships for different phases of unsaturated are presented below.

3.2.1.1 The Soil Structure Constitutive Relationship

The constitutive relationships for the soil structure can be written in an incremental elasticity form as follows (Fredlund and Rahardjo, 1993):

$$\varepsilon_x = \frac{1+\nu}{E} d(\sigma_x - u_a) - \frac{\nu}{E} d(\sigma_y + \sigma_z - 2u_a) + \frac{d(u_a - u_w)}{H}$$

$$\varepsilon_y = \frac{1+\nu}{E} d(\sigma_y - u_a) - \frac{\nu}{E} d(\sigma_x + \sigma_z - 2u_a) + \frac{d(u_a - u_w)}{H} \qquad (3.1)$$

$$\varepsilon_z = \frac{1+\nu}{E} d(\sigma_z - u_a) - \frac{\nu}{E} d(\sigma_x + \sigma_y - 2u_a) + \frac{d(u_a - u_w)}{H}$$

Where:

ε_x, ε_y, ε_z: strain in the x-, y-, z-direction.

σ_x, σ_y, σ_z: normal stress in x-, y-, z-direction.

u_a: pore air pressure.

u_w: pore water pressure.

(u_a-u_w): matric suction.

E: elasticity parameter for the soil structure with respect to a change in the net normal stress.

H: elasticity parameter for the soil structure with respect to a change in matric suction.

ν : Poisson's ratio

Equation (3.1) can be used to write the equation for volumetric strain in a compressibility form as follows:

$$d\varepsilon_v = m_1^s(\sigma_{mean} - u_a) + m_2^s d(u_a - u_w) \tag{3.2}$$

Where:

ε_v : Volumetric strain ($\varepsilon_v = \varepsilon_x + \varepsilon_y + \varepsilon_z$)

$\sigma_{mean} = \dfrac{\sigma_x + \sigma_y + \sigma_z}{3}$: mean total stress.

$m_1^s = \dfrac{3(1-2\nu)}{E}$: coefficient of volume change with respect to a change in net normal stress.

$m_2^s = \dfrac{3}{H}$: coefficient of volume change with respect to a change in matric suction.

3.2.1.2 The Water Phase Constitutive Relationship

The water phase constitutive relationship can be presented in an incremental elasticity form as follows (Fredlund and Rahardjo, 1993):

$$d\theta = \frac{dV_w}{V_o} = \frac{1}{E_w} d(3\sigma_{mean} - 3u_a) + \frac{1}{H_w} d(u_a - u_w) \tag{3.3}$$

Where:

$\theta = \dfrac{V_w}{V_o}$: volumetric water content.

E_w: water volumetric modulus with respect to a change in the net normal stress.

H_w: water volumetric modulus with respect to a change in matric suction.

Equation (3.3) can also be written in compressibility form as follows:

$$d\theta = \frac{dV_w}{V_o} = m_1^w d(\sigma_{mean} - u_a) + m_2^w d(u_a - u_w) \tag{3.4}$$

Where:

$m_1^w = \dfrac{3}{E_w}$: coefficient of water volume change with respect to a change in net normal stress.

$m_2^w = \frac{1}{H_w}$: coefficient of water volume change with respect to a change in matric suction.

Using Equation (3.2) for mean net normal stress, Equation (3.4) becomes:

$$d\theta = \frac{dV_w}{V_o} = \beta_{w1} d\varepsilon_v + \beta_{w2}(u_a - u_w) \tag{3.5}$$

Where:

$\beta_{w1} = \frac{m_1^w}{m_1^s}$, or in the elasticity form, $\frac{E}{(1-2\nu)E_w}$

$\beta_{w2} = m_2^w - \frac{m_1^w m_2^s}{m_1^s}$, or in the elasticity form, $\frac{1}{H_w} - \frac{3E}{(1-2\nu)E_w H}$

Equation (3.5) shows that change in the volume of the soil mass would result in a change to the volume of the water within the soil. Additionally, volumetric water content is related to the matric suction. Therefore, a change in matric suction produces a direct change in the volumetric water content of the soil (and vice versa). Further, a change in matric suction will also act like a change in the applied stress, in that it will produce a change in the soil structure, hence leading to variation in the volume of voids. This will produce a further change in the volumetric water content of the soil.

3.2.1.3 The Air Phase Constitutive Relationship

The continuity requirement for an element of unsaturated soil allows the volume change of air phase be computed from the volume change of soil structure and volume change of water phase. The air phase constitutive relationship can be presented in the elasticity form as follows (Fredlund and Rahardjo, 1993):

$$\frac{dV_a}{V_o} = \frac{1}{E_a} d(3\sigma_{mean} - 3u_a) + \frac{1}{H_a} d(u_a - u_w) \tag{3.6}$$

Where:

E_a : air volumetric modulus with respect to change in net normal stress.

H_a : air volumetric modulus with respect to change in matric suction.

Equation (3.6) is written in compressibility form as follows:

$$\frac{dV_a}{V_o} = m_1^a d(\sigma_{mean} - u_a) + m_2^a d(u_a - u_w) \tag{3.7}$$

Where:

$m_1^a = \frac{3}{E_a}$: coefficient of air volume change with respect to change in net normal stress

$m_2^a = \frac{1}{H_a}$: Coefficient of air volume change with respect to change in matric suction.

Using Equation (3.2) for mean net normal stress, Equation (3.7) becomes:

$$\frac{dV_a}{V_o} = \beta_{a1} d\varepsilon_v + \beta_{a2}(u_a - u_w) \tag{3.8}$$

Where:

$\beta_{a1} = \frac{m_1^a}{m_1^s}$: or in the elasticity form, $\frac{E}{(1-2\nu)E_a}$

$\beta_{a2} = m_2^a - \frac{m_1^a m_2^s}{m_1^s}$: or in the elasticity form, $\frac{1}{H_a} - \frac{3E}{(1-2\nu)E_a H}$

Because of the continuity requirement for an element of unsaturated soil (i.e., $dV_v = dV_w + dV_a$), the parameters β_{a1} and β_{a2} are related to β_{w1} and β_{w2} as follows:

$$\beta_{w1} + \beta_{a1} = 1 \tag{3.9}$$

$$\beta_{w2} + \beta_{a2} = 0 \tag{3.10}$$

Equation (3.8) can be written as follows:

$$\frac{dV_a}{V_o} = (1 - \beta_{w1}) d\varepsilon_v - \beta_{w2}(u_a - u_w) \tag{3.11}$$

3.2.2 Flow Laws

The air and water phases both require a flow law. Darcy's law can be used for the water phase and Fick's law can be used for the air phase.

3.2.2.1 Flow of Water

Darcy's law relates the water flow rate to the hydraulic head (i.e., pressure head plus elevation head) as follows:

$$v_{wi} = -k_{wi} \nabla\left(\frac{u_w}{\rho_w g} + y\right) \tag{3.12}$$

Where:

v_{wi} : Darcy's Flux in *i*-direction

u_w: pore water pressure

k_{wi} : hydraulic conductivity in *i*-direction

ρ_w : density of water

g : gravitational acceleration

y : elevation head

3.2.2.2 Flow of Air

Fick's law relates the mass rate of air with pore-air pressure as follows:

$$J_{ai} = -D_a^* \frac{\partial u_a}{\partial x_i} \tag{3.13}$$

Where:

J_{ai} : mass rate of air in *i*-direction.

D_a^* : coefficient of transmission for air phase.

$\frac{\partial u_a}{\partial x_i}$: pore air pressure gradient in *i*-direction.

3.2.3 Basic Equation of Physics

A rigorous formulation to describe the swelling behaviour of an unsaturated expansive soil requires the following system of equations (Fredlund and Rahardjo, 1993):

i) Static equilibrium of the soil medium;

ii) The water phase continuity equation; and

iii) The air phase continuity equation.

3.2.3.1 Equilibrium Equations

The equations of overall static equilibrium for an unsaturated soil can be written as follows:

$$\sigma_{ij} + b_i = 0 \tag{3.14}$$

Where:

σ_{ij} : components of the net total stress tensor.

b_i : components of the body force vector.

3.2.3.2 Water Continuity Equation

The water continuity equation for an unsaturated soil can be written as follows (Freeze and Cherry, 1979):

$$\frac{\partial(\rho_w ns)}{\partial t} + \nabla.(\rho_w v_w) = 0 \tag{3.15}$$

Where:

n: porosity.

s: degree of saturation.

ρ_w: water density.

v_w: Darcy's Flux (discharge velocity)

$\nabla = \frac{\partial}{\partial x} i + \frac{\partial}{\partial y} j + \frac{\partial}{\partial z} k$: the divergence operator.

Water is commonly considered incompressible in geotechnical engineering practice (i.e., water density is a constant) and Eq. (3.15) can be written as follows:

$$\frac{\partial (ns)}{\partial t} + \nabla .(v_w) = \frac{\partial \theta}{\partial t} + \nabla .(v_w) = 0 \qquad (3.16)$$

Where:

$\theta = ns$: volumetric water content.

With the assumption that deformations are infinitesimal, Equation (3.16) becomes:

$$\frac{\partial (V_w / V_o)}{\partial t} + \nabla .(v_w) = 0 \qquad (3.17)$$

Where:

V_w: current water volume in the referential element.

V_o: referential volume of the element.

3.2.3.3 Air Continuity Equation

Fredlund and Rahardjo (1993) presented the air continuity equation as follows:

$$\frac{\partial}{\partial t}[\rho_a n(1-S)] + \nabla.(J_a) = 0 \tag{3.18}$$

Where:

ρ_a: density of air.

n: porosity.

s: degree of saturation.

J_a: mass flow rate of air.

With the assumption that deformations are infinitesimal, equation (3.18) becomes:

$$\frac{\partial(M_a / V_a)}{\partial t} + \nabla.(J_a) = 0 \tag{3.19}$$

Where:

$M_a = \rho_a V_a$: mass of air in the soil element.

$V_a = n\ (1 - S)\ V_o$: the air volume in the soil element.

Equation (3.18) can be written in an expanded form as follows:

$$\rho_a \frac{\partial(V_a / V_o)}{\partial t} + n(1-S)\frac{\partial \rho_a}{\partial t} + \nabla.(J_a) = 0 \tag{3.20}$$

The air phase is a highly compressible medium and its density is a function of the air pressure. Assuming that air behaves as an ideal gas, the equation for air density can be written as follows:

$$\rho_a = \frac{\omega_a}{RT}\overline{u}_a \tag{3.21}$$

Where:

ω_a: molecular mass of air,

R: universal (molar) gas constant.

T: absolute temperature,

$\overline{u}_a$: absolute pore-air pressure (i.e., $\overline{u}_a = u_a + \overline{u}_{atm}$).

u_a : gauge-pore-air pressure.

$\overline{u}_{atm}$: atmospheric pressure (i.e., 101kPa).

Equation (3.20) can be rearranged as follows:

$$\frac{\partial(V_a / V_o)}{\partial t} + \frac{n(1-S)}{\overline{u}_a}\frac{\partial u_a}{\partial t} + \frac{RT}{\omega_a \overline{u}_a}\nabla.(J_a) = 0 \tag{3.22}$$

3.3 Finite Element Formulations of Fredlund's Model for Two Dimensional Space

Many geotechnical problems can be simplified to a two-dimensional form using the concept of plane strain loading or axisymmetric loading. Let *x* be the horizontal direction and *y* be vertical direction, strains are considered only in the *xy*-plane, while strain in the *z*-direction is assumed to be negligible (i.e., $\Delta\varepsilon_z = 0$).

3.3.1 Strain-Displacement Relations

Let *u, v* and *w* be displacements in the *x*-, *y*- and *z*-direction, respectively. The incremental strain vector for infinitesimal deformation can be written as follows:

$$\{\Delta\varepsilon\} = \begin{Bmatrix} \Delta\varepsilon_x \\ \Delta\varepsilon_y \\ \Delta\varepsilon_z \\ \Delta\gamma_{xy} \end{Bmatrix} = \begin{Bmatrix} \dfrac{\partial u}{\partial x} \\ \dfrac{\partial v}{\partial y} \\ \dfrac{\partial w}{\partial z} \\ \dfrac{\partial u}{\partial y} + \dfrac{\partial v}{\partial x} \end{Bmatrix} \tag{3.23}$$

The incremental strain-stress relationship for an unsaturated soil medium can be written as follows (Fredlund and Rahardjo, 1993):

$$\begin{Bmatrix} \Delta\varepsilon_x \\ \Delta\varepsilon_y \\ \Delta\varepsilon_z \\ \Delta\gamma_{xy} \end{Bmatrix} = \frac{1}{E}\begin{bmatrix} 1 & -\nu & -\nu & 0 \\ -\nu & 1 & -\nu & 0 \\ -\nu & -\nu & 1 & 0 \\ 0 & 0 & 0 & 2(1+\nu) \end{bmatrix}\begin{Bmatrix} \Delta(\sigma_x - u_a) \\ \Delta(\sigma_x - u_a) \\ \Delta(\sigma_x - u_a) \\ \Delta\tau_{xy} \end{Bmatrix} + \frac{1}{H}\begin{bmatrix} 1 & 0 & 0 & 0 \\ 0 & 1 & 0 & 0 \\ 0 & 0 & 1 & 0 \\ 0 & 0 & 0 & 0 \end{bmatrix}\begin{Bmatrix} \Delta(u_a - u_w) \\ \Delta(u_a - u_w) \\ \Delta(u_a - u_w) \\ \Delta(u_a - u_w) \end{Bmatrix}$$

(3.24)

3.3.2 Constitutive Relationships

The soil structure constitutive relationship for plane strain conditions can be written as follows:

$$\begin{Bmatrix} \Delta(\sigma_x - u_a) \\ \Delta(\sigma_x - u_a) \\ \Delta(\sigma_x - u_a) \\ \Delta\tau_{xy} \end{Bmatrix} = \frac{E(1-\nu)}{(1+\nu)(1-2\nu)} \begin{bmatrix} 1 & \frac{\nu}{1-\nu} & \frac{\nu}{1-\nu} & 0 \\ \frac{\nu}{1-\nu} & 1 & \frac{\nu}{1-\nu} & 0 \\ \frac{\nu}{1-\nu} & \frac{\nu}{1-\nu} & 1 & 0 \\ 0 & 0 & 0 & \frac{1-2\nu}{2(1-\nu)} \end{bmatrix} \begin{Bmatrix} \Delta\varepsilon_x \\ \Delta\varepsilon_y \\ \Delta\varepsilon_z \\ \Delta\gamma_{xy} \end{Bmatrix}$$

$$-\frac{1}{H} \begin{bmatrix} 1 & \frac{\nu}{1-\nu} & \frac{\nu}{1-\nu} & 0 \\ \frac{\nu}{1-\nu} & 1 & \frac{\nu}{1-\nu} & 0 \\ \frac{\nu}{1-\nu} & \frac{\nu}{1-\nu} & 1 & 0 \\ 0 & 0 & 0 & \frac{1-2\nu}{2(1-\nu)} \end{bmatrix} \begin{bmatrix} 1 & 0 & 0 & 0 \\ 0 & 1 & 0 & 0 \\ 0 & 0 & 1 & 0 \\ 0 & 0 & 0 & 0 \end{bmatrix} \begin{Bmatrix} \Delta(u_a - u_w) \\ \Delta(u_a - u_w) \\ \Delta(u_a - u_w) \\ \Delta(u_a - u_w) \end{Bmatrix} \quad (3.25)$$

Alternatively, this incremental stress-strain relationship can be written as:

$$\{\Delta(\sigma - u_a)\} = [D]\{\Delta\varepsilon\} - [D]\{m_H\}\Delta(u_a - u_w) \quad (3.26)$$

Equation (3.26) can be rearranged as follow:

$$\{\Delta\sigma\} = [D]\{\Delta\varepsilon\} - [D]\{m_H\}\Delta(u_a - u_w) + \{\Delta u_a\} \quad (3.27)$$

Where:

$\{\Delta\sigma\}$: incremental total stress vector.

[D]: drained constitutive matrix.

$\{m_H\}^T$: $\begin{bmatrix} \frac{1}{H} & \frac{1}{H} & \frac{1}{H} & 0 \end{bmatrix}$: transpose of constitutive suction vector.

It can be further assumed that air pressure remains atmospheric at all times, Equation (3.27) becomes:

$$\{\Delta\sigma\} = [D]\{\Delta\varepsilon\} + [D]\{m_H\}\Delta(u_w) \quad (3.28)$$

3.3.3 Finite Element Formulation for Equilibrium Equations

Finite element equilibrium equations are formulated using the principle of virtual work which states that for a system in equilibrium, the total internal virtual work is equal to the external virtual work. In the simple case when only external point loads $\{F\}$ are applied, the virtual work equation can be written as:

$$\int \{\varepsilon^*\}^T \{\Delta\sigma\} dV = \{\delta^*\}^T \{F\} \tag{3.29}$$

Where:

$\{\delta^*\}$: virtual nodal displacements

$\{\varepsilon^*\}$: virtual strains

$\{\Delta\sigma\}$: internal stresses

$$\{\Delta\varepsilon\} = \begin{Bmatrix} \Delta\varepsilon_x \\ \Delta\varepsilon_y \\ \Delta\varepsilon_z \\ \Delta\gamma_{xy} \end{Bmatrix} = \begin{Bmatrix} \dfrac{\partial u}{\partial x} \\ \dfrac{\partial v}{\partial y} \\ \dfrac{\partial w}{\partial z} \\ \dfrac{\partial u}{\partial y} + \dfrac{\partial v}{\partial x} \end{Bmatrix} = [B]\{\delta\} \tag{3.30}$$

The strain matrix, $[B_i]$, for node, i, is given by:

$$[B_i] = \begin{bmatrix} \dfrac{\partial N_i}{\partial x} & 0 \\ 0 & \dfrac{\partial N_i}{\partial y} \\ \dfrac{N_i}{x} & 0 \\ \dfrac{\partial N_i}{\partial y} & \dfrac{\partial N_i}{\partial x} \end{bmatrix} \tag{3.31}$$

Where:

N_i: shape function (interpolation function) for node i

Substituting Equations (3.28) and (3.30) into Equation (3.29) gives that:

$$\int \{\delta^*\}^T B^T \left([D]B\{\delta\} + [D]\{m_H\}\Delta u_w\right) dV = \{\delta^*\}^T \{F\} \tag{3.32}$$

The nodal displacement vector is a constant, thus it can go out of integration:

$$\int B^T [D]B\{\delta\} dV + \int B^T [D]\{m_H\}\Delta u_w dV = \{F\} \tag{3.33}$$

The field pore water pressure vary over the finite element mesh according to:

$$\Delta u_w = \langle N_p \rangle \{\Delta u_w\} \tag{3.34}$$

where:

u_w : field pore water pressure.

$\langle N_p \rangle$: pore water pressure shape function.

$\{u_w\}$: nodal pore water pressure vector.

Substituting Equation (3.34) into Equation (3.33) gives that:

$$\int B^T [D] B \{\Delta\delta\} dV + \int B^T [D] \{m_H\} \langle N_p \rangle \{\Delta u_w\} dV = \{\Delta F\} \tag{3.35}$$

Equation (3.35) may be written in other simplified form as:

$$\int [K] dV \{\Delta\delta\} + \int [L_d] dV \{\Delta u_w\} = \{\Delta F\} \tag{3.36}$$

Where:

$[K] = \int B^T [D] B dV$: stiffness matrix.

$[L_d] = \int B^T [D] \{m_H\} \langle N_p \rangle dV$: linking matrix.

Applying numerical integration, it can be shown that the finite element equations are given by:

$$[K] = \sum_{i=1}^{NGP} [B_i]^T [D_i] [B_i] |J| w_i \tag{3.37}$$

$$[L_d] = \sum_{i=1}^{NGP} [B_i]^T [D_i] \{m_H\} \langle N_p \rangle |J| w_i \tag{3.38}$$

where:

$|J|$: determinant of Jacobian matrix.

w_i: weight for integration point i.

NGP: number of integration point in element.

For 6-node triangular element which used in this research, geometry of element is evident from Figure (3.1). Degrees of freedom of element (nodal displacement vector) can be presented as follow:

$$\{\delta\} = [u_1 \quad u_2 \quad u_3 \quad u_4 \quad u_5 \quad u_6 \quad v_1 \quad v_2 \quad v_3 \quad v_4 \quad v_5 \quad v_6]^T \tag{3.39}$$

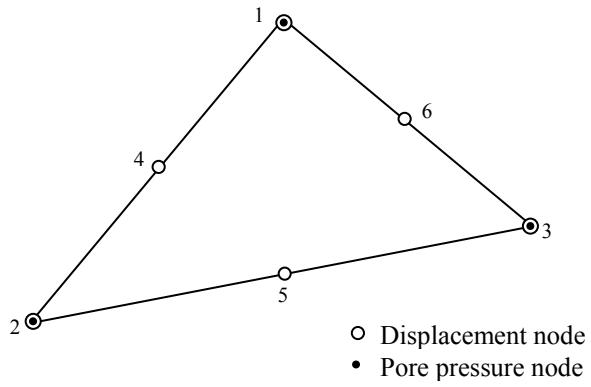

Figure (3.1): Geometry of Linear Strain Triangular Element

The displacement field inside the element is uniquely described by the above nodal displacement are:

$$u = \sum_{j=1}^{n} N_j u_j \tag{3.40}$$

$$v = \sum_{j=1}^{n} N_j v_j \tag{3.41}$$

Where:

n: the number of element nodes.

N_j: shape function (interpolation function) for node j

u_j: nodal displacement in local direction r for node j

v_j: nodal displacement in local direction s for node j

The displacement interpolation functions for 6-node element are listed in Table (3.1). The strain matric [B] has dimensions (4x12) and may be written as follow:

$$[B] = \begin{bmatrix} \frac{\partial N_1}{\partial x} & \frac{\partial N_2}{\partial x} & \frac{\partial N_3}{\partial x} & \frac{\partial N_4}{\partial x} & \frac{\partial N_5}{\partial x} & \frac{\partial N_6}{\partial x} & 0 & 0 & 0 & 0 & 0 & 0 \\ 0 & 0 & 0 & 0 & 0 & 0 & \frac{\partial N_1}{\partial y} & \frac{\partial N_2}{\partial y} & \frac{\partial N_3}{\partial y} & \frac{\partial N_4}{\partial y} & \frac{\partial N_5}{\partial y} & \frac{\partial N_6}{\partial y} \\ 0 & 0 & 0 & 0 & 0 & 0 & 0 & 0 & 0 & 0 & 0 & 0 \\ \frac{\partial N_1}{\partial y} & \frac{\partial N_2}{\partial y} & \frac{\partial N_3}{\partial y} & \frac{\partial N_4}{\partial y} & \frac{\partial N_5}{\partial y} & \frac{\partial N_6}{\partial y} & \frac{\partial N_1}{\partial x} & \frac{\partial N_2}{\partial x} & \frac{\partial N_3}{\partial x} & \frac{\partial N_4}{\partial x} & \frac{\partial N_5}{\partial x} & \frac{\partial N_6}{\partial x} \end{bmatrix} \tag{3.42}$$

Table (3.1): Interpolation Functions for 6-Node Triangular Element

Node, i	Function, N_i
1	*r(2r-1)*
2	*s(2s-1)*
3	*(1-r-s)(1-2r-2s)*
4	*4rs*
5	*4s(1-r-s)*
6	*4r(1-r-s)*

The quadratic 6-node element is integrated at 7 integration points. Locations of integration points within parent elements and its weight are stored in Table (3.2).

Table (3.2): Integration Points for 6-Node Triangular Element

Integration Point	Coordinate r_i	Coordinate s_i	Weight w_i
1	0.7974269853531	0.1012865073235	0.1259391805448
2	0.1012865073235	0.7974269853531	0.1259391805448
3	0.1012865073235	0.1012865073235	0.1259391805448
4	0.0597158717898	0.4701420641051	0.1323941527885
5	0.4701420641051	0.0597158717898	0.1323941527885
6	0.4701420641051	0.4701420641051	0.1323941527885
7	0.3333333333333	0.3333333333333	0.2250000000000

The Jacobian matrix, *J(r,s)* is given by:

$$[J]=\begin{bmatrix}\frac{\partial x}{\partial r} & \frac{\partial y}{\partial r}\\ \frac{\partial x}{\partial s} & \frac{\partial y}{\partial s}\end{bmatrix}=\sum_{j=1}^{n}\begin{bmatrix}\frac{\partial N_j}{\partial r}x_j & \frac{\partial N_j}{\partial r}y_j\\ \frac{\partial N_j}{\partial s}x_j & \frac{\partial N_j}{\partial s}y_j\end{bmatrix} \qquad (3.43)$$

A new approach is considered for solution of Equation (3.36) in finite element programming. The effect of suction change which represented by second term in the left hand side of Equation (3.36), $\int[L_d]dV\ \{\Delta u_w\}$, is calculated and added to the external force load vector as additional nodal loads. Then, the equations are solved by frontal solution method to find the nodal displacement due to change in nodal forces from external loads and soil suction change.

3.3.4 Finite Element Formulation for Flow Equations

The flow equation can similarly be formulated for finite element analysis using the principle of virtual work in terms of pore water pressure and volumetric strains. If virtual pore water pressures, u_w^*, are applied to the Flow Equation (3.17) and integrate over the volume, the following virtual work equation can be obtained:

$$\int u_w^* \left[\frac{k_x}{\gamma_w} \frac{\partial^2 u_x}{\partial x} + \frac{k_y}{\gamma_w} \frac{\partial^2 u_y}{\partial y} + \frac{\partial \theta}{\partial t} \right] dV = 0 \tag{3.44}$$

Applying integration by parts to Equation (3.44) gives:

$$-\int \left[\frac{k_x}{\gamma_w} \frac{\partial u_w^*}{\partial x} \frac{\partial u_w}{\partial x} + \frac{k_y}{\gamma_w} \frac{\partial u_w^*}{\partial y} \frac{\partial u_w}{\partial y} + \frac{\partial \theta}{\partial t} \right] dV + \int u_w^* \frac{\partial \theta}{\partial t} dV = -\int u_w^* v_n dA \tag{3.45}$$

The resultant equation describing the flow of water in saturated/unsaturated soil is:

$$\beta_{w2} [L_f] \{\Delta\delta\} - \left(\Delta t [\Phi] + \beta_{w1} [M_n] \right) \{\Delta u_w\} = \Delta t \left(\{Q\}\big|_{t+\Delta t} + [\Phi] \{\Delta u_w\}\big|_t \right) \tag{3.46}$$

where:

$[L_f] = \int \langle N_p \rangle^T \{m\}^T [B] dV$: linking matrix for flow.

$[\Phi] = \int \frac{1}{\gamma_w} [E]^T [K_w] [E] dV$: sub-permeability matrix.

$[M_n] = \langle N_p \rangle^T \langle N_p \rangle$: mass matrix.

Thus, analysis for saturated/unsaturated soils is formulated using incremental displacement and incremental pore water pressure as field variables. In uncoupled analysis, equations for finite element analysis are the equilibrium equation (3.36) and the flow equation (3.46) are solved separately. In this research, flow equations are simulated using SEEP/W while, equilibrium equation are implemented into the CRISP code.

3.4 Soil Properties Required for Volume Change Prediction of Expansive Soils

For an analysis involving unsaturated soils, flow analysis required the hydraulic conductivity function, K_w. In addition, the factors β_{w1} and β_{w2} are required for solving the flow equations. Factor β_{w1} may be calculated using equation (3.47) and factor β_{w2} may be calculated using equation (3.48).

$$\beta_{w1} = \frac{m_1^w}{m_1^s} = \frac{E}{(1-2\nu)E_w} \tag{3.47}$$

$$\beta_{w2} = m_2^w - \frac{m_1^w m_2^s}{m_1^s} = \frac{1}{H_w} - \frac{3E}{(1-2\nu)E_w H} \tag{3.48}$$

The volume change analysis required the constitutive matrix, [D] and constitutive suction vector, $\{m_H\}$. The elasticity parameter for the soil structure with respect to a change in the net normal stress, E, and Poisson's ratio, ν, are required for estimating the constitutive matrix [D]. In addition, the elasticity parameter for soil structure with respect to a change in matric suction, H, for estimating the constitutive suction vector $\{m_H\}$. In summary, six soil parameters required for the analysis of unsaturated soil. These parameters are E, H, E_w, H_w, ν and K_w.

For a uncoupled analysis, when solving flow equation, the net normal stress do not be taken into consideration thus the water volumetric modulus associated with a change in net normal stress equals infinity (∞). Consequently, the factor β_{w1} equals to zero and factor β_{w2} equals the inverse of the water volumetric modulus associated with a change in soil suction ($1/H_w$), i.e. the factor β_{w2} equals the slope of soil water characteristic curve, m_2^w. In summary, five soil parameters required for the uncoupled analysis of unsaturated soil. These parameters are E, H, H_w, ν and K_w.

3.5 Critical State Program (CRISP)

CRISP is frequently used as a test bed for new constitutive models, which can be bolted on to the existing finite element code. The code of CRISP has a great flexibility for implementing new soil models and new elements type. Also, user model for modifying and implemented different subroutines in CRISP code is available. These are the reasons why CRISP is used in this study.

CRISP operates in either two-dimensional plane strain or axis-symmetry. The effective stress principal is an integral part of the finite element analysis engine. Thus, CRISP can perform drained, undrained and fully coupled (Biot) consolidation analyses. The adequacy of a finite element solution is largely dependent upon the constitutive models used. CRISP incorporates various soil models. These models include linear elastic, and critical state soil models. CRISP provides sufficient element types to give accurate solutions to most geotechnical problems. One and two-dimensional elements are available. New element types can also be added into CRISP with relatively little effort.

CRISP uses Tangent Stiffness Technique to analyze non-linear problems. In the incremental or Tangent Stiffness Technique, the user divides the total load acting into a number of small increments and the program applies each of these incremental loads in turn. During each increment, the stiffness properties appropriate for the current stress levels are used in the calculations.

3.5.1 Soil Element Types

Plane 6-node and 15-node isoparametric triangular elements are available in CRISP. Six-noded element is a linear strain element where, fifteen-noded element is a cubic strain element. Also, Linear and cubic strain triangle elements with excess pore pressure degree of freedom for consolidation analysis are available in CRISP. The pore pressure nodes are deployed such that the strains and pore pressures have the same order of variation across the elements.

3.5.2 Soil Models

A material model is a set of mathematical equations that describes the relationship between stress and strain. The mechanical behavior of soils may be modelled at various degrees of accuracy.There are different soil models that differ from very simple one to very complicated. CRISP program package included some models such as elastic model and Cam clay models

3.5.2.1 Elastic Constitutive Model for Soil (Model 1)

This is the standard elastic model which allows for cross (transverse) anisotropy. Fully isotropic behaviour is covered as a special case. Although not realistic for soils the program makes possible to analyze a purely elastic anisotropic material. A typical stress-strain curve for a linear elastic material is plotted in Figure (3.2). Note that such a model assumes that the loading and unloading branches coincide.

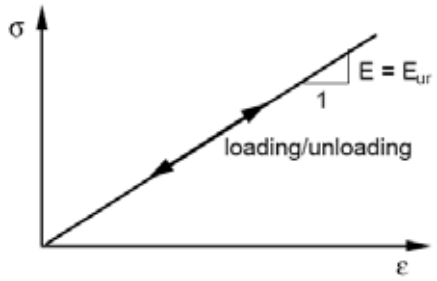

Figure (3.2): Linear Elastic Constitutive Model for Soil

The stiffness parameters required are:

- Young's modulus in the horizontal direction, E_h
- Young's modulus in the vertical direction, E_v
- Poisson's ratio linking vertical and horizontal directions, ν_{vh}
- Poisson's ratio linking both horizontal directions, ν_{hh}
- Shear modulus in *v*-*h* plane, G_{vh}

3.5.2.2 Non Homogeneous Isotropic Linear Elastic (Model 2)

This model is particularly suited to soil materials, where increasing confining pressure (with depth) often leads to a linearly increasing stiffness with depth. Poisson's ratio is not allowed to vary, so shear modulus, *G*, will be linked to Young's modulus through a constant ratio. This model is sometimes referred to as 'Gibson soil'.

The stiffness parameters required are:

- Young's modulus at the datum elevation, E_0.
- Rate of increase of Young's modulus with depth, m.
- Datum elevation at which ($E = E_0$), y_o
- Poisson's ratio, ν.

The elastic Young's modulus at an elevation *y* is given by the equation (3.49):

$$E = E_o + m(y_o - y) \tag{3.49}$$

3.5.2.3 Cam Clay and Modified Cam Clay Models (Models 3 and 4)

CRISP includes the Cam clay model (Schofield & Wroth, 1968) and modified Cam clay model (Roscoe and Burland,1968). All of these models are specific formulations within the framework of critical state soil mechanics (CSSM). The stiffness parameters required for these models are:

- Slope of isotropic compression line in v : ln(p'), λ
- Slope of unload-reload lines in v : ln(p'), k
- Reference void ratio on critical state line when p' = 1, e_{cs}
- Slope of critical state line in $q : p'$, M

3.5.3 Initial Stresses Genration

Initial stresses are of vital importance in geotechnical finite element work. The stiffness matrix of a finite element depends on the stress state within the element. In general, the stress state will vary across an element and the stiffness terms are calculated by integrating expressions dependent on these varying stresses over the volume of each element. The purpose of the initial stress input data is to enable the program to calculate the stresses before the analysis starts. In CRISP, initial stresses are only allowed to vary in the vertical direction.

For the purposes of specifying initial stresses, the mesh is divided into a number of horizontal layers. For most problems the initial stresses do not vary in the horizontal direction and it is assumed that the stresses vary only with depth. Therefore, you specify a set of reference elevations (differentiating the layers) along a vertical section, together with the stresses at these elevations. The in situ stresses at the integration points are interpolated from the stresses specified at these elevations. If all the initial stress values vary linearly throughout the mesh, then it is sufficient to define these values at just 2 elevations (at the top and bottom of the mesh).

A separate option is available to directly specify the in situ stresses at the integration points. This option may be used if the stress variation is such that the above simple option can not deal with the specific situation. For example, where the ground surface has a slope and where the stresses are not the same in the horizontal direction. In some analyses, the simple option of no initial stresses may have been selected. However, in most geotechnical problems the in situ stresses play an important role.

3.5.4 Types of Analysis

One of the principal features of any dedicated geotechnical finite element package should be its ability to work explicitly in terms of effective stress and pore pressure. Soils are at least 2-phase materials (solids and water), and many constitutive models are developed within an effective stress framework.

CRISP works in effective stresses and if you wish to work in total stress terms, this is also possible. Undrained, drained or fully coupled (Biot) consolidation analysis of two dimensional plane strain or axi-symmetric are available in CRISP

3.5.5 Finite Element Analysis

CRISP allows you to sub-divide the analysis into one or more increment blocks, with each increment block comprising one or more increments. The number of increment blocks required will depend on the analysis. In general, a block will be required whenever there is a distinct operation involving element removal or addition, application of boundary loads and changes to boundary drainage conditions (consolidation analyses only).

In some analyses as few as one block is sufficient, in others; several tens of blocks might be needed. When modeling construction activities it is convenient to use a separate block for each new phase of activity (e.g. wall installation, excavation stage, prop removal).

CRISP uses the incremental method which, in contrast to iterative methods, tends to give a response which continually drifts away from the true response where the stress strain behavior is non-linear. Any analysis which uses purely linear elastic models does not require more than one increment. However if you mix linear elastic models with other soil models then it is the latter which will govern the required number of increments.

CRISP allows soil constructions or excavations to be modeled in an analysis via the addition or removal of elements as the analysis proceeds. All the elements that appear at any stage in the analysis must have been included in the input data. Any number of finite elements can be removed from the parent finite element mesh to form the primary mesh before the analysis is started. These elements are added later at appropriate stages to simulate construction. Element which has a stress history cannot be added in analysis, hence elements which are added to represent a construction event cannot have CSSM material

3.6 Modeling of Water Flow Using SEEP/W Program

SEEP/W is a finite element software product that can be used to model the movement of water and pore-water pressure distribution within porous materials such as soil and rock. SEEP/W is a general seepage analysis program that models both saturated and unsaturated flow. SEEP/W is rigorously formulated with hydraulic conductivity and water content as a function of pore-water pressure, thus giving a seamless transition from the saturated to the unsaturated zone in the model. Saturated flow is simply a special case of this formulation, and as such, SEEP/W can model groundwater flow in confined systems.

The two-dimensional plane geometry is useful for modeling seepage in two-dimensions, such as a vertical cross-sectional plane or a plan view of the system. Axi-symmetric geometry is useful for situations where there is symmetry about a vertical axis, such as near a single vertical well.

Selection of SEEP/W for this research is due to it included the same element types (triangular-element) as CRISP consequently, the results of SEEP/W can be used as input data for CRISP. In addition, the flow equations are formulated using two independent stress state variables; total normal stress and soil suction as stated by Fredlund's model. Also, SEEP/W has the same assumptions for modeling of water flow as considered in Fredlund's model.

3.6.1 Soil Elements Types

Isoparameteric quadrilateral and triangular finite elements are included and each may have various numbers of optional secondary nodes to provide higher order interpolation of nodal values within the element. Infinite elements can be used at the boundaries of the problem domain that are for practical purposes unbounded. The local and global coordinate systems are related by a set of interpolation functions. SEEP/W uses the same functions for relating the coordinate systems as for describing the variation of the field variable (head) within the element. The elements are consequently isoparametric elements.

3.6.2 Flow Law

SEEP/W is formulated on the basis that the flow of water through both saturated and unsaturated soil follows Darcy's Law which states that:

$$q = k\, i \tag{3.50}$$

Where:

q: specific discharge

k: hydraulic conductivity

i: gradient of fluid head or potential

Darcy's Law was originally derived for saturated soil, but later research has shown that it can also be applied to the flow of water through unsaturated soil (Richards, 1931). The only difference is that under conditions of unsaturated flow the hydraulic conductivity is no longer a constant but varies with changes in water content and indirectly varies with changes in pore-water pressure.

3.6.3 Governing Equations

The governing differential equation used in the formulation of SEEP/W is:

$$\frac{\partial}{\partial x}\left(k_x \frac{\partial H_t}{\partial x}\right)+\frac{\partial}{\partial y}\left(k_y \frac{\partial H_t}{\partial y}\right)+Q=\frac{\partial \theta}{\partial t} \qquad (3.51)$$

Where:

H_t: total head

k_x: hydraulic conductivity in the x-direction

k_y: hydraulic conductivity in the y-direction

Q: applied boundary flux

θ: volumetric water content

t: time

This equation states that the difference between the flow (flux) entering and leaving an elemental volume at a point in time is equal to the change in the volumetric water content. More fundamentally, it states that the sum of the rates of change of flows in the x- and y- directions plus the external applied flux is equal to the rate of change of the volumetric water content with respect to time.

Under steady-state conditions, the flux entering and leaving an elemental volume is the same at all times. The right side of the equation consequently vanishes and the equation reduces to:

$$\frac{\partial}{\partial x}\left(k_x \frac{\partial H_t}{\partial x}\right)+\frac{\partial}{\partial y}\left(k_y \frac{\partial H_t}{\partial y}\right)+Q=0.0 \qquad (3.52)$$

Changes in volumetric water content are dependent on changes in the stress state and the properties of the soil. The stress state for both saturated and unsaturated conditions can be described by two state variables. These stress state variables are (σ - u_a) and (u_a - u_w). SEEP/W is formulated for conditions of constant total stress; that is, there is no loading or unloading of the soil mass. The second assumption is that the pore-air pressure remains constant at atmospheric pressure during transient processes. This means that (σ - u_a)

remains constant and has no effect on the change in volumetric water content. Changes in volumetric water content are consequently dependent only on changes in the (u_a - u_w) stress state variable, and with u_a remaining constant, the change in volumetric water content is a function only of pore-water pressure changes. A change in volumetric water content can be related to a change in pore-water pressure by the equation:

$$\partial\theta = m_2^w \partial u_w \tag{3.53}$$

Where:

m_2^w : the slope of the soil water characteristic curve.

The total hydraulic head is defined as:

$$H_t = \frac{u_w}{\gamma_w} + y \tag{3.54}$$

Where:

u_w: pore-water pressure

γ_w: unit weight of water

y: elevation head

Equation (3.6) can be rearranged as:

$$u_w = (H_t - y) \tag{3.55}$$

Substituting Equation (3.55) into (3.53) gives the following equation:

$$\partial\theta = m_2^w \gamma_w \partial(H_t - y) \tag{3.56}$$

Now can be substituted into Equation (3.52), leading to the following expression:

$$\frac{\partial}{\partial x}\left(k_x \frac{\partial H_t}{\partial x}\right) + \frac{\partial}{\partial y}\left(k_y \frac{\partial H_t}{\partial y}\right) + Q = m_2^w \gamma_w \frac{\partial(H_t - y)}{\partial t} \tag{3.57}$$

Since the elevation is a constant, the derivative of y with respect to time disappears, leaving the following governing differential equation:

$$\frac{\partial}{\partial x}\left(k_x \frac{\partial H_t}{\partial x}\right) + \frac{\partial}{\partial y}\left(k_y \frac{\partial H_t}{\partial y}\right) + Q = m_2^w \gamma_w \frac{\partial(H_t)}{\partial t} \tag{3.58}$$

3.7 Implementation of Fredlund's Model in finite Element Code

Implementation of Fredlund's model required some modifications and additions to the CRISP source code. The main steps for implementation are as follow:

1. Prepare a subroutine to estimate the constitutive matrix [D] which is varied with change of net normal stress (nonlinear model).
2. Prepare a subroutine to read initial and final total head from the results of SEEP/W. Then, calculate the pore pressure head and soil suction from total head.
3. Prepare a subroutine to calculate the linking matrix, [L_d]
4. Prepare a subroutine to estimate the equivalent suction loads and insert them in the external nodal load vector, $\{F\}$.
5. Modify subroutine which calculating internal stress vector $\{\Delta\sigma\}$ from Strain vector $\{\Delta u_w\}$.

3.8 Evaluation of the Elasticity Parameter Functions from Volume Change Indices

The stress–deformation analysis in two and three dimensions requires the characterization of the elasticity parameters E and H, which are functions of stress state. The elasticity parameters can be calculated from the coefficients of volume change, m_s^1 and m_s^1.

Several testing conditions can be used to obtain the void ratio constitutive surface (i.e., K_0 condition, plane strain condition, or isotropic condition). It is important to note that three fundamental elasticity parameters are required in the constitutive equations (i.e., E, H, andν). However, there are only two coefficients of volume change obtained from the constitutive surface for soil structure (i.e., m_s^1 and m_s^1). Therefore, it is suggested that Poisson's ratio be assumed (or measured) to convert the coefficients of volume change for different loading conditions to the fundamental elasticity parameters.

The elasticity parameter functions can be calculated from various testing conditions and then used for different types of analyses. Table (3.3) presents the calculation of these elasticity parameter functions for various loading conditions (Fredlund and Rahardjo, 1993). The coefficients obtained from one loading condition can be converted to other loading conditions using the assumed value of Poisson's ratio (Fredlund and Rahardjo, 1993):

$$m_1^s = \frac{3(1-\nu)}{(1+\nu)} m_{1-1D}^s = \frac{3}{2(1+\nu)} m_{1-2D}^s \qquad (3.59)$$

$$m_2^s = \frac{3(1-\nu)}{(1+\nu)} m_{2-1D}^s = \frac{3}{2(1+\nu)} m_{2-2D}^s \tag{3.60}$$

The coefficients of volume change can be obtained through the conversion of the semi-logarithmic plot of void ratio to an arithmetic plot (Hung, 2000). The swelling indices, C_t and C_m, are the slope of the void ratio versus logarithm of net normal stress or matric suction as shown in Figure (3.4). The semi-logarithmic plot of the void ratio constitutive surface for an unsaturated soil is approximately linear on the extreme planes over a relatively large stress range (Ho et al., 1992). The volume change indices obtained from K_0 loading have been shown to be essentially the same as those obtained from isotropic loading conditions, (Al-Shamrani and Al-Mhaidib, 2000).

Table (3.3): Relations between Elasticity Parameters and Coefficients of Volume Change

Stress State Variables	Coefficient of volume Change	Elasticity Parameter
Three-Dimensional Loading (3D):		
$(\sigma_{mean}-u_a);(u_a-u_w)_{3D}$	$m_1^s = \frac{\partial \varepsilon_v}{\partial(\sigma_{mean}-u_a)} = \frac{0.434}{(1+e_o)}\frac{C_s}{(\sigma_{mean}-u_a)}$ $m_2^s = \frac{\partial \varepsilon_v}{\partial(u_a-u_w)} = \frac{0.434}{(1+e_o)}\frac{C_m}{(u_a-u_w)}$	$E = 3\frac{(1-2\nu)}{m_1^s}$ $H = \frac{3}{m_2^s}$
K_o Loading, One-Dimensional Loading (1D):		
$(\sigma_y-u_a);(u_a-u_w)_{1D}$	$m_{1-1D}^s = \frac{\partial \varepsilon_y}{\partial(\sigma_y-u_a)} = \frac{0.434}{(1+e_o)}\frac{C_s}{(\sigma_y-u_a)}$ $m_{2-1D}^s = \frac{\partial \varepsilon_y}{\partial(u_a-u_w)_{1D}} = \frac{0.434}{(1+e_o)}\frac{C_m}{(u_a-u_w)_{1D}}$	$E = \frac{(1+\nu)(1-2\nu)}{(1-\mu)m_{1-1D}^s}$ $H = \frac{(1+\nu)}{(1-\nu)m_{2-1D}^s}$
Plane Strain Loading, Two-Dimensional Loading (2D):		
$(\sigma_{av}-u_a);(u_a-u_w)_{2D}$	$m_{1-2D}^s = \frac{\partial(\varepsilon_x+\varepsilon_y)}{\partial(\sigma_{av}-u_a)} = \frac{0.434}{(1+e_o)}\frac{C_s}{(\sigma_{av}-u_a)}$ $m_{2-2D}^s = \frac{\partial(\varepsilon_x+\varepsilon_y)}{\partial(u_a-u_w)_{2D}} = \frac{0.434}{(1+e_o)}\frac{C_m}{(u_a-u_w)_{2D}}$	$E = \frac{2(1+\nu)(1-2\nu)}{m_{1-2D}^s}$ $H = \frac{2(1+\nu)}{m_{2-2D}^s}$

The elasticity parameter functions E and H can also be calculated directly from volume change indices C_s (from net normal stress plane) and C_m (from matric suction plane), respectively. Figure (3.3) shows the typical void ratio constitutive surface plotted in semi-logarithmic scale and volume change indices. The elasticity parameters are calculated

from the coefficient of volume change as shown in Table (3.3). The elasticity parameter E can be expressed as a function of the volume change index with respect to net normal stress, C_s, initial void ratio, and Poisson's ratio. The elasticity parameter H can be expressed as a function of the volume change index with respect to matric suction, C_m, initial void ratio, and Poisson's ratio. The equations for these elasticity parameters can be written for general three-dimensional loading conditions as follows:

$$E = \frac{3.908(1-2\nu)(1+e_o)}{C_s}(\sigma_{mean} - u_a) \tag{3.61}$$

$$H = \frac{6.908(1+e_o)}{C_m}(u_a - u_w) \tag{3.62}$$

Equations (3.61) and (3.62) can be written for two dimensional plane strain conditions as follows:

$$E = \frac{4.605(1+\nu)(1-2\nu))(1+e_o)}{C_s}(\sigma_{av} - u_a) \tag{3.63}$$

$$H = \frac{4.605(1+\nu)(1+e_o)}{C_m}(u_a - u_w) \tag{3.64}$$

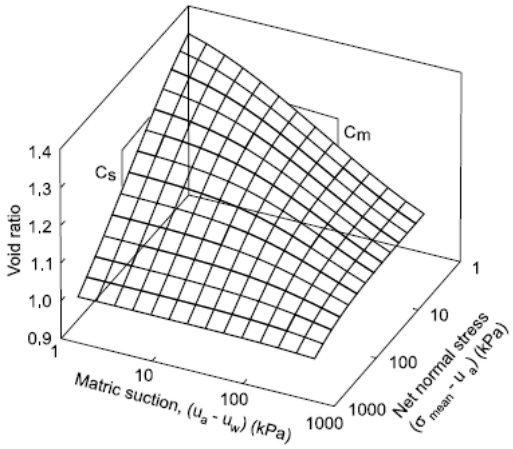

Figure (3.3): A Typical Void Ratio Constitutive Surface Plotted in Semi-logarithmic Scale.

3.9 Steps of Analysis

As mentioned before, in the uncoupled approach, the water phase continuity (i.e., seepage) equation is solved separately from the equilibrium (i.e., stress-deformation) equations. First, the seepage analysis is performed using SEEP/W. Seepage analysis required the hyraulic conductivity function, k_w, soil water characteristic curve and initial soil suction. Final soil suction results are used as input for the stress-deformation analyis. The stress-deformation analysis is performed with Fredlund's model in the Modified CRISP. This

analysis required the elasticity parameters and Poison's ratio. Also, the initial soil stress is important for stress deformation analysis. Soil displacement and stresses in the domain of modal are obtained from Modified CRISP. The steps of analysis are illustrated as a flow chart in Figure (3.4)

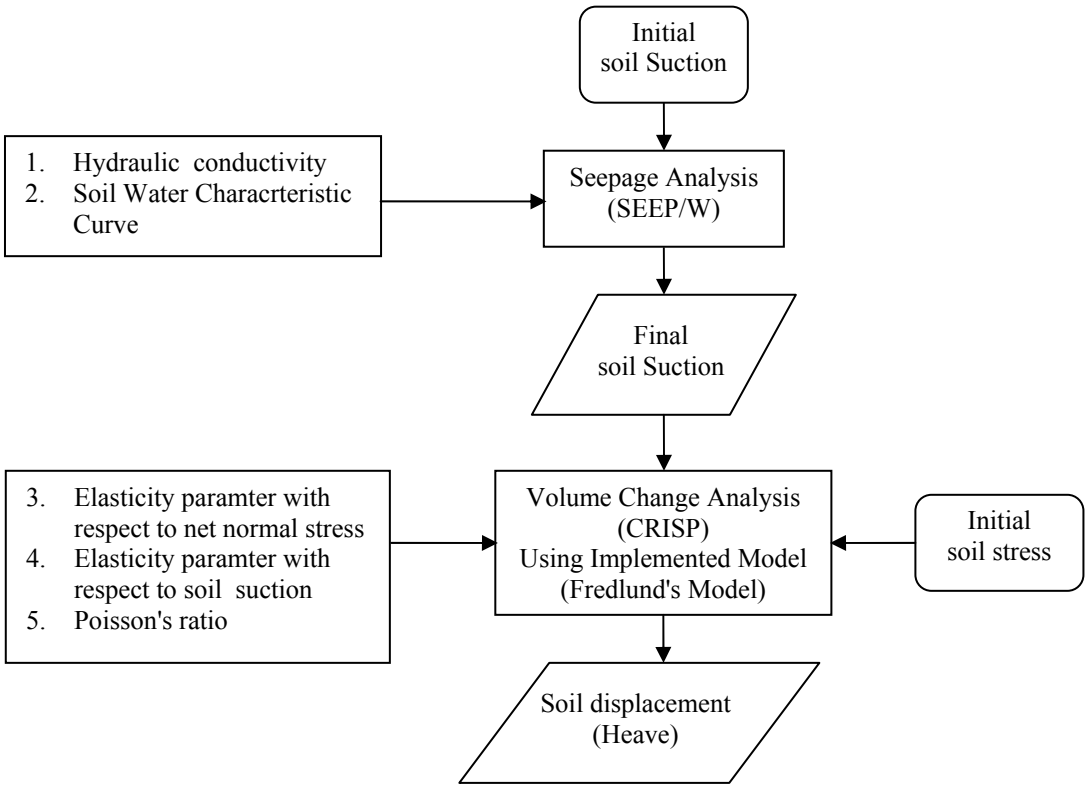

Figure (3.4): Flow Chart for Analysis Steps of Unsaturated Expansive Soils

CHAPTER (4)
PROGRAM VERIFICATION AND VALIDATION

4.1 Introduction

This chapter provides verification of the results obtained from Modified CRISP by comparing the analysis results performed by Modified CRISP with that reported in the field or with the results presented in the literature. For the purpose of this verification, one case history and three example problems were used. The example problems include simple heave problem presented by Fredlund and Rahardjo (1993) to evaluate heave using analytical method depending on oedometer tests. Also, example problem presented by Hung (2000) to estimate the influence of trees on surrounding soil using finite element approach was used for verification of the modified program. Finally, example problem simulates the influence of ground surface flux on soil heave presented by Hung (2000) is used.

4.2 Simple Heave Problem (Fredlund and Rahardjo, 1993)

Fredlund and Rahardjo (1993) conducted an analysis to evaluate the total heave of expansive soil layer due to change in soil suction. In this analysis, a 2.0 m thick layer of expansive clay was subjected to change in soil suction due to covering with an impermeable layer of asphalt as shown in Figure (4.1). The initial void ratio, e_o, of the soil is 1.0, the total unit weight is 18.0 kN/m^3, and the swelling index, C_s is 0.10. Only one oedometer test was performed on a sample taken from a depth of 0.75 m. The test data showed a corrected swelling pressure, P_s, of 200 kPa. It was assumed that the corrected swelling pressure is constant throughout the 2.00 m layer.

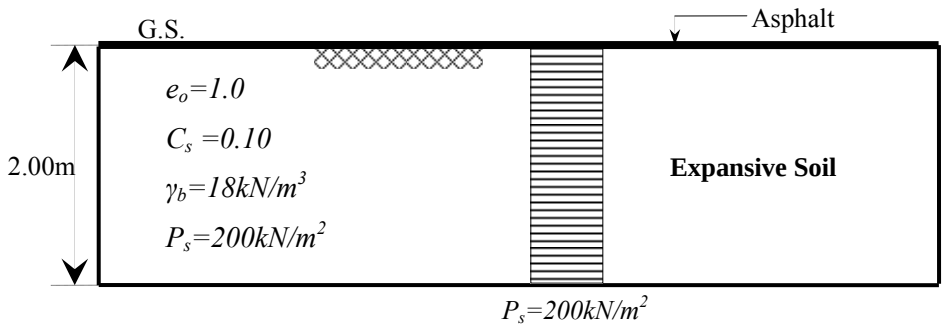

Figure (4.1): Simple Heave Problem (Fredlund and Rahardjo, 1993)

It is anticipated that with time, the negative pore-water pressure in the soil below the asphalt will increase as a result of the discontinuance of evaporation and evapotranspiration. For analysis purposes, it was assumed that the final pore-water pressure will increase to zero throughout the entire depth. Calculations performed by Fredlund showed a total heave of 11.4 cm, approximately 36% of the total heave occurs in the upper quarter of the clay strata.

4.2.1 Analysis with Modified CRISP

This example was re-analyzed using the modified program. The initial soil suction is estimated from the swelling pressure using the following equation (Fredlund and Rahardjo, 1993):

$$(u_a - u_w)_o = \frac{P_s - (\sigma_y - u_a)}{f} \quad (4.1)$$

Where:

$(u_a\text{-}u_w)_o$: initial soil suction.

P_s: swelling pressure.

$(\sigma_y\text{-}u_a)$: net normal overburden vertical stress.

f: equivalent factor (equal to degree of saturation)

Initial soil suction may be introduced as function in soil depth using the previous equation. The factor, *f,* is taken equal to soil degree of saturation. The degree of saturation is estimated to be equal 0.90 based on bulk unit weight (18kN/m^3) and initial void ratio (1.0) and assuming (2.70) for specific gravity of solid particles. Therefore, the initial soil suction may be given by Equation (4.2) (Fredlund and Hung, 2004):

$$(u_a - u_w)_o = 222.25 - 20Z \quad (4.2)$$

Where:

$(u_a\text{-}u_w)_o$: initial soil suction.

Z: depth of soil from ground surface.

According to equation (4.2), initial soil suction varies linearly with soil depth. Initial soil suction at ground surface equals 222.25kPa and initial soil suction at end of layer (2.00m depth) equals 182.25kPa. Similar to Fredlund and Rahardjo (1993), the final soil suction is assumed to equal zero over the layer due to covering soil with impermeable layer as proposed by Fredlund and Rahardjo (1993).

Soil properties are estimated from the given data by Fredlund and Rahardjo (1993). Poisson's ratio, ν, is assumed to equal 0.40 and at rest coefficient of earth pressure, K_o, equals 0.67. The modulus of elasticity with respect to change in net normal stress is not required because there are no applied loads in the analyzed example problem. The modulus of elasticity with respect to change in soil suction, H, is estimated using equations (4.3) and (4.4) with the assumption that coefficient of volume change with respect to soil suction, C_m, equals the coefficient of volume change with respect to total stress, C_s, (0.10) as proposed by Fredlund and Hung (2004). Thus, modulus of elasticity with respect to change in soil suction, H, is introduced as function in soil suction by equation (4.5) according to Fredlund and Hung (2004) .

$$m^s_{2-2D} = \frac{0.434}{(1+e_o)} \frac{C_m}{(u_a - u_w)_{2D}} \tag{4.3}$$

$$H = \frac{2(1+\nu)}{m^s_{2-2D}} \tag{4.4}$$

$$H = 130(u_a - u_w) \tag{4.5}$$

Properties of the soil layer used in the analyses of example problem can by summarized as shown in Table (4.1).

Table (4.1): Properties of Soil for Simple Heave Problem

No.	Property	Unit	Value
1	Modulus of elasticity with respect to soil suction, H	kN/m^2	$130(u_a-u_w)$
2	Poisson's Ratio, ν	-	*0.40*
3	At rest coefficient of earth pressure	-	*0.67*

The problem is simulated by a finite element mesh with dimension 20 X 2.0m using triangular linear strain elements. The dimensions of finite element mesh and distribution of elements are shown in Figure (4.2).

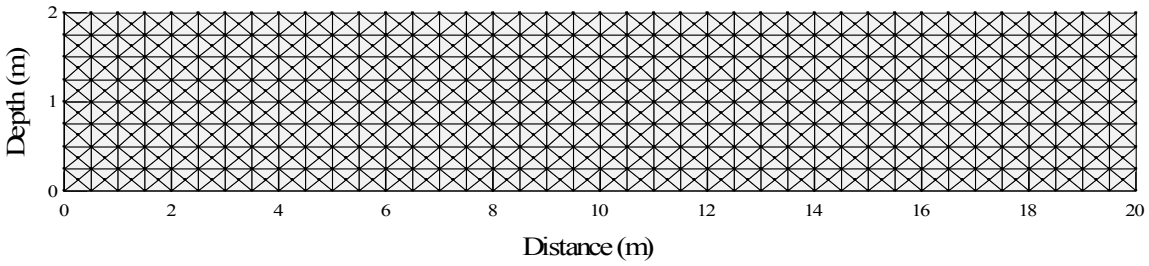

Figure (4.2): Dimension of Finite Element Mesh and Distribution of Elements
Validation Example No. 1

The results of analysis give a ground surface heave 10.40 cm. This value is almost in good agreement with the results from analytical procedure presented by Fredlund and Rahardjo (1993). The difference in results may be attributed to the assumption that the coefficient of volume change due to soil suction change, C_m, equals the coefficient of volume change due to net total stress change, C_s. The distribution of vertical heave with depth is shown in Figure (4.3).

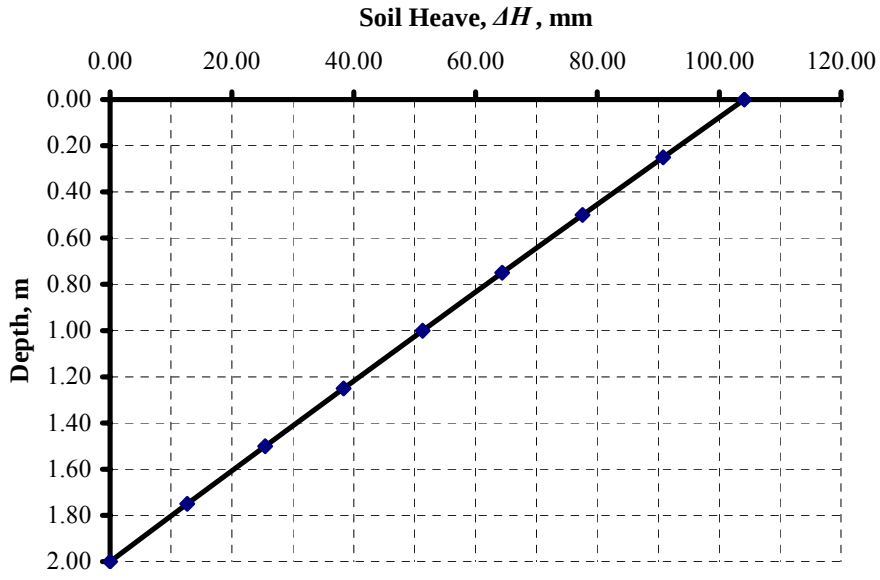

Figure (4.3) Predicted Vertical Displacements with Modified CRISP Program

4.3 Case History of a Slab on Grade Floor on Regina Clay

The heave of a floor slab of a light industrial building in north central Regina, Saskatchewan is reported and analyzed by Fredlund and Hung, 2004. Construction of the building and instrumentation took place during August 1961. Instrumentation installed at the site included a deep benchmark, vertical movement gauges, and a neutron moisture meter access tube. Vertical ground movement was monitored at depths of 0.58, 0.85, and 2.39 m below the original ground surface (Yoshida et al., 1983).

The owner of the building noticed heave and cracking of the floor slab in early August 1962, about a year after construction. An unexpected increase in water consumption of approximately 35000L was recorded. The line of hot water was cracked under the floor slab. The location of the cracks and contours of the heave are shown in Figure (4.4).

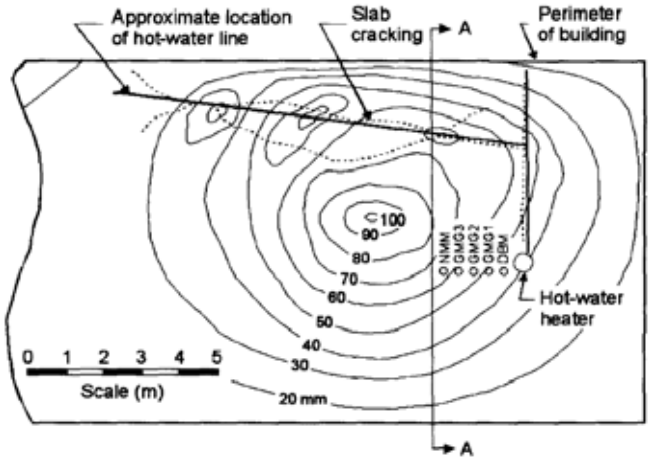

(NMM: neutron moisture meter, GMG: ground movement gauge, DBM: depth benchmark)

Figure (4.4): Floor Plan of Study Site and Contours of Measured Heave (Yoshida et al., 1983)

Laboratory analysis for samples at the site was performed. Atterberg limits, insitu water content, grain size distribution and swelling pressure of samples were evaluated. Swelling pressure and swelling index were obtained by constant volume oedometer test for three samples. The summary of the analysis results of oedometer tests are introduced in Table (4.2).

Table (4.2): Results of Constant Volume Oedometer Tests for Slab on Floor, Regina (Fredlund and Hung, 2004)

Depth (m)	Initial void ratio, e_o	Swelling Index, C_s	Corrected Swelling pressure, p_s (kPa)
0.69	0.927	0.095	490
1.34	0.985	0.081	325
2.20	0.974	0.094	81

4.3.1 Analysis of Case History by Fredlund and Hung, (2004)

Fredlund and Hung (2004) present two dimensional numerical study of this site. The analyses were performed for water flow and stress-deformation. Soil suctions were estimated from saturated-unsaturated seepage analysis. The results were then used as input for the prediction of displacements in a stress-deformation analysis. A general purpose partial differential equation solver, called FlexPDE was used in the study (PDE Solutions Inc., 2004). The details of study for seepage and stress-deformation analyses are presented in the following sections.

4.3.1.1 Seepage Analysis

A seepage analysis was performed to predict changes in matric suction conditions in the soil. The initial matric suction was estimated from the corrected swelling pressures. The initial matric suction conditions required for seepage analysis can be estimated as follows (Fredlund and Hung, 2004):

$$(u_a - u_w) = \frac{P_s - (\sigma_y - u_a)}{f} \tag{4.6}$$

Where:

f: function set equal to degree of saturation.

P_s : swelling pressure.

The variation of corrected swelling pressure and initial soil suction with depth were introduced in Figure (4.5) based on Equation (4.3).

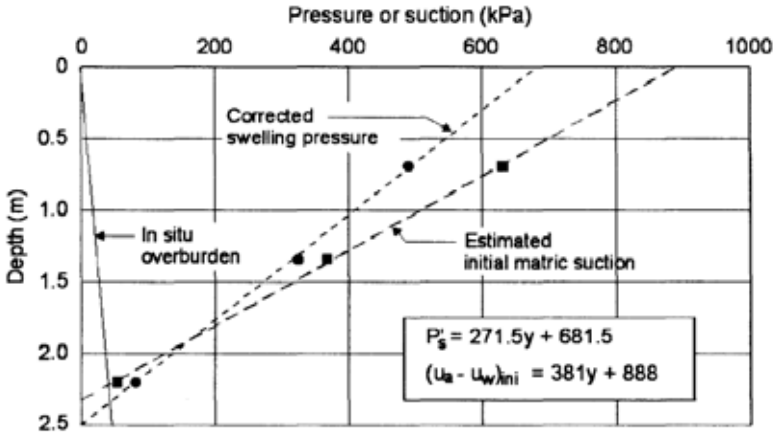

Figure (4.5): Distribution of Corrected Swelling Pressure and Estimated Initial Suction with Depth (Fredlund and Hung, 2004)

An approximate soil-water characteristic curve was defined using measured water contents at various values of soil suction. The Fredlund and Xing (1994) equation for Soil Water Characteristic Curve, Equation (2.9), was used to describe the soil-water characteristic curve, the fitting parameters for the relation between the volumetric water content and soil suction were $a_f = 300$, $n_f = 0.6$ and $m_f = 0.7$ where the fitting parameters for relation between degree of saturation and soil suction were $a = 300$, $n = 0.5$ and $m = 0.7$. Figures (4.6) and (4.7) show the soil water characteristic curve relations.

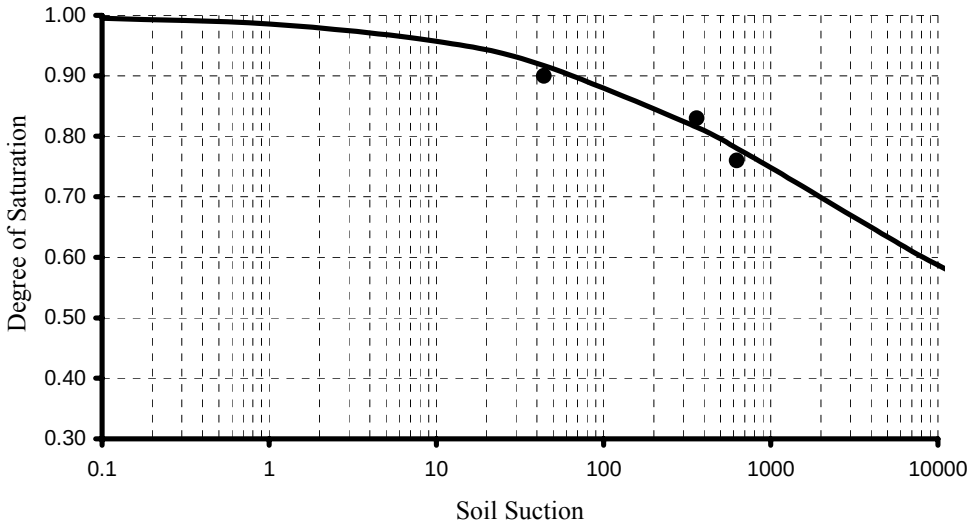

Figure (4.6): Degree of saturation versus Soil Suction for Regina Clay (SWCC), (Fredlund and Hung, 2004)

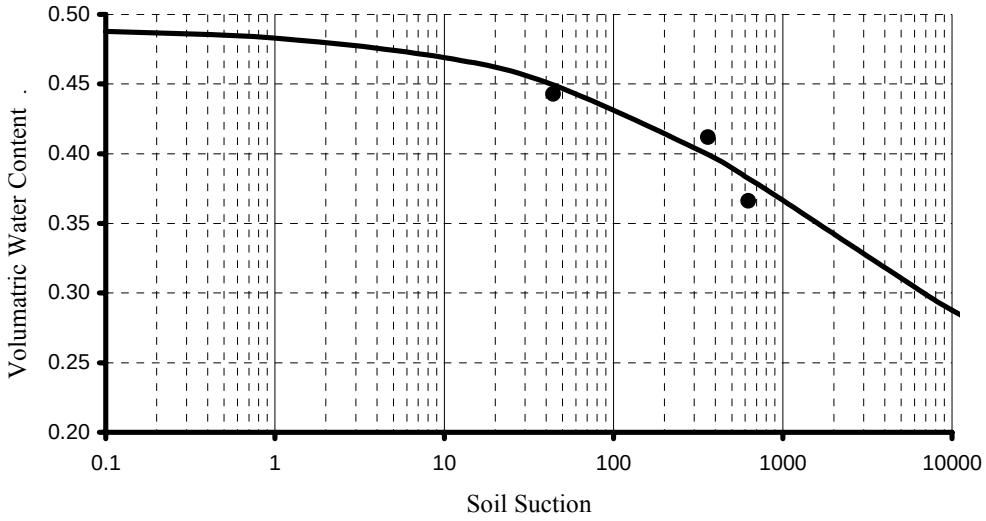

Figure (4.7): Volumetric Water Content versus Soil Suction for Regina Clay (SWCC), (Fredlund and Hung, 2004)

A coefficient of permeability function for compacted Regina Clay measured by Shuai, (1996) was used for seepage analysis of this case history by Fredlund and Hung, (2004). The coefficient of permeability function described by Leong and Rahardjo, (1997) is provided as Equation (4.7) and shown graphically in Figure (4.8).

$$k = k_s \left[\left(\frac{1}{\ln\left(e + \left(\frac{\Psi}{a_f}\right)^{n_f}\right)} \right)^{m_f} \right]^{p} \qquad (4.7)$$

Where:

k_s: the saturated coefficient of permeability (7.9×10^{-10} m/s)

a_f: fitting parameter corresponding to (553.5kPa)

n_f: fitting parameter corresponding to (1.09)

m_f: fitting parameter corresponding to (2.2)

P: fitting parameter corresponding to (1.06)

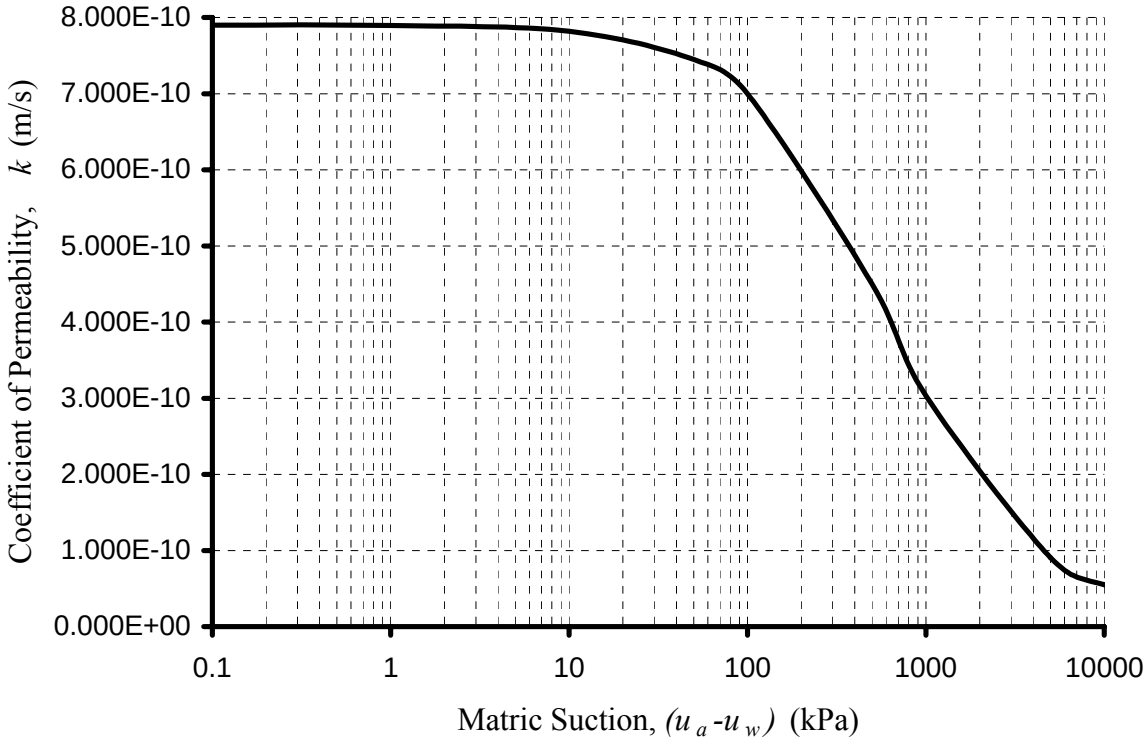

Figure (4.8): Coefficient of Permeability Function for Regina Clay
(Fredlund and Hung, 2004)

The geometry and boundary conditions for the seepage analysis are illustrated in Figure (4.9). It is assumed that water leaked from the water line along 2 m length of the line. It was assumed that the initial suction conditions did not change outside of the concrete slab and at the lower boundary of the domain. A moisture flux equal to zero was specified elsewhere along the boundaries.

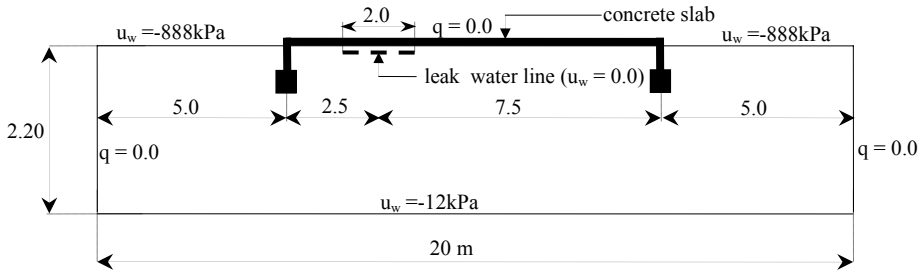

Figure (4.9): Geometry and Boundary Conditions for Seepage Analysis
(Fredlund and Hung, 2004)

4.3.1.2 Stress-Deformation Analysis

The elasticity parameter function with respect to changes in net normal stress, *E*, was calculated considering two dimensional conditions using Equations (4. 8) and (4.9).

$$m^{s}_{1-2D} = \frac{\partial(\varepsilon_x + \varepsilon_y)}{\partial(\sigma_{av} - u_a)} = \frac{0.434}{(1+e_o)} \frac{C_s}{(\sigma_{av} - u_a)} \tag{4.8}$$

$$E = \frac{2(1+\nu)(1-2\nu)}{m^{s}_{1-2D}} \tag{4.9}$$

The average values of swelling index measured using conventional oedometer test , C_s, and initial void ratio, e_o, were taken as 0.09 and 0.962 respectively. The Poisson's ratio, ν, was assumed to be equal to 0.40. The final expression for the elasticity modulus can be introduced as follows (Fredlund and Hung, 2004):

$$E = 28.11(\sigma_{ave} - u_a) \tag{4.10}$$

The elasticity parameter function with respect to changes in matric suction, *H*, can be calculated for two-dimensional analysis using Equation (3.66). The swelling index with respect to changes in matric suction, C_m, was not measured for this case history. Fredlund and Hung (2004) suggested that a value of C_s to be used for C_m. The elasticity parameter with respect to soil suction may be expressed as follows (Fredlund and Hung, 2004):

$$H = 140.5(u_a - u_w) \tag{4.11}$$

Fredlund and Hung (2004) stated that deformation of the slab associated with this case was due to applied load and wetting. Deformation of the slab and the soil mass due to loading can be assumed to respond immediately, while the deformations due to wetting are a time dependent process. Therefore, the stress-deformations due to loading and due to wetting need to be analyzed independently. Figure (4.10) shows the stress path followed in the analysis. The stress-deformation analysis was first performed to predict the displacements and induced stress due to the loading of the slab. The deformations due to changes in matric suction were then predicted for steady state conditions from the seepage analysis (Fredlund and Hung, 2004).

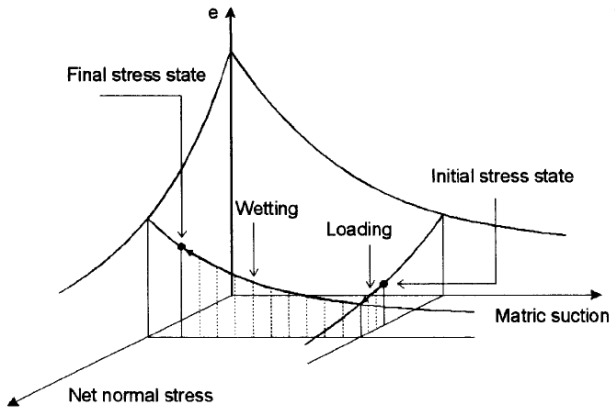

Figure (4.10): Stress Path Followed in The Stress-deformation Analysis (Fredlund and Hung, 2004)

Figure (4.11) shows the geometry and boundary conditions for stress-deformation analysis. A load equal to 5.76 kPa is applied on the surface of a 100mm thick concrete slab. This surcharge is made up of 180 mm of fill with unit weight of 18.88 kN/m^3 and 100 mm concrete with a unit weight of 23.6kN/m^3. An accurate perimeter load is unknown, however, a typical value of 15 kN/m was assumed. The soil is free to move in a vertical direction and fixed in the horizontal direction at the left and right sides of the domain. The lower boundary is fixed in both directions.

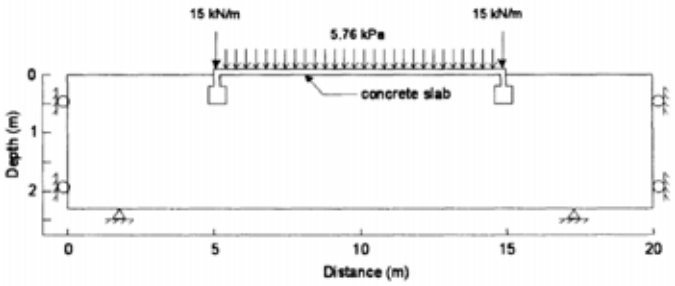

Figure (4.11): Boundary Conditions for Stress-deformation Analysis

4.3.2 Results of Analysis from Fredlund and Hung (2004)

Figure (4.12) shows the matric suction distribution in the soil at steady state conditions. It can be noted that under the specified boundary conditions the matric suction at steady state conditions is about 20kPa under the center of the slab.

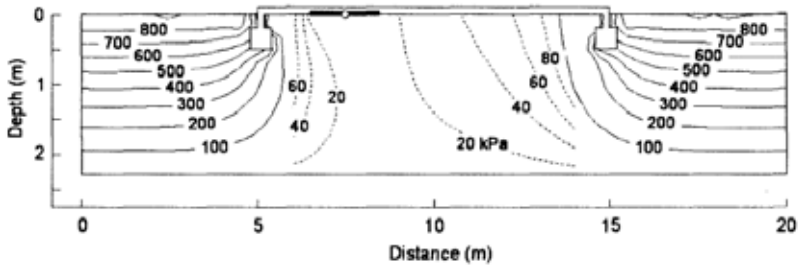

Figure (4.12): Matric Suction at Steady State Conditions (Fredlund and Hung, 2004)

The predicted vertical displacements at various final suction conditions with the measured total heave at the center of the slab are presented in Figure (4.13). The agreement between the predicted and the measured heave at different depths differ to some degree. The amounts of heave measured at depths of 0.58 and 0.85 m correspond to the predicted heave at 100 days, while the total heave of 106 mm at the ground surface corresponds to the case when the pore-water pressure goes to zero under the slab. It must be noted that a heave of 106 mm represents the maximum heave observed on the slab. The maximum heave observed at the cross-section (A-A) under consideration is only 80 mm (Fredlund and Hung, 2004)

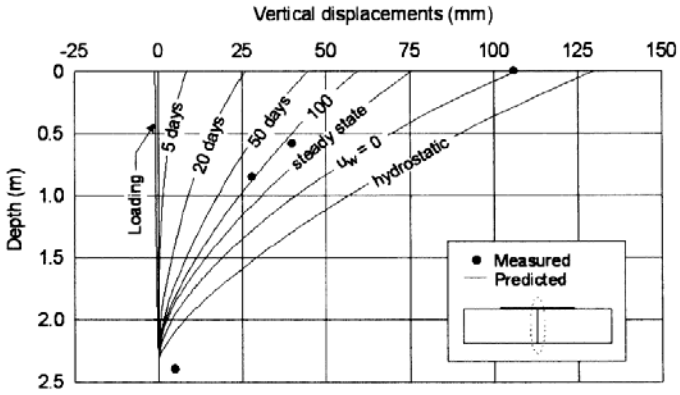

Figure (4.13): Measured and Predicted Vertical Displacements near The Center of Slab (Fredlund and Hung, 2004)

4.3.3 Results of Analysis from Modified CRISP

The case history was re-analyzed using the Modified CRISP with the same soil properties. Dimensions of finite element mesh and distribution of elements are presented in Figure (4.14). Figure (4.15) shows the matric suction distribution in the soil at steady state conditions obtained using SEEP/W program with same soil properties introduced by Fredlund and Hung (2004). The suction distribution is well compared to the results of

Fredlund. However, final soil suction at steady state conditions under the center of slab was approximately zero.

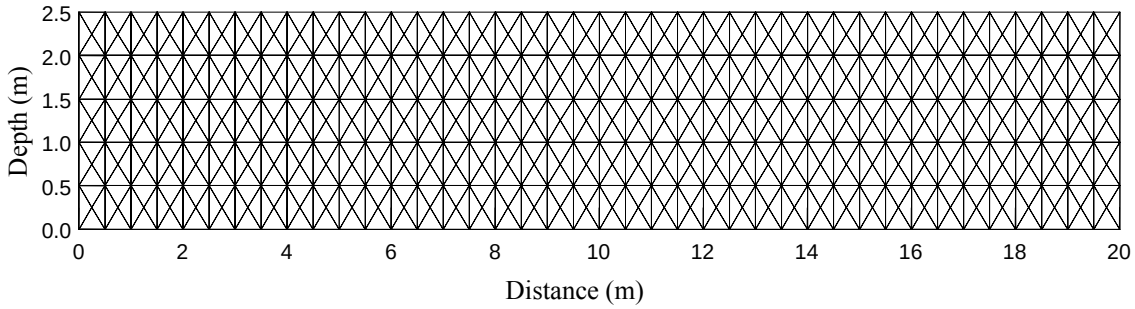

Figure (4.14): Dimension of Finite Element Mesh and Distribution of Elements for Slab on Floor in Regina Clay Case History

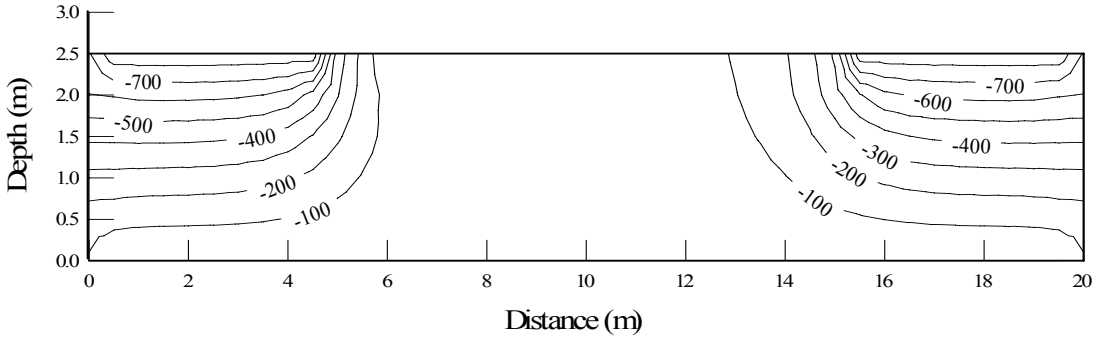

Figure (4.15): Matric Suction Distribution at Steady State Conditions with SEEP/W

The results of the stress-deformation analysis at steady state conditions are shown in Figure (4.16). When analyzing the problem using Modified CRISP for steady state conditions, the results of analysis showed good agreement with the results reported by Fredlund and Hung (2004) for the case of final pore water pressure under the entire slab equal to zero.

It should be noted that the maximum predicted heave at ground surface (94 mm) resulting from steady state condition analysis is greater than that measured at the site (80 mm) and reported by Fredlund and Hung (2004). This because the final soil suction distribution assumed in the field did not reach the steady state conditions as considered in the current analysis.

In general, the results of Modified CRISP are in good agreement with the measured results considering assumptions of the soil properties and the accuracy of the initial suction values.

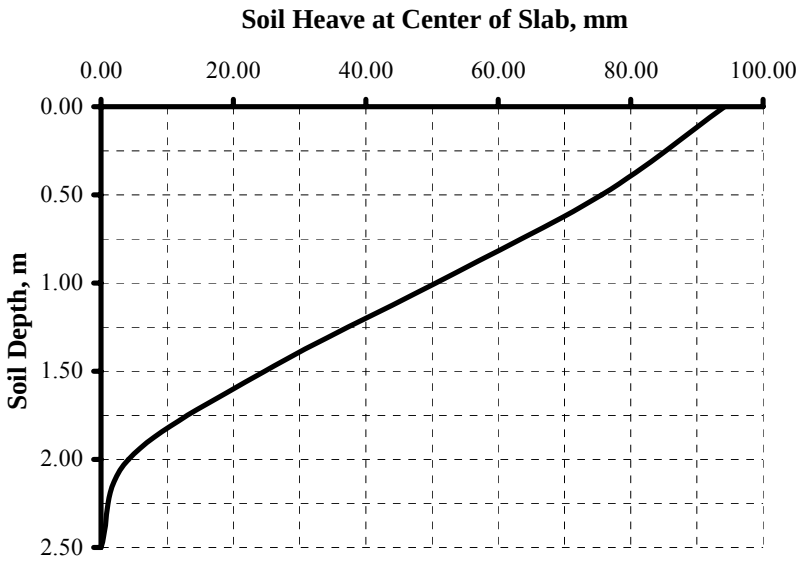

Figure (4.16): Predicted Vertical Displacements with Depth near The Center of Slab at Steady State Conditions (Modified CRISP Program)

4.4 Influence of Trees on Surrounding Soil (Hung, 2003)

Hung (2003) analyzed the influence of a line of trees on the surrounding soil. It was assumed that the trees are planted in a line at every 5 m. In this analysis, a 10 m thick layer of clay soil is considered. The coefficient of permeability of the soil is described using Gardner's (1958) equation with a saturated coefficient of permeability equal to 5.79×10^{-8} m/s (i.e., 5 mm/day), parameters a and n equal to 0.001 and 2, respectively. The initial void ratio of the soil is equal to 1.0, and the volume change index with respect to matric suction, C_m is equal to 0.2.

Hung (2003) proposed that the initial matric suction is taken to be hydrostatic with an unchanged ground water table at the 15 m depth. This represents the water content conditions in soils in the winter when water uptake by the trees is low. It is then assumed that one tree will extract 0.3 m^3 of water per day in summer and the steady state condition is attained (Hung, 2003). The water uptake zone for the trees is from the 1 m to 3 m depth, with uptake rate decreasing linearly with depth.

Deformations in the soil profile due to water uptake by trees from initial to final matric suction state were predicted. The elastic modulus function with respect to matric suction for the soil was computed using a given initial void ratio, e_o, swelling index, C_s, and assumed Poisson's ratio, ν, equal to 0.3. The function can be calculated from Equation (4.4) as follows (Hung, 2003):

$$H = 59.9(u_a - u_w)_{ave} \qquad (4.12)$$

The initial and final matric suction conditions used to predict deformations in the stress-deformation analysis were obtained from the steady state seepage analysis using the coefficient of permeability function shown in Figure (4.17). Boundary conditions for initial matric suction condition, a -15 m total head was specified at the lower boundary and a zero total head was specified at other boundaries. While, for final matric suction conditions, a -15 m total head was specified at the lower boundary, a boundary outflow value was specified along the left side of the soil domain at a depth from 1 m to 3 m and zero total head was specified at other boundaries. The outflow value decreases linearly from 15 mm/day at the 1.0 m depth to zero mm/day at the 3 m depth. This boundary condition represents 0.3 m^3/day of water being extracted by one tree from the soil (i.e., 2 sides x 2 m depth x 5 m wide x 15 mm/day = 0.3 m^3/day).

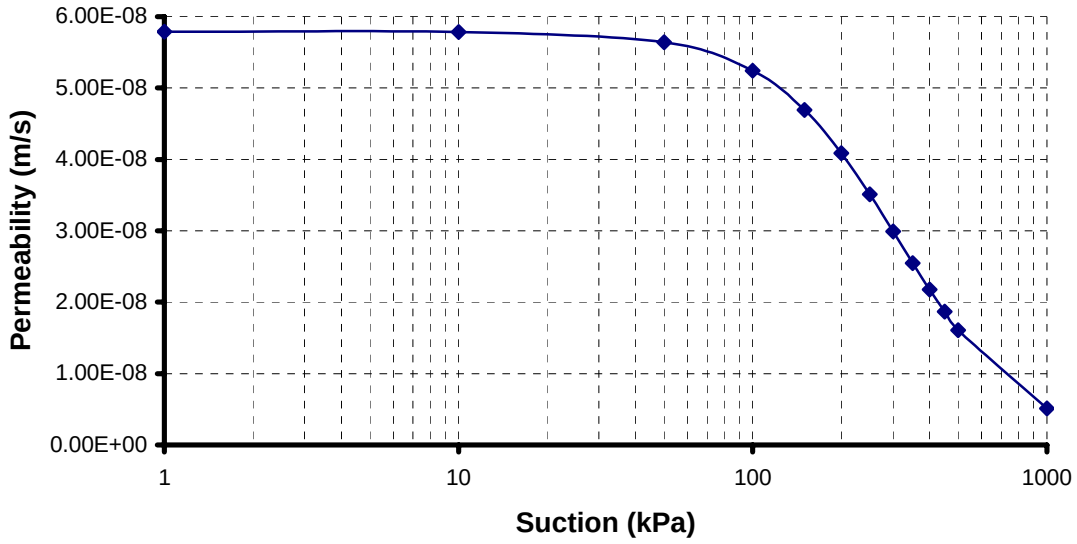

Figure (4.17): Permeability Function of Soil for Influence of Trees Example (Hung, 2002)

The matric suction distribution in the soil at equilibrium is estimated from seepage analysis. The deformations in the soil profile due to water uptake by tree roots were then predicted through the use of the stress-deformation analysis. The boundary condition for the stress-deformation analysis involved free moving of soil in the vertical direction and fixed in horizontal direction at the left and right sides of the domain. The lower boundary was fixed in both directions.

4.4.1 Results of Analysis from Hung (2003)

The final matric suction profiles are shown in Figure (4.18). The ground movements at various depths are shown in Figure (4.19). It can be seen that the movements near the ground surface were quite large within a horizontal distance of about 4 m from the trees. The movements decreased rapidly with distance until at 12 m. The displacements also decreased rapidly with depth. At ground surface, a value of settlement of 85 mm at tree location decreased to 40 mm at 8 m from the trees. At 4 m from the trees, a settlement of 65 mm at ground surface decreased to 40 mm at the 3 m depth, and about 20 mm at the 5 m depth.

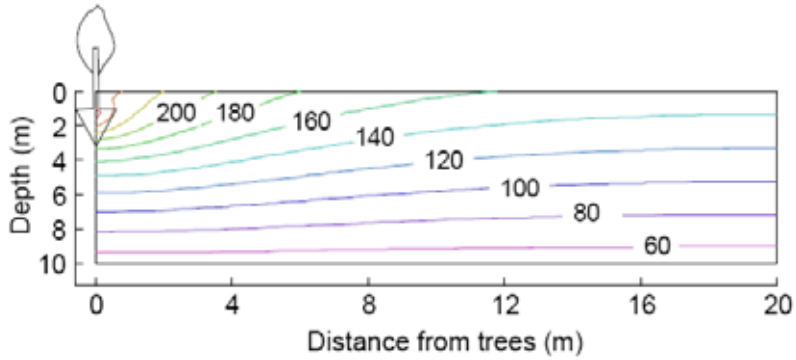

Figure (4.18): Final Matric Suction (kPa) Profile (Hung, 2003)

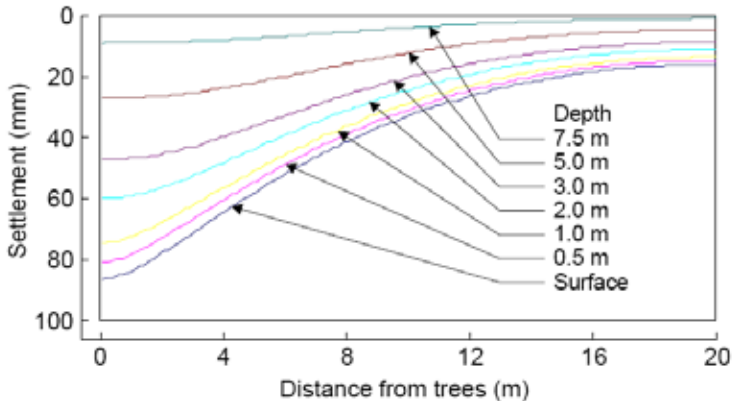

Figure (4.19): Variation of Ground Movements with Depth near a Line of Trees, (Hung, 2003)

4.4.2 Results of Analysis from Modified CRISP

The same problem was analyzed using the SEEP/W program for seepage analysis and modified CRISP for stress-deformation analysis. Dimensions of the finite element mesh and distribution of elements are illustrated in Figure (4.20). Initial soil suction profile is presented in Figure (4.21), while final soil suction profile at steady state conditions is presented in Figure (4.22). Deformations due to trees are introduced in Figure (4.23). Comparison show good agreement of the results from Hung, (2003) and the results from Modified CRISP are similar to a great extent. For example, the displacement at ground surface near the trees root is 85 mm from Modified CRISP and 80 mm from Hung, (2003). Therefore, the Modified CRISP is considered a satisfactory tool for estimating the effect of trees on the surrounding soil and structures.

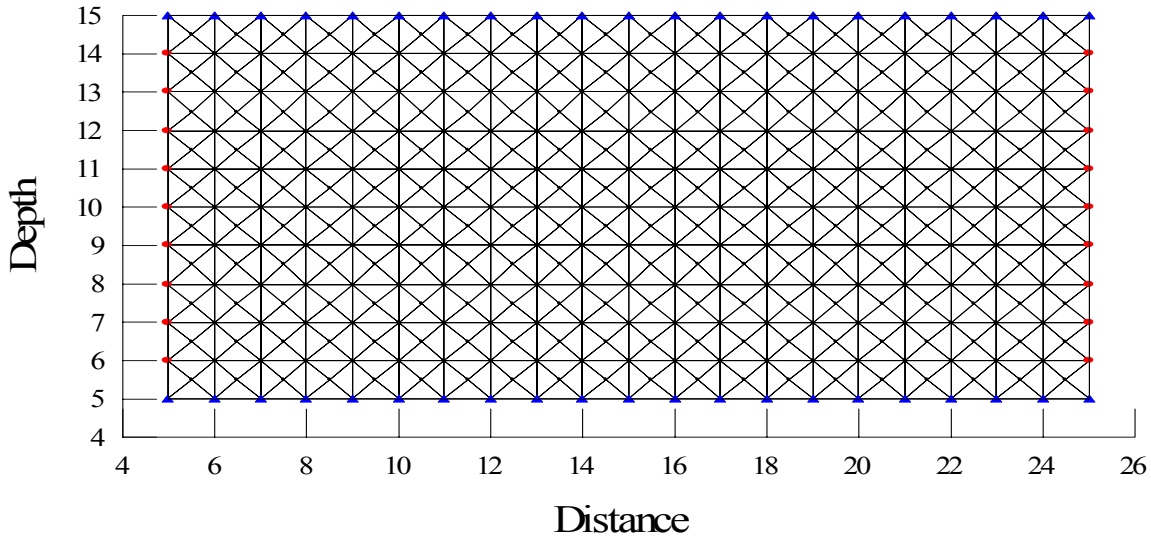

Figure (4.20): Dimension of Finite Element Mesh and Distribution of Elements
Validation Example No. 3

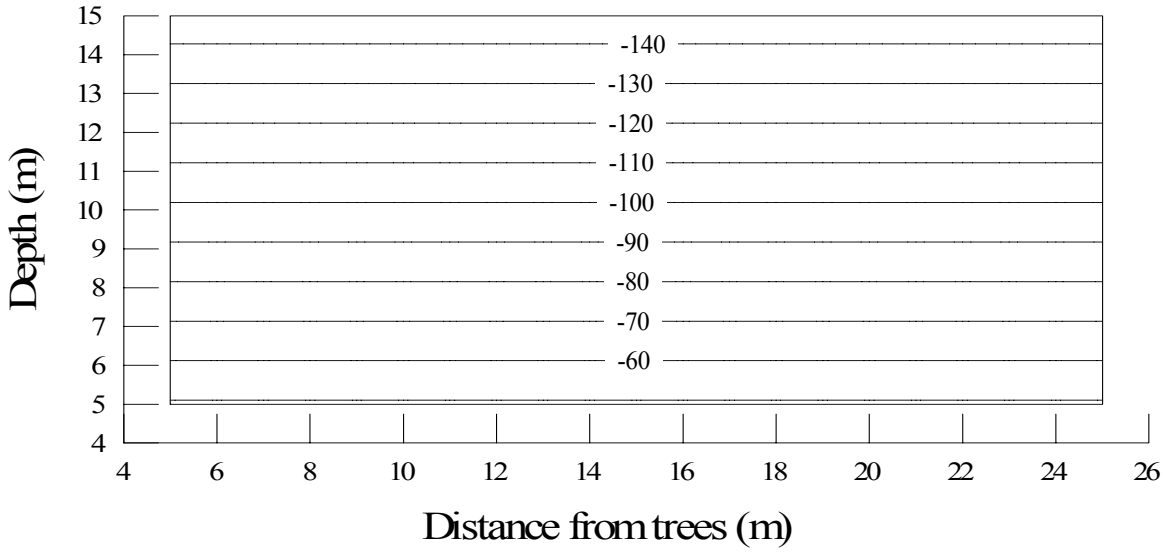

Figure (4.21): Initial Suction Distribution, SEEP/W

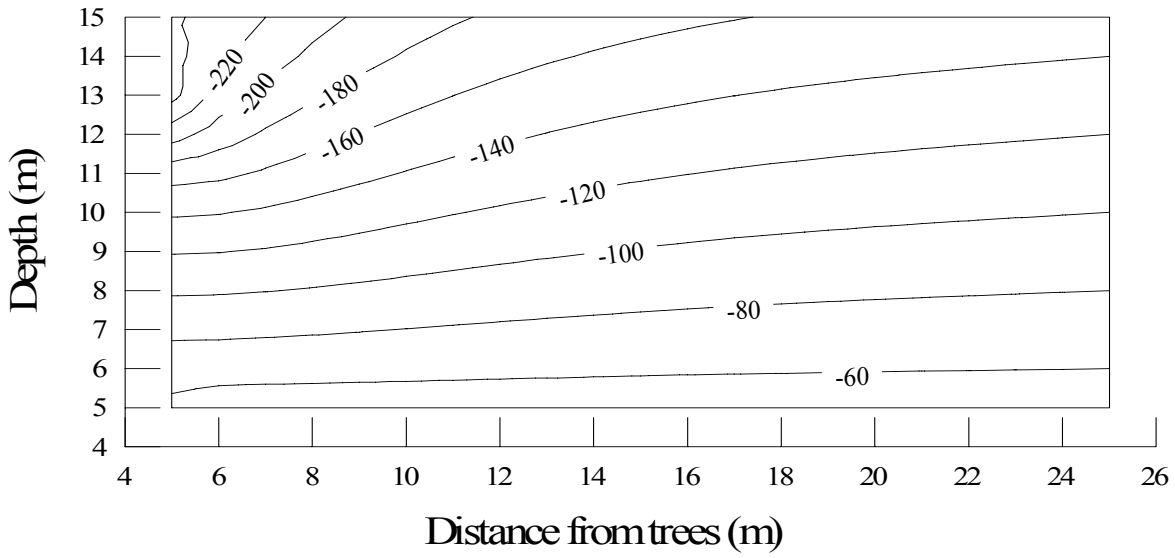

Figure (4.22): Final Suction Distribution near Trees, SEEP/W

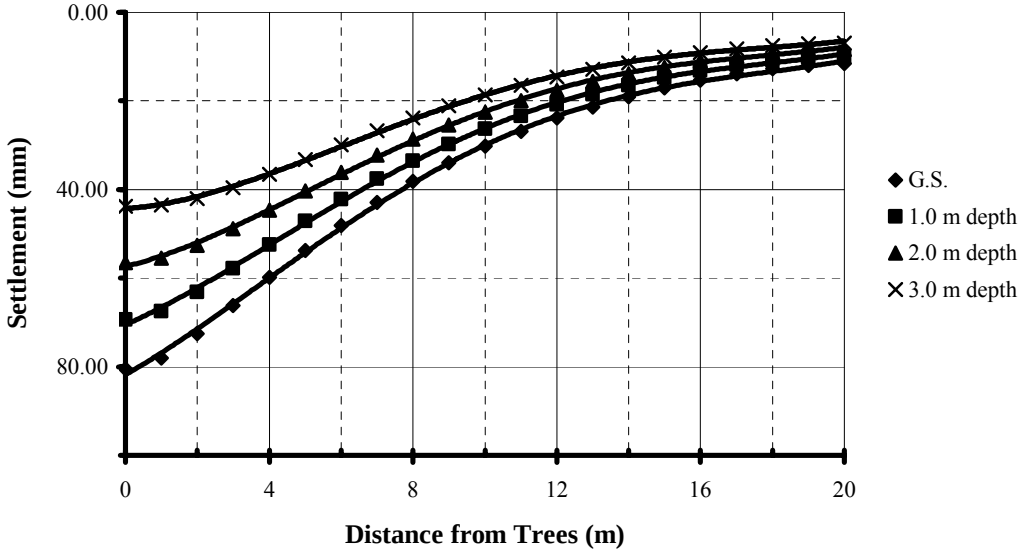

Figure (4.23): Variation of Ground Movements with Depth near a Line of Trees, Modified CRISP Program

4.5 Influence of Ground Surface Flux (Hung, 2003)

This example considers the hypothetical case of a 5- m thick deposit of swelling clay considered by Hung (2003). The surface is assumed partially covered with a flexible cover. Figure (4.24) presents the geometry and key variables for this problem. Experimental data used for this analysis were obtained from tests on compacted specimens of Regina clay (Hung, 2000). Poisson's ratio was assumed to be 0.4. The elasticity parameters (*E, H*) are presented graphically in Figures (4.25) through (4.28)

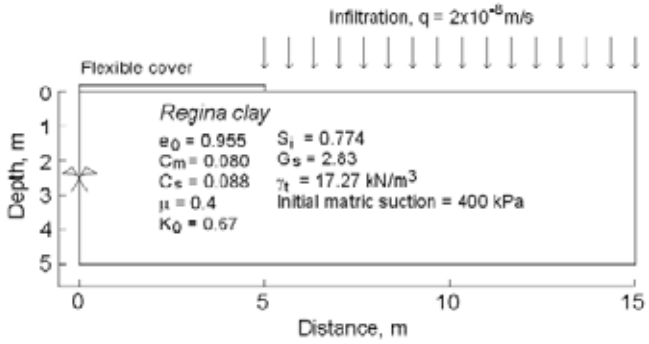

Figure (4.24): Geometry and Key Variable of Soil

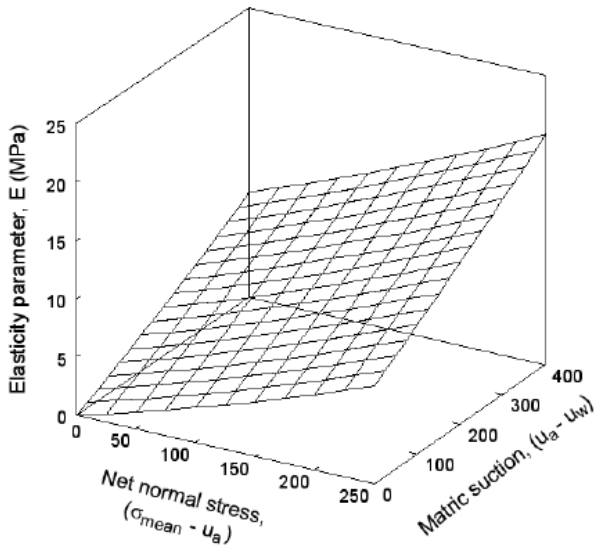

Figure (4.25): Elasticity Parameter for Soil Structure with Change in Net Normal Stress, *E*

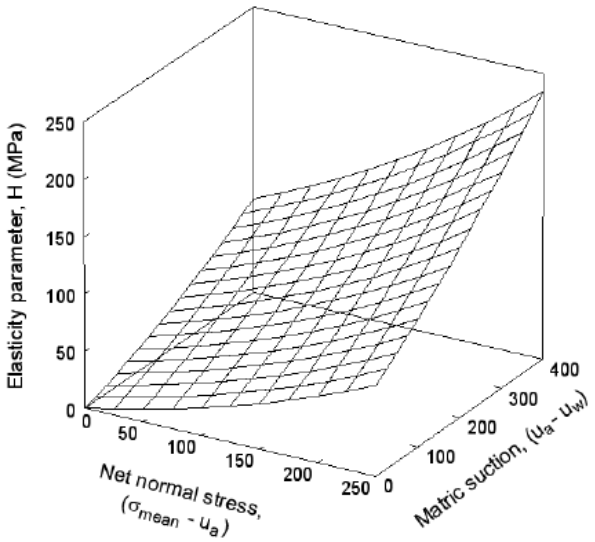

Figure (4.26): Elasticity Parameter for Soil Structure with Change in Soil Suction, *H*

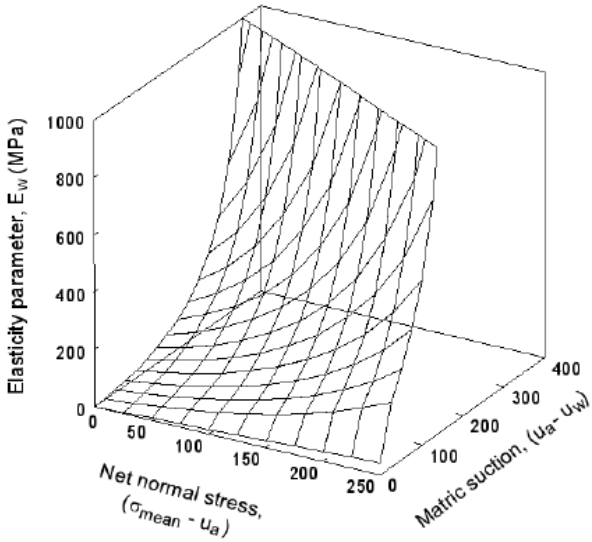

Figure (4.27): Elasticity Parameter for Water Phase with Change in Net Normal Stress, E_w

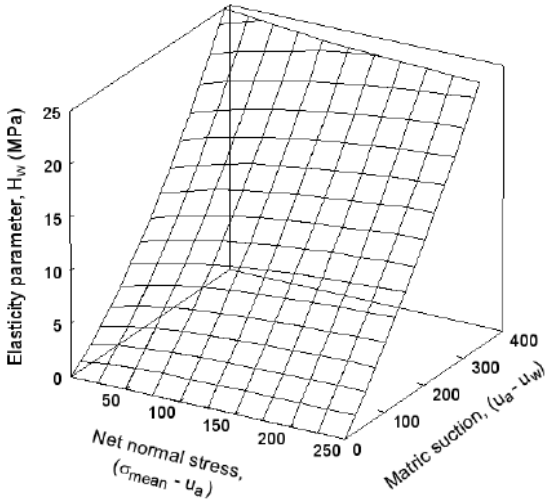

Figure (4.28): Elasticity Parameter for Water Phase with Change in Soil Suction, H_w

The initial matric suction in the soil mass was assumed to be constant and equal to 400 kPa. The coefficient of earth pressure at-rest, K_0, was assumed to be 0.67 for the calculation of initial stress condition. The transient wetting process was introduced by imposing a water infiltration rate equal to $2x10^{-8}$ m/s at the uncovered portion of the ground surface. Such a wetting condition simulates the water infiltration into the soil mass due to the watering of a lawn or a light rain. The analysis is performed to track both the swelling soil behavior and matric suction changes as the transient wetting front advances into the soil mass.

Boundary conditions for this example as assumed by Hung (2003), the left and right sides of the domain were free to move in the vertical direction and fixed in horizontal direction. The lower boundary was considered fixed in both directions.

4.5.1 Results of Analysis from Hung (2003)

Hung, (2003) analyzed the problem with uncoupled and coupled approaches. The uncoupled solutions are obtained through the use of the general partial equation solver, FlexPDE, while coupled solution was performed using COUPSO program. The uncoupled and coupled solutions at day 53 after infiltration begins were used to simulate the effect of infiltration. The comparisons are presented for the distribution of matric suction and vertical displacement in Figures (4.29) and (4.30). Immediately after wetting was introduced into the soil from the uncovered surface, water infiltrated downward and to the left of the soil domain. Matric suction reduced to less than 100 kPa near ground surface. Most of the soil suction changes occurred below the uncovered portion where infiltration took place.

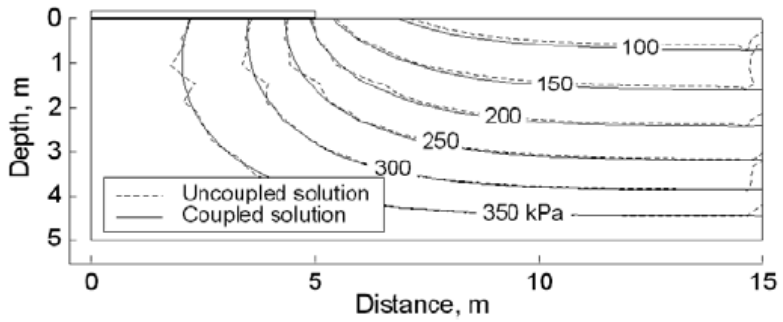

Figure (4.29) Matric Suction Distribution at Day 53 Using Coupled and Uncoupled Approaches (Hung, 2003)

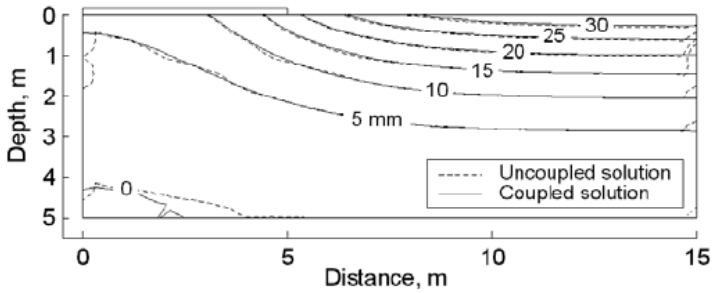

Figure (4.30): Vertical Displacement Distribution at day 53 Using Coupled and Uncoupled Approaches (Hung, 2003)

4.5.2 Results of Analysis from Modified CRISP

The infiltration example was re-analyzed with uncoupled approach using Modified CRISP. The seepage analysis for the infiltration process through unsaturated soil is modeled using SEEP/W program. Then, the final soil suction profiles were used to perform the stress-deformation analysis. Dimensions of finite element mesh and distribution of elements are presented in Figure (4.31). The final soil suction profiles after 53 due to infiltration are introduced in Figure (4.32). The vertical displacement due to wetting from surface infiltration was predicted using modified CRISP program. Total heave due to wetting for 53 days is presented in Figure (4.33).

Results of the analyses appear to be reasonable and consistent with predicted values reported by Hung (2000). It can be noted that heave at the center of flexible cover is about 6 mm from analysis by Hung (2000) and 7.5 mm from analysis using Modified CRISP.

It is possible to use unsaturated soil theory for seepage and stress analysis using Modified CRISP program to study the influence of infiltration conditions on soil heave.

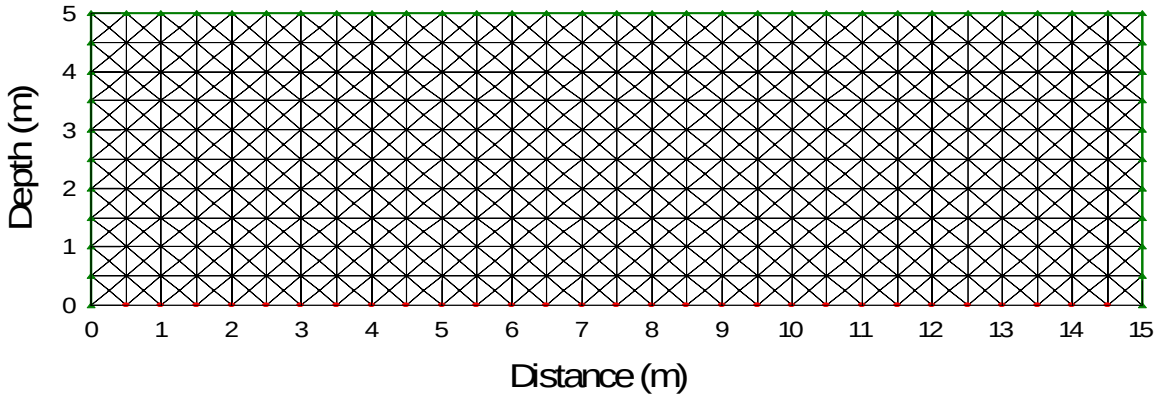

Figure (4.31): Dimension of Finite Element Mesh and Distribution of Elements Validation Example No. 4

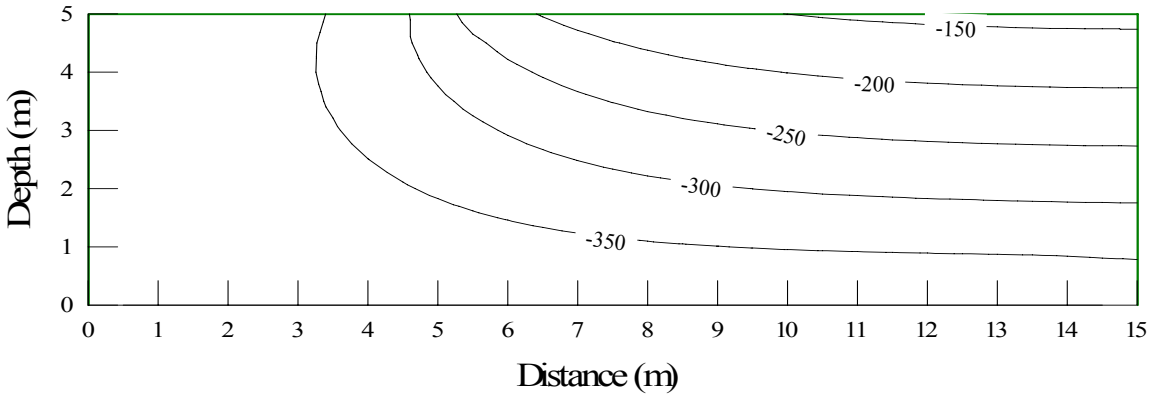

Figure (4.32) Matric Suction Distribution at Day 53 Using SEEP/W Program

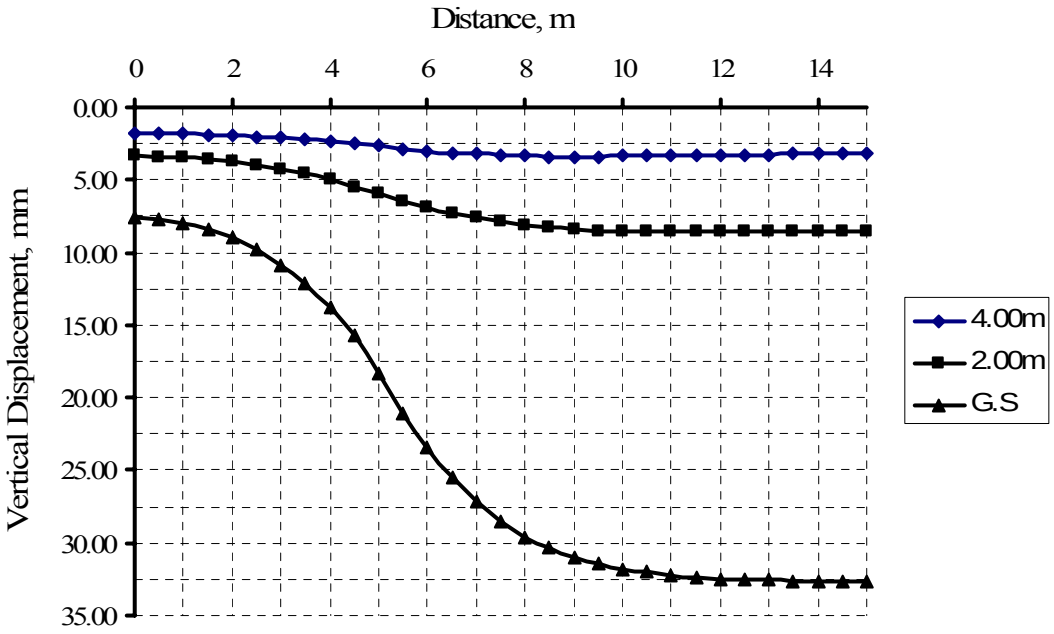

Figure (4.33): Vertical Displacement Distribution at day 53 (Modified CRISP)

CHAPTER (5)
EVALUATION OF HEAVE
DUE TO WATER CONTENT CHANGES

5.1 Introduction

Volume change of expansive soils upon wetting may cause extensive damage to structures, in particular, light buildings and pavements. The changes in water content of soil can originate from the environment or man-made causes.

Changes in water content due to environmental conditions may be attributed to significant variations in climate, such as long droughts and heavy rains. Climate variations cause cyclic water content changes resulting in edge movement of structures. Also, the changes in depth to the water table lead to changes in soil water content.

Man-made construction process leads to changes in water content profiles. Covered areas reduce natural evaporation of moisture from the ground, thereby increasing the soil water content. Inadequate drainage of surface water from the structure leads to ponding and localized increases in soil water content. Defective rain gutters and downspouts contribute to localized increases in soil water content. Seepage into foundation subsoils at soil foundation interfaces and through excavations made for basements or shaft foundations leads to increased soil water content beneath the foundation

Watering of lawns leads to increase in soil water content. Planting and growth of heavy vegetation, such as trees, at distances from the structure less than 1.0 to1.5 times the height of mature trees, aggravates cyclic edge heave. Drying of soil beneath heated areas of the foundation, like furnace rooms, leads to soil shrinkage. Leaking underground water and sewer lines can cause foundation heave and differential movement.

For the purpose of this research, the impact of several water content variation sources on the heave of expansive soils was investigated. Sources of water content variations considered for this research are shown in Figure (5.1). These factors will be analyzed using uncoupled finite element approach implemented in the Modified CRISP program presented in Chapter (3).

For the purpose of this research, soil properties of Regina clay will be adopted for these analyses. Regina clay was selected because of the abundance of data in the literature

regarding the physical and mechanical properties that were evaluated under different stress state variables.

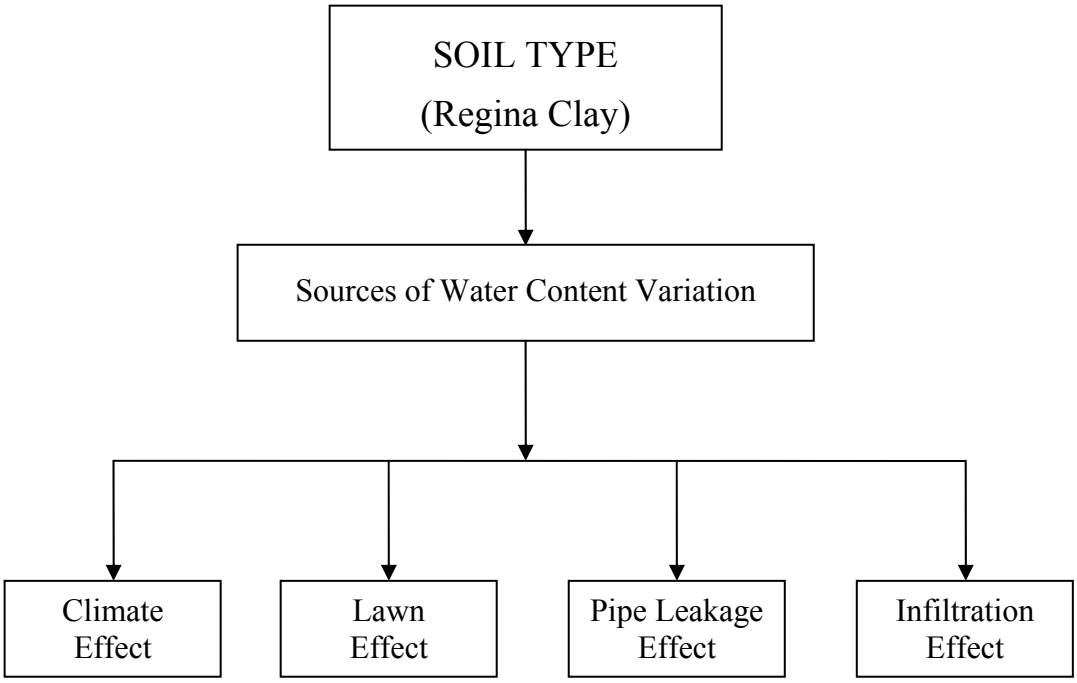

Figure (5.1): Water Content Variation Sources

5.2 Regina Clay Properties

As stated earlier, Regina Clay was considered as the modeling soil for the analyses presented hereinafter. Data on Regina Clay characteristics as provided in the technical literature are summarized herein after.

Regina Clay is classified as highly expansive, post-glacial lake deposit found beneath the city of Regina, Saskatchewan (Shuai, 1996). The unified Classification system places the soil in the class of organic clay with high plasticity. The index properties of soil, together with the mineralogical composition and the cations in the pore-water, are presented in Table (5.1). The particle size distribution curve for the soil is shown in Figure (5.2). The mineralogical composition of clay friction was determined by Krahn and Fredlund (1972) which indicated that the main clay minerals are Ilitte 42% and Montmorillonite 20%. The high content of Montmorillonite is responsible for high swelling potential of Regina clay. The exchangeable cations are mostly calcium (Shuai, 1996).

Table (5.1): Index Properties of Regina Clay (Shuai, 1996)

Location	Regina area - Saskatchewan- Canada
Specific gravity	2.83
Atterberg limits	Liquid Limit, W_L = 69.9% Plastic Limit, W_p = 31.9% Plasticity Index, I_p = 38.0%
Grain size Distribution	Sand = 2.2% Silt = 32.9% Clay = 64.0%
Unified Soil Classification system	CH – Inorganic clay of high plasticity
Standard Compaction	Maximum dry unit weight = 1.640 t/m^3 Optimum Moisture Content = 28.5 %
Mineralogical Composition (X-ray diffraction)	Montmorillonite 20% Illite 42% Kaolinite 14% Mixed mineral layer 24%
Cations in pore water (Milliequivalents/100 grams dry soil)	Sodium 1.05 Calcium 3.16 Magnesium 1.66 Potassium 0.33

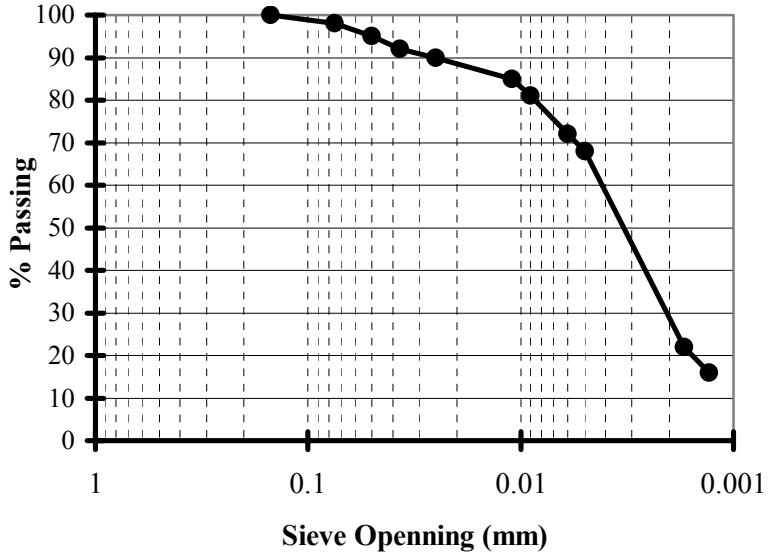

Figure (5.2) Particle size Distribution Curve for Regina Clay (Shuai, 1996)

Soil water characteristic curve of Regina clay was presented by Fredlund and Hung, (2004). Fredlund and Hung, (2004) used the Fredlund and Xing equation to fit the volumetric water content versus soil suction data. Constants of equations are θ_{sat}=49.3%, a = 300kPa, n_f = 0.60, and m_f = 0.70. Figure (5.3) presents the fitted soil water characteristic curve for Regina clay

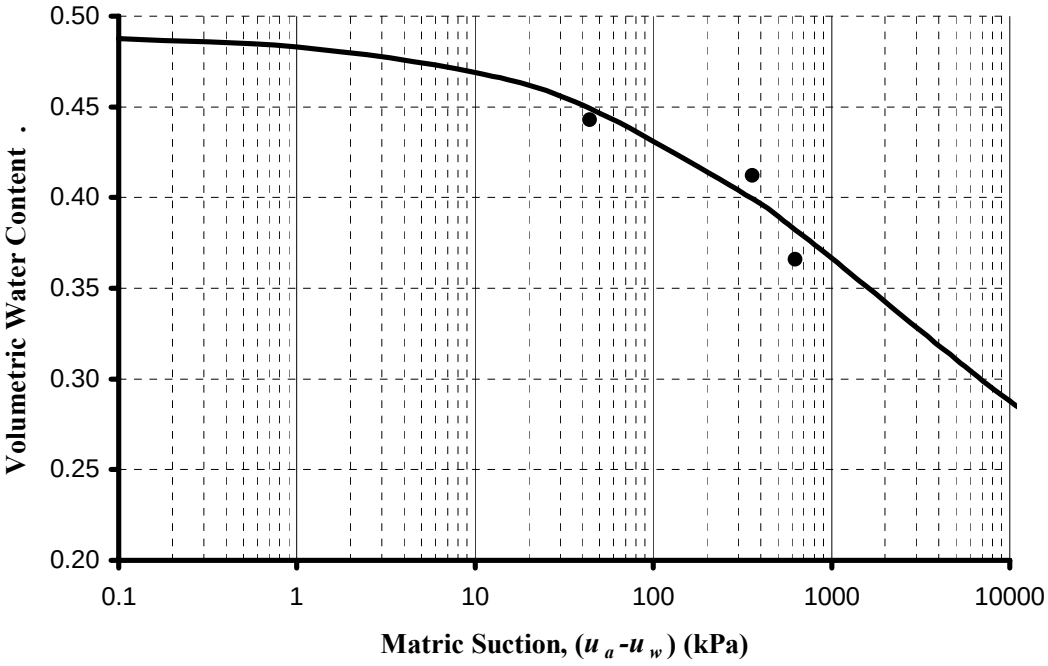

Figure (5.3): Soil Water Characteristic Curve Relationship for Regina Clay

A coefficient of permeability function (i.e., variation of coefficient of permeability with soil suction) for compacted Regina clay (Shuai, 1996) is considered as integral input to the analysis of this study. The coefficient of permeability function was derived using Leong and Rahardjo (1997) equation and presented graphically in Figure (5.4)

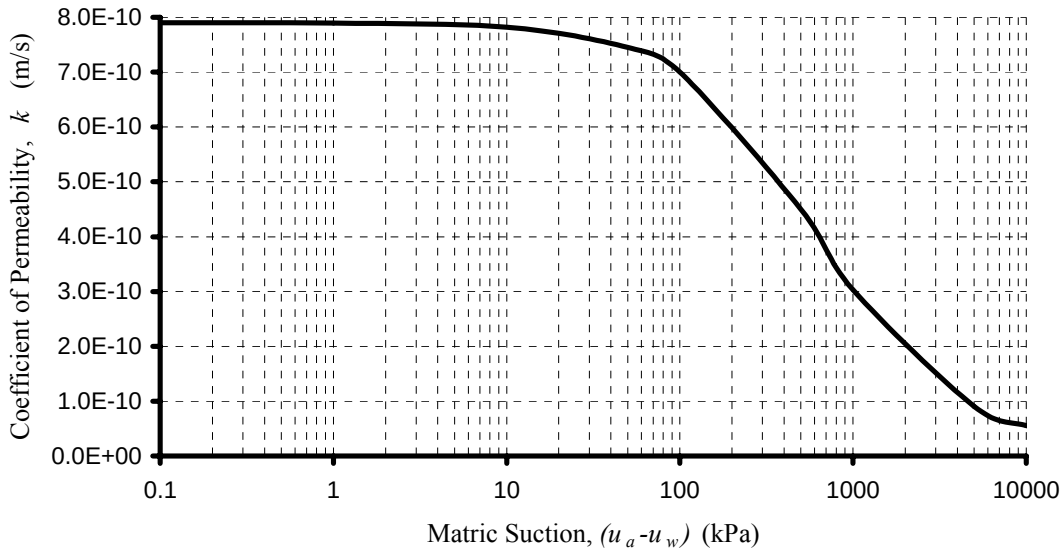

Figure (5.4): Coefficient of Permeability Function for Regina Clay

Lytton (1994) presented typical values for coefficients of at rest earth pressure, K_o, that were back calculated from field observations of heave and shrinkage for unsaturated expansive soils as shown in Equation (5.1).

$$K_o = \begin{cases} 0 & \text{Soil is dry and cracked} \\ 0.333 & \text{Soil is dry and cracks are opening} \\ 0.500 & \text{Cracks are closed and suction is at a steady state condition} \\ 0.667 & \text{Cracks are closed and soil is wetting} \\ 1 & \text{Soil is wetting and is in hydrostatic stress conditions} \\ 2\text{-}3 & \text{Soil is approaching passive earth pressure} \end{cases} \qquad (5.1)$$

A coefficient of earth pressure equal to 0.667 was considered by Fredlund and Hung, (2004) for Regina Clay. A Poisson's ratio, ν, equal to 0.40 was suggested by Fredlund and Hung, (2004) from K_o using the following equation:

$$\nu = \frac{K_o}{1 + K_o} \qquad (5.2)$$

The elasticity parameter function with respect to changes in normal stress, *E*, for Regina clay may presented by equation (5.3) according to Fredlund and Hung, (2004).

$$E = 28.11(\sigma_{av} - u_a) \tag{5.3}$$

The elasticity parameter function with respect to changes in soil suction, *H*, for Regina clay was presented by equation (5.4) according to Fredlund and Hung, (2004).

$$H = 140.5(u_a - u_w) \tag{5.4}$$

Properties that have been presented in the literature for Regina clay and used in this research are summarized in Table (5.2).

Table (5.2): Mechanical and Physical Properties of Regina Clay

No.	Properties	Symbol	value	units
1	Unit weight	γ_b	18.88	kN/m^3
2	At rest earth pressure coefficient	K_o	0.67	-
3	Poisson's ratio	ν	0.40	-
4	The elasticity parameter function with respect to changes in normal stress	E	$28.11(\sigma_{av} - u_a)$	kN/m^2
5	The elasticity parameter function with respect to changes in normal stress	H	$140.5(u_a - u_w)$	kN/m^2
6	Soil water characteristic curve function	$SWCC$	$\theta = \frac{49.30}{\left[\ln\left(e + (\frac{\psi}{300})^{0.6}\right)\right]^{0.7}}$	%
7	Permeability function	k	$k = \frac{7.9*10^{-10}}{\left[\ln\left(e + (\frac{\psi}{553.5})^{1.09}\right)\right]^{2.25}}$	m/s

As described in Chapter (3), uncoupled analysis of expansive soil behavior due to different water variation effects was performed in two stages, namely, seepage analysis and stress-deformation analysis. Seepage analysis requires the initial soil suction profiles, the permeability function, *k* and soil water characteristic curve (SWCC). Stress-deformation analysis requires the elasticity parameters with respect to change of net normal stress, *E*,

elasticity parameter with respect to change of soil suction, H, and passion's ratio, ν. For the cases where, final soil suction profile and active zone depth are obtained using field measurements, seepage analysis for estimation of final soil suction is not required.

5.3 Active Zone

Adequate design of foundations on expansive soil must consider the maximum amount of heave that may occur during the lifetime of the structure. Prediction of the maximum heave requires that the largest zone of expansive soil that can be wetted be defined, variations of expansive soil properties in that zone must be determined, and the greatest heave potential of that zone must be predicted. Active zone is that zone of soil that is contributing to heave due to soil expansion at any particular time. The active zone will normally vary with time.

If the ground water level is shallow, the depth of active zone, Z_a, may be assumed equal to the depth of water table for ground water levels less than 6.00 m in clay soil. The pore water pressure at ground water table is assumed to be zero. If the ground water level is deep, the depth of active zone, Z_a, may be determined by field measurements of soil suction. If depths to groundwater exceed 6.00 m beneath the foundation and no other information is available, the depth of active zone can be assumed to be 6.00 m for dry profiles below the base of foundation. However, the depth should not be estimated less than three times the width of foundation (TM 5-818-7, 1983).

The pore water pressure or soil suction change is often approximately constant with increasing depth below active zone depth. Sometimes active zone depth can be estimated as the depth below which the water content/plastic limit ratio or soil suction is constant. If the soil suction is not approximately constant with increasing depth below depths of 3.50 to 6.00m, the active zone depth may be approximated by being set to a depth 0.35 to 0.75m below the first major change in the magnitude of the soil suction (TM 5-818-7, 1983).

Lytton (1995) provided several profiles of field suction measurements and estimated the depths of moisture active zone where total suction reaches equilibrium suction level or there is an inferred presence of a water table.

5.4 Soil Suction Profiles

The magnitude of swelling of expansive clay depends on the magnitude of change from the initial to the equilibrium or final suction profile that will be observed to take place in the active zone of expansive soils.

The vertical distribution of matric suction in a horizontally layered unsaturated soil generally depends on several factors: in particular, the soil properties as given by the soil water characteristic curve (SWCC) and the soil permeability function, environmental factors including precipitation or evaporation rates, and boundary drainage conditions including the location of the water table. The combination of these factors results in different suction profiles as shown in Figure (5.5).

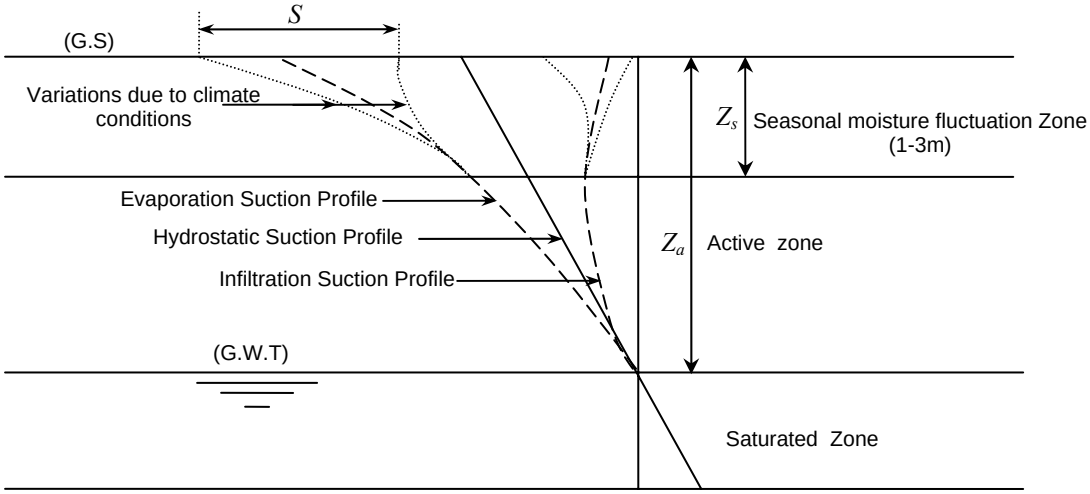

Figure (5.5): Change in Soil suction profiles due to Environmental Conditions

Initial suction profile may be assumed as suction increases with increase in vertical distance above the groundwater level in proportion to the unit weight of water. If shallow water table does not exist, suction profile also becomes more negative with increasing vertical distance above the bottom boundary of active zone in proportion to the weight of water.

The final suction profile can be estimated either analytically using a moisture diffusion analysis for steady-state flow or by field measurements. In absence of field or analytical data, Fredlund and Rahardjo (1993) proposed that there are three possibilities for the estimation of final pore-water pressure conditions, first, it can be assumed that the water table will rise to the ground surface, creating a hydrostatic condition. This assumption predicts the greatest amount of total heave. Second, it can be assumed that the

pore-water pressure approaches a zero value throughout its depth. This may appear to be a realistic assumption; however, it should be noted that it is not an equilibrium condition. In many situations, this assumption may provide a suitable estimate for the final pore-water pressure state. Third, it can be assumed that under long-term equilibrium conditions, the pore-water pressure will remain slightly negative. This assumption predicts the smallest amount of total heave. It is also possible to have variations of the above assumptions with depth (Fredlund and Rahardjo, 1993).

5.5 Climate Conditions Effect

Amount and variation of precipitation and evaporation greatly influence the moisture availability and depth of seasonal moisture fluctuation zone, Z_s. Greatest seasonal suction variation occurs in arid or semi-arid climates that have pronounced and short wet periods.

Many researchers stated that matric suction profile within the seasonal moisture fluctuation zone could be important to the stability of many shallow geotechnical structures (Rahardjo and Leong, 1997; Totoev and Kleeman, 1998; Fredlund et al., 2001).

5.5.1 Depth of Seasonal Moisture Fluctuation Zone, Z_s

The depth of seasonal moisture fluctuation, Z_s, is defined as the least soil depth near the surface in which the water content varies due to climate after construction of foundation as shown in Figure (5.5). The depth of this zone would be less than or equal to the depth of active zone, Z_a. The deeper seasonal moisture fluctuation zone is, the larger the region over which soil expansion can occur and thus the larger the potential for heave due to soil expansion.

The depth of seasonal moisture fluctuation zone is related to the climate and clay soil properties. When a marked separation occurred between wet and dry seasons, a large seasonal variation in soil moisture content occurred, a large seasonal moisture fluctuation zone depth is expected, whereas in areas which were either predominantly dry or predominantly wet for most part of the year, the changes in soil moisture content is not so marked (Mitchell, 1979).

Fityus et al. (1998) have proposed that the Thornthwaite Moisture Index (TMI) can be used to determine the depth of seasonal moisture fluctuation, Z_s, for the purpose of site

classification. The proposed correlation between TMI and depth of seasonal moisture fluctuation zone is shown in Table (5.3).

Seasonal moisture fluctuation zone depth can be inferred from the suction measurements using psychrometers in the field or using laboratory tests. Mitchell (1979) presented several field suction profiles measured in the area of Adelaide, South Australia (Mediterranean Climate) with the depth seasonal moisture fluctuation zone close to 1.5-2.5m.

Table (5.3): Depth of Seasonal Moisture Fluctuation Zone based on TMI Values (Fityus et al., 1998)

Climate classification	Thornthwaite Moisture Index, TMI	Depth of seasonal moisture fluctuation, (m)
Wet (Coastal/Alpine)	>40	1.50
Wet temperate	10 to 40	1.80 to 1.50
Temperate	-5 to 10	2.30 to 1.80
Dry temperate	-25 to -5	3.0 to 2.30
Semi-arid	< -25	3.0

5.5.2 Soil Suction Change at Ground Surface, *S*

Variations in climate conditions produce changes in the pore-water pressure or suction distribution, which in turn result in shrinking and swelling of the soil deposit. The pore water pressure distribution with depth can take a wide variety of shapes as a result of climate changes as shown in Figure (5.5)

An idealized soil suction profile in a uniform soil at an undeveloped site in a dry climate is shown by evaporation suction profile in Figure (5.5). Below the depth of active zone, Z_a, equilibrium water content exists and above it, the water content decreases due to water losses from the ground surface, usually evapo-transpiration. If a cover is placed on the ground surface that is large enough that edge effects can be neglected, surface water losses are eliminated, and the suction profile will come into equilibrium with the environment, for example, by infiltration suction profile as shown in Figure (5.5). If the ground surface is subjected to temperature fluctuations such as due to summer and winter climates, suction in this zone affected by temperature changes will fluctuate about infiltration suction profile.

The Australian standards (AS 2870) estimated the soil moisture conditions in terms of soil suction, (u_a-u_w) with units of pF. When a soil is saturated, it has a relatively low suction value of 3.2 pF (158kPa) or less which increases to 4.2 pF (1585kPa) when soil dries to the wilting point of vegetation. Recommended soil suction change values at ground surface and depth of seasonal moisture fluctuation zone, Z_s, for various locations in Australia are given in Table (5.4). The change in suction profile is assumed to decrease linearly with increasing depth below ground surface and becoming zero at end of seasonal moisture fluctuation zone, Z_s.

Table (5.4): Soil Suction Change Profiles for Various Locations in Australia (AS 2870)

Location	Change in soil suction at The soil surface, S (pF)	Depth of seasonal moisture fluctuation, Z_s (m)
Adelaide	1.20	4.0
Albury/Wodonga	1.20	3.0
Brisbane/Ipswich	1.20	1.50 to 2.30
Hobart	1.50	2.0
Hunter Valley	1.50	2.0
Newcastle/Gosford	1.50	1.50
Sydney	1.50	1.50

There are no measurements for seasonal moisture fluctuation zone or soil suction profiles in Egypt. Thus, the suction profile used here will be estimated from data available in the literature. Figure (5.6) presents different parameters used in the analysis of the effect of climate variations on footing heave. In this analysis, the seasonal moisture fluctuation zone depth, Z_s, is selected 1.0, 2.0, 3.00 m based on values reported in the technical literature. The suction change at ground surface varied as 1.0, 1.20, 1.50 pF. The final soil suction is assumed to be hydrostatic with soil suction value of 3.2 pF (150kPa) at ground surface which simulates wet conditions in winter and infiltration suction profile as illustrated before in Figure (5.5). The initial soil suction is estimated by subtracting the soil suction change from final soil suction. The idealized profiles used in analysis of climate effect through this research are shown in Figure (5.7).

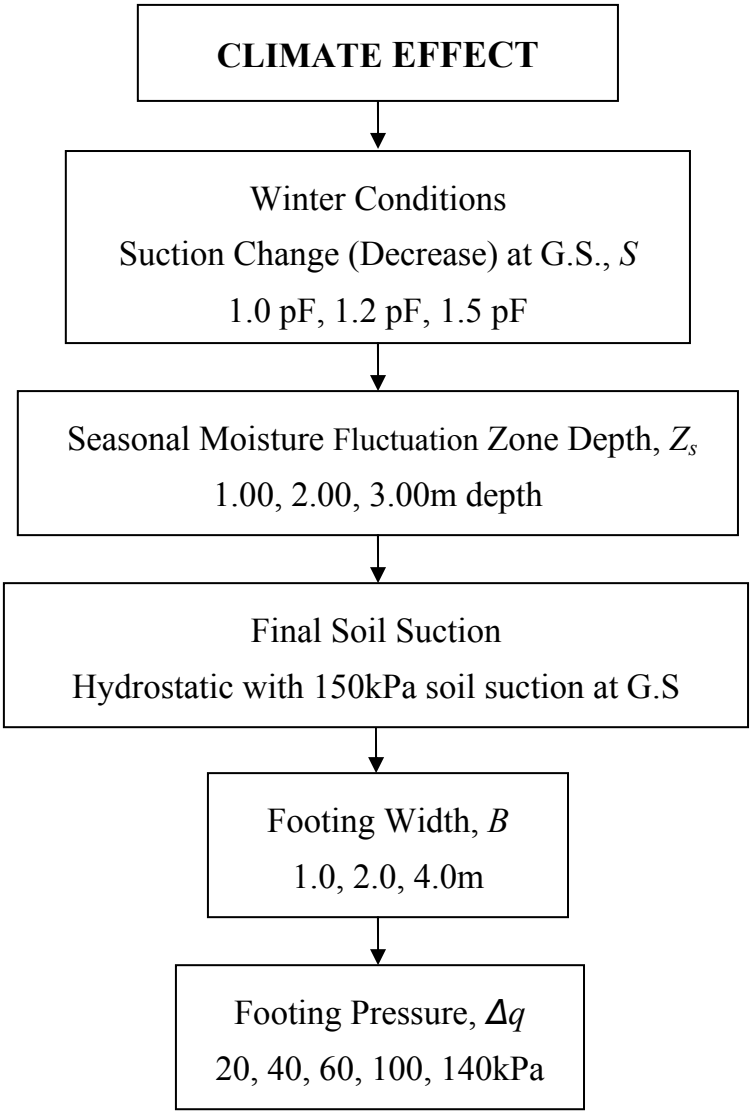

Figure (5.6): Parameters of Climate Effect Study

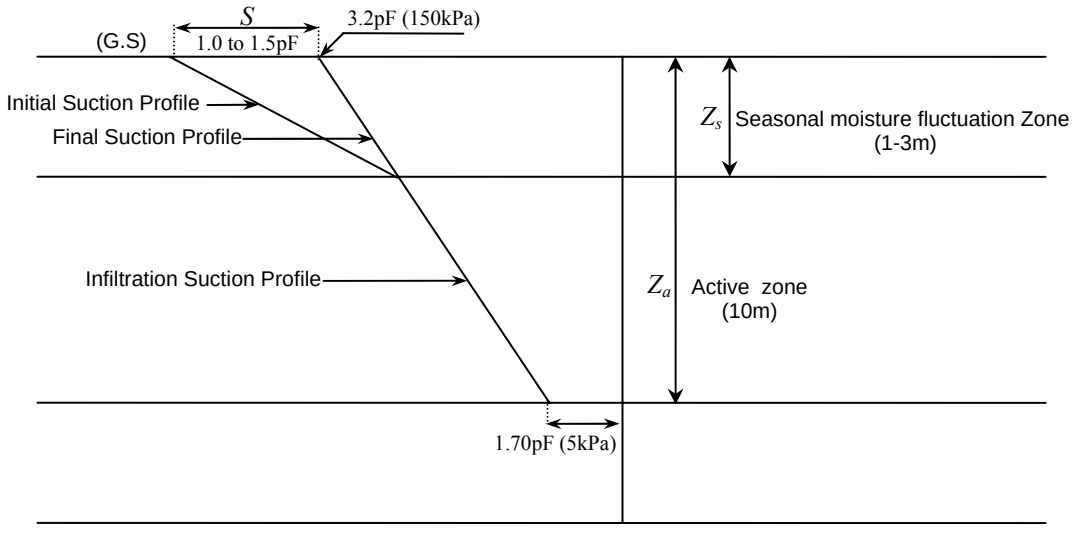

Figure (5.7): The Idealized Profiles Used in Analysis

5.5.3 Results of Climate Conditions Effect

Results of analysis for the effect of climate conditions parameters such as, depth of seasonal moisture fluctuation zone, Z_s, and suction change at ground surface, $S_,$ on the heave of shallow foundation are presented in Tables from (5.4) to (5.6). In addition, the effect of footing width and footing pressures were investigated. Table (5.5) summarizes the results for heave under different footing pressures, footing widths and different soil suction change in case of 1.00 m seasonal moisture fluctuation zone depth. Similarly, Tables (5.6) and (5.7) presented the results for 2.00 m and 3.00 m seasonal moisture fluctuation zone depth respectively.

Table (5.5): Footing Heave for 1.00 m Depth Seasonal Moisture Fluctuation Zone

Footing width, B (m)	1.00			2.00			4.00		
Suction Change at G.S., (pF) / Footing Pressure, Δq (kPa)	1.0	1.2	1.5	1.0	1.2	1.5	1.0	1.2	1.5
0.0	26.37	32.86	42.94	26.37	32.86	42.94	26.37	32.86	42.94
20	24	30.09	39.62	24.54	30.67	40.25	24.95	31.11	40.71
40	23.02	28.89	38.13	24.13	30.14	39.53	24.82	30.94	40.44
60	22.48	28.23	37.27	23.98	29.93	39.22	24.8	30.95	40.46
100	21.89	27.49	36.3	23.51	29.38	38.73	24.14	30.08	39.58
140	21.48	27.01	35.72	22.54	28.33	37.48	22.75	28.68	38.10

Table (5.6): Footing Heave for 2.00 m Depth Seasonal Moisture Fluctuation Zone

Footing width, *B* (m)	1.00			2.00			4.00		
Suction Change at G.S., (pF) / Footing Pressure, Δq (kPa)	1.0	1.2	1.5	1.0	1.2	1.5	1.0	1.2	1.5
0.0	53.42	66.46	86.63	53.42	66.46	86.63	53.42	66.46	86.63
20	50.26	62.82	82.37	50.24	62.77	82.29	50.74	63.32	82.89
40	48.66	60.91	80.04	48.92	61.17	80.28	49.81	62.19	81.46
60	47.64	59.68	78.5	48.12	60.18	79	49.29	61.53	80.55
100	46.35	58.09	76.46	46.76	58.54	77.19	47.27	59.03	78.01
140	45.45	57.04	75.11	44.9	56.37	74.71	44.61	56.16	74.51

Table (5.7): Footing Heave for 3.00 m Depth Seasonal Moisture Fluctuation Zone

Footing width, *B* (m)	1.00			2.00			4.00		
Suction Change at G.S., (pF) / Footing Pressure, Δq (kPa)	1.0	1.2	1.5	1.0	1.2	1.5	1.0	1.2	1.5
0.0	81.35	101.04	131.36	81.35	101.04	131.36	81.35	101.04	131.36
20	77.83	97.02	126.67	77.51	96.64	126.2	77.86	97.01	126.54
40	75.89	94.73	123.9	75.63	94.38	123.39	76.21	94.95	123.93
60	74.56	93.15	121.91	74.33	92.76	121.32	74.86	91.01	121.85
100	72.73	90.88	119.02	71.94	89.89	118.04	71.21	88.91	117.43
140	71.3	89.17	116.85	69.09	86.52	114.4	67.23	84.56	112.00

5.5.4 Analysis of Results for Climate Conditions

The effect of each parameter of climate conditions is investigated and analyzed to estimate its significance on footing heave. The relationships between heave at mid point of footing and climate parameters are presented graphically to predict the order of these relationships.

As will be stated later, the results indicate that the climate condition parameters (i.e. soil suction change at ground surface, S, and seasonal moisture fluctuation zone depth, Z_s) have a significant effect on the footing heave. However, the footing width, B, and footing pressures, Δq, have a less significant effect on footing heave than the climate parameters.

5.5.4.1 Effect of Seasonal Moisture Fluctuation Zone Depth, Z_s

Figure (5.8) presents the effect of seasonal moisture fluctuation zone depth on footing heave under zero pressures. Seasonal moisture fluctuation zone depth, Z_s, has a significant effect on footing heave. Increase in seasonal moisture fluctuation zone depth leads to increase of heave. In addition, the relationship between seasonal moisture fluctuation zone depth and footing heave is linear. Slope of linear relationship increases with increase of the soil suction change at ground surface, S. It may be noted that slope of relationship for 1.50 pF soil suction at ground surface is one and half times slope of relationship for 1.00 pF.

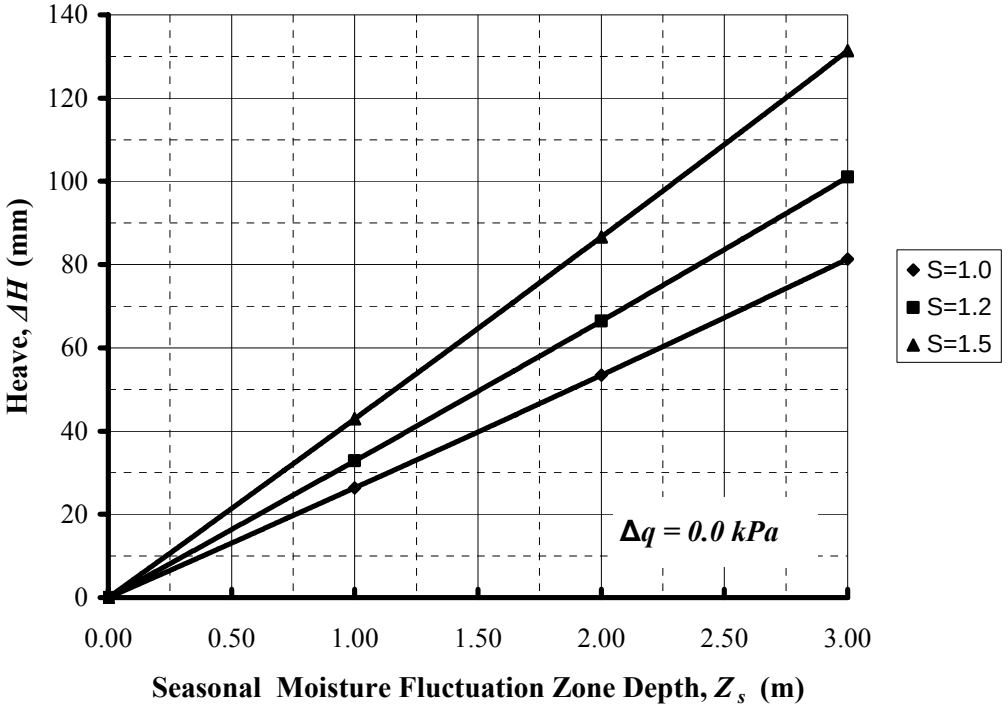

Figure (5.8): Effect of Seasonal Moisture Fluctuation Zone Depth, Z_s, on Footing Heave under Zero Applied Pressures

Figures (5.9) and (5.10) illustrate the effect of seasonal moisture fluctuation zone depth on footing heave under 60 kPa and 100 kPa footing pressures; respectively and for 2.00m footing width. The relationship between seasonal moisture fluctuation zone depth and heave of the mid point of footing is linear. Slope of linear relationship increases with increasing of soil suction change at ground surface. Furthermore, the slope decreases with increase of footing pressure for the same soil suction change at ground surface.

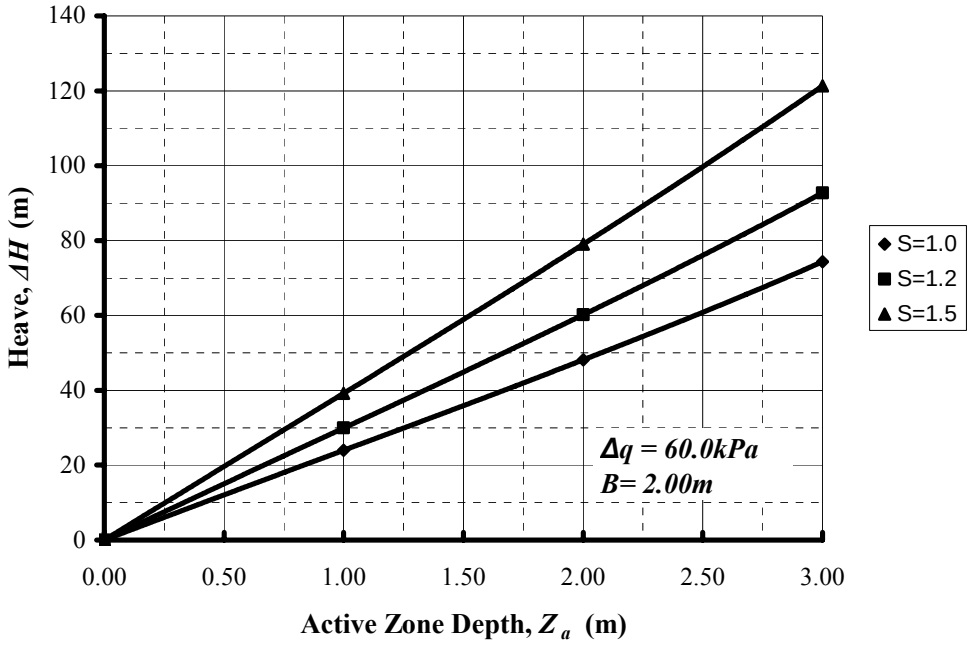

Figure (5.9): Effect of Seasonal Moisture Fluctuation Zone Depth, Z_s, on Footing Heave under 60 kPa Footing Pressure for 2.0 m Footing Width

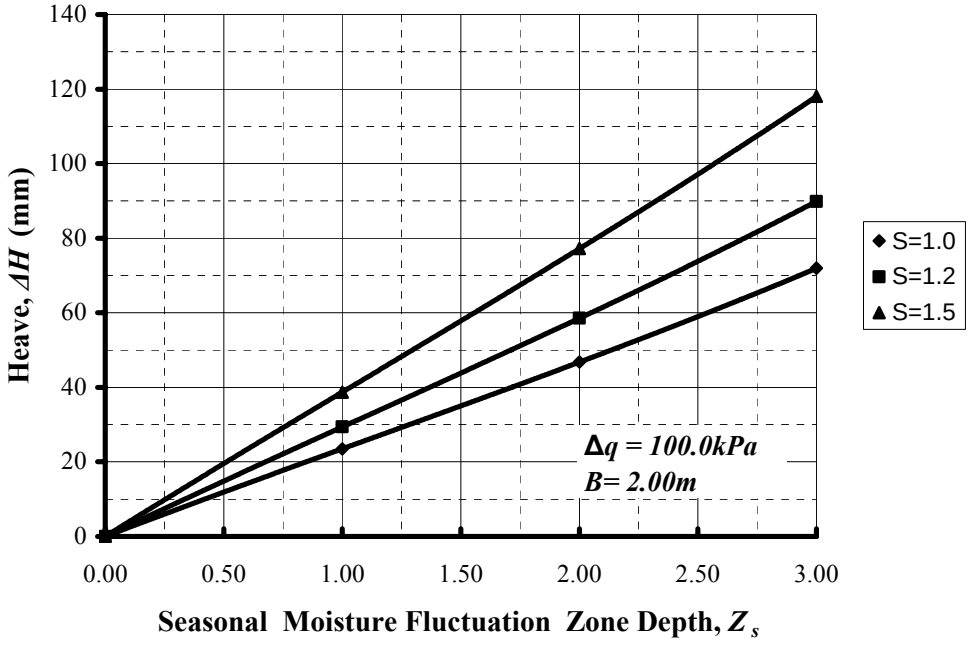

Figure (5.10): Effect of Seasonal Moisture Fluctuation Zone Depth, Z_s on Footing Heave under 100 kPa Footing Pressure for 2.0 m Footing Width

5.5.4.2 Effect Soil Suction Change at Ground Surface, *S*

Figure (5.11) presents the effect of soil suction change at ground surface on footing heave under zero pressure. According to the results shown in the figure, soil suction change at ground surface, *S*, has a significant effect on the heave of soil. Increase in soil suction change by 20% leads to increase of heave by 25% for 1.0 m seasonal moisture fluctuation depth under zero footing pressure. In addition, the relationship between Soil suction change at ground surface and footing heave is linear.

Under different footing pressures, Figure (5.12) and (5.13) presents the effect of soil suction change at ground surface on footing heave for 60 and 100 kPa footing pressure; respectively. The relationship between soil suction change at ground surface and footing heave is linear under different footing pressures. The slope of linear relationship is almost equal for different footing widths. Also, the effect of soil suction change on footing heave is slightly influenced by footing pressure.

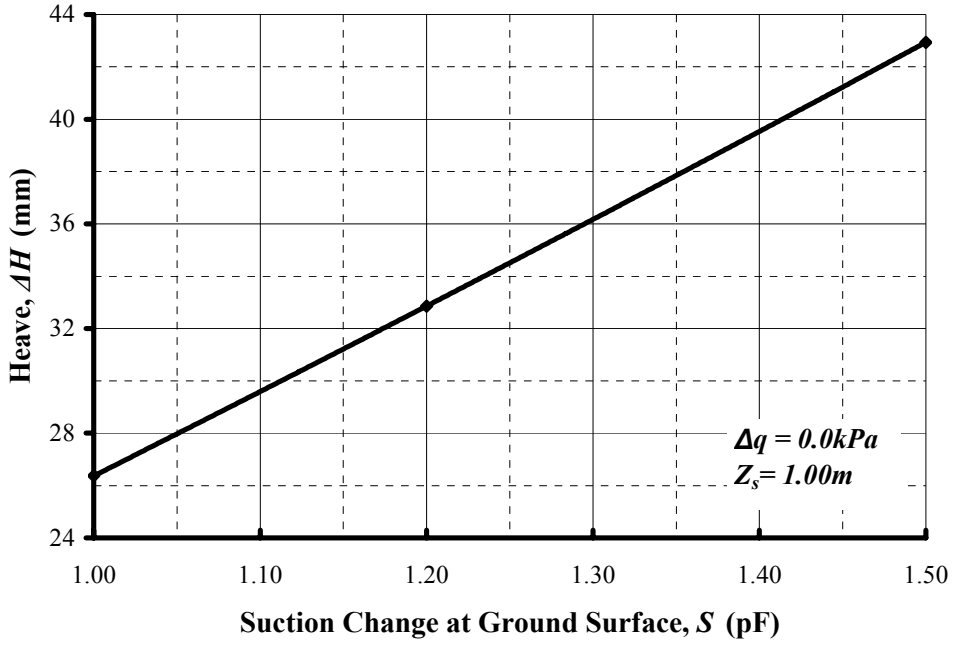

Figure (5.11): Effect of Suction Change at Ground Surface, *S* on Footing Heave under Zero Applied Pressure

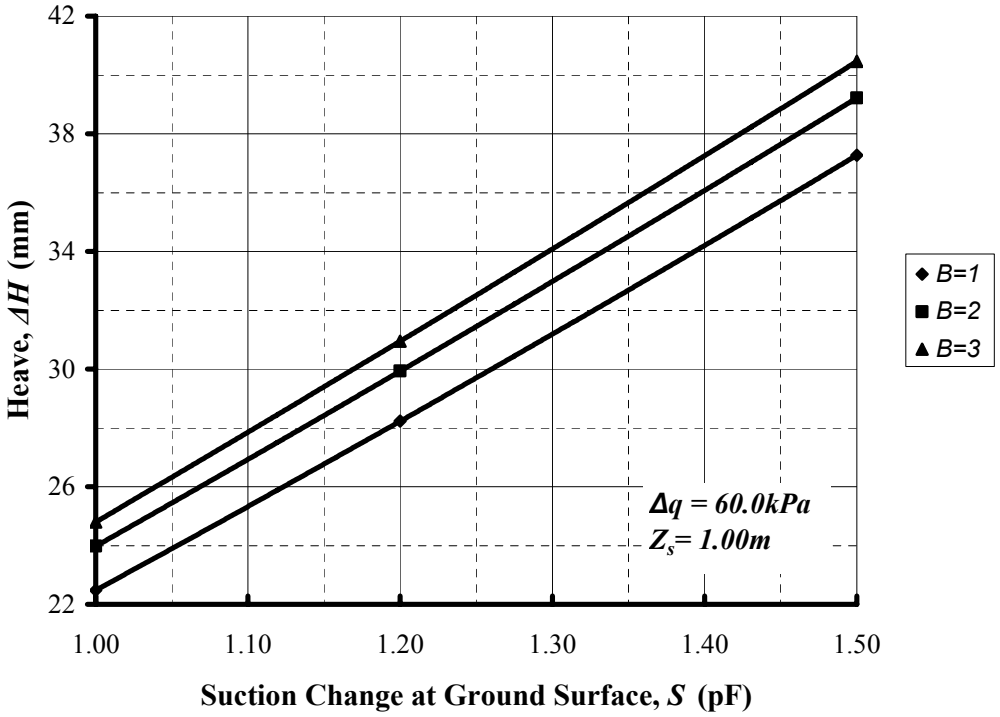

Figure (5.12): Effect of Suction Change at Ground Surface, *S* on Footing Heave under 60 kPa Footing Pressure for 1.00 m Seasonal Moisture Fluctuation Zone Depth

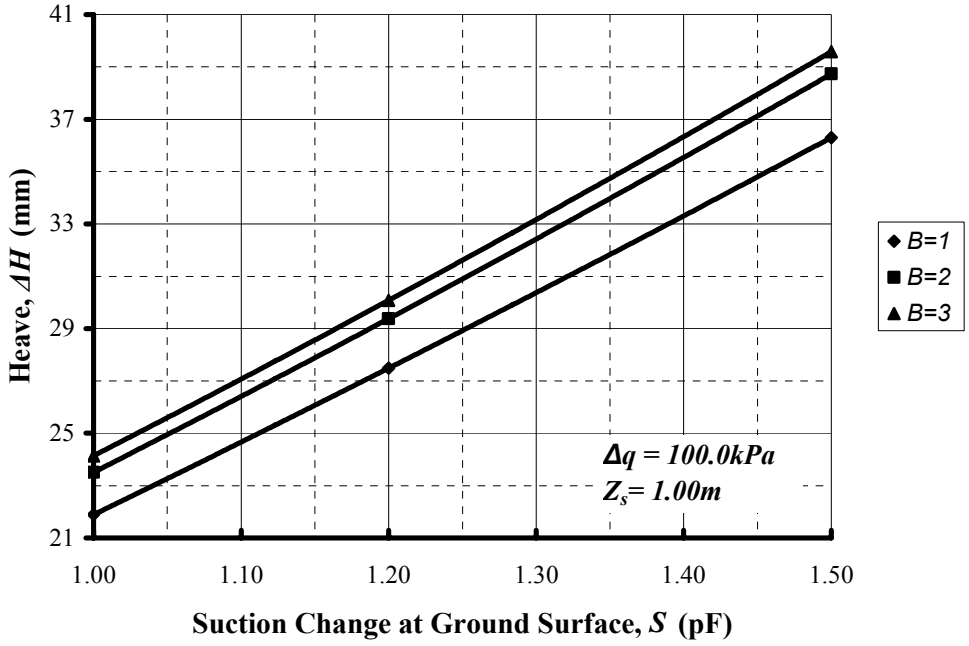

Figure (5.13): Effect of Suction Change at Ground Surface, *S* on Footing Heave under 100 kPa Footing Pressure for 1.00m Seasonal Moisture Fluctuation Zone Depth

5.5.4.3 Effect of Footing Width, *B*

Figure (5.14) illustrates the effect of footing width on footing heave due to climate effect under different pressures for 1.00 m active zone depth. Increase of footing width results in a slight increase in footing heave. The rate of increase of footing heave changes sharply at certain footing width. The increase of footing width from 1.00 to 4.00 m (i.e. 300%) leads to an 8% increase in footing heave. Furthermore, it is observed that the rate of change in heave decreases with increase in footing width thus, the effect of footing width on footing heave deceases with increasing of footing pressure.

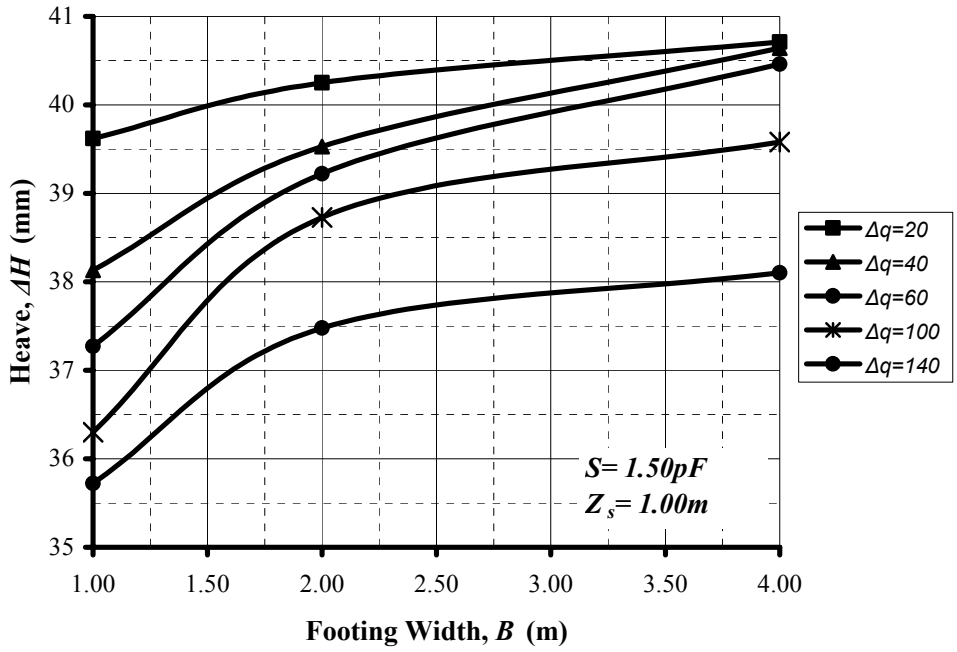

Figure (5.14): Effect of Footing width, *B* on Footing Heave
under 1.5 pF Soil Suction Change for 1.00m Seasonal Moisture Fluctuation Zone Depth

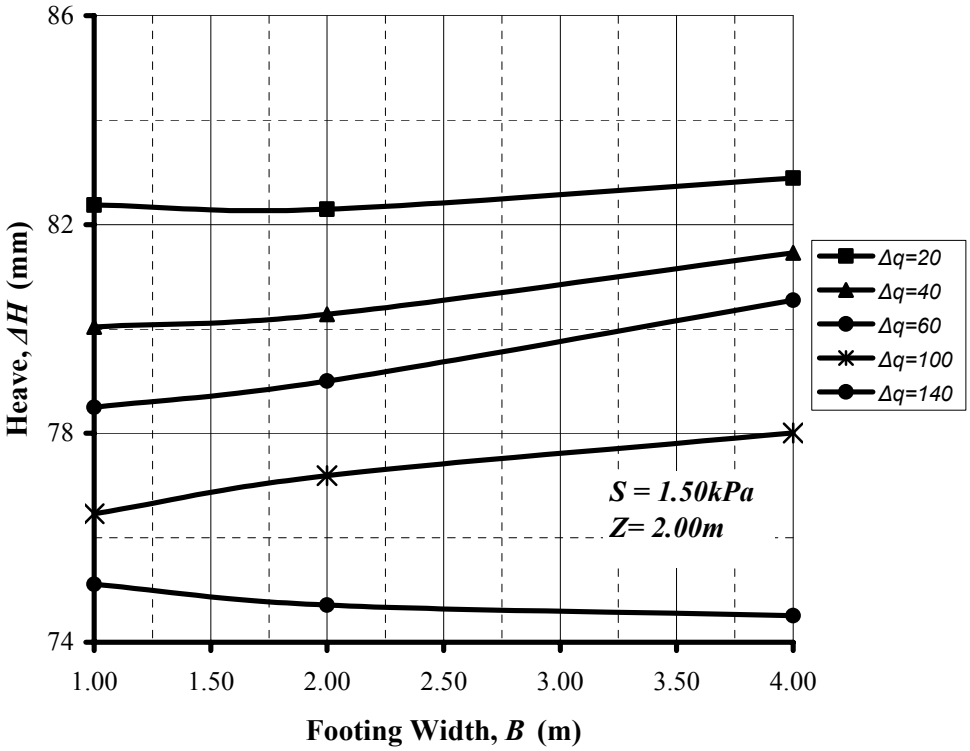

Figure (5.15): Effect of Footing width, *B* on Footing Heave
under 1.5 pF Soil Suction Change for 2.00m Seasonal Moisture Fluctuation Zone Depth

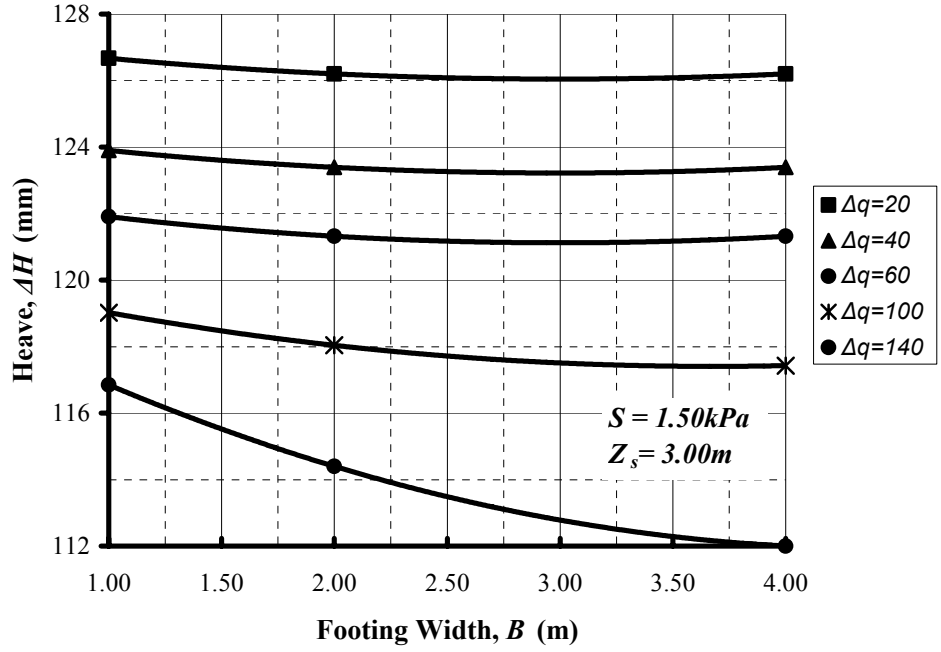

Figure (5.16): Effect of Footing width, *B* on Footing Heave
under 1.5 pF Soil Suction Change for 3.00m Seasonal Moisture Fluctuation Zone Depth

5.5.4.4 Effect of Footing Pressure, Δq

The effect of footing pressure on the heave of expansive soil resulting from soil suction changes due to climate effect is investigated and presented in Figure (5.17). This figure, presents the results for heave versus footing pressure for 1.0m footing depth and 1.00 m seasonal moisture fluctuation zone depth. According to this figure, footing heave decreases with increase of footing pressure. The slope of relationship decreases with increasing of footing pressure. For example, the heave decreases by 6% when footing pressure increases by 300% from 20 to 60 kPa.

The results indicate similar trends for footing heave versus footing pressure under different soil suction change. In other words, heave decreases by almost 6% when footing pressure increases from 20 to 60 kPa for suction soil change at ground surface by 1.0 or 1.2 or 1.5 pF.

Figure (5.18) presents the results for 1.0 m footing width and 3.0 m seasonal active zone depth. Similar to Figure (5.17), it is noted that footing heave due to suction changes at ground surface decreases with increasing of footing pressure. Comparison between the results for 1.0 m and 3.0 m seasonal moisture fluctuation zone depth indicates that the

effect of footing pressure on footing heave increases with increase of seasonal moisture fluctuation zone depth.

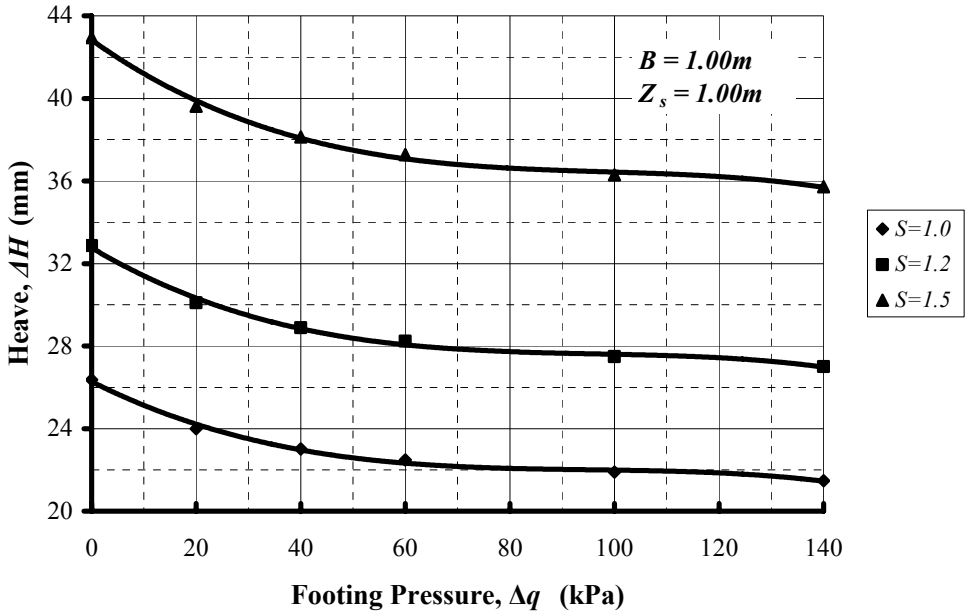

Figure (5.17): Effect of Footing Pressure, Δq on Footing Heave
for 1.00 m Footing Width and 1.00 m Seasonal Moisture Fluctuation Zone Depth

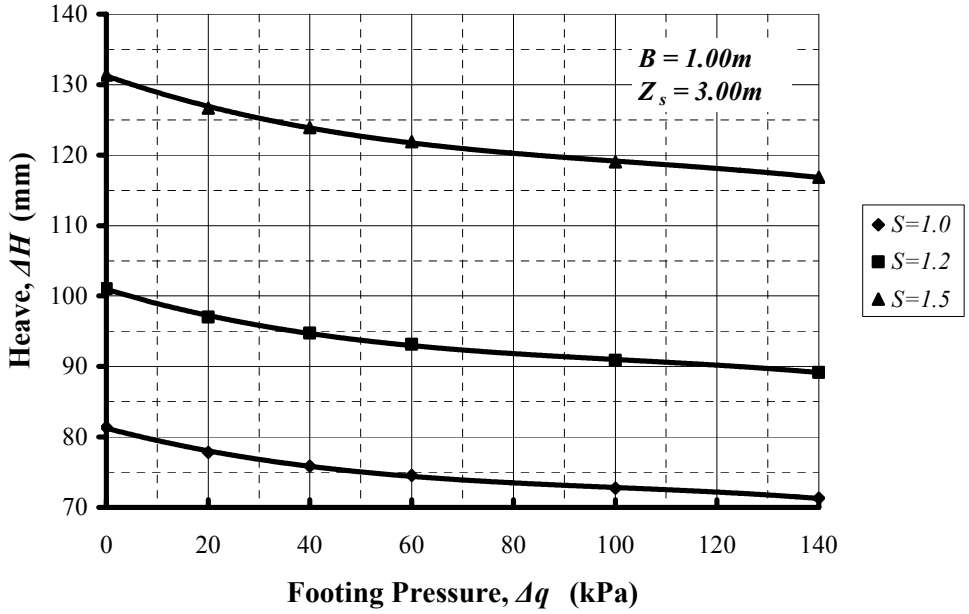

Figure (5.18): Effect of Footing Pressure, Δq *on* Footing Heave
for 1.00 m Footing Width and 3.00 m Seasonal Moisture Fluctuation Zone Depth

5.5.4.5 Summary

The parametric study to investigate the effects of soil suction changes due to climate on footing heave show the importance of collecting data about the climate over the year and measuring the depth of seasonal moisture fluctuation zone in several regions in Egypt to estimate heave due to climate changes. Table (5.8) summarized the effect of climate parameters on shallow foundations.

Table (5.8): Effect of Climate Parameters on Heave Shallow Foundation

Parameter	Symbol	Relation	Change of Footing heave due to increase of the parameter	Significance
Seasonal moisture fluctuation zone depth	Z_s	Linear	Increase	High
Suction change at G.s.	S	Linear	Increase	High
Footing width	B	Non-Linear	Variable depending on Z_s	Low
Footing pressure	Δq	Non-Linear	Decrease	Medium

5.6 Lawn (Trees) Effect

Trees that are often planted in small landscape areas near buildings may impact their performance. Shallow foundations may suffer distress due to shrinkage of the clays resulting from moisture demand of trees. This is attributed to the fact that the roots of trees extract water from the subsoils by suction which in turn extracts water from the soil beyond the root system resulting in appreciable volume change especially in clayey soils.

5.6.1 Root Zone Depth, R_L

Root zone depth is an important parameter for the consideration of drying effects caused by trees. The root system of a tree can be grouped as either tap or lateral as shown in Figure (5.19) (Mitchell, 1979). The vertical tap roots grow vertically downwards to considerable depths (root zone depth) to convey water and trace elements from the soil at depth, and to anchor the tree. Normally, it is considered that tap roots are confined to the vicinity of the tree trunk itself, and are thought to have only an insignificant effect on the tree surroundings. The laterals grow horizontally and parallel to the soil surface and form a mat over a certain limited depth where microbiological processes are most active. These lateral root systems extend a considerable distance from the trunk and extract moisture from surrounding soils.

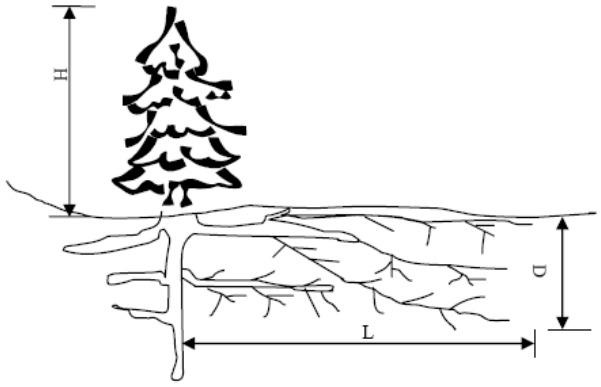

Figure (5.19) Lateral and vertical extent of tree root system (Mitchell, 1979)

Root zone has been reported to reach a depth of 6.00 m (Biddle, 1983). A recorded root fiber of 4.3m was reported by Lytton (1995) near a large oak tree in Texas during a hot, dry summer. Normally, roots can fracture the soil approximately 0.6 m beyond or deeper than the location of the root fiber.

Root zone depth located in shallow soils or those with root zone limiting conditions can be much less. The root zone limiting conditions can be caused by soil texture and

structure, such as fine textured soils with poor internal drainage characteristics and /or poor structure or soils with dense, compact, or cemented sub-soils and layered or stratified soils where abrupt, significant changes in soil texture may disrupt water movement in the vicinity of the interface. Other factors like rock and water table whether static or fluctuating can limit the depth of root zone.

Besides the soil structure, the irrigation system and the amount of rainfall can also have an influence on root zone depth. The use of moisture measuring devices can help define the root zone over the season by monitoring the soil water disappearance at soil depths in and below the suspected root zone.

5.6.2 Planting Distance, D_L

The influence of trees on expansive soils was investigated by several researchers. Ward (1953) recommended safe planting distance of trees of height, H, from buildings a distance, D_L, away. He prescribed "proximity rule" of D_L: $H = 1$ to ensure buildings were not damaged by the soil desiccation.

In Canada, Bozozuk (1962) demonstrated the decrease of drying settlements with distance from a row of 17 m high elm trees. In the UK, in the mid 70's, a severe drought caused much shrinkage settlement and it was realized that a large proportion of the ground movement under footings was related to the drying effects of trees.

Biddle (1983) conducted several studies of soil moisture deficits around specimens of certain tree species in open grassland. Five different clay soil profiles were investigated at three locations underlain by clay soils. Soil moisture was monitored with a down-hole neutron moisture meter to a maximum depth of 4 m. Generally, it was seen that the lateral extent of drying was contained within a radius equal to the height of the tree. However, the depth and radius of drying, both horizontally and vertically, appeared to be species dependent. Poplars caused drying to a radius of over 1.5 times the tree height and caused the deepest drying close to the trees, probably to a depth in excess of 4 m.

In New Zealand, Wesseldine (1982) demonstrated the influence of the silver dollar gum (E. cinerea) on houses. The research indicated a threshold value of D_L : H of 0.75 for single trees to cause damage and 1.0 to 1.5 for groups of these trees. The extent of damage was not mentioned in this research.

In Texas, USA, Tucker and Poor (1978) investigated a housing estate, which was in the process of being demolished because of the extent of damage to the houses (masonry veneer walls on slabs). Tree species were mulberry, elm, cottonwood and willows. Differential movements were measured and compared with D_L : H ratios. The results of the study revealed an average background movement of approximately 50 mm due to trees, which was apparent at D_L: H ratios above two. The data strongly indicated that tree effects were significant at D_L: H values greater than one and smaller than two. Differential movements in excess of 120 mm were observed where trees were close to the building.

5.6.3 Tree Water Demand, Q_L

The term water demand may be defined as the amount of water required by a tree in order to keep its metabolism functioning at optimum levels to meet its physiological requirements. The water demand of individual trees is not known and is difficult to measure. Attempts to do this using a combination of leaf area index and pan evaporation rates have yielded some success although the methods need to be refined.

National House Building Council (NHBC, 1985) presented a table of relative water demands and mature height of trees in that table, trees are ranked as high, moderate or low in their demand for water. Yet there are no published scientific data on water demand of mature trees to support such a classification. Perpich et al. (1965) proposed that the water demand of trees ranges from 0.25 to 0.50 m^3/day. Al-Shrief (1986) estimated the water demand of some pieces of trees as shown in Table (5.9).

Table (5. 9) Water Demand of Planted Trees and Bamboo (Al-Shrief, 1986)

Species	Water demand
Citrus tree	33.3 m^3/tree/year
Palm tree	93 m^3/tree/year
Olive tree	37 m^3/tree/year
Bamboo	1.75 m^3/m^2/year

It must be remembered; however, that the amount of water taken up by the tree can and will vary through the seasons and with changes in physiological activity. It is important that the amount of moisture extracted from soil by trees is examined and quantified separately from the other mechanisms by which moisture is lost to the soils, i.e., evaporation, surface run off, etc.

5.6.4 Soil Suction Changes around Trees

Knowledge of the in situ soil suction changes around trees is essential to reliably estimate the ground movement in expansive clay soils. Once the magnitude and pattern of the ground movement is known, footings can be structurally designed to mitigate adverse effects and to facilitate an acceptable performance of the structures they support.

Design soil suction changes due to tree are provided in the guidelines of the Footings Group, (1996). These suction changes do not recognize either any influence from tree species or the concept of wilting point. Furthermore, its major drawback is that it is based on limited data and has yet to be tested rigorously. Cameron (2001) recommended a suction profile that could be used to account for the influence of tree groups, as shown in Figure (5.20)

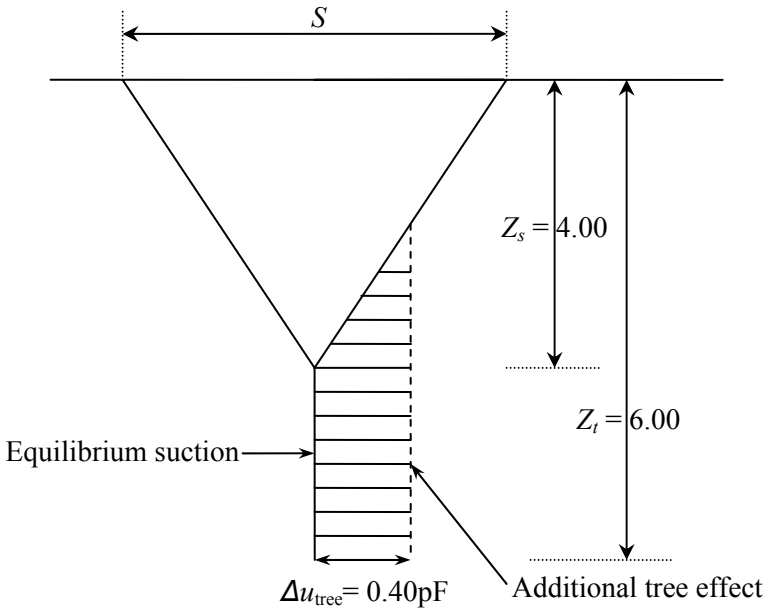

S: suction change at the ground surface; Z_s: depth of seasonal moisture fluctuation zone;
Δu_{tree} :design suction change due to tree; Z_t: depth of suction change due to tree

Figure (5. 20)**:** Suction change profile for a group of trees for $D_L/H_L < 0.6$ (Cameron, 2001)

Post Tensioning Institute (PTI) (2005) recommends equilibrium suction values for specific field conditions. When a shallow water table is present, the method recommends using equilibrium suction equal to 2.0 pF. When large trees are evident at the site, the equilibrium suction should be equal to 4.5 pF throughout the tree root zone. For the scenario that the soil is cemented or known to have high osmotic suction, the equilibrium suction value has to be determined experimentally.

5.6.5 Results of Lawn Effect

The effect of lawn on the settlement of footing was investigated. The different parameters that effect the settlement due lawn effect include root zone depth, R_L, planting distance, D_L, and water demand, Q_L were considered in analyses. The proposed values for these parameters were assumed as shown in Figure (5.21) based on data presented in the technical literature.

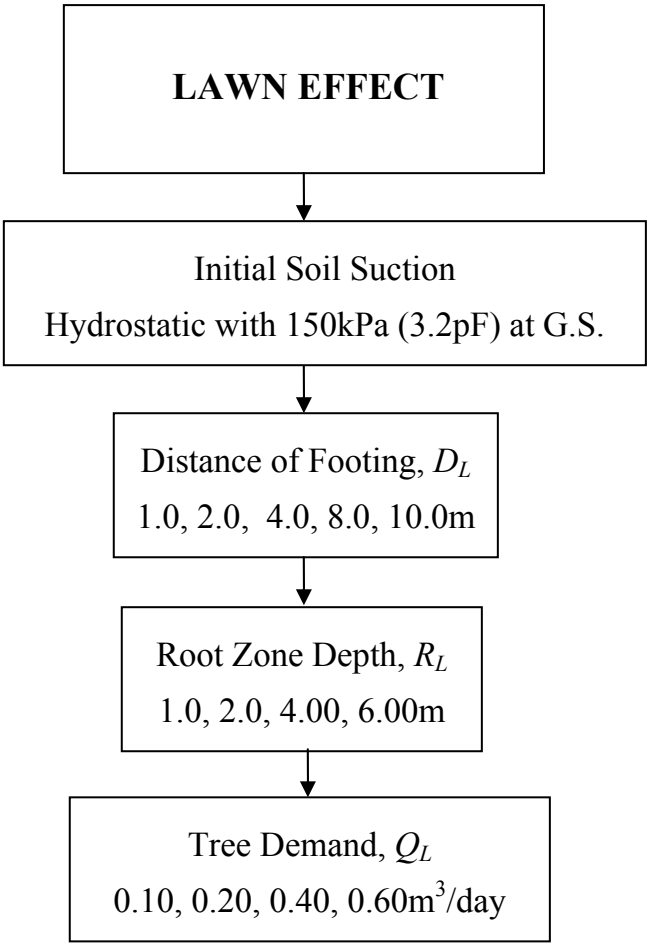

Figure (5.21): Lawn Effect Study

The effect of lawn on soil suction distribution was modeled using SEEP/W. The initial soil suction profile was assumed to be hydrostatic with 150 kPa (3.2pF) which simulate wet conditions. The final soil suction profiles due to different water demand for 2.0 m root zone depth are presented in Figures (5.22) to (5.24). While, the final soil suction profiles due to 0.40 m^3/day water demand for different root zone depth are presented in Figures (5.25) to (5.27).

Based on results of seepage analysis, stress-deformation analyses were performed using Modified CRISP to simulate the effect of lawn on soil volume change. Results of analysis for the effect of lawn parameters such as, planting distance from footing edge, root zone depth and tree demand on settlement of soil are presented in Tables (5.10) and (5.11). Table (5.10) summarizes the results for settlement of edge point of footing near tree line for different planting distance and root zone depth in case of Q_L=0.10 and Q_L= 0.20 m^3/day tree water demand. Similarly, Table (5.11) summarizes the results for 0.40 and 0.60 m^3/day tree water demand.

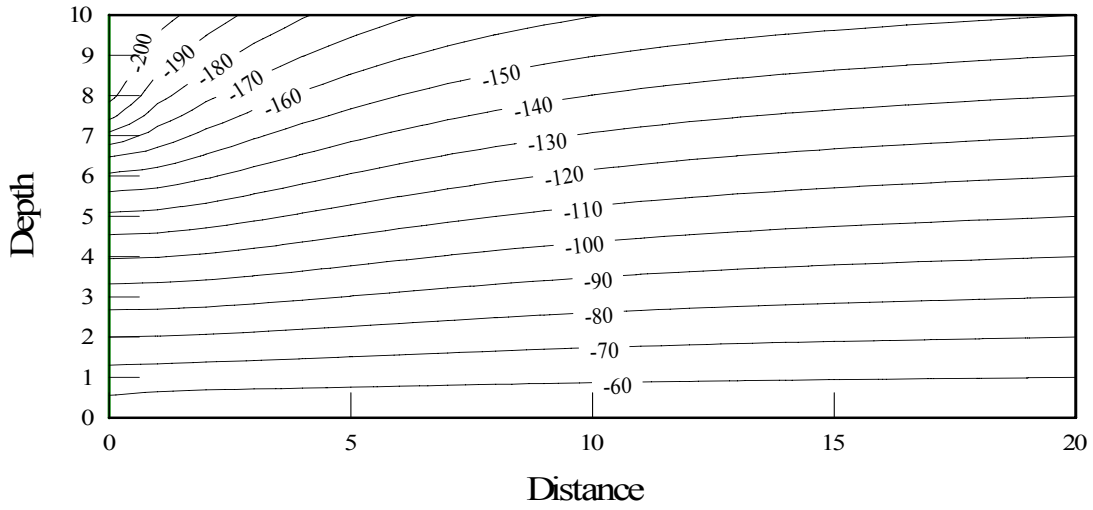

Figure (5.22): Final Soil Suction Distribution due to Lawn Effect for 0.20m^3/day Tree Water Demand and 2.00m Root Zone Depth

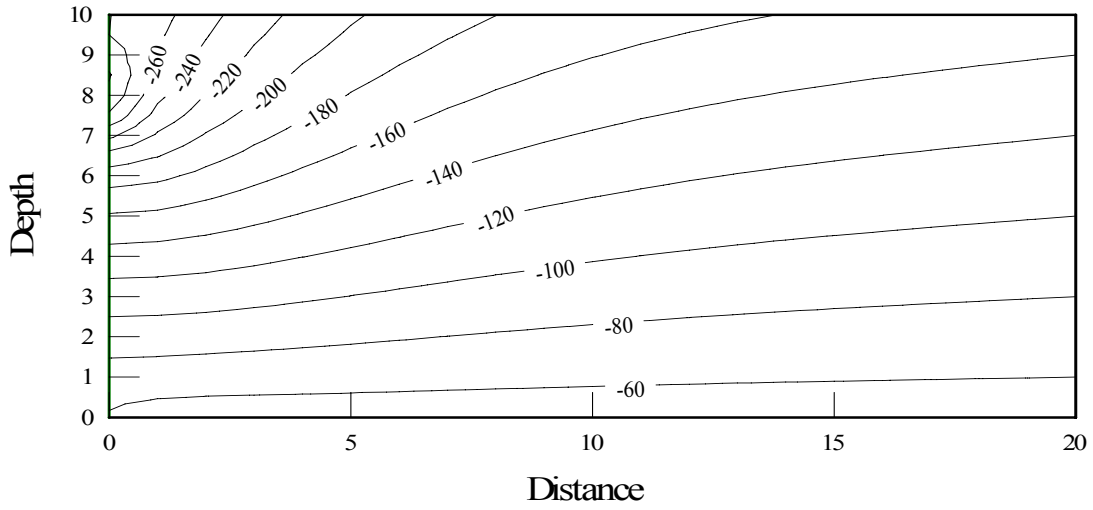

Figure (5.23): Final Soil Suction Distribution due to Lawn Effect for 0.40m^3/day Tree Water Demand and 2.00m Root Zone Depth

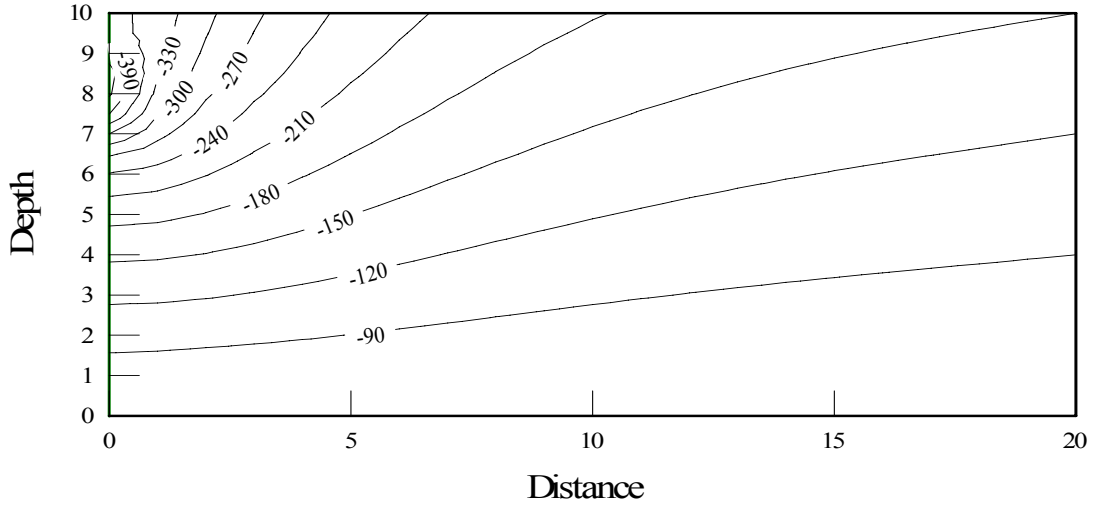

Figure (5.24): Final Soil Suction Distribution due to Lawn Effect for 0.60m^3/day Tree Water Demand and 2.00m Root Zone Depth

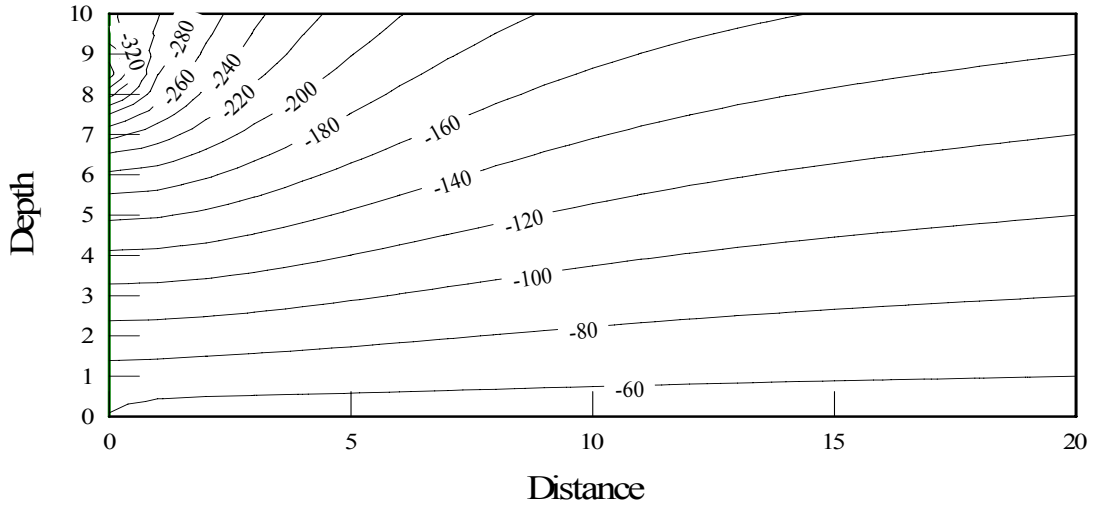

Figure (5.25): Final Soil Suction Distribution due to Lawn Effect for 0.40m^3/day Tree Water Demand and 1.00m Root Zone Depth

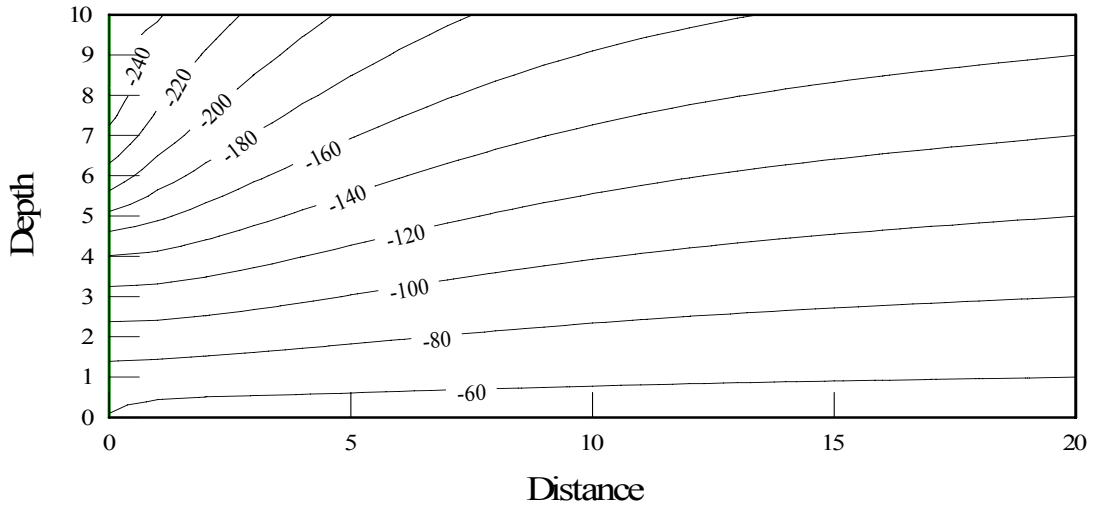

Figure (5.26): Final Soil Suction Distribution due to Lawn Effect for 0.40m^3/day Tree Water Demand and 4.00m Root Zone Depth

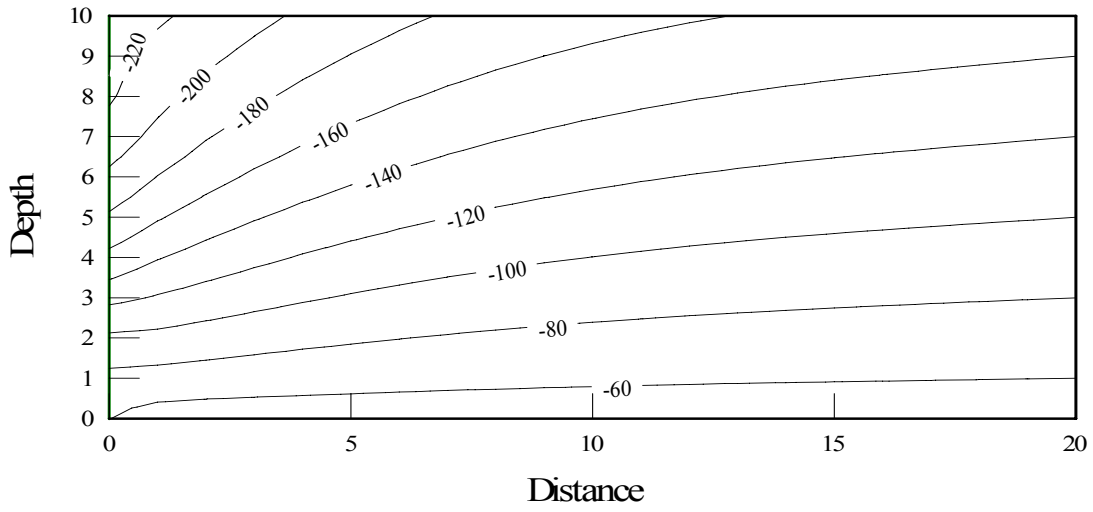

Figure (5.27): Final Soil Suction Distribution due to Lawn Effect for 0.40m^3/day Tree Water Demand and 6.00m Root Zone Depth

Table (5.10): Footing Settlement for 0.10 and 0.20 m^3/day Tree Water Demand

Tree demand	0.10 m^3/day				0.20 m^3/day			
Root zone Depth, (m) / Planting Distance, (m)	1.00	2.00	4.00	6.00	1.00	2.00	4.00	6.00
1.00	18.37	11.9	10.81	9.46	28.89	23.06	21.06	18.57
2.00	17.64	10.91	10.03	8.84	26.47	21.2	19.58	17.39
4.00	12.99	8.74	8.16	7.28	21.35	17.11	16.02	14.39
8.00	8.06	5.39	5.08	4.58	13.36	10.07	9.8	9.11
10.00	6.37	4.25	4.01	3.63	10.57	8.43	7.95	7.22

Table (5.11): Footing Settlement for 0.40 and 0.60 m^3/day Tree Water Demand

Tree demand	0.40 m^3/day				0.60 m^3/day			
Root zone Depth, (m) / Planting Distance, (m)	1.00	2.00	4.00	6.00	1.00	2.00	4.00	6.00
1.00	50.09	43.93	40.3	35.77	70.63	63.79	58.49	52.1
2.00	45.91	40.51	37.59	33.57	64.56	58.81	54.6	48.95
4.00	37.25	32.96	30.98	26.48	52.4	47.99	45.18	40.91
8.00	23.61	20.85	19.69	17.88	33.49	30.65	28.98	26.4
10.00	18.76	16.55	15.64	14.23	26.71	24.42	23.11	21.08

5.6.5.1 Effect of Planting Distance from Footing Edge, D_L

Figure (5.28) presents the effect of planting distance on soil settlement for 0.10 m^3/day tree water demand . According to Figure (5.28), it is evident that planting distance, D_L, has a significant effect on the settlement of soil. The relationship between the planting distance and soil settlement is nonlinear. In addition, increase of planting distance leads to decrease of settlement. Settlement decreases by 26% when planting distance increases from 2.00 to 4.00m. The slope of relationship decreases with increasing of planting distance.

Also, for the same water demand, effect of planting distance decreases with increasing of root zone depth. The average slope of relationship between settlement and planting distance decreases by 26% when root zone depth increase from 1.00 m to 4.00 m for Q_L=0.10 m^3/day.

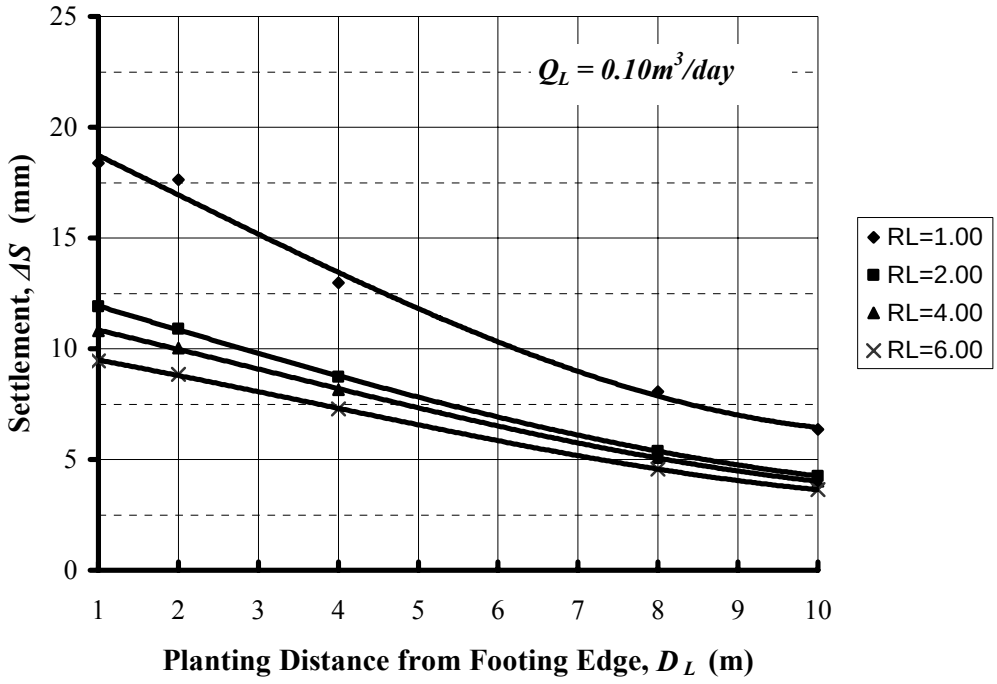

Figure (5.28): Effect of Planting Distance, D_L on Footing Settlement for 0.10m^3/day Tree Water Demand

Figures from (5.29) to (5.30) present the effect of planting distance on settlement of footing for 0.20, 0.40 and 0.60 m^3/day tree water demand. For the same planting distance, as the tree water demand increase, the settlement of footing significantly increases. Thus, selection of safe planting distance to protect buildings of damage is highly depending on tree water demand (i.e., tree species).

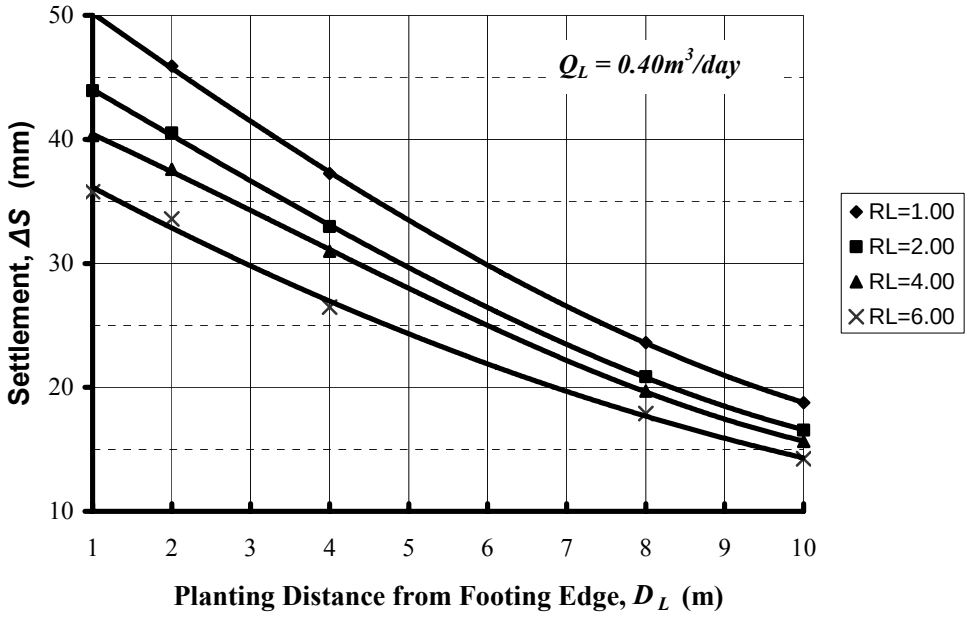

Figure (5.29): Effect of Planting Distance, D_L on Footing Settlement for 0.40 m^3/day Tree Water Demand

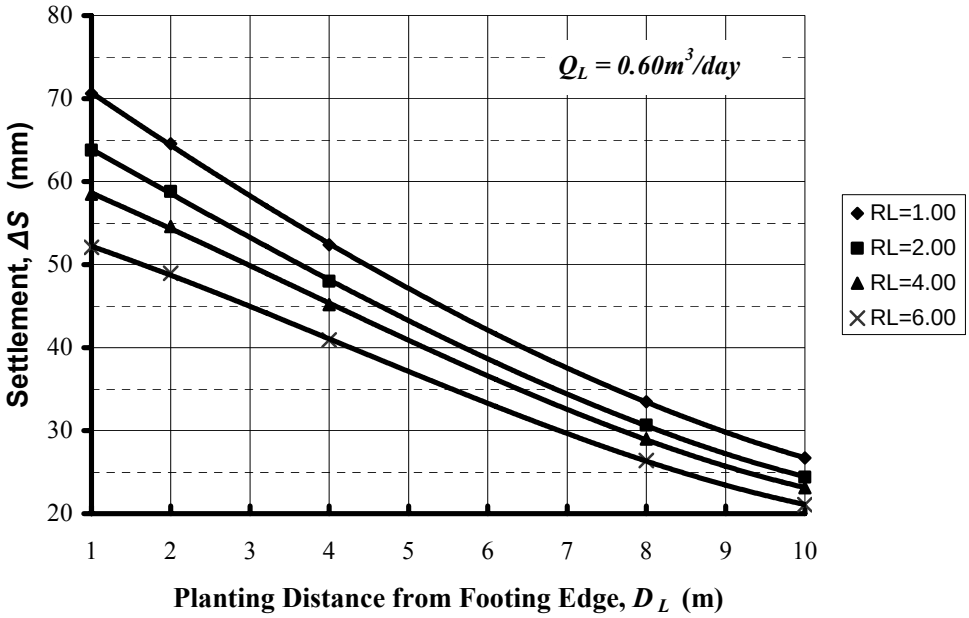

Figure (5.30): Effect of Planting Distance, D_L on Footing Settlement for 0.60 m^3/day Tree Water Demand

5.6.5.2 Effect of Root Zone Depth, R_L

Figure (5.31) presents the effect of root zone depth, R_L, on footing settlement for 0.10m^3/day tree water demand. According to the results shown in this figure, footing settlement decreases with increase of root zone depth. Also, the relationship between footing settlement and root zone depth is nonlinear. Root zone depth has a significant effect on settlement of soil when it is less than 2.00 m. For example, footing settlement deceases by 35% when root zone depth increases from 1.0 to 2.0 m (i.e., 100%) for 0.10 m^3/day tree water demand and 1.0 m planting distance. If root zone depth is greater than 2.00 m, it has limited effect on settlement. The effect of root zone depth on settlement decreases with increasing of planting distance.

For large planting distance, the effect of root zone depth becomes negligible especially, for root zone depth greater than 2.00 m. Therefore, it is important to identify the limiting conditions of root zone depth which may caused by soil texture and structure because this conditions may lead to higher effect of lawn on the buildings.

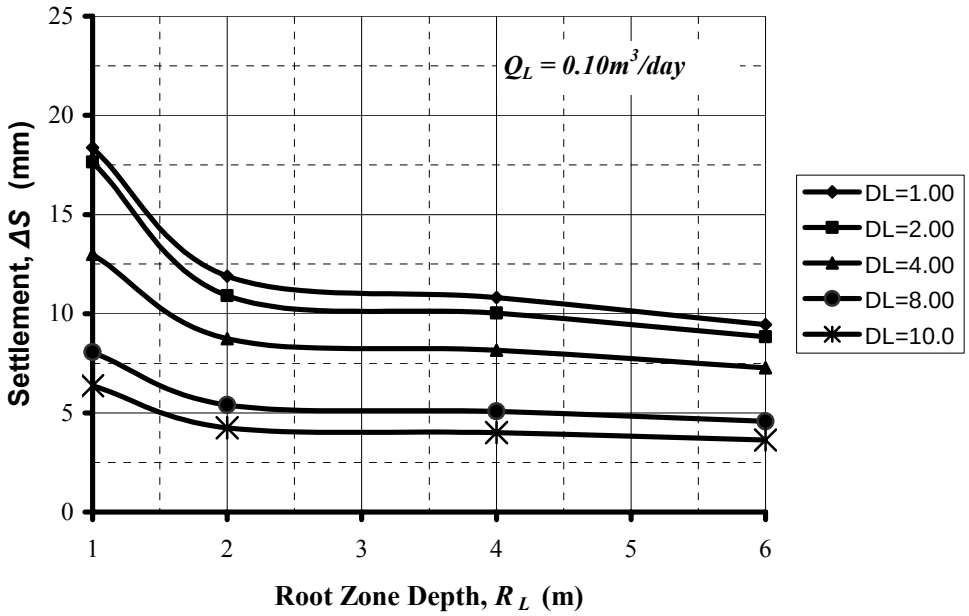

Figure (5.31): Effect Root Zone Depth, R_L on Footing Settlement for 0.10 m^3/day Tree Water Demand

Figures (5.32) and (5.33) present the effect root zone depth on settlement of footing for 0.40 and 0.60 m^3/day tree water demand. Based on these figures, it is apparent that for the same tree water demand, settlement decreases as root zone depth increases. Also, effect of root zone depth on footing settlement increases with increase of water demand.

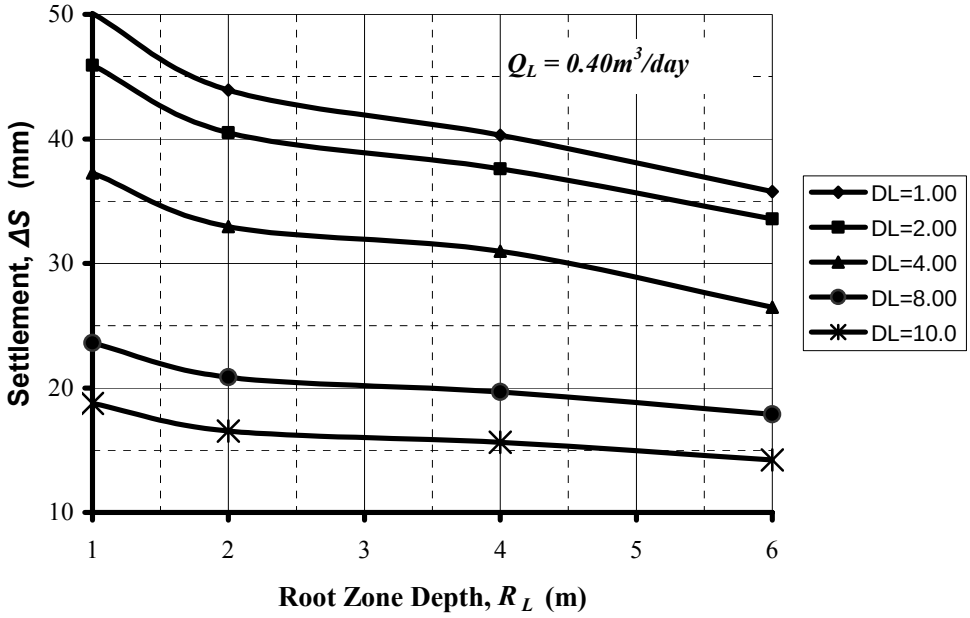

Figure (5.32): Effect Root Zone Depth, R_L, on Footing Settlement for 0.40 m^3/day Tree Water Demand

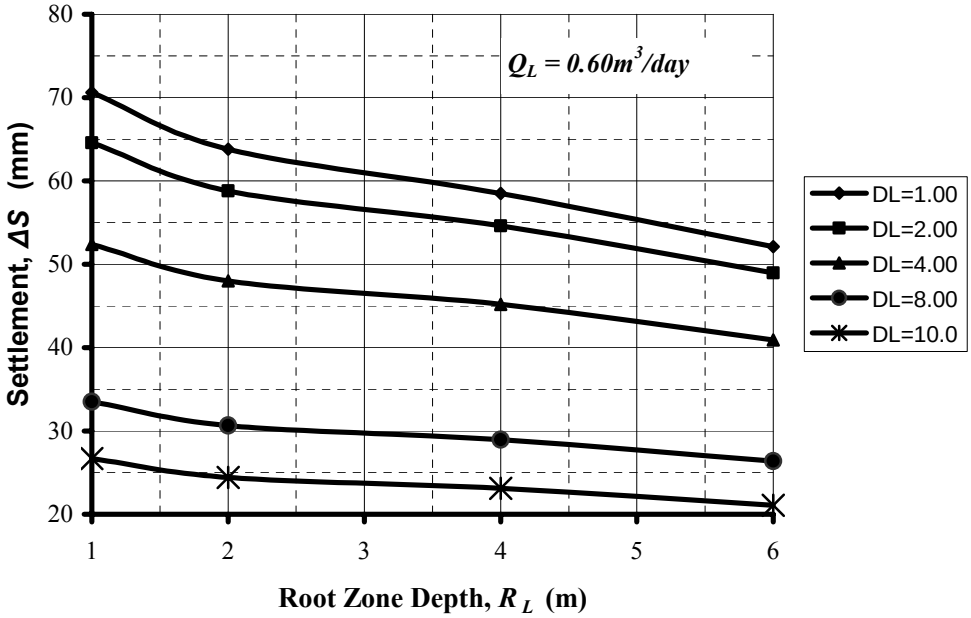

Figure (5.33): Effect Root Zone Depth, R_L, on Footing Settlement for 0.60 m^3/day Tree Water Demand

5.6.5.3 Effect of Tree Water Demand, Q_L

Figures (5.34) and (5.35) present the effect of tree water demand on soil settlement for different planting distances in case of 2.00 m and 3.00 m root zone depth; respectively. Based on results shown in these figures, the relationship between tree water demand and soil settlement is linear. Tree water demand, Q_L, has a significant effect on settlement of soil. Increase of tree water demand by 50% leads to increase of settlement by 45% for 1.00 m planting distance and 2.00 m root zone depth. However, it should be noted that the effect of tree water demand on footing settlement decreases with increase of planting distance.

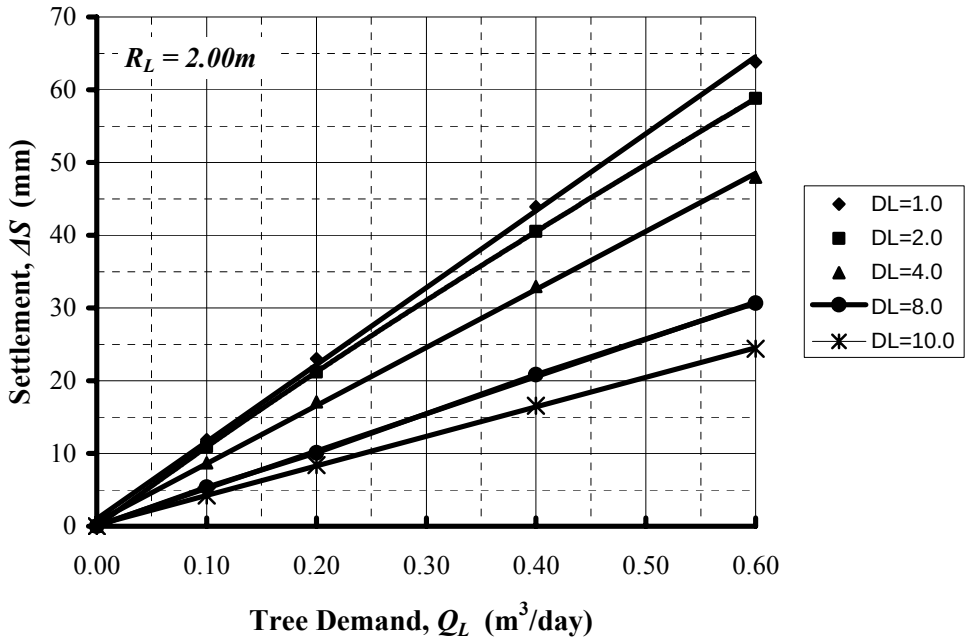

Figure (5.34): Effect Tree Water Demand, Q_L, on Footing Settlement for 2.00 m Root Zone Depth

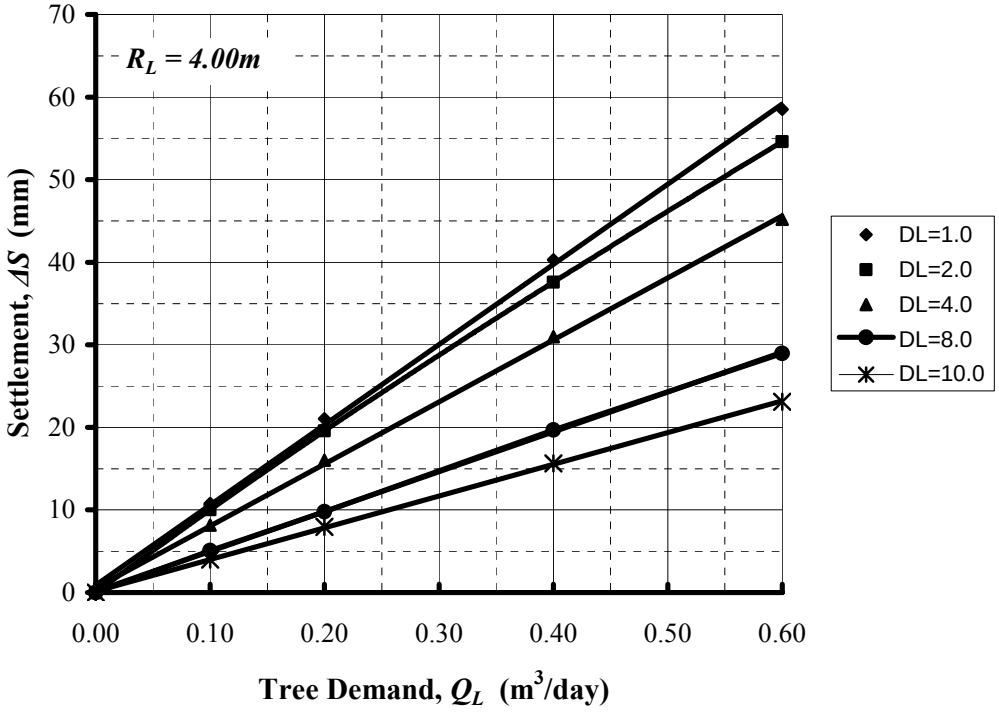

Figure (5.35): Effect Tree Water Demand, Q_L, on Footing Settlement for 2.00 m Root Zone Depth

5.6.5.4 Summary

The parametric study for the parameters of lawn effect on soil settlement shows the importance of collecting data about the parameters of lawn especially the tree water demand for different types of lawn or tree species. The effect of these parameters can be taken into account during the design of light loaded structures and pavements. Also, the study illustrates the high significance of selecting the safe planting distance to avoid the damage from lawn on building foundations. Furthermore, the root zone depth has a considerable effect especially for short root zone depth (i.e., limiting soil conditions). Table (5.12) summarized the effect of lawn parameters on footing settlement.

Table (5.12): Effect of Lawn on Settlement of Shallow Foundation.

Parameter	Symbol	Relationship	Change in footing settlement due to increase of parameter	Significance
Planting distance	D_L	Non-linear	Decrease	High
Root zone Depth	R_L	Non-linear	Decrease	Low
Tree water demand	Q_L	Linear	Increase	High

5.7 Infiltration Effect

Infiltration of water into ground leads to changes in soil suction. The reduction in soil suction causes heave of soil and loss of soil shear strength. Sources of infiltrated water include rainfall, watering of lawn and run water in open canals. Change in soil suction due to infiltration depends on rate of infiltration, width of infiltration surface and distance of infiltration from the building foundation. In this study, the uncoupled approach was used to simulate footing heave due to infiltration process and its related parameters. The research also considered the effect of shallow foundation dimensions and footing pressures on footing heave. It is important to note that the study does not consider the effect of infiltration on the shear strength of soil.

5.7.1 Infiltration Rate, q_i

Water infiltration into the ground is controlled by the rate and duration of water application. The rate of infiltration is affected by soil physical properties, slope, vegetation, and surface roughness. Water can infiltrate into the soil as quickly as it is applied, and the supply rate determines the infiltration rate. This type infiltration process has been termed as supply controlled. However, once the infiltration rate exceeds the soil infiltrability, it is the latter which determines the actual infiltration rate, and thus the process becomes profile controlled. therefore, whenever water is ponded over the soil surface, the rate of water application exceeds the soil infiltrability. On the other hand, if water is applied slowly, the application rate may be smaller than the soil infiltrability (Hillel, 1982).

Generally, water infiltration has a high rate at the beginning, decreasing rapidly, and then slowly until it approaches a constant rate. As shown in Figure (5.36), the infiltration rate will eventually become steady and approach the value of the saturated hydraulic conductivity, k_s. The initial soil water content and saturated hydraulic conductivity of the soil media are the primary factors affecting the soil water infiltration process. The wetter the soil initially, the lower will be the initial infiltrability (due to a smaller suction gradient), and a constant infiltration rate will be attained more quickly. In general, the higher the saturated hydraulic conductivity of the soil, the higher the infiltrability.

As might be expected, the slope of the land can also indirectly impact the infiltration rate. Steep slopes will result in runoff, which will impact the amount of time the water will be available for infiltration. In contrast, gentle slopes will have less of an impact on the infiltration process due to decreased runoff.

When compared to the bare soil surface, vegetation cover tends to increase infiltration by retarding surface flow, allowing time for water infiltration. Plant roots may also increase infiltration by increasing the hydraulic conductivity of the soil surface. Due to these effects, infiltration may vary widely under different types of vegetation.

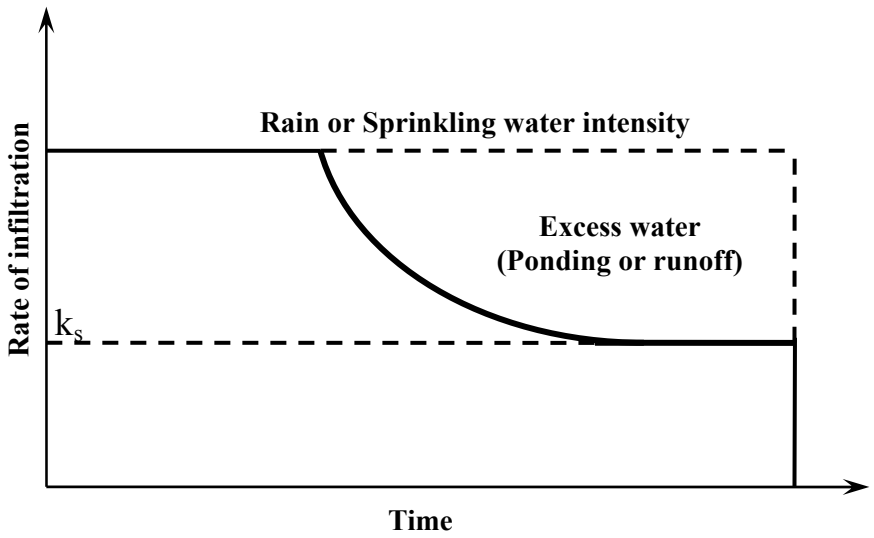

Figure (5.36): Decrease of Infiltration rate with time (Hillel, 1982).

Source of infiltrated water may be the rainfall or irrigation or any source of water. Rainfall is considered one of the main sources especially in wet regions. The annual rainfall in most parts of Egypt is less than 50 mm. Table (5.13) presents the average rainfall in Egypt according to world climate site.

Table (5. 13): Average Rainfall in Egypt According to World Climate Site

Month	Jan	Feb	Mar	Apr	May	Jun	Jul	Aug	Sep	Oct	Nov	Dec
Rainfall (mm)	4.0	4.0	3.0	1.0	2.0	0.5	0.0	0.0	0.5	1.0	3.0	7.0

5.7.2 Results of Infiltration Effect

The effect of infiltration on footing heave was investigated. The different parameters that effect footing heave due to water infiltration such as infiltration rate, q_i, infiltration width, w_i, and infiltration distance, D_i, were considered in analyses. Figure (5.37) presents the definition of these parameters and dimensions of finite element mesh used in the analysis. The proposed values for these parameters were assumed as shown in Figure (5.38).

The effect of infiltration on soil suction change was modeled using seepage analysis. The initial soil suction profile was assumed to be hydrostatic with 1500 kPa (4.2pF) which

represent the wilting point of vegetation at ground surface which used to simulate dry conditions. The final soil suction profiles in response to different infiltration rate for 3.00 m surface infiltration width are presented in Figures (5.39) to (5.41).

Based on these figures, it can be observed that infiltration results in decrease of soil suction around the infiltration area. Soil suction changes increases due to increase of infiltration rate. The change of soil suction extends to larger lateral dimensions with increase of infiltration rate. The decrease of soil suction will lead to increase footing heave. Footing heave was estimated using stress-deformation analysis with Modified CRISP.

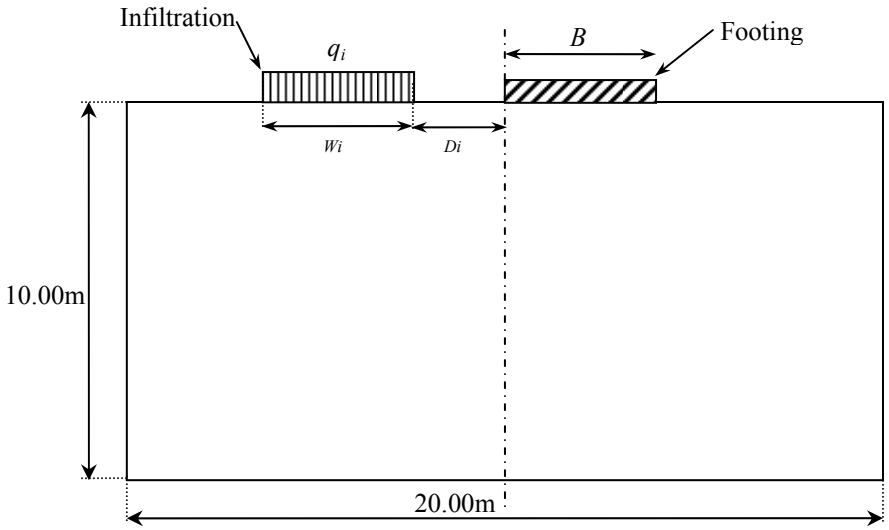

Figure (5.37): Infiltration Parameters and Dimensions of Finite Element Model

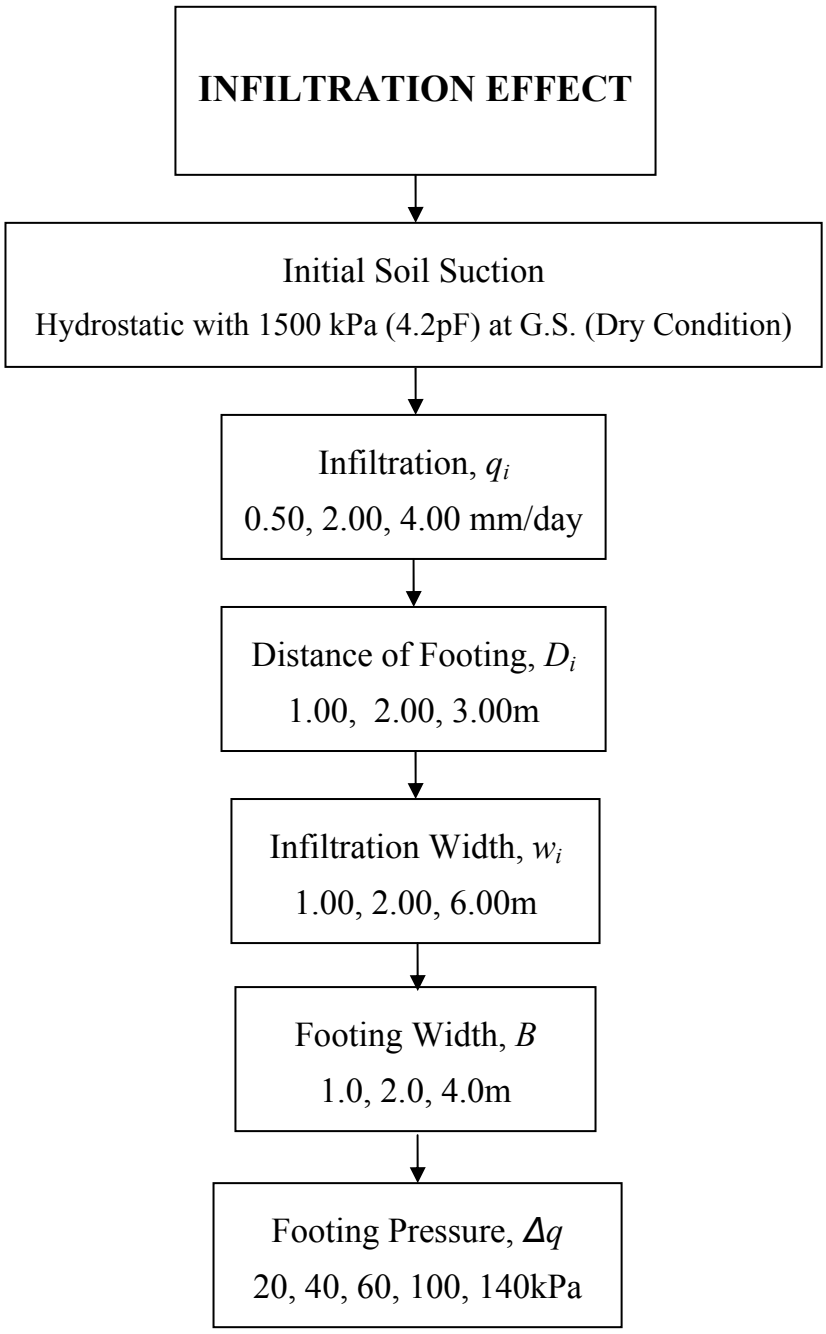

Figure (5.38): Infiltration Effect Study

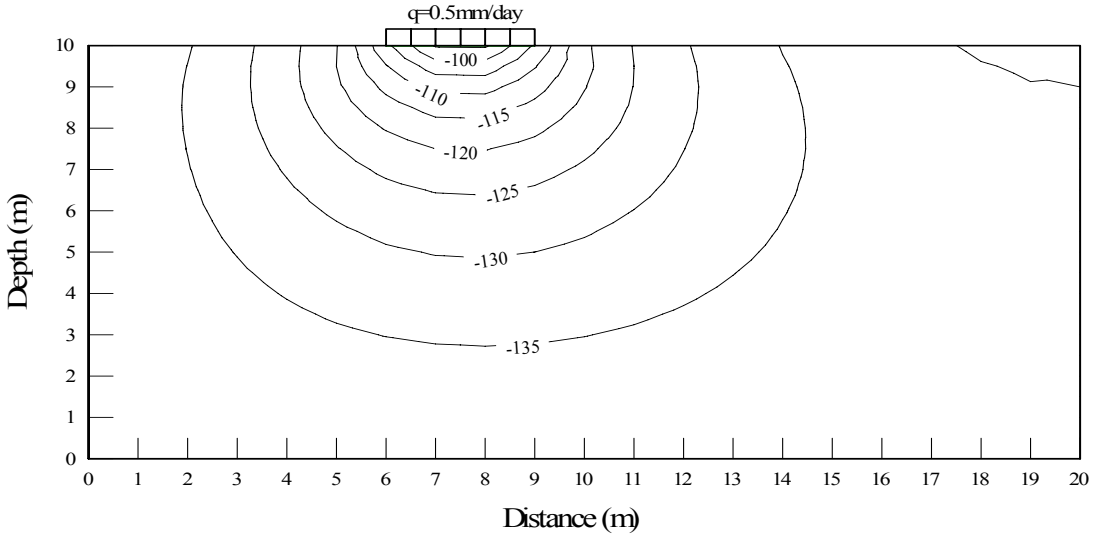

Figure (5.39): Final Soil Suction Distribution due to 0.50mm/day Infiltration Rate and 3.00 m Infiltration Width

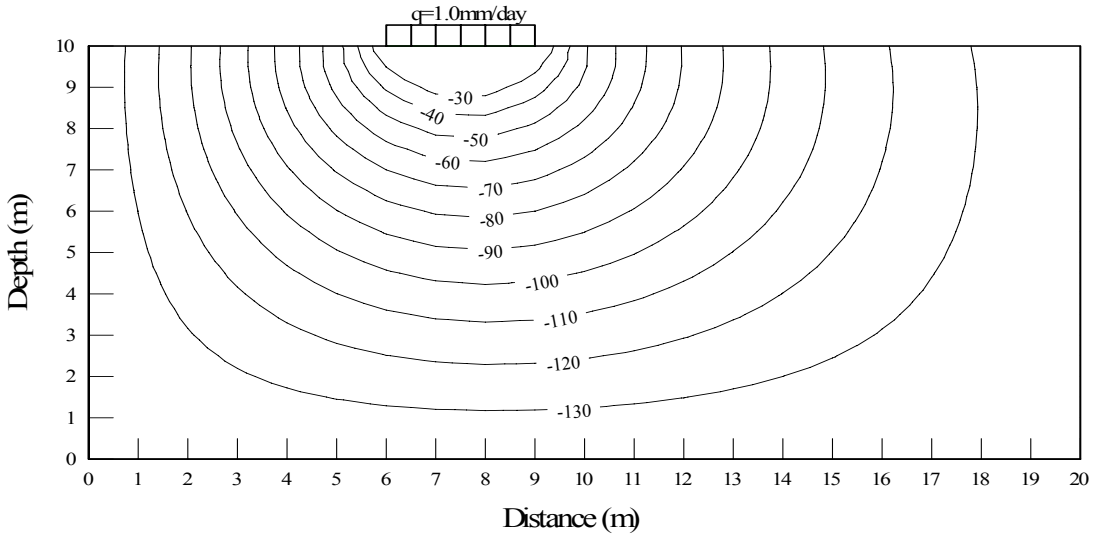

Figure (5.40): Final Soil Suction Distribution due to 1.00 mm/day Infiltration Rate and 3.00 m Infiltration Width

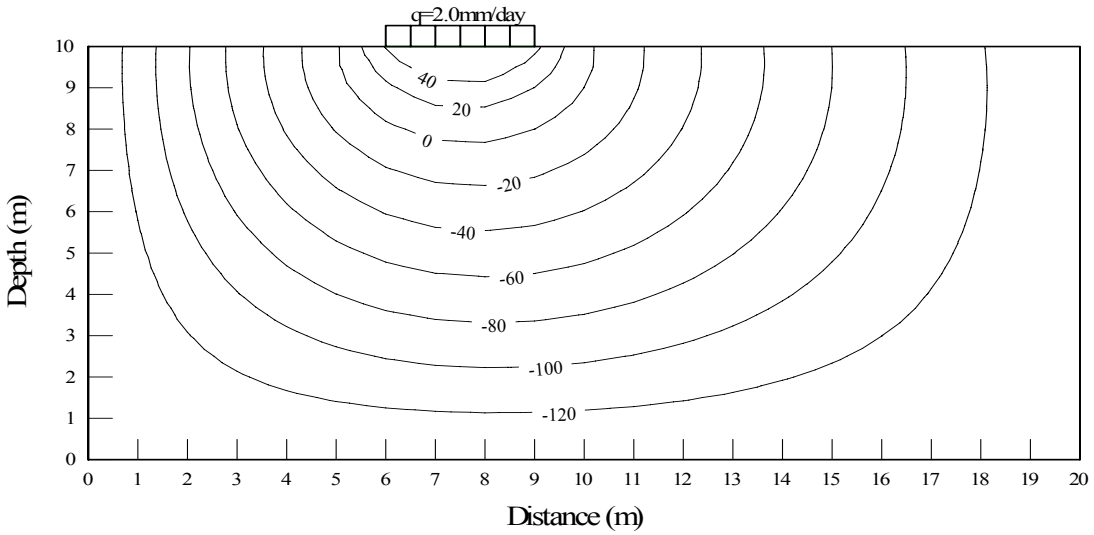

Figure (5.41): Final Soil Suction Distribution due to 2.00 mm/day Infiltration Rate and 3.00 m Infiltration Width

Results of stress-deformation analyses for the effect of infiltration parameters such as infiltration distance from footing edge, D_i, width of surface infiltration, w_i, and infiltration rate, q_i, on heave of shallow foundation are presented in the following tables. In addition, the effect of footing width and footing pressures are presented in the results. Table (5.14) summarizes the results of heave under different footing pressures, footing widths and different infiltration distances in case of 0.50 mm/day infiltration rate. Similarly, Tables (5.15) and (5.16) present the results for 1.00 mm/day and 6.00 mm/day infiltration rate; respectively. Also, Table (5.17) presents footing heave for different infiltration rates.

Table (5.14): Footing Heave for 1.00m Infiltration Width and 0.50mm/day Infiltration Rate

Footing Width, *B* (m)	1.00			2.00			4.00		
Infiltration Distance, *B*, (m) / Footing Pressure, *Δq*, (kPa)	1.00	2.00	4.00	1.00	2.00	4.00	1.00	2.00	4.00
0.0	7.79	7.15	5.93	7.79	7.15	5.93	7.79	7.15	5.93
20	7.6	6.96	5.76	7.58	6.95	5.75	7.58	6.95	5.75
40	7.5	6.87	5.68	7.46	6.83	5.64	7.45	6.82	5.63
60	7.43	6.8	5.61	7.38	6.75	5.57	7.36	6.72	5.55
100	7.33	6.7	5.52	7.27	6.64	5.46	7.22	6.6	5.43
140	7.26	6.63	5.46	7.18	6.55	5.39	7.13	6.51	5.34

Table (5.15): Footing Heave for 3.00m Infiltration Width and 1.00mm/day Infiltration Rate

Footing Width, (m)	1.00			2.00			4.00		
Infiltration Distance, *B*, (m) / Footing Pressure, *Δq*, (kPa)	1.00	2.00	4.00	1.00	2.00	4.00	1.00	2.00	4.00
0.0	16.48	14.43	10.65	16.48	14.43	10.65	16.48	14.43	10.65
20	16.1	14.08	10.35	16.07	14.05	10.33	16.07	14.05	10.33
40	15.91	13.89	10.2	15.83	13.82	10.14	15.82	13.81	10.13
60	15.76	13.76	10.08	15.67	13.67	10.01	15.63	13.63	9.98
100	15.57	13.57	9.93	15.44	13.45	9.83	15.38	13.38	9.77
140	15.42	13.43	9.81	15.27	13.29	9.69	15.18	13.21	9.63

Table (5.16): Footing Heave for 6.00m Infiltration Width and 6.00mm/day Infiltration Rate

Footing Width, (m)	1.00			2.00			4.00		
Infiltration Distance, *B*, (m) / Footing Pressure, *Δq*, (kPa)	1.00	2.00	4.00	1.00	2.00	4.00	1.00	2.00	4.00
0.0	25.52	21.25	21.25	25.52	21.25	21.25	25.52	21.25	21.25
20	24.91	20.7	20.7	24.86	20.65	20.65	24.86	20.65	20.65
40	24.58	20.41	20.41	24.47	20.3	20.3	24.45	20.29	20.29
60	24.32	20.2	20.2	24.21	20.07	20.07	24.15	20.02	20.02
100	24.03	19.91	19.91	23.82	19.73	19.73	23.72	19.64	19.64
140	23.8	19.71	19.71	23.55	19.49	19.49	23.42	19.38	19.38

Table (5.17): Footing Heave for 3.00m Infiltration Width and 2.00 m Footing Width

Infiltration Rate, q_i, (mm/day)	1.00			2.00			4.00		
Infiltration Distance, *B*, (m) / Footing Pressure, *Δq*, (kPa)	1.00	2.00	4.00	1.00	2.00	4.00	1.00	2.00	4.00
0.0	16.48	14.43	10.65	70.29	58.49	38.47	217.79	153.52	87.23
20	16.1	14.08	10.35	68.62	56.98	37.33	211.28	148.96	84.24
40	15.91	13.89	10.2	67.65	56.1	36.66	204.64	146.15	82.54
60	15.76	13.76	10.08	66.99	55.5	36.21	199.09	144.15	81.36
100	15.57	13.57	9.93	66.05	54.65	35.56	190.44	141.24	79.71
140	15.42	13.43	9.81	65.4	54.06	35.1	183.89	139.13	78.57

5.7.2.1 Effect of Infiltration Distance from Footing Edge, D_i

A parametric study for the effect of infiltration distance from footing edge on footing heave is performed. Figure (5.42) presents graphically the relationship between heave of edge point of footing near infiltration area and infiltration distance under zero pressure. Heave linearly decreases with increase of infiltration distance. The distance of infiltration has a moderate effect on footing heave. The heave decreases by 8% with increase of infiltration distance by 100%.

Similarly, Figures (5.43) and (5.44) present the effect of infiltration distance on footing heave under 20kPa and 100kPa footing pressure respectively. The relationship between heave and infiltration distance is linear. According to Figures (5.43) and (5.44), the effect of footing pressure and footing width is considered negligible. Furthermore, study illustrates the high significance of increasing infiltration distance from footing to avoid the intolerable heave of foundation. The increasing of infiltration distance may by performed using impermeable platform around the buildings. Also, horizontal barriers around the buildings have a significant effect on reducing footing heave.

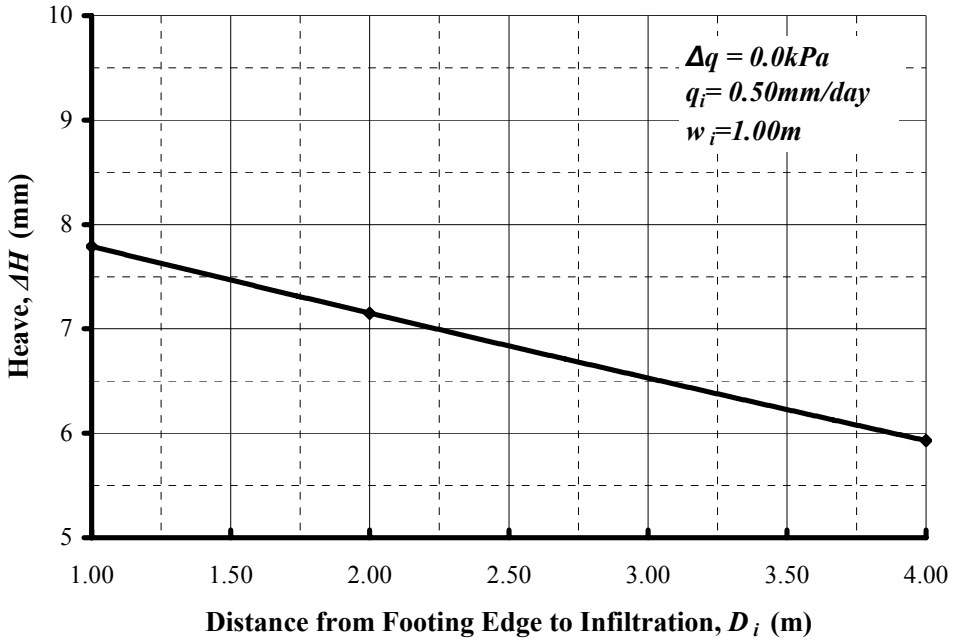

Figure (5.42): Effect of Infiltration Distance, D_i on Footing Heave
under Zero footing Pressure, 0.50mm/day Infiltration Rate and 1.00m Infiltration Width

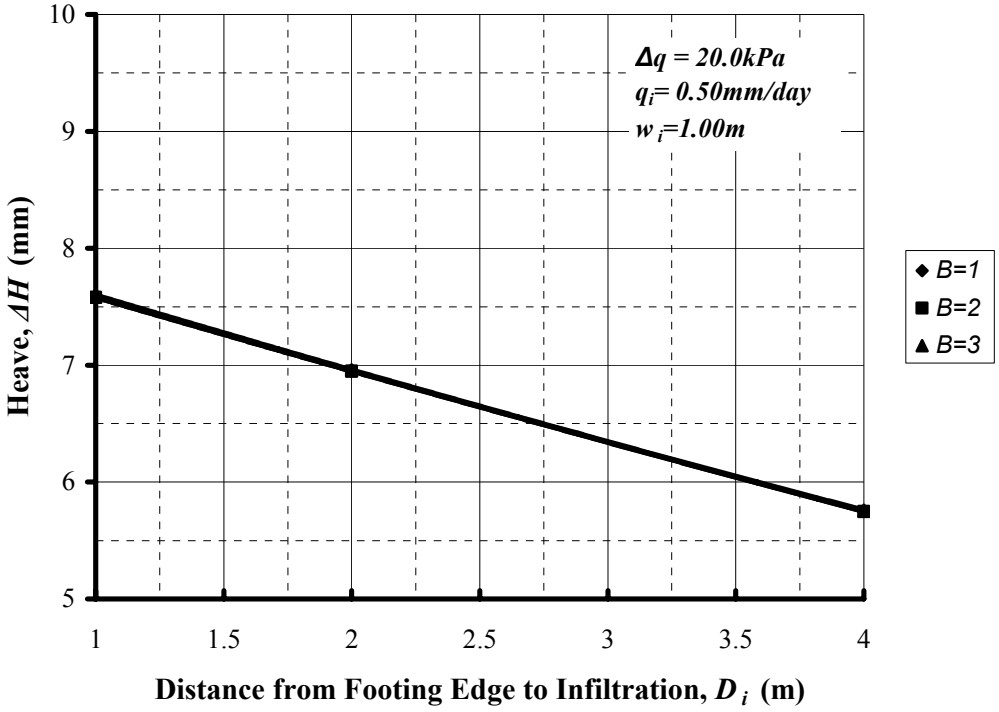

Figure (5.43): Effect of Infiltration Distance, D_i on Footing Heave
under 20kPa footing Pressure, 0.50mm/day Infiltration Rate and 1.00m Infiltration Width

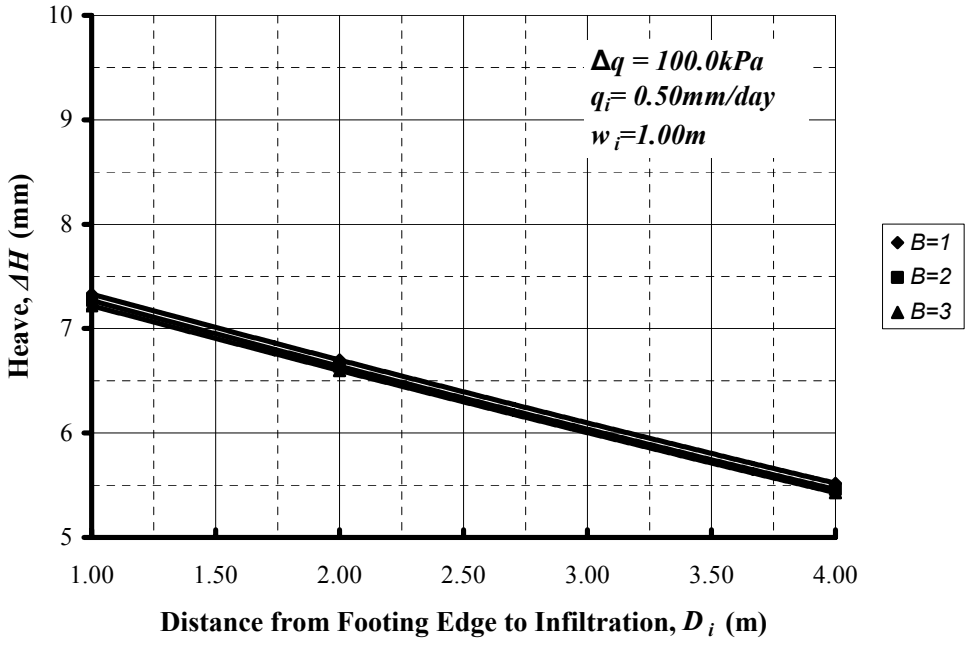

Figure (5.44): Effect of Infiltration Distance, D_i on Footing Heave
under 100kPa footing Pressure, 0.50mm/day Infiltration Rate and 1.00m Infiltration Width

5.7.2.2 Effect of Infiltration Width, w_i

The effect of infiltration width on the footing heave is studied to asses its significance on the foundation heave. Figure (5.45) presents the relationship between heave of edge point of footing adjacent to the infiltration area and infiltration width for different infiltration distance in case of zero footing pressure and 0.50 mm/day infiltration rate. The heave increases nonlinearly with increasing of infiltration width. Footing heave increases by 100% when infiltration width increases from 1.0 to 3.0 m (i.e., by 200%) for 0.50mm/day tree water demand and 1.0 m infiltration distance. The slope of relationship decreases with increasing of infiltration distance. The effect of infiltration width is more significant for smaller infiltration distance. Figure (5.46) presents the relationship between heave of footing edge and infiltration width for different infiltration distance, 2.00m footing width, 60 kPa footing pressure, and 0.50 mm/day infiltration rate. Based on results shown in Figure (5.46), it is noted that footing heave slightly decreases with increase of footing pressure.

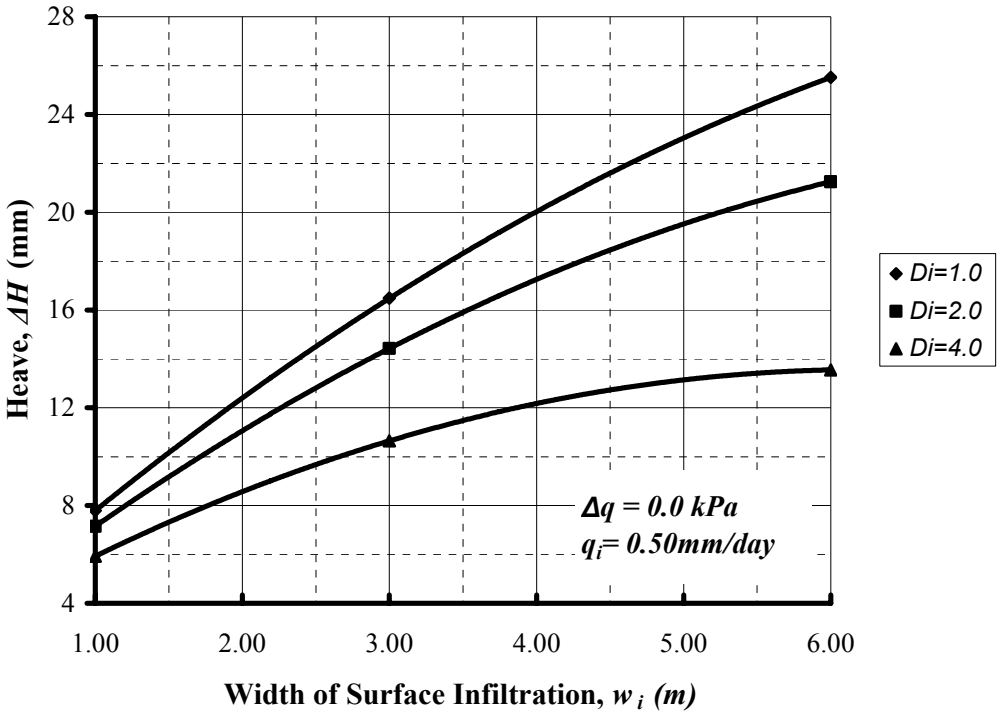

Figure (5.45): Effect of Infiltration Width, w_i on Footing Heave under Zero footing Pressure, 0.50 mm/day Infiltration Rate

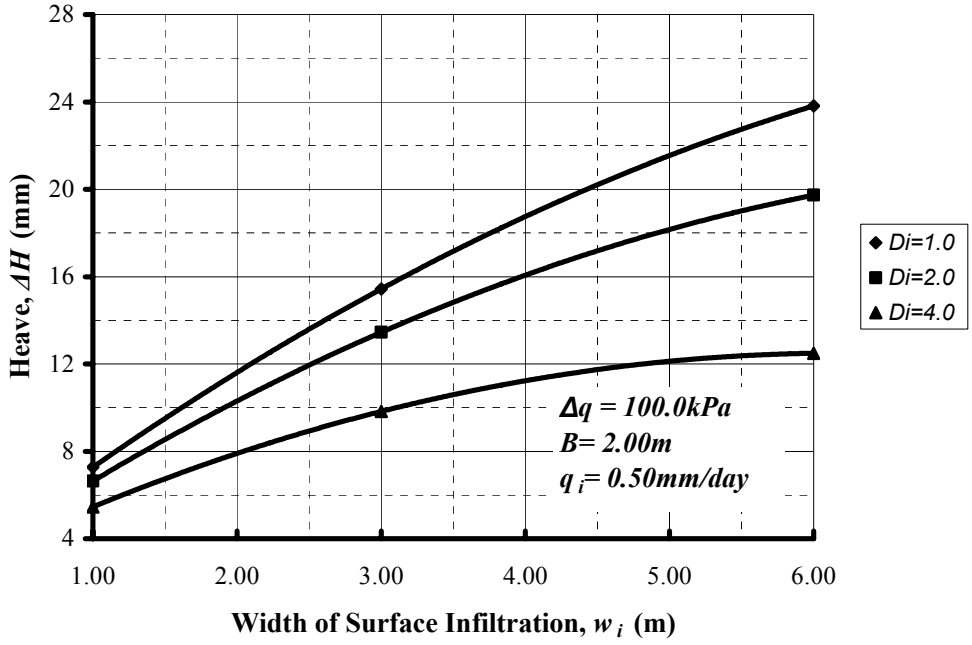

Figure (5.46): Effect of Infiltration Width, w_i on Footing Heave
under 100kPa footing Pressure, 0.50mm/day Infiltration Rate and 2.00m footing Width

5.7.2.3 Infiltration Rate Effect, q_i

Infiltration rate is considered one of the most important parameters of infiltration process. The effect of infiltration rate on the heave of footing has been modeled using the modified CRISP to investigate the significance of its effect. Figure (5.47) and Figure (5.48) present the relationship between the heave of footing edge adjacent to the infiltration area and infiltration rate for 2.00m footing width, 3.00m infiltration width, and 60 and 100 kPa footing pressure; respectively. Based on these figures, it is apparent that heave increases nonlinearly with increase of infiltration rate. The relationship curves showed very steep slope indicating that, infiltration rate is a highly significant parameter. In other words, the heave increases by 85% when rate of infiltration increases from 2.00 to 3.00 mm/day (i.e., increase by 50%).

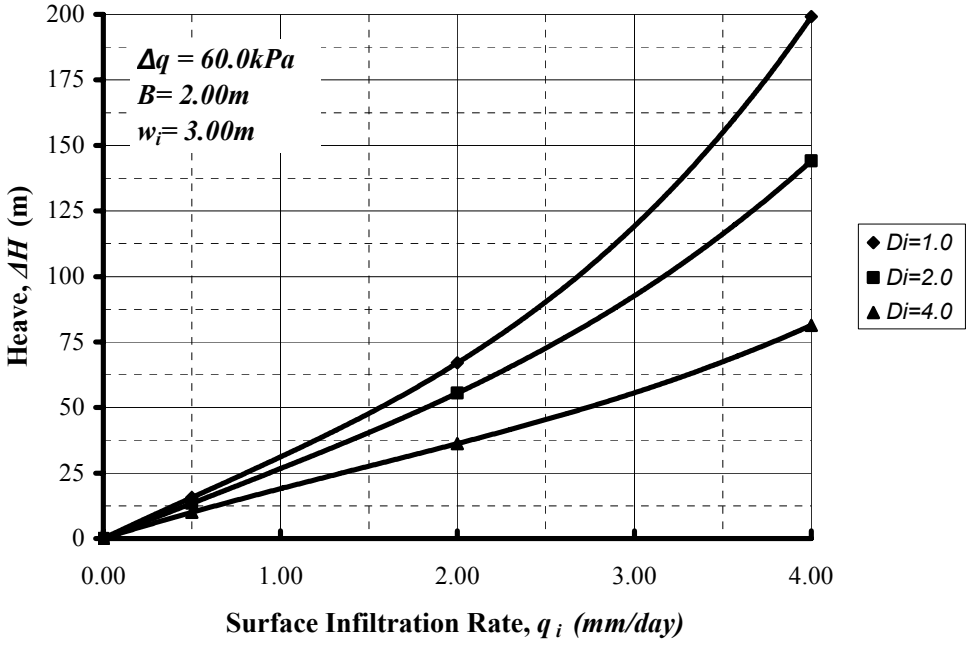

Figure (5.47): Effect of Infiltration Rate, q_i on Footing Heave
under 60kPa footing Pressure, 3.00m Infiltration Width and 2.00m footing Width

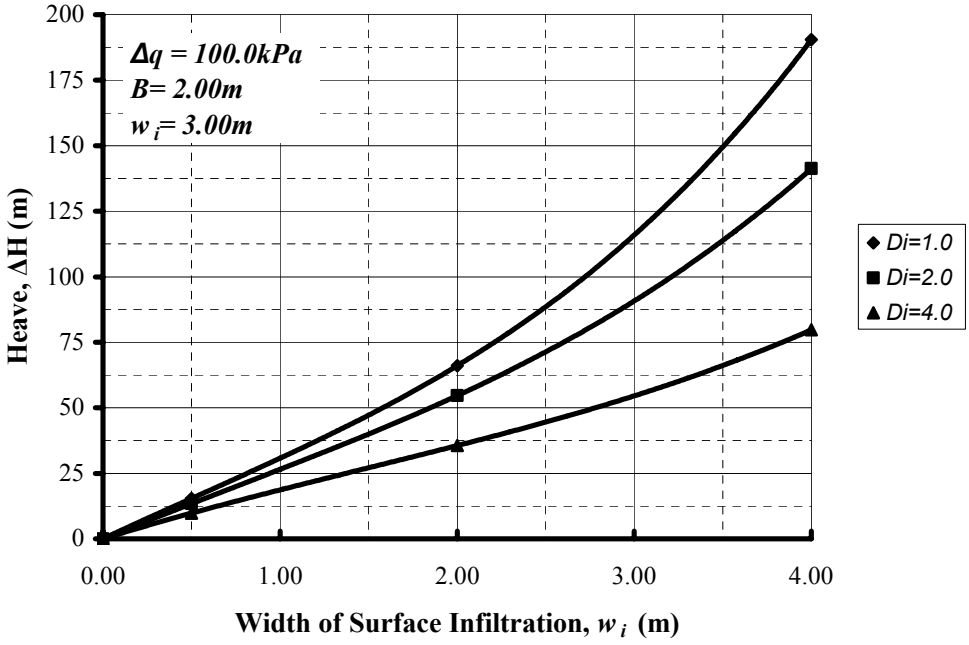

Figure (5.48): Effect of Infiltration Rate, q_i on Footing Heave
under 60kPa footing Pressure, 3.00m Infiltration Width and 2.00m footing Width

5.7.2.4 Summary

The parametric study for the effect of infiltration parameters on footing heave indicates the importance of infiltration rate which depend on rainfall rate and soil properties. Consequently, the effect of infiltration rate should be taken into account during the design of light loaded structures and pavements. Also, the study illustrates the high significance of infiltration distance and width to avoid the building damage due to heave. The infiltration around building may be decreased by decreasing infiltration width and decreasing infiltration distance which, may performed through reduction of planting areas and using horizontal barrier. Also the permeability of top layer of soil may be decreased using soil improvement techniques to decrease infiltration and increase water runoff. Table (5.18) summarized the effect of infiltration parameters on heave of shallow foundation.

Table (5.18): Effect of Water Infiltration Parameters on Heave of Shallow Foundation

Parameter	Symbol	Relation	Change in footing heave due to increase of parameter	Significance
Infiltration distance	D_i	Non-linear	Decrease	High
Infiltration Width	w_i	Non-linear	Increase	High
Infiltration rate	q_i	Linear	Increase	Very High
Footing width	B	Non-Linear	Decrease	Insignificant
Footing pressure	Δq	Non-Linear	Decrease	Insignificant

5.8 Pipe Leakage Effect

Leaks in sewer or water lines into expansive soils provide localized source of water result in localized heave of foundation that may lead to differential movement between footings. If water or sewage pipes break, then the resultant leaking moisture could exacerbate swelling damage to nearby structures. Rogers et al. (1993) reported that shallow pipes, especially plastic pipes, buried in the zone of seasonal moisture fluctuation, were exposed to enormous stresses by shrinking soils. Stresses from soil shrinking caused small cracks of pipes and leak of water through these cracks. Consequently, localized heaving near the leak due to change of soil moisture led to structural damage to nearby light structures such as cracks, floor humps, and movement of foundation. Pryke (1975) reported that for a site leak near light structures, particularly near foundations, heave was severe especially during rainy seasons.

A two-dimensional finite element model experimented by Li (2006) indicated that a leaking underground water pipe could cause more severe distortion of the footing than the seasonal climate changes. It also showed that a water pipe leaking directly beneath the footing could cause a much larger distortion in the foundation than if it had leaked outside of the footing (Li, 2006).

Using numerical modeling, Sorochan and Kim (1994) showed that wetting of expansive soil creates vertical and horizontal stresses that can ultimately crack objects enclosed in the soil. Moreover, the lateral pressure component associated with swelling increases with increase of vertical load. The load prevents loosening of the soil, leading to a stress increase in the backfill around the structure. This is especially true for water and sewage lines, where even minor damage can create leaks, once a leak occurs; the water saturates the soil next to the leak, compounding the problem by causing continued expansion.

5.8.1 Results of Pipe Leakage Effect

The effect of different pipe leakage parameters on footing heave was studied. The different parameters that effect footing heave due pipe leakage include depth of leaking pipe below foundation level, D_P, and distance of leaking pipe from footing edge, L_P. Footing width, B, and footing pressures, Δq, were also considered in these analyses. Figure (5.49) presents the definition of these parameters and dimensions of finite element mesh used in the analysis. The proposed values for these parameters are provided as shown in Figure (5.50).

The depth and distance of the leaking pipe with respect to foundation are selected according to the usual practice in Egypt.

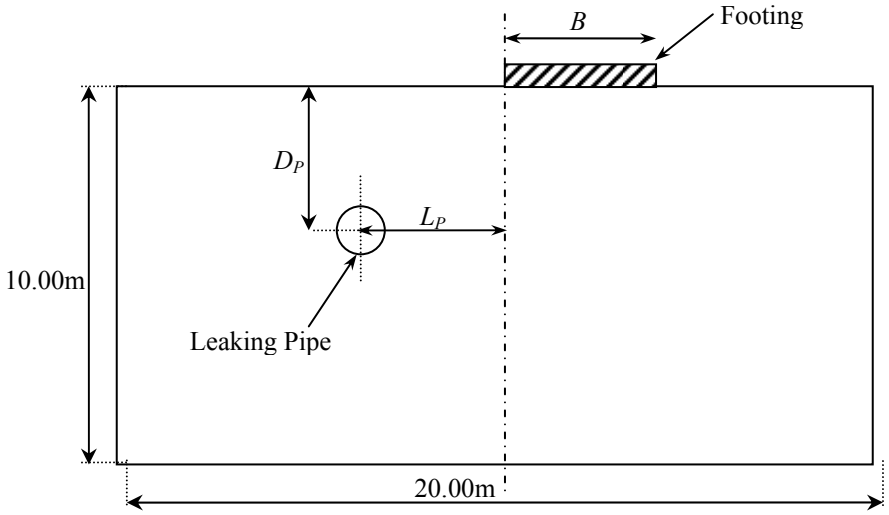

Figure (5.49): Parameters of Pipe Leakage and Dimensions of Finite Element Mesh

The effect of pipe leakage on soil suction change was modeled using seepage analysis. The leaking pipe is simulated in seepage analysis by applying zero-pressure head on nodes of finite element grid defining the boundaries of the pipe. The zero-pressure head is applied at all nodes at 1m distance from the pipe center line. The initial soil suction profile was assumed to be hydrostatic with 1500kPa (4.2pF) which represents wilting point of vegetation at ground surface and simulates dry conditions. Pipe leakage results in a decrease of soil suction around the leaking pipe. The final soil suction profiles estimated using SEEP/W for different pipe depths and for 4.00 m pipe distance from footing edge are presented in Figures (5.51) to (5.53). Footing heave was estimated using stress-deformation analysis with Modified CRISP.

Results of analysis for the effect of pipe leakage parameters such as, depth of leaking pipe below foundation level and distance of pipe from footing edge on the heave of shallow foundation are presented in Tables from (5.19) to (5.21). Furthermore, the effect of footing width and footing pressures are included in the tables. Table (5.19) presents the expected footing heave for different footing pressures, footing widths, and different pipe distances and for 1.00m depth of leaking pipe below foundation level. Similarly, Tables (5.20) and (5.21) presented the expected footing heave for 4.00m and 6.00m depth of leaking pipe; respectively.

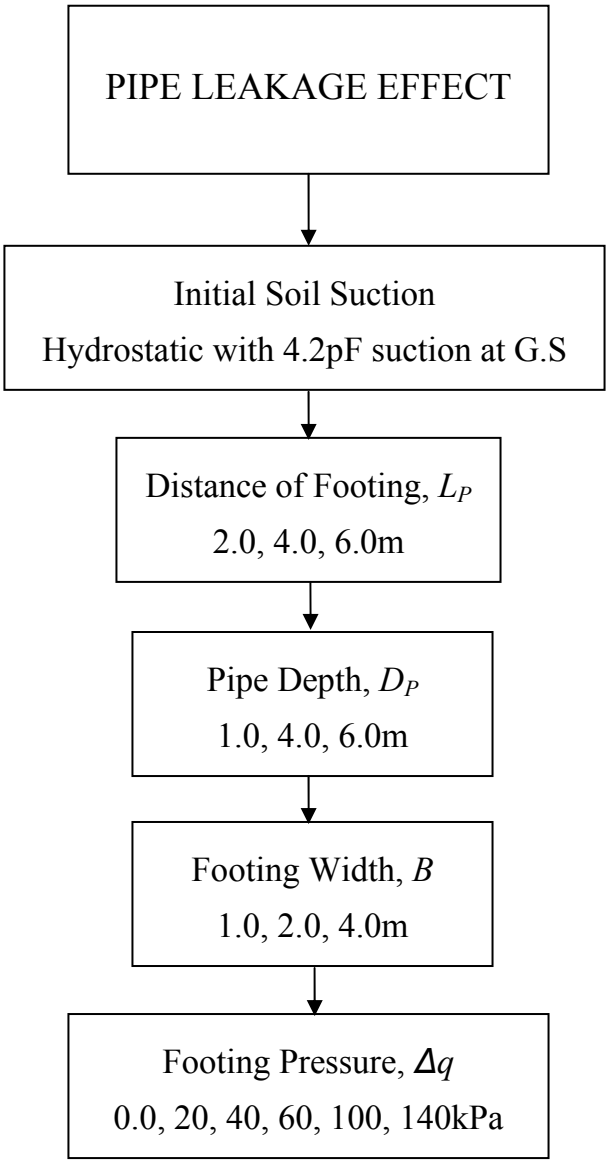

Figure (5.50): Pipe Leakage Effect Study

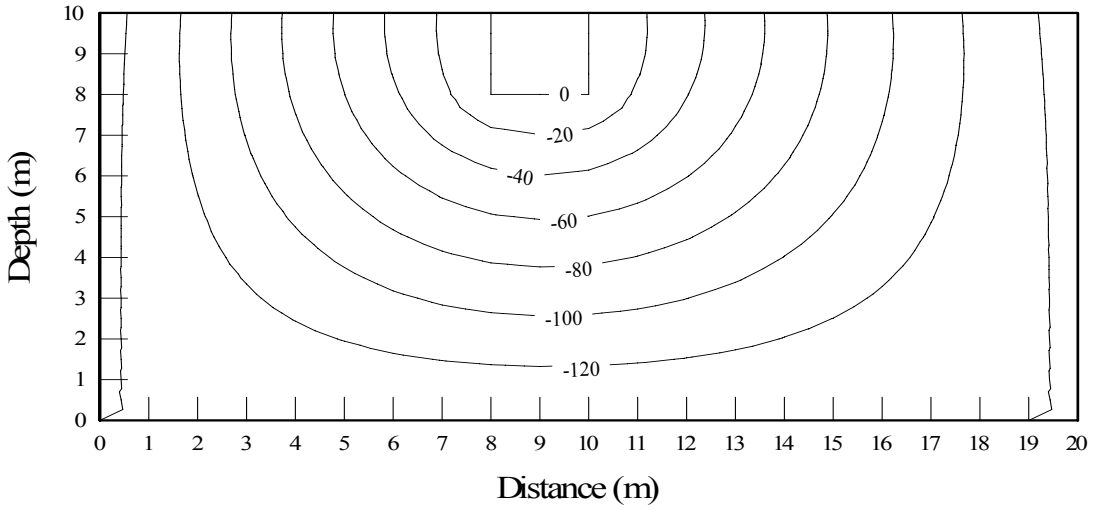

Figure (5.51): Final Soil Suction Profile for 1.00 m Depth Leaking Pipe

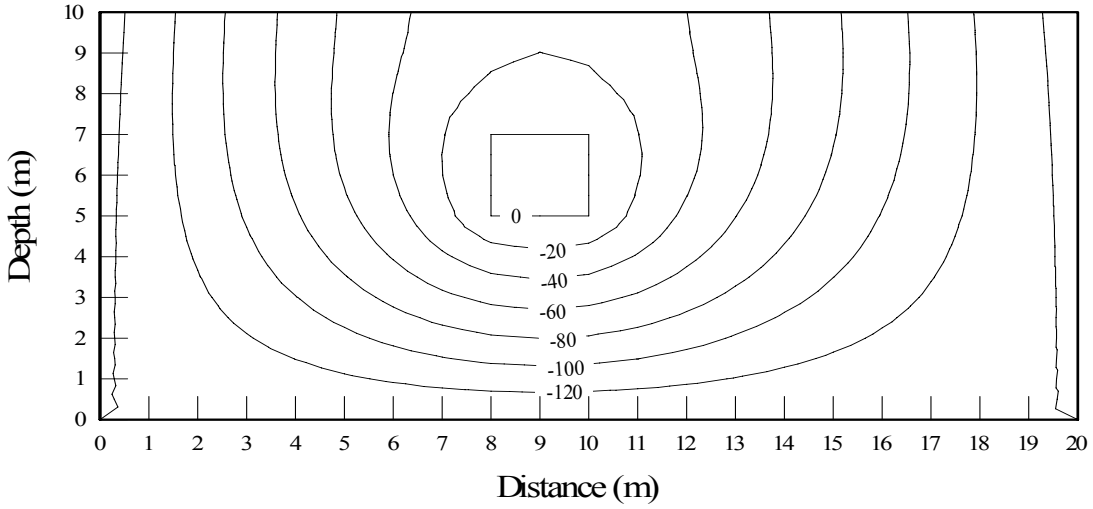

Figure (5.52): Final Soil Suction Profile for 4.00 m Depth Leaking Pipe

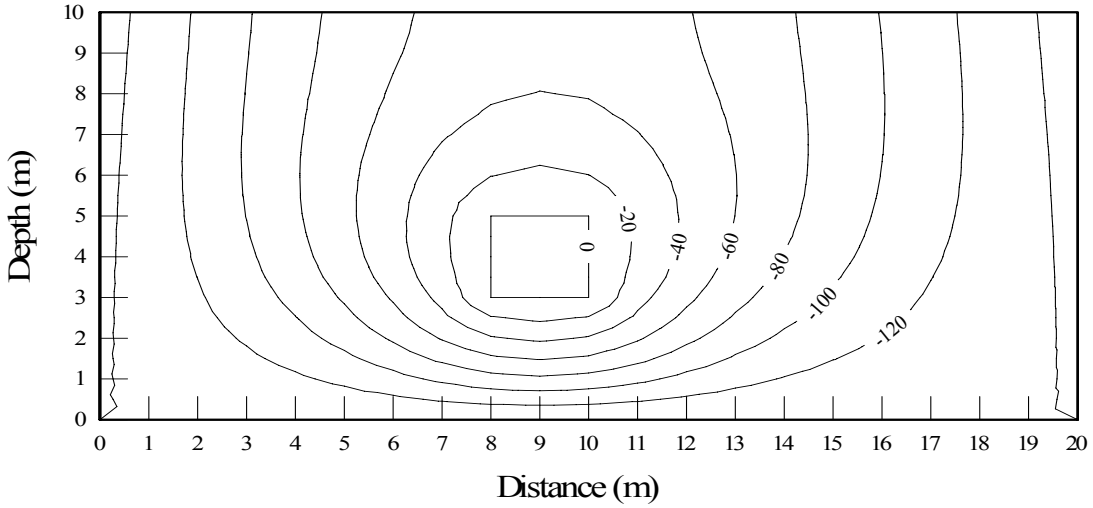

Figure (5.53): Final Soil Suction Profile for 6.00 m Depth Leaking Pipe

Table (5.19): Footing Heave for 1.00m Depth of Leaking Pipe

Footing Width, (m)	1.00			2.00			4.00		
Pipe Distance L_p, (m) / Footing Pressure, Δq, (kPa)	2.00	4.00	6.00	2.00	4.00	6.00	2.00	4.00	6.00
0.0	143.76	97.33	69.07	143.76	97.33	69.07	143.76	97.33	69.07
20	140.85	94.55	66.55	140.49	94.33	66.33	140.45	94.35	66.23
40	139.14	93.04	65.16	138.42	92.55	64.62	138.1	92.37	64.16
60	137.91	91.99	64.17	136.9	91.31	63.42	136.33	90.92	62.47
100	136.07	90.49	62.75	134.64	89.52	61.66	133.71	88.81	60.21
140	134.67	89.41	61.71	132.96	88.26	60.38	131.7	87.29	58.44

Table (5.20): Footing Heave for 4.00m Depth of Leaking Pipe

Footing Width, (m)	1.00			2.00			4.00		
Pipe Distance L_p, (m) / Footing Pressure, Δq, (kPa)	2.00	4.00	6.00	2.00	4.00	6.00	2.00	4.00	6.00
0.0	167.31	130.27	97	167.31	130.27	97	167.31	130.27	97
20	166.55	127.86	94.13	165.92	127.41	93.72	165.47	127.17	93.44
40	165.74	126.42	92.47	164.55	125.51	91.62	163.53	124.83	90.74
60	165.01	125.36	91.26	163.34	124.09	90.05	161.85	122.99	88.61
100	163.66	123.74	89.47	161.25	121.91	87.71	159.04	120.17	85.29
140	162.46	122.48	88.11	159.5	120.26	85.93	156.7	118	82.75

Table (5.21): Footing Heave for 6.00m Depth of Leaking Pipe

Footing Width, (m)	1.00			2.00			4.00		
Pipe Distance L_p, (m) / Footing Pressure, Δq, (kPa)	2.00	4.00	6.00	2.00	4.00	6.00	2.00	4.00	6.00
0.0	143.43	120.44	94.95	143.43	120.44	94.95	143.43	120.44	94.95
20	143.56	118.97	92.63	143.12	118.55	92.21	142.71	118.26	91.89
40	143.33	118.03	91.26	142.51	117.1	90.41	141.64	116.43	89.45
60	143.04	117.31	90.25	141.89	116	89.04	140.62	114.94	87.48
100	142.41	116.17	88.73	140.7	114.22	86.93	138.79	112.56	84.36
140	141.78	115.24	87.55	139.62	112.8	85.29	137.2	110.67	81.91

5.8.2 Analysis of Results Pipe Leakage Effect

The effect of each parameter associated with pipe leakage is studied and analyzed to estimate its significance on footing heave. The relationships between footing heave and pipe leakage parameters are presented graphically to predict its order of magnitude.

In general, the results indicate that the distance of leaking pipe from footing edge, L_P and depth of leaking pipe below foundation level, D_P, have a significant effect on the footing heave. However, the footing width and footing pressures have insignificant effect on footing heave. Detailed analyses of pipe leakage parameters are presented herein.

5.8.1.1 Effect of Depth of Leaking Pipe below Foundation Level, D_P

Figure (5.54) illustrates the variations of footing heave with depth of leaking pipe below foundation level. As shown in Figure (5.54), increase of leaking pipe depth results in increase of heave to a maximum value, after which, further increase in leaking pipe depth results in decrease in footing heave. In other words, there is a critical pipe depth at which the heave is expected to be maximum. Thus, the selected in-situ depth of pipe should be selected shallower or deeper than the critical depth. It is also noted that the critical depth depends on the distance of leaking pipe from the footing. Increase of leaking pipe distance leads to higher critical depth as shown in Figure (5.54). Furthermore, increase of leaking pipe distance increases the effect of pipe depth. For example, footing heave increases by 30% when pipe depth increase from 1.00 to 3.00m for 4.00 pipe distance where it increases by 16% for 2.00 pipe distance.

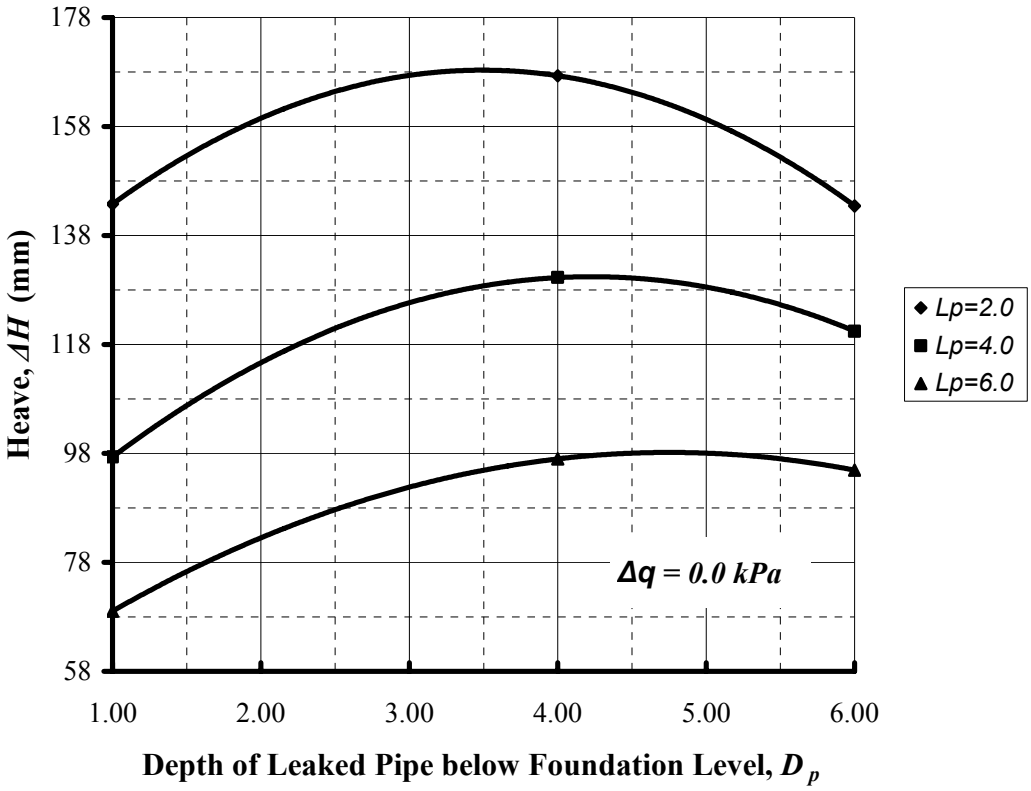

Figure (5.54): Effect of Leaking Pipe Depth, D_P on Footing Heave under Zero Applied Pressures

Figures (5.55) and (5.56) illustrate the effect of leaking pipe depth on footing edge heave under 60 and 100 kPa footing pressures; respectively and for 2.00 m footing width. According to these figures, it is observed that the relationship between the leaking pipe depth and footing heave is similar to that shown in Figure (5.54) for zero footing pressure. The relationships indicate that there is a critical soil depth where heave is maximum; however, the critical depth is independent from footing pressure. Increase of footing pressure has insignificant effect on heave change due to pipe depth change. For example, footing heave increase by the same percent (30%) for zero and 60 kPa footing pressure for 4.00m leaking pipe distance when leaking pipe depth changes from 1.00 to 3.00 m.

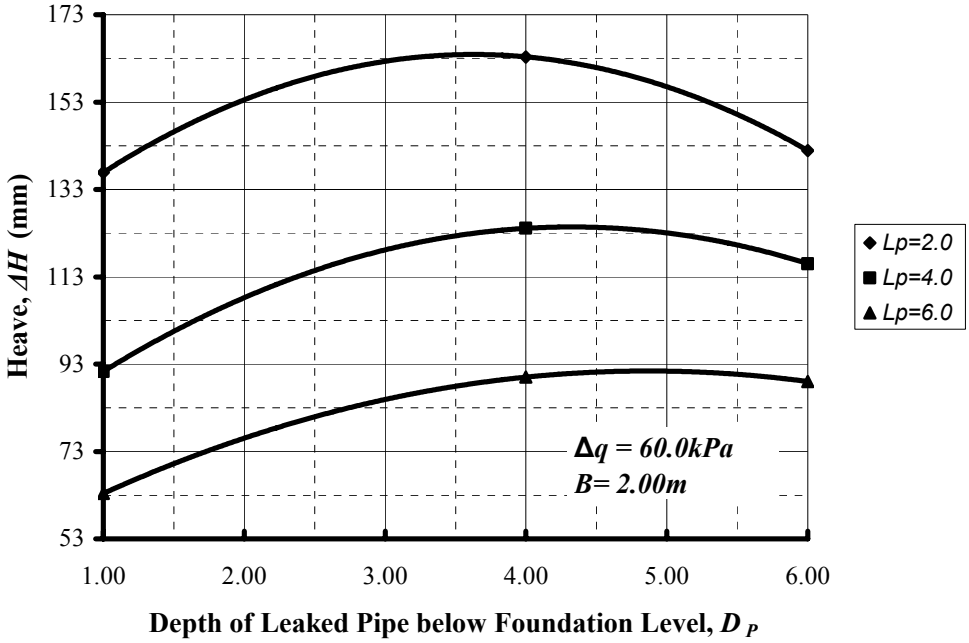

Figure (5.55): Effect of Leaking Pipe Depth, D_P on Footing Heave under 60 kPa Footing Pressure for 2.0 m Footing Width

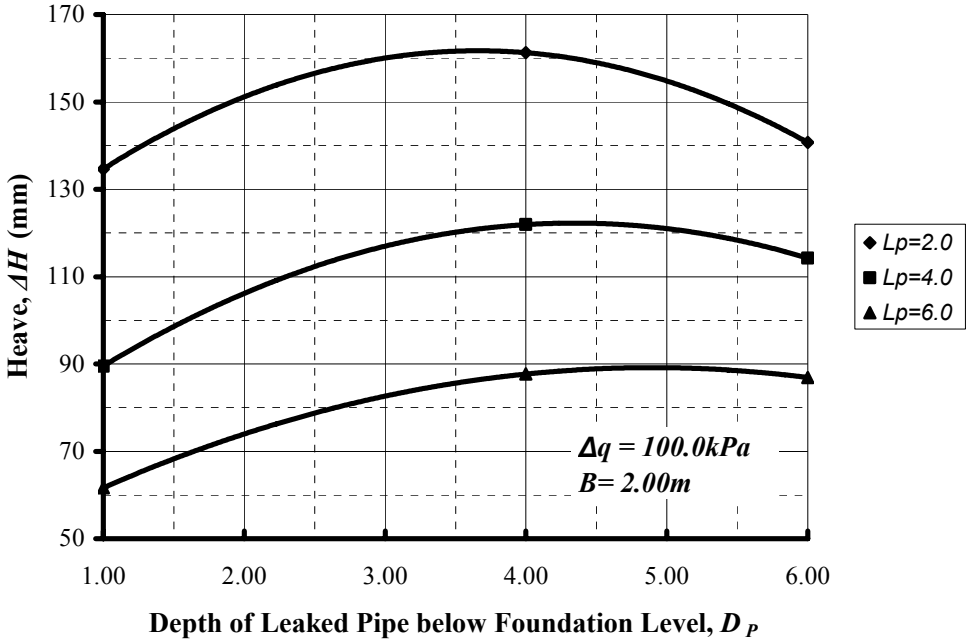

Figure (5.56): Effect of Leaking Pipe Depth, D_P on Footing Heave under 100 kPa Footing Pressure for 2.0m Footing Width

5.8.2.2 Effect of Distance of Leaking Pipe from Footing Edge, L_P

Figure (5.57) presents the effect leaking pipe distance from footing edge on footing edge heave under zero footing pressure. According to the results shown in this figure, distance of leaking pipe has a significant effect on footing heave. Increase in leaking pipe distance by 33% (from 3.00 to 4.00 m) leads to decrease of footing heave by 18%. Furthermore, the relationship between distance of leaking pipe form footing and footing heave is linear.

Under different footing pressures, Figure (5.58) and (5.59) presents the effect of leaking pipe distance on footing heave for 60 and 100kPa footing pressure; respectively. Also, the relationship between leaking pipe distance form footing and footing edge heave is linear under different footing pressures.

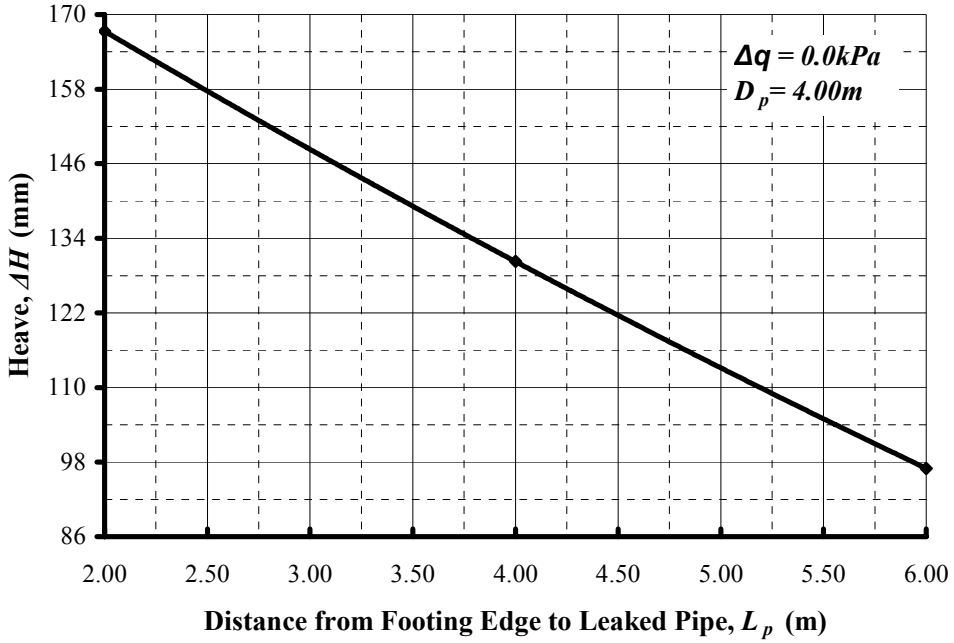

Figure (5.57): Effect of Leaking Pipe Distance, L_P on Footing Edge Heave under Zero Applied Pressure

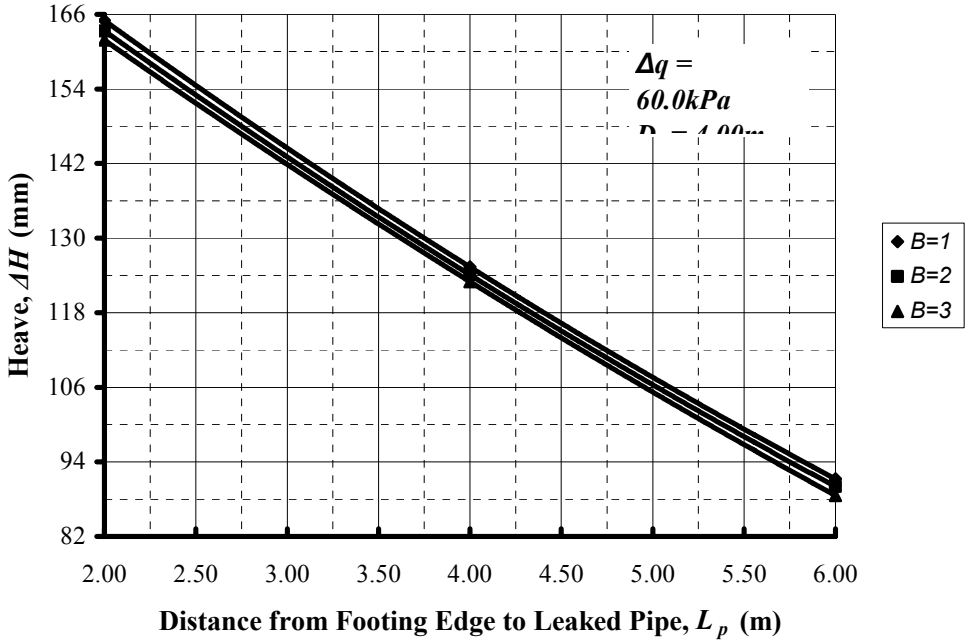

Figure (5.58): Effect of Leaking Pipe Distance, L_P on Footing Edge Heave under 60 kPa Footing Pressure for 4.00 m Pipe Depth

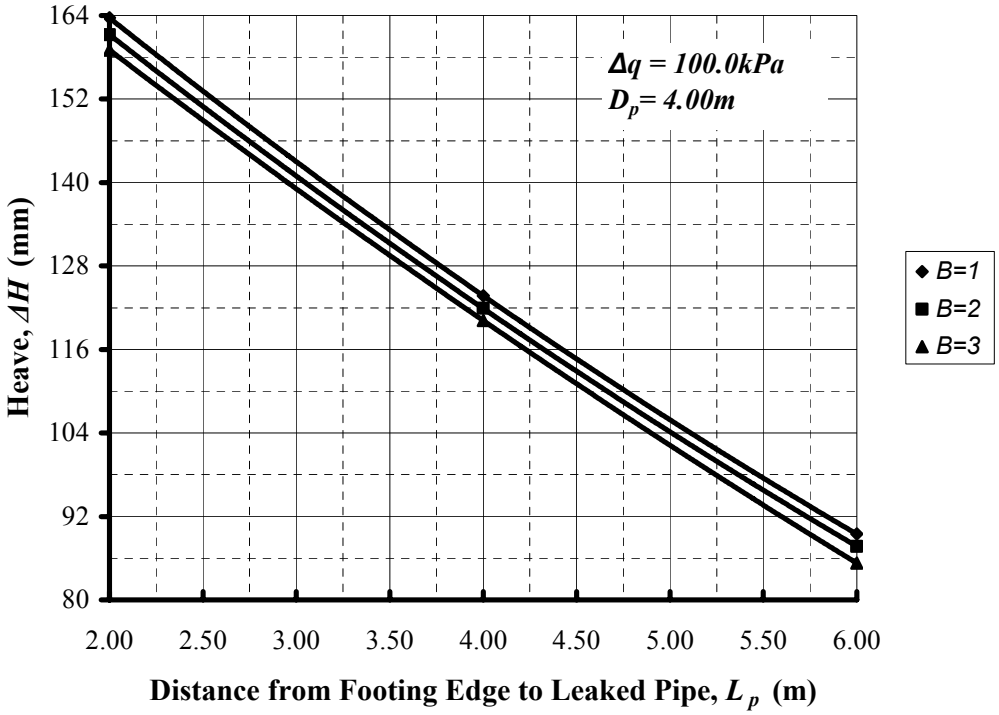

Figure (5.59): Effect of Leaking Pipe Distance, L_P on Footing Edge Heave under 100 kPa Footing Pressure for 4.00 m Pipe Depth

5.8.2.3 Effect of Footing Width, *B*

Figure (5.60) presents the effect of footing width on footing heave due to pipe leakage under different pressures for 1.00 m pipe depth and 2.00 m pipe distance. It is observed that, the effect of footing width on heave is insignificant. For example, the increase of footing width from 1.00 to 4.00 m (i.e. 300%) leads to 2% heave decrease under 140 kPa footing pressure. Furthermore, the effect of footing width on footing heave deceases with increasing of footing pressure.

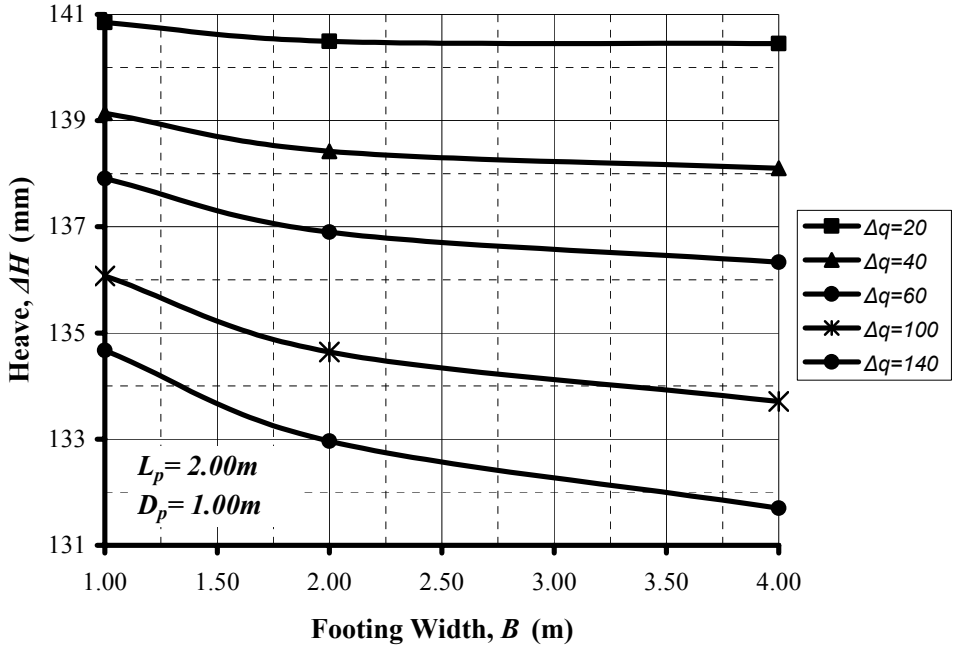

Figure (5.60): Effect of Footing width, *B* on Footing Edge Heave for 2.0m Pipe Distance and 1.00m Pipe Depth

5.8.2.4 Effect of Footing Pressure, Δq

The effect of footing pressure on the footing heave is studied and presented graphically. Figure (5.61) presents the results for heave versus footing pressure for 1.0m leaking pipe depth and 2.00m leaking pipe distance. According to this figure, footing heave decreases with increase of footing pressure. For example, heave decreases by 1% when pressure increases by 50% (from 40 to 60 kPa). Results indicate that footing pressure has insignificant effect on footing heave.

Figures (5.62) and (5.63) present the results for 4.0m and 6.0m pipe distance respectively, for 1.00m footing width. Also, results indicate that the footing pressure has insignificant effect on footing heave.

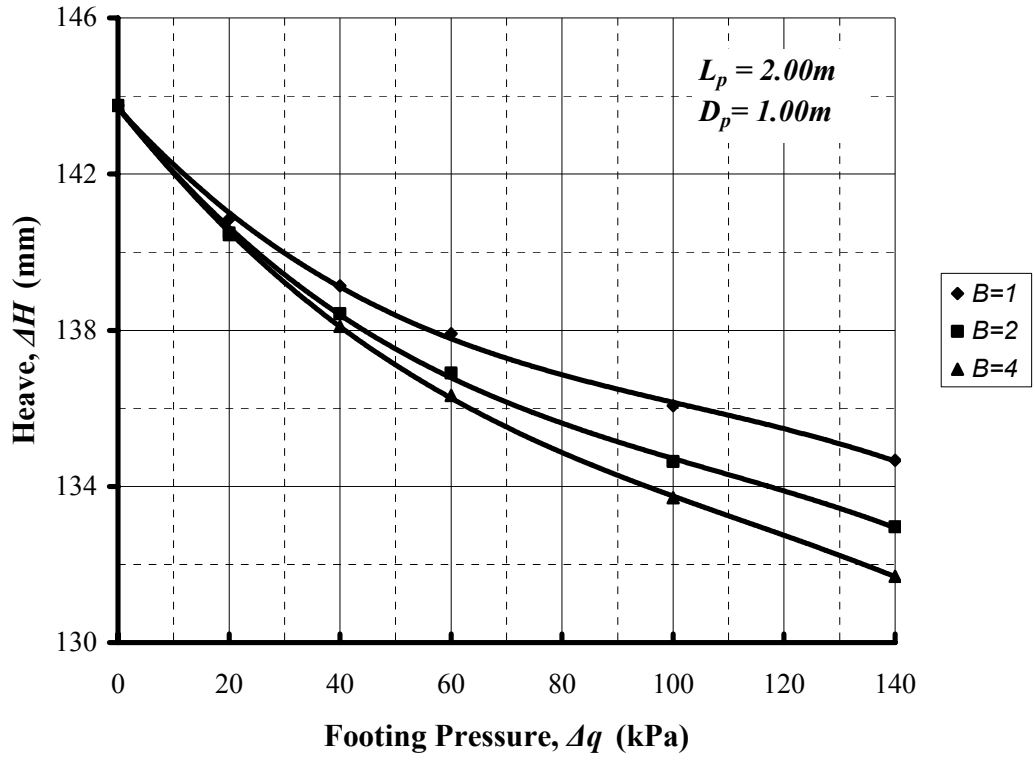

Figure (5.61): Effect of Footing Pressure, Δq on Footing Edge Heave for 1.00 m Pipe depth and 2.00 m Pipe Distance

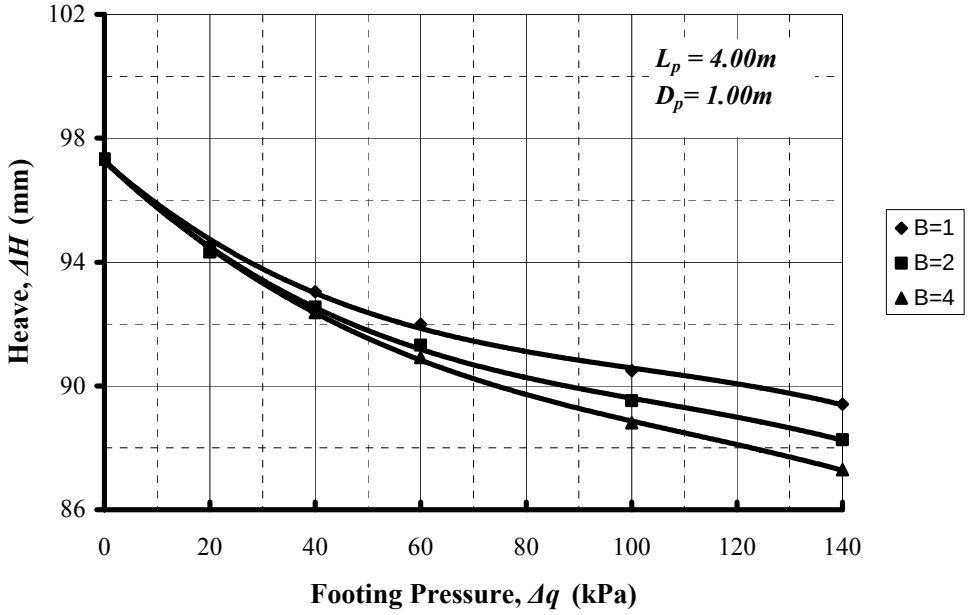

Figure (5.62): Effect of Footing Pressure, Δq on Footing Edge Heave for 1.00 m Pipe depth and 4.00 m Pipe Distance

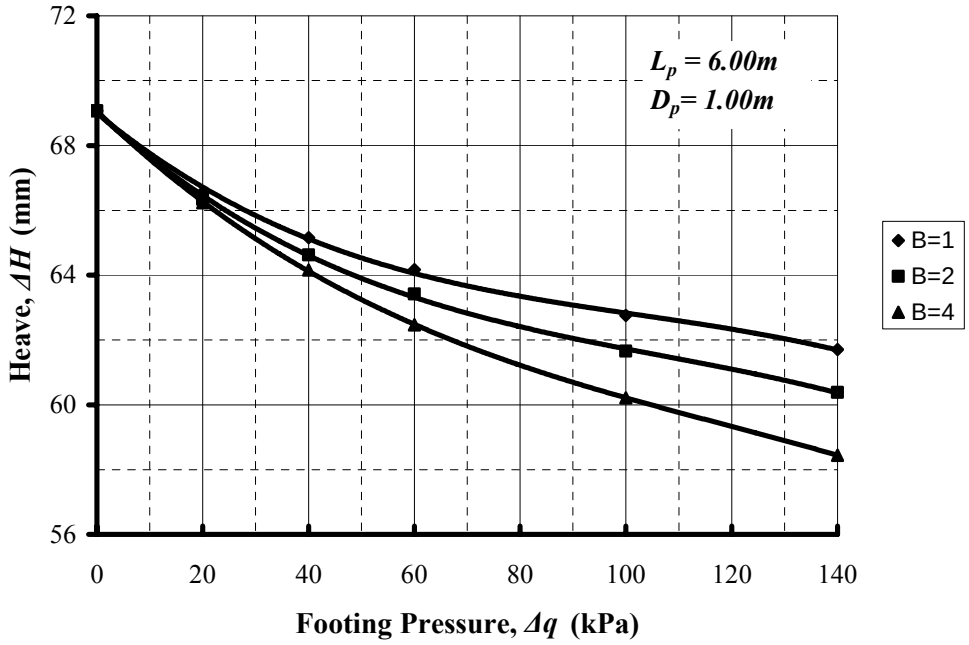

Figure (5.63): Effect of Footing Pressure, Δq on Footing Edge Heave for 1.00m Pipe depth and 6.00m Pipe Distance

5.8.2.5 Summary

The parametric study for the parameters associated with pipe leakage conditions and shallow foundation dimension and loading shows that there is critical depth of leaking pipe at which heave is maximum. Furthermore, the distance leaking pipe from footing edge has a considerable effect in footing. However, footing pressure and footing width have negligible effects on footing heave due to high suction changes from leaking pipes. Table (5.22) summarized the effect of pipe leakage parameters on shallow foundations.

Table (5.22): Effect of Pipe Leakage on Heave of Shallow Foundations.

Parameter	Symbol	Relation	Change of heave due to increase of the parameter	Significance
Leaking Pipe Depth	D_P	Non-linear	Increase/Decrease	High
Leaking Pipe Distance	L_P	Linear	Decrease	High
Footing Width	B	Non-linear	Decrease	Insignificant
Footing Pressure	Δq	Non-linear	Decrease	Insignificant

CHAPTER (6)
SAND CUSHION EFFECT

6.1 Introduction

Removal and replacement of expansive soils with non-expansive soils is one the most popular methods to minimize the effect of heave on foundations. Zeitlen (1969), Snethen et al (1979), Chen (1988) and Satyanarayana (1969) have suggested the full removal of expansive soil in case of shallow thickness or partially when it extends to considerable depth to counteract the anticipated heave with an applied load.

Satyanarayana (1969), further reported that pressure under footing due to swelling of clay varies inversely as the thickness of the sand layer and directly as its density. Therefore, generally, sand cushions are formed in their loosest possible state without, however, violating the bearing capacity criterion (Satyanarayana, 1969).

Although soil replacement is considered the most economic solution for expansive soils, there are some disadvantages associated with soil replacement. The main disadvantages are that the required thickness of soil replacement may be too great to be practical. In addition, the high permeability of sand creates conditions conducive to easy entry and accumulation of water from surface runoff thus; granular fill may serve as a source of water to sub-grade soils.

Nelson and Miller (1992) stated that the depth to which non-expansive backfill should be placed is governed by the weight necessary to restrain the expected uplift pressures and the ability of the backfill to mitigate differential displacements. There are no definitive guidelines, for depth of sand cushion, have been developed. Most of the foundation engineers often suggest some arbitrary thickness for the sand cushion without consideration to the depth of the zone of potential volume change which itself is difficult to determine (Nelson and Miller, 1992). Chen (1988) recommends a minimum of 1.00 to 1.30 m for thickness of soil replacement

In this research, a parametric study for the effect of sand cushion on soil settlement and soil heave was performed using the modified CRISP. Regina clay properties were used in this study as presented in the previous chapter. The study was performed under the effect of climate conditions with 3.00 m seasonal moisture fluctuation zone depth and

1.50pF soil suction change at ground surface. Parametric study included the effect of different sand cushion parameters such as; depth, lateral extension, and relative density of sand cushion as shown in (6.1). Illustration of different parameters considered in parametric study is shown in Figure (6.2).

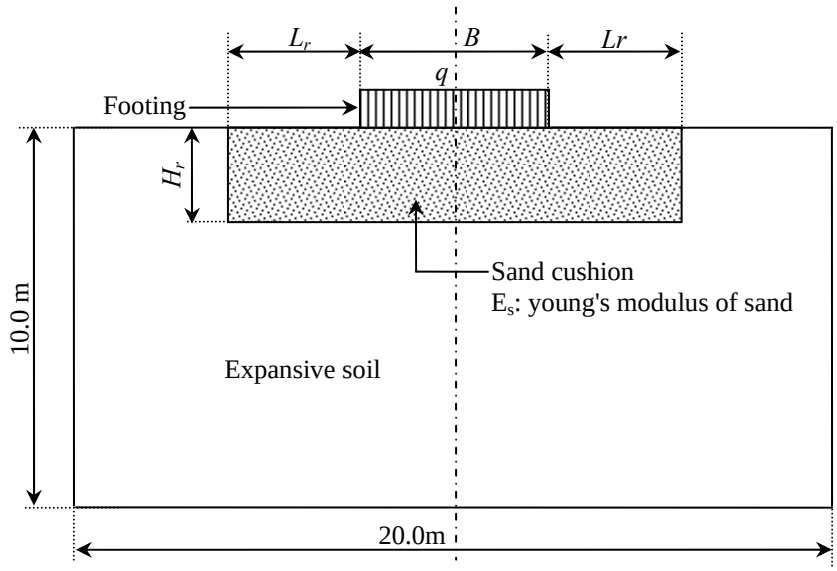

Figure (6.1): Dimensions and Parameters for Sand Cushion Effect

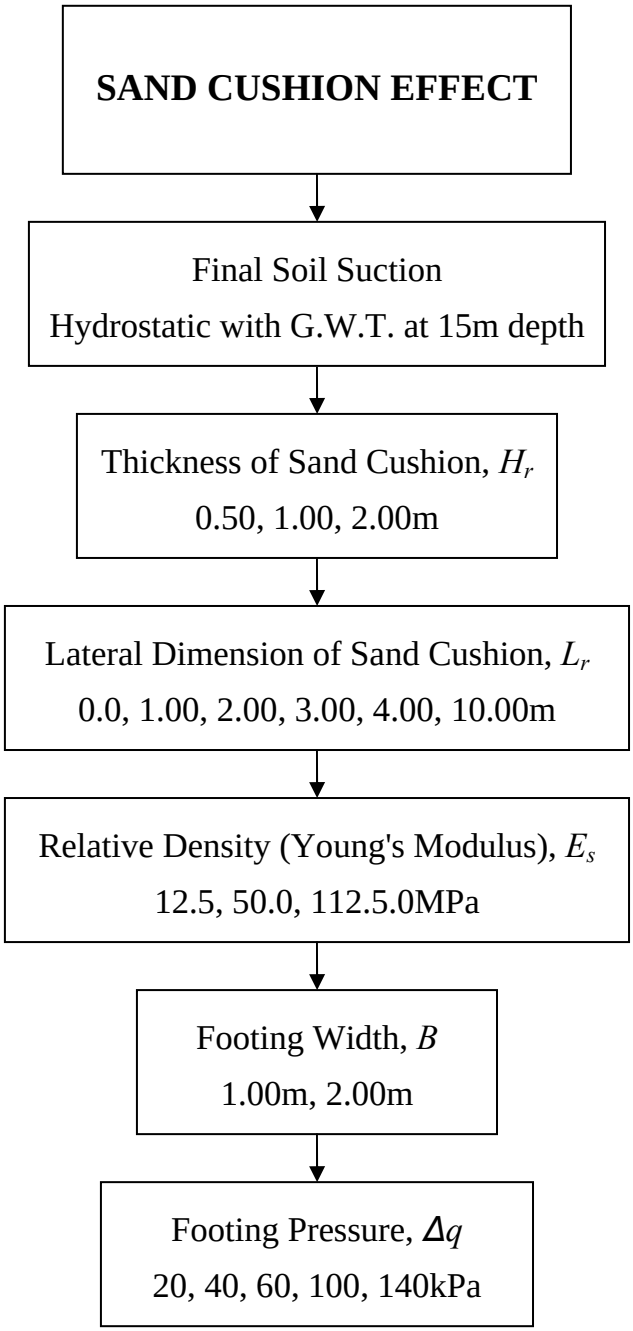

Figure (6.2): Sand Cushion Effect Study

6.2 Effect of Sand Cushion Depth, H_r

As shown in Figure (6.2), the depth of cushion, the depth of cushion was selected to range between 0.50 m and 2.00 m. The lateral extension of sand cushion is assumed to be 10.0 m which represents infinity lateral extension where further increase has insignificant effect (end of model boundary).

The modulus of elasticity of sand cushion used in this analysis equals 50 MPa to simulate medium dense sand. The sand is modeled in analysis using the linear elastic model with Poisson's ratio equals to 0.30.

The loading are applied in two stages. The footing pressure was applied in first stage and soil suction change was applied in the second stage. In second stage, final soil suction is assumed to be hydrostatic with soil suction value of 3.2 pF (150kPa) at ground surface which simulates wet conditions in winter. At the end of the first stage, settlement, ΔS, is estimated due to applying footing pressure. At the end of the second stage, soil heave, ΔH, is estimated due to decrease in soil suction. The results of analysis are summarized in Table (6.1) for 1.00m footing width for different sand cushion depth. The reported results are predicted at the mid point of footing width.

Table (6.1): Footing Displacements for Different Sand Cushion Depth for 1.00m Footing Width

Load (kPa)	H_r =0.50m		H_r =1.00m		H_r =1.50m		H_r =2.0m	
	ΔS	ΔH	ΔS	ΔH	ΔS	ΔH	ΔS	ΔH
0.0	0.00	103.49	0.00	77.22	0.00	52.34	0.00	29.75
20	-10.63	101.33	-6.43	76.22	-4.01	51.93	-3.55	29.52
40	-20.23	99.46	-12.59	75.25	-7.93	51.5	-7.04	29.26
60	-29.95	97.85	-18.53	74.27	-11.78	51.06	-10.48	28.99
100	-45.3	95.17	-29.82	72.44	-19.27	50.17	-17.22	28.43
140	-59.95	92.92	-40.47	70.67	-26.49	49.22	-23.79	27.89

(Note: -ve values represent settlement and +ve values represent heave)

The results of analysis are introduced in Figures (6.3) and (6.4) for 1.00m footing width. Figure (6.3) presents the settlement due to applying footing pressure before applying soil suction. Figure (6.4) presents soil heave due to decrease in soil suction.

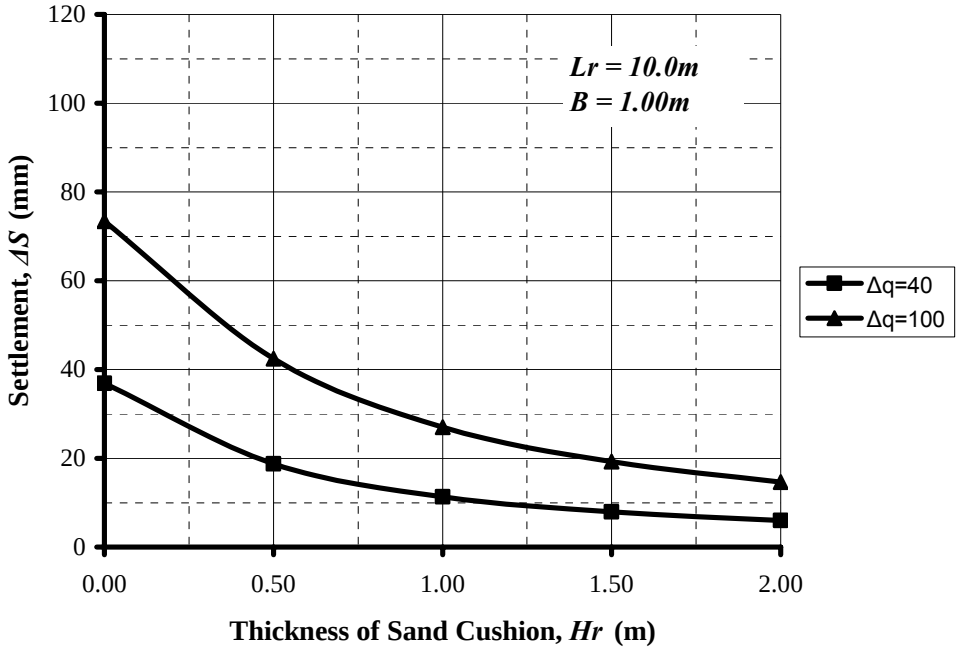

Figure (6.3): Effect of Thickness of Sand Cushion on Footing Settlement
(1.00 m Footing Width and 10.0 m Lateral Extension of Replacement)

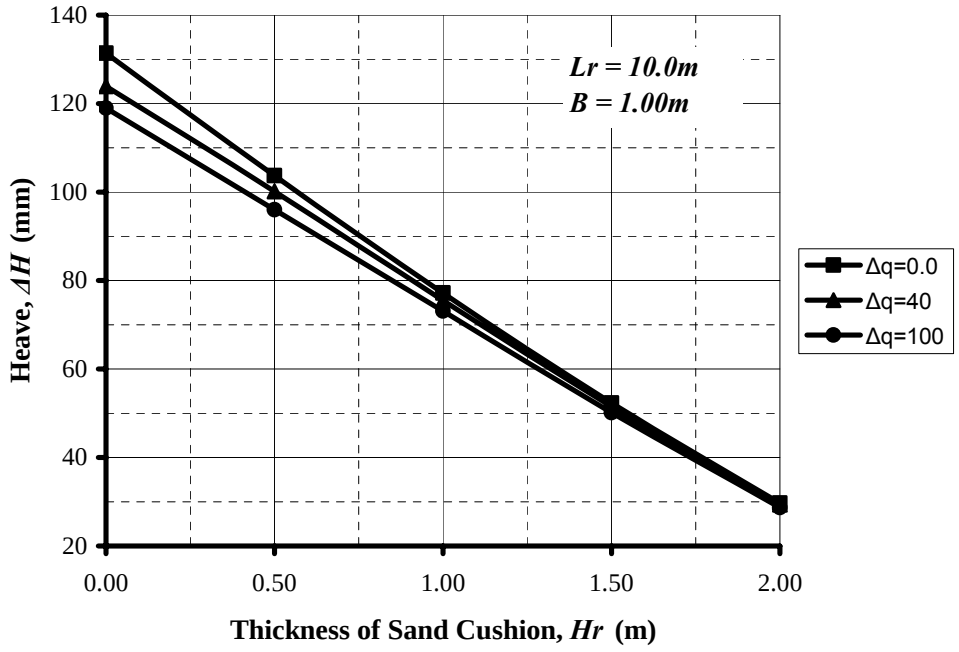

Figure (6.4): Effect of Thickness of Sand Cushion on Footing Heave
(1.00 m Footing Width and 10.0 m Lateral Extension of Replacement)

Similarly, the results of analysis are illustrated in Table (6.2) for 2.00 m footing width for different sand cushion depth. Graphical presentation for results is introduced in Figure (6.5) and Figure (6.6).

Table (6.2): Footing Displacements for Different Sand Cushion Depth for 2.00m Footing Width

Load (kPa)	*Hr* =0.50m		*Hr* =1.00m		*Hr* =1.50m		*Hr* =2.0m	
	ΔS	*ΔH*	*ΔS*	*ΔH*	*ΔS*	*ΔH*	*ΔS*	*ΔH*
0.0	0.00	103.67	0.00	77.21	0.00	52.34	0.00	29.75
20	-18.81	100.12	-11.34	75.52	-7.94	51.5	-3.55	29.52
40	-35.11	97.17	-21.95	73.91	-15.57	50.61	-7.04	29.26
60	-49.78	94.65	-31.96	72.34	-22.93	49.69	-10.48	28.99
100	-72.83	89.87	-50.59	69.09	-36.96	47.75	-17.22	28.43
140	-98.82	85.49	-67.73	66.02	-50.19	45.96	-23.79	27.89

(Note: -ve values represent settlement and +ve values represent heave)

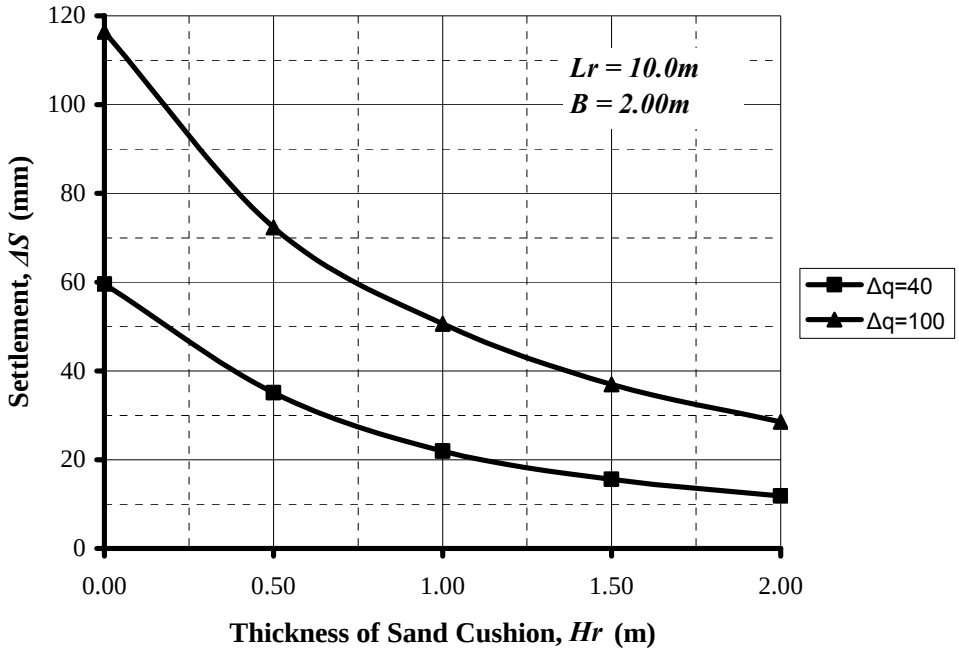

Figure (6.5): Effect of Thickness of Sand Cushion on Footing Settlement (2.00 m Footing Width and 10.00 m Lateral Extension of Replacement)

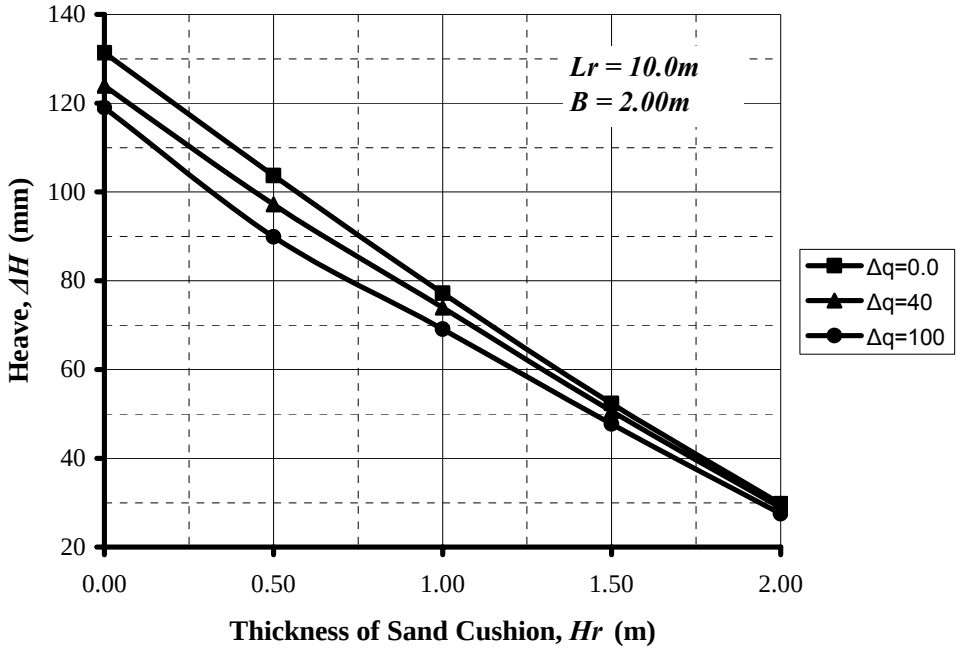

Figure (6.6): Effect of Thickness of Sand Cushion on Footing Heave
(2.00 m Footing Width and 10.00 m Lateral Extension of Replacement)

From the previous results for sand cushion with different depths, it is clear that the sand cushion depth has a significant effect on decreasing soil heave and soil settlement. The relationship between soil heave and depth of sand cushion is linear, where; the relationship between soil settlement and depth of sand cushion is non-linear. Increase replacement depth causes decrease in depth of seasonal moisture fluctuation zone thus, footing heave decreases. Heave decreases by 21% when using 0.50 m depth sand cushion and by 41% when using 1.00 m depth sand cushion for 1.00 m footing depth under zero footing pressure.

From Figures (6.6) and (6.4), it is apparent that, footing width has insignificant effect on the heave of footing especially when using sand cushion. Also, the slope of relationship between soil heave and depth of sand cushion decreases with increasing of footing pressure, thus the effect of sand cushion depth on footing heave decreases with increase of footing pressure as shown in Figure (6.4) and Figure (6.6). However, the effect of footing pressure on the footing heave is generally insignificant.

6.3 Effect of Lateral Extension of Sand Cushion, L_r

Parametric study for the effect of lateral extension of sand cushion on the heave of footings was performed. Depth of sand cushion is selected equal to 0.50, 1.00 and 2.00 m. Footing with 1.00 m width was considered in this analysis. The lateral extension of sand cushion is assumed to vary from 1.00m to 10.00 m (end of model boundary). Sand is modeled using linear elastic soil model. In this analysis, modulus of elasticity of sand cushion is assumed equal 50MPa to simulate medium dense sand and its Poisson's ratio is considered equal to 0.30.

The results for lateral extension effect are presented in Table (6.3) for 0.50m depth sand cushion and different footing width. Similarly, results of analysis for lateral extension effect for 1.00m and 2.00m sand cushion depth are presented in Tables (6.4) and (6.5) respectively. Figures (6.7), (6.9) and (6.11) illustrate the effect of lateral extension on footing settlement for 0.50, 1.00 and 2.00 m sand cushion depth; respectively. Similarly, Figures (6.8), (6.10) and (6.12) present the effect of lateral extension on footing heave for 0.50, 1.00 and 2.00 m sand cushion depth; respectively.

The lateral extension of sand cushion has a significant effect on the settlement of footing. For 1.00 m sand cushion depth and under 20 kPa footing pressure, the settlement of footing decreases by about 36.5% when lateral extension increases from zero to 1.00 m as shown in Figure (6.9). If the lateral extension is greater than two times the depth of sand cushion, further decrease of settlement will be noted. Therefore, increasing lateral extension more than twice the depth of sand cushion is not recommend.

The effect of lateral extension on footing settlement decreases with increase of sand cushion depth. For 2.00 m depth sand cushion, the decease in settlement is about 17.5% (compared to 36.5% for 1.00 m sand cushion depth) when lateral extension increases from zero to 1.00 m under 20 kPa footing pressure as shown in Figure (6.11).

The effect of lateral extension slightly decreases with increase of footing pressure. For example, for 1.00m sand cushion depth, the decrease in settlement is 36.5% under 20kPa, while, the decrease is 32% under 100 kPa for increase of lateral extension from zero to 1.00 m for 1.00 m footing width as shown in Figure (6.9).

Table (6.3): Footing Displacement for Different Lateral Extensions of Sand Cushion
(0.50 m Depth Sand Cushion and 1.00 m Footing Width)

Lateral Extension	L_r = 0.00m		L_r =1.00m		L_r = 2.00m		L_r = 3.00m		L_r =10.0m	
Load (kPa)	ΔS	ΔH	ΔS	ΔH	ΔS	ΔH	ΔS	ΔH	ΔS	ΔH
0.0	0.00	106.9	0.00	104.37	0.00	103.54	0.00	103.49	0.00	103.49
20	-15.24	104.04	-10.98	102.09	-10.85	101.33	-10.63	101.33	-10.63	101.33
40	-27.99	102.18	-20.85	100.22	-20.62	99.46	-20.23	99.46	-20.23	99.46
60	-39.29	100.77	-29.94	98.62	-29.64	97.85	-29.95	97.85	-29.95	97.85
100	-59.18	98.56	-46.44	96	-46.02	95.17	-45.3	95.17	-45.3	95.17
140	-76.69	96.44	-61.32	93.82	-60.81	92.92	-59.95	92.92	-59.95	92.92

(Note: -ve values represent settlement and +ve values represent heave)

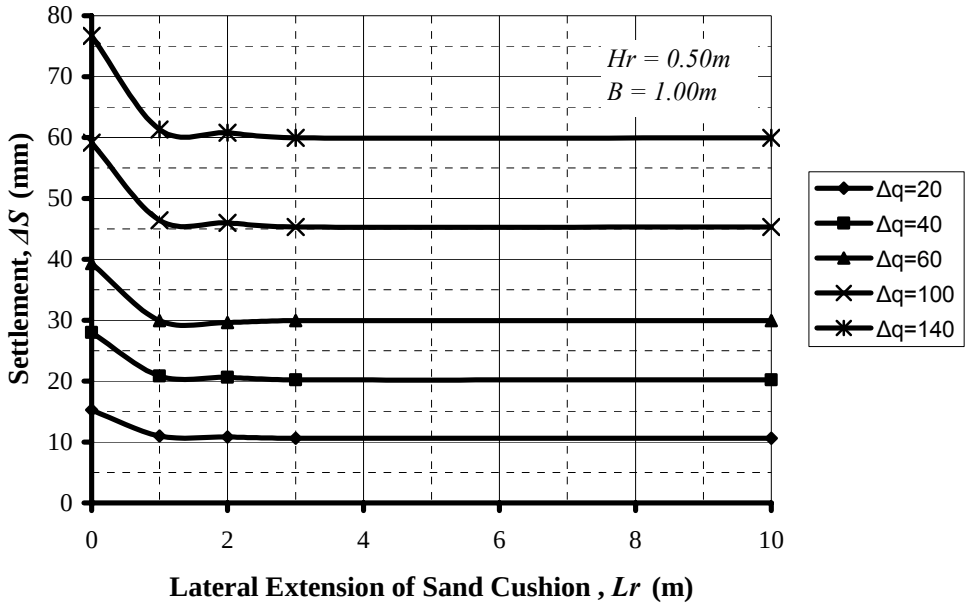

Figure (6.7): Footing Settlement for Different Lateral Extensions
(0.50 m Depth Sand Cushion and 1.00 m Footing Width)

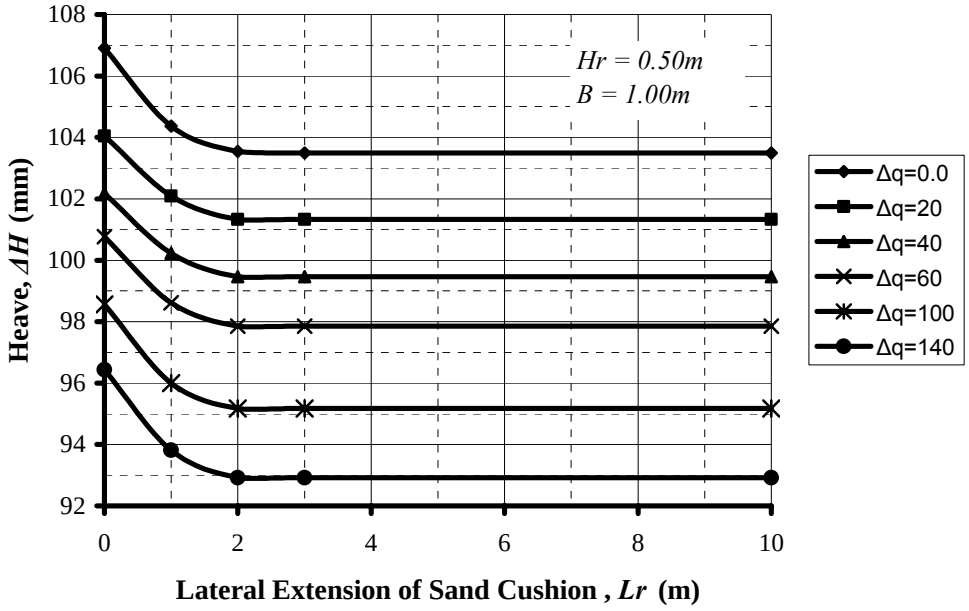

Figure (6.8): Footing Heave for Different Lateral Extensions
(0.50m Depth Sand Cushion and 1.00m Footing Width)

Table (6.4): Footing Displacement for Different Lateral Extensions of Sand Cushion
(1.00m Depth Sand Cushion and 1.00m Footing Width)

Lateral Extension	L_r =0.0m		L_r =1.00m		L_r =2.00m		L_r = 3.00m		L_r =10.0m	
Load (kPa)	ΔS	ΔH	ΔS	ΔH	ΔS	ΔH	ΔS	ΔH	ΔS	ΔH
0.0	0.00	86.41	0.00	81.15	0.00	78.64	0.00	77.39	0.00	77.22
20	-11.26	84.54	-7.15	79.79	-6.7	77.49	-6.66	76.29	-6.43	76.22
40	-21.4	83.16	-13.92	78.58	-13.1	76.4	-13.02	75.25	-12.59	75.25
60	-30.74	82.05	-20.37	77.48	-19.24	75.38	-19.14	74.27	-18.53	74.27
100	-47.69	80.17	-32.49	75.51	-30.9	73.51	-30.75	72.44	-29.82	72.44
140	-63.00	78.34	-43.79	73.67	-41.86	71.74	-41.66	70.67	-40.47	70.67

(Note: -ve values represent settlement and +ve values represent heave)

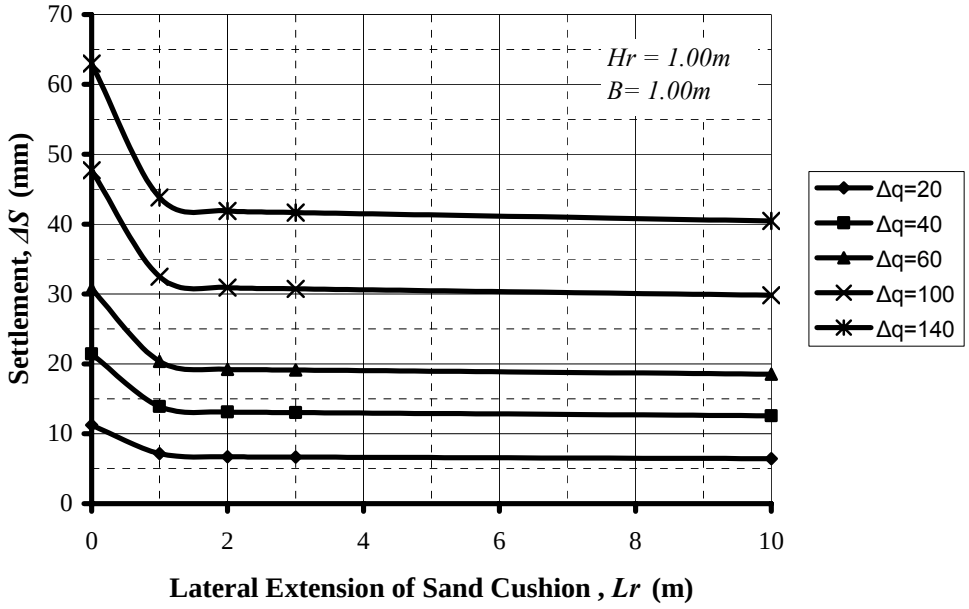

Figure (6.9): Footing Settlement for Different Lateral Extensions
(1.00m Depth Sand Cushion and 1.00m Footing Width)

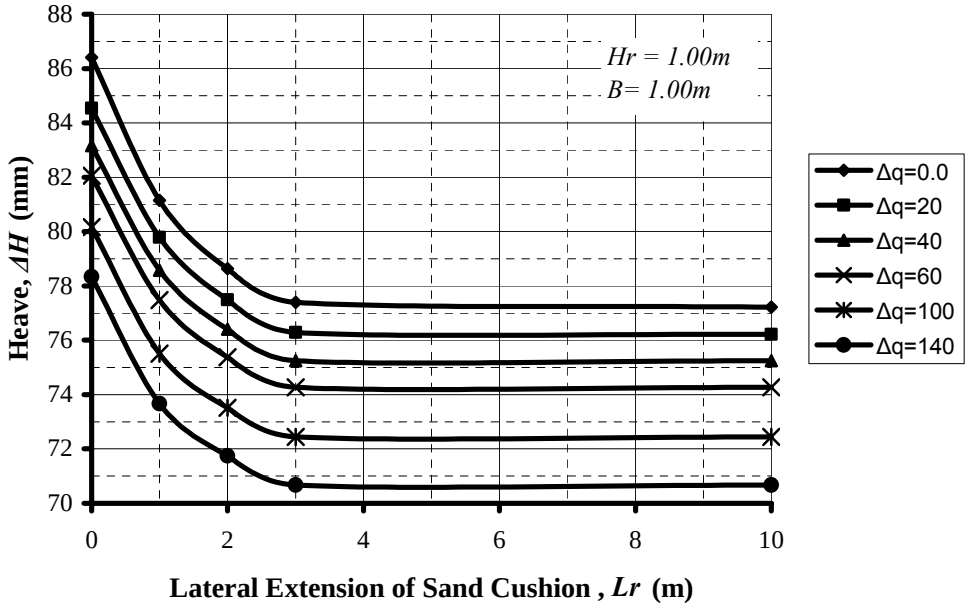

Figure (6.10): Footing Heave for Different Lateral Extensions
(1.00 m Depth Sand Cushion and 1.00 m Footing Width)

Table (6.5): Footing Displacement for Different Lateral Extensions of Sand Cushion (2.00m Depth Sand Cushion and 1.00m Footing Width)

Lateral Extension	L_r = 0.0m		L_r = 1.00m		L_r = 2.00m		L_r = 3.00m		L_r = 10.0m	
Load (kPa)	ΔS	ΔH	ΔS	ΔH	ΔS	ΔH	ΔS	ΔH	ΔS	ΔH
0.0	0.00	53.75	0.00	42.76	0.00	38.03	0.00	32.21	0.00	29.75
20	-7.60	53.19	-6.28	41.74	-3.93	37.61	-3.69	31.91	-3.55	29.52
40	-14.84	52.75	-13.74	41.24	-7.78	37.19	-7.33	31.59	-7.04	29.26
60	-21.78	52.37	-22.34	40.24	-11.57	36.76	-10.9	31.25	-10.48	28.99
100	-34.92	51.66	-30.56	39.32	-18.93	35.89	-17.9	30.58	-17.22	28.43
140	-47.23	51.13	-30.56	39.32	-26.06	35.06	-24.7	29.95	-23.79	27.89

(Note: -ve values represent settlement and +ve values represent heave)

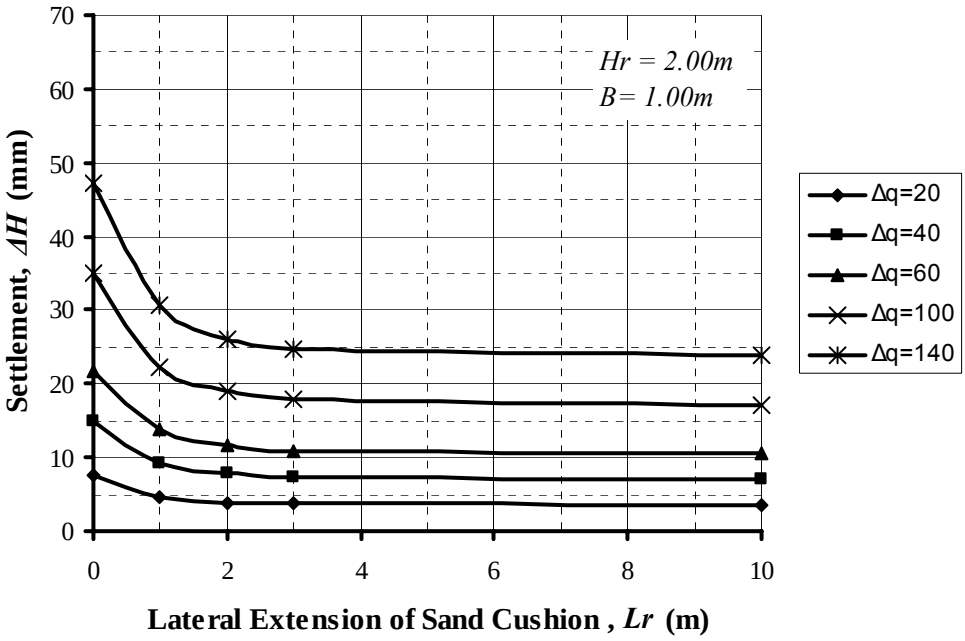

Figure (6.11): Footing Settlement for Different Lateral Extensions (2.00 m Depth Sand Cushion and 1.00 m Footing Width)

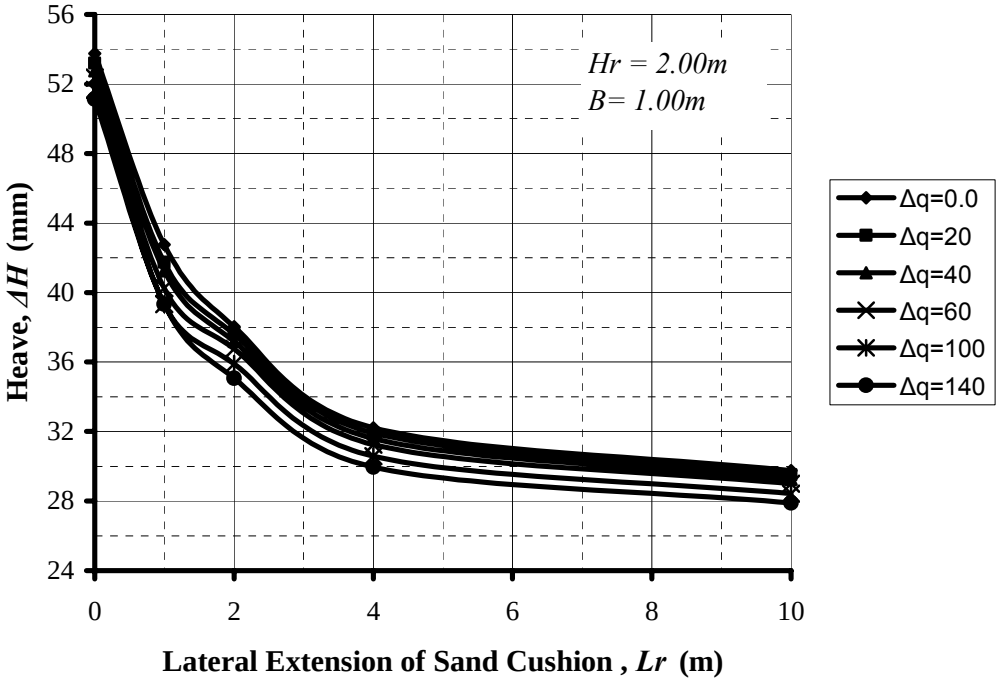

Figure (6.12): Footing Heave for Different Lateral Extension of Sand Cushion
(2.00 m Depth Sand Cushion and 1.00 m Footing Width)

As shown in Figure (6.8) and Figure (6.10), the lateral extension of sand cushion has less significant effect on footing heave than its effect on footing settlement. For sand cushion depths smaller than 1.00 m, the effect of lateral extension is insignificant. Decrease in heave is 2% when the lateral extension increases from zero to 1.00m for 0.50 m depth sand cushion for 20 kPa footing pressure as shown in Figure (6.8). Also, the reduction of footing heave decreases with decrease of footing pressure, for example, it becomes 1.90% under 20 kPa footing pressure. The effect of lateral extension on footing heave increases with increase of sand cushion depth. The heave of footing resting on 1.00 m depth sand cushion decreases by 6%, when lateral extension increases from zero to 1.00m under 20 kPa footing pressure as shown in Figure (6.10) (compared to 2% for 0.50 sand cushion depth).

6.3.1 Summary

Finally, it may be noted that the lateral extension has a less significant effect on footing heave than its effect on footing settlement. Also, lateral extension of sand cushion equal to one time its depth is practical for footing settlement but this value is impractical for footing heave in all cases. Comparison between effect of lateral extension of sand cushion on footing settlement and footing heave is presented in Table (6.6).

Table (6.6)**:** Comparison between Effects of Lateral Extension of Sand Cushion on Footing Settlement and Footing Heave

Parameter	Settlement	Heave
Relationship with length of lateral extension	Non-Linear	Non-Linear
Significance of lateral extension	High	Medium
Practical length of lateral extension (times depth of sand cushion)	One time	Varied (2 to 3 times)

6.4 Effect of Sand Cushion Relative Density

Parametric study for effect of relative density or degree of relative compaction of sand cushion on footing heave and settlement was performed. Sand cushion is classified to three types according to relative density: loose, medium and dense sand. The modulus of elasticity of each type is estimated according to the Egyptian Code of Practice part 3, 2001. Values of 12.5, 50 and 112.5 MPa were selected for loose, medium and dense sand; respectively. Analysis was performed for 1.00 m footing width and sand cushion of 0.50 and 2.00m depth. The lateral extension of sand cushion is assumed to be 10.0 m which represents infinity lateral extension where further increase has insignificant effect (end of model boundary).

Results of analysis for the effect of sand cushion type on footing settlement and heave are shown in Table (6.7) for 0.50 m sand cushion depth. Similarly, Table (6.8) presents results for 2.00 m sand cushion depth. Figures (6.13) and (6.14) present the relationship between footing settlement and modulus of elasticity of sand cushion for 0.50 m and 2.0 m sand cushion depth; respectively. Similarly, Figures (6.15) and (6.16) present the relationship between footing heave and modulus of elasticity of sand cushion for 0.50 m and 2.0 m sand cushion depth; respectively.

Effect of modulus of elasticity of sand cushion on footing settlement is significant. Settlement decreases with increase of modulus of elasticity of sand cushion as shown in Figures (6.13) and (6.14). This effect decreases with increase of footing pressure. On the other hand, effect of modulus of elasticity of sand cushion on footing heave is considered negligible as shown in Figures (6.15) and (6.16). It is important to note that increase of modulus of elasticity leads to increase of footing heave however this increase is considered insignificant. This means that increase of relative density of sand cushion causes increase

of footing heave. Also, the effect of modulus of elasticity decreases with increase of footing pressure. This increase of heave due to increase of modulus of elasticity of sand cushion is attributed to increase in rigidity of sand cushion to adapt its volume due to heave. Finally, it is good practice to compact the sand cushion to minimize the effect of heave without violating the required settlement and bearing capacity of footings.

Table (6.7): Footing Displacement for Different Elasticity Modulus of Sand Cushion (0.50m Depth Sand Cushion and 1.00m Footing Width)

Load (kPa)	*E*s=12.5MPa		*E*s = 50 MPa		*E*s =112.5MPa	
	ΔS	*ΔH*	*ΔS*	*ΔH*	*ΔS*	*ΔH*
0.0	0.00	103.68	0.00	103.49	0.00	103.63
20	-11.75	101.27	-10.63	101.33	-8.58	102.16
40	-22.21	99.31	-20.23	99.46	-16.58	100.78
60	-31.80	97.67	-29.95	97.85	-24.04	99.46
100	-49.12	95.00	-45.3	95.17	-37.95	97.10
140	-64.70	92.80	-59.95	92.92	-50.75	94.96

(Note: -ve values represent settlement and +ve values represent heave)

Table (6.8): Footing Displacement for different Elasticity Modulus of Sand Cushion (2.00m Depth Sand Cushion and 1.00m Footing Width)

Load (kPa)	*E*s =12.5MPa		*E*s =50MPa		*E*s =112.5MPa	
	ΔS	*ΔH*	*ΔS*	*ΔH*	*ΔS*	*ΔH*
0.0	0.00	29.75	0.00	29.75	0.00	29.72
20	-4.75	29.44	-3.55	29.52	-2.30	29.61
40	-9.42	29.10	-7.04	29.26	-4.58	29.49
60	-14.01	28.74	-10.48	28.99	-6.83	29.35
100	-23.00	28.04	-17.22	28.43	-11.25	29.03
140	-31.75	27.39	-23.79	27.89	-15.59	28.70

(Note: -ve values represent settlement and +ve values represent heave)

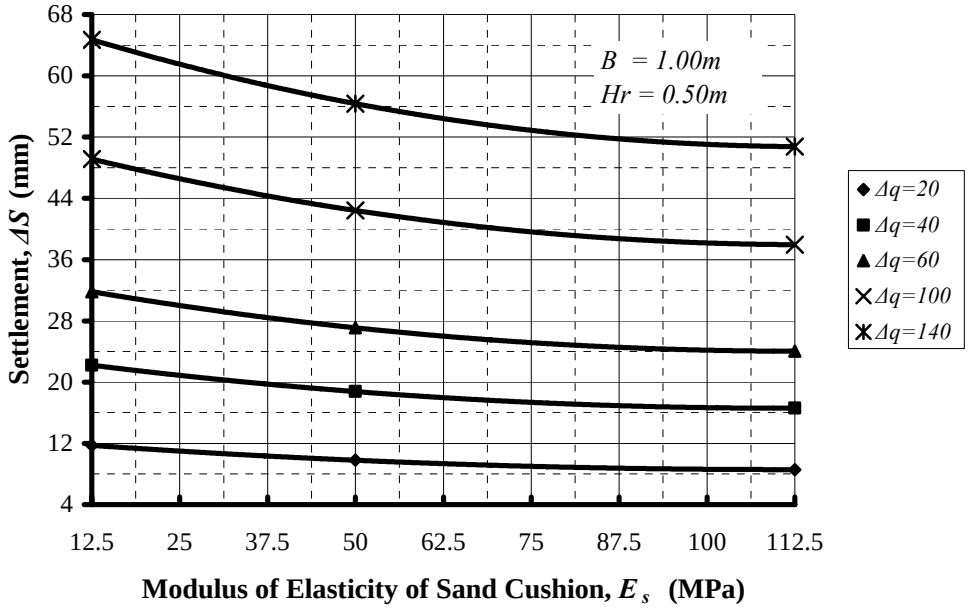

Figure (6.13): Effect of Elasticity Modulus of Sand Cushion on Footing Settlement (0.50m Depth Sand Cushion and 1.00m Footing Width)

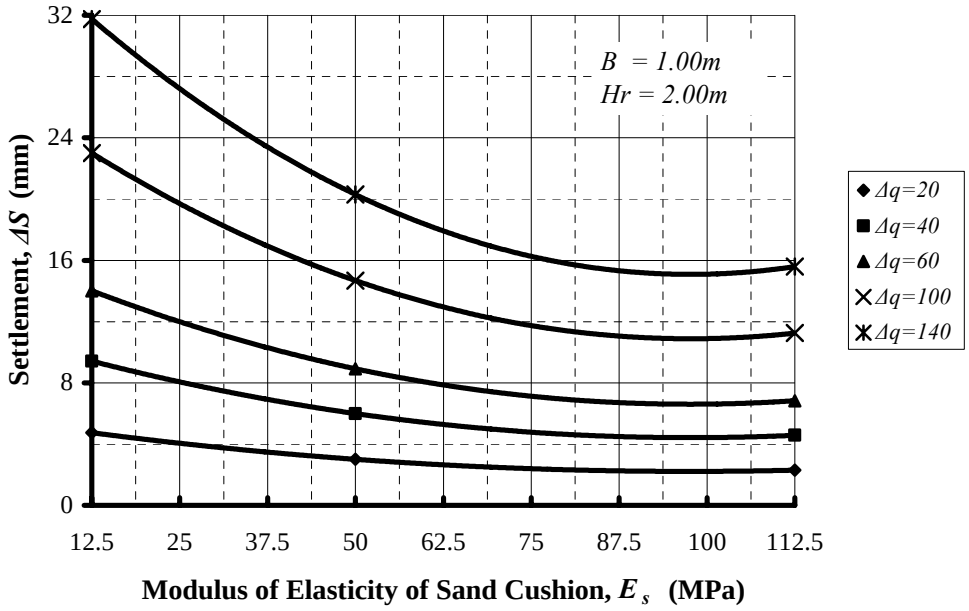

Figure (6.14): Effect of Elasticity Modulus of Sand Cushion on Footing Settlement (2.00m Depth Sand Cushion and 1.00m Footing Width)

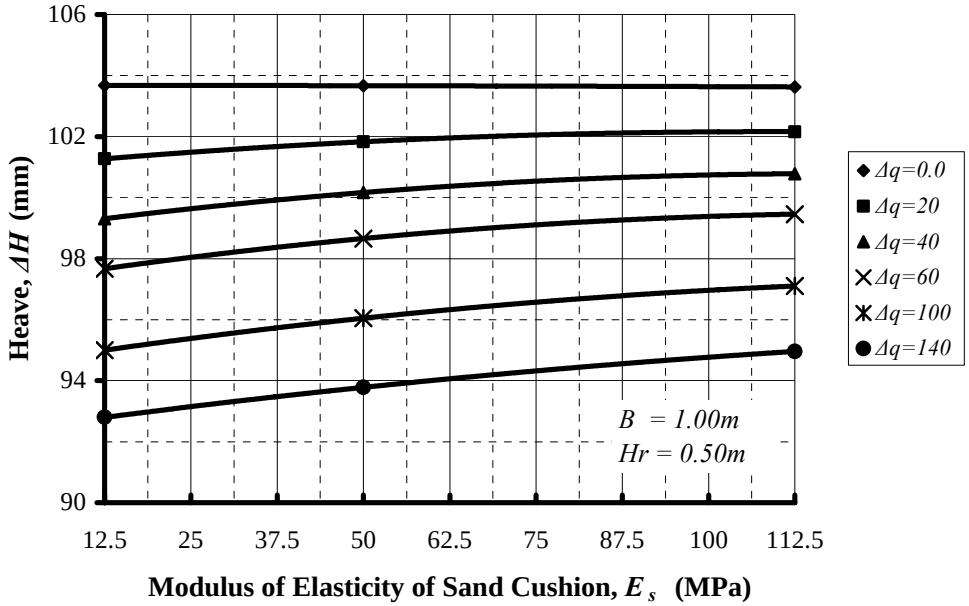

Figure (6.15): Effect of Elasticity Modulus of Sand Cushion on Footing Heave (0.50m Depth Sand Cushion and 1.00m Footing Width)

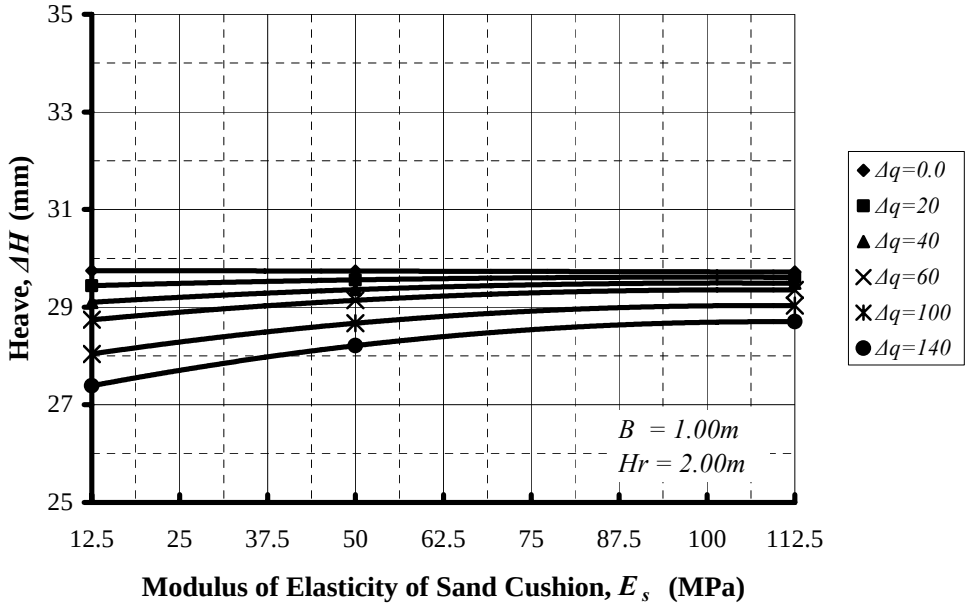

Figure (6.16): Effect of Elasticity Modulus of Sand Cushion on Footing Heave (2.00m Depth Sand Cushion and 1.00m Footing Width)

CHAPTER (7)

CONCLUSIONS AND RECOMMENDATIONS FOR FUTURE WORK

Expansive soils in developed areas undergo volume change with variations in soil moisture. This volume change may cause movement of foundations that adversely affects its performance. Sources of soil water variations in developed areas can be introduced by man-made causes such as lawn and garden watering and leaky pipes. In addition, the annual cycle of wetting and drying due to climate changes causes soils to shrink and swell each year. Thus, the arid regions of the country are much more susceptible to damage due to expansive soils.

The primary purpose of that work is to develop a powerful tool for evaluating and predicting volume change problems associated with unsaturated expansive soils. Furthermore, to evaluate the heave potential of expansive soils on shallow foundation due to the different sources of water variations namely, climate, lawn, water infiltration and pipe leakage. The relevant findings of that thesis give a step to augment our understanding of the cause of damage to pavement, infrastructure and light-loaded structures due to expansive soils.

The mechanical behaviour of unsaturated expansive soils is one of the challenging topics in the field of geotechnical engineering. In this research, an analytical study has been undertaken for the implement unsaturated nonlinear elastic model in finite element framework that performs a sequentially uncoupled flow-displacement analysis for the prediction of effect of soil suction and the induced volume change on civil infrastructures. The flow equations have been solved by the commercial program called SEEP/W (Seepage analysis Program). Where, the stress-deformation equations have been implemented in CRISP (CRItical State soil mechanics Program). The Modified CRISP was used to investigate effect of expansive soils on shallow foundation due to water variation causes.

Modified CRISP validation was performed to evaluate the accuracy of program in predicting volume change of expansive soils. Case history of heave of a floor slab of a light industrial building in north central Regina, Saskatatchewan due to water pipe leakage was modeled using implemented model. The results of case history analysis showed good agreement with measured displacements. In addition, three example problems from literature were re-analyzed to verify the program formulation and performance.

The capabilities of the program are illustrated through studying the effect of soil suction change on heave of footings. Parametric studies of the different causes of moisture content changes soil heave were conducted. The program was used to investigate the effect of climate conditions, pipe leakage, surface infiltration and lawn on the volume change of expansive soils. Regina Clay was considered as the modeling soil for the analyses presented in this research. Regina clay was selected because of abundance of data on properties that were measured under different stress state variables with acceptable accuracy.

Furthermore, the Modified CRISP was used to evaluate the effect of the sand cushions as one of the most effective method to avoid the danger of expansive soil on shallow foundation. Parametric study of sand cushion dimensions and properties was performed. The study try to asses the effectiveness of depth, lateral extension and relative density of sand cushion on the heave of shallow foundation. Analysis of sand cushion with the Modified CRISP showed the capability of the program to estimate the most effective depth and lateral extension of the sand cushion with considering the properties of expansive soil and causes of water content variations in the practical problems.

7.1 Conclusions

The program of research described in this has provided considerable insight into the behaviour of expansive soils. In the following sections, conclusions from various aspects of this research are summarized as follows:

7.1.1 Modified Program and Implemented Model

1. Uncoupled approach for analysis of behaviour of unsaturated expansive soil is considered a simple and suitable method for practicing the volume change of unsaturated expansive soils.

2. Modified CRISP for the modeling of unsaturated expansive soil behaviour forms a powerful computing tool for solving volume change problems associated with shallow foundation resting on unsaturated expansive soils.

3. Modified CRISP provides flexibility for the description of elasticity parameters as constant values or as mathematical expressions of stress variables and soil suction.

4. SEEP/W program is considered a suitable tool for simulating the flow through saturated and unsaturated soils and for evaluating soil suction distributions through the soil. The final suction distributions serve as input for the stress deformation analysis program to predict the volume change using the implemented unsaturated expansive soil model.

7.1.2 Effect of Sources of water variations on Shallow Foundation Heave

1. The footing pressure has a low significant effect on heave reduction for shallow foundation on expansive soils.

2. The effect of footing width on heave of shallow foundation is insignificant.

7.1.2.1 Climate Conditions Effect

3. Seasonal moisture fluctuation zone depth, Z_s, has a significant effect on footing heave. Increase in seasonal moisture fluctuation zone depth leads to increase of footing heave. In addition, the relationship between seasonal moisture fluctuation

4. Soil suction change at ground surface, S, has a significant effect on footing heave. Increase in soil suction change at ground surface leads to increase of footing heave. In addition, the relationship between soil suction change at ground surface and footing heave is linear. For example, Increase in soil suction change at ground surface by 20% leads to increase of heave by 25% for 1.0 m seasonal moisture fluctuation depth under zero footing pressure.

7.1.2.2 Effect of Lawn (Trees)

5. Planting distance, D_L, has a significant effect on the settlement of shallow foundation rested on expansive soils. Increase of planting distance leads to decrease of footing settlement. Relationship between the planting distance and footing settlement is nonlinear. For example, footing settlement decreases by

26% when planting distance increases from 2.00 to 4.00m for 0.10 m^3/day tree water demand and 1.0 root zone depth.

6. For the same tree water demand, footing settlement significantly decreases with increase of root zone depth, R_L, especially when it is less than 2.00 m. For example, footing settlement deceases by 35% when root zone depth increases from 1.0 to 2.0 m (i.e., by 100%) for 0.10 m^3/day tree water demand and 1.0 m planting distance.

7. The effect of root zone depth on footing settlement decreases with increase of planting distance from footing edge. For large planting distance, the effect of root zone depth becomes negligible especially, for root zone depth larger than 2.00 m. Also, the effect of root zone depth increases with increase of tree water demand.

8. Tree water demand, q_L, has a significant effect on settlement of shallow foundation rested on expansive soils. Increase of tree water demand leads to increase of shallow foundation settlement. Relationship between tree water demand and footing settlement is linear. For example, Increase of tree water demand by 50% leads to increase of settlement by 45% for 1.00 m planting distance and 2.00 m root zone depth.

7.1.2.3 Water Infiltration Effect

9. Infiltration distance from footing edge, D_i, has a moderate effect on heave of shallow foundation resting on expansive soils. Footing heave is linearly decreased with increase of infiltration distance. For example, The heave decreases by 8% with increase of infiltration distance by 100%.

10. Horizontal barriers around the buildings have a significant effect on the reduction of heave. Modified CRISP for modeling the behaviour of unsaturated expansive can be used to simulate the field cases with barriers and select the appreciate width of horizontal barrier or platform.

11. Infiltration width, w_i, has a significant effect on heave of shallow foundation on expansive soils. Heave increases nonlinearly with increasing of infiltration width. Footing heave increases by 100% when infiltration width increases from 1.0 to

3.0 m (i.e., by 200%) for 0.50mm/day tree water demand and 1.0 m infiltration distance.

12. Infiltration rate, q_i, has a significant effect on heave of shallow foundation on expansive soils. Heave increases nonlinearly with increasing of infiltration rate. For example, footing heave increases by 85% when rate of infiltration increases from 2.00 to 3.00 mm/day (i.e., increase by 50%).

7.1.2.4 Pipe Leakage Effect

13. The pipe leakage induce significant heave compared to other water variation sources. Consequently, it is considered the most significant with respect to foundation problems.

14. Depth of leaking pipe below foundation level, D_p, has a significant effect on soil heave. Increase of leaking pipe depth results in increase of footing heave to a maximum value, after which, further increase in leaking pipe depth results in decrease in footing heave. Thus, there is a critical pipe depth at which heave is maximum. Thus, the selected in-situ depth should be selected shallower or deeper than the critical depth.

15. Distance of leaking pipe, L_p, form footing edge has a significant effect on footing heave. Increase in leaking pipe distance leads to decrease of footing heave. Furthermore, the relationship between distance of leaking pipe form footing edge and footing heave is linear. For example, footing heave decrease by 18% when leaking pipe distance increase by 33% (from 3.00 to 4.00 m).

7.1.3 Sand Cushion Effect

1. Sand cushion depth, H_r, has a significant effect on decreasing footing heave and footing settlement.

2. Relationship between footing heave and depth of sand cushion is linear, where; the relationship between footing settlement and depth of sand cushion is non-linear.

3. Footing width and footing pressure have an insignificant effect on footing heave especially when using sand cushion.

4. The lateral extension of sand cushion has a significant effect on the settlement of footings. Increasing lateral extension more than once the depth of sand cushion is insignificant on footing settlement.

5. Lateral extension of sand cushion has less significant effect on footing heave than its effect on footing settlement

6. The effect of lateral extension of sand cushion on footing heave is negligible for sand cushion depths less than 1.00 m.

7. The effect of lateral extension of sand cushion on footing heave increases with increase of sand cushion depth.

8. Optimum lateral extension of sand cushion increases with increase of sand cushion depth but it is not equal to one time the sand cushion depth as often assumed in practice. The optimum lateral extension for 0.50, 1.00, 2.00m sand cushion depth are 1.00, 3.00, 6.00m respectively. Therefore, , lateral extension of sand cushion equal to one time its depth is adequate for safe settlement requirements but this value is non-adequate for heave.

9. Effect of modulus of elasticity of sand cushion on footing settlement is significant. Settlement decreases with increase of modulus of elasticity of sand cushion.

10. Effect of modulus of elasticity of sand cushion on footing heave is insignificant.

11. Increase of modulus of elasticity of sand cushion leads to increase of footing heave. This means that increase of relative density of sand cushion causes increase of footing heave thus, loose sand is more suitable for heave conditions.

12. It is good practice to compact the sand cushion to minimize the effect of heave without violating the required settlement and bearing capacity of footings

7.2 Recommendation for Future Research

The research reported in this thesis has resulted in a better understanding of the behaviour of shallow foundations resting on expansive soils. However, many questions are still unanswered and there are several lines of research which could usefully be pursued in the future. These future research opportunities include development of constitutive models, improvement to laboratory testing techniques and other areas. The work described in this thesis is limited to theoretical work. The study may extensively extend to cover the following suggested points:

7.2.1 Theoretical work

1. The uncoupled approach was performed through this research. The study may be extend to the coupled approach then a comparison are made between these approaches.

2. This analysis may be performed for anisotropic expansive soils by modifying the nonlinear elastic model to account the anisotropy properties of the soil.

3. The seepage-deformation numerical analysis utilizes a nonlinear elastic deformation model, which provides accurate prediction for the scenario of elastic behavior and combinations of soil stress state below the critical state. It is recommended that an incorporation of plastic yielding into the program to address plastic effects

4. The elastoplastic models of expansive soils may be used for studying the effect of the environmental conditions and replacement on the behaviour of shallow foundation rested on expansive soils.

5. The implemented model may be used for studying the behaviour of deep foundations in expansive and evaluated the uplift forces on piles from expansive soils.

6. The implemented model may used to study the stability of slopes under infiltration process and other sources of water variations.

7. Program should be verified against further measured data and field case histories.

8. The effect of each soil property function on the solutions of water flow and stress-deformation problems should be studied. The results of such analyses may assist in the simplification of the soil property functions used in the analysis.

9. This research was limited to the two dimensional problems, the numerical modeling of expansive soil may be extended to include the axisymmetric problems and three dimensional problems.

10. It is suggested that the mathematical equations of constitutive relationships for unsaturated soils used for obtaining the elasticity parameters by differentiating these equations. Then, these parameters can be expressed as functions of net normal stress and matric suction and consequently it is not necessary to assume a lower limit for each stress state variable.

7.2.2 Laboratory and field work

11. Estimate the state surface for soil structure and water phases with respect to total stress and suction for different soil types in Egypt.

12. Measurement soil suction profiles for different regions in Egypt over the all times on year.

13. Measurement the soil water characteristic curves for the different soils type in Egypt.

13. Verify the accuracy of current expansive soil models for describe the mechanical behavior of expansive shale soils in Egypt through experimental work.

In spite of the need for further work, this research has advanced the numerical modeling of expansive soils significantly in three respects. Firstly, a simple numerical tool for analysis of expansive soils is proposed and its capability for simulating different practical problems is evaluated. Secondly, the effect of different causes of water variations such as climate conditions, lawn, pipe leakage and water infiltration were investigated. Finally, investigation of the effect of sand cushion on volume change behaviour of expansive soil heave was conducted.

REFERENCES

1. Abdullah, W. S. (2002). "Bi-dimensional Swell Effect on Accuracy of Footing Heave Prediction", Geotechnical Testing Journal, GTJODJ, Vol. 25, No. 2, June 2002, pp. 177–186.
2. Aitchison G. (1973). “Preface to Set of Papers on the Quantitve Description of the Stress Deformation Behavior of Expansive Soils” Proc. 3rd International Research and Engineering Conference on Expansive soils, Heifa, pp.75-77.
3. Aitchison, G. and el. (1973). "A Microscopic Model of Expansive Clay" Proc. 3rd International Research and Engineering Conference on Expansive soils, Heifa, pp.75-77.
4. Aitchison, G.D. (1973). "The Quantitative Description of the Stress-Deformation of Expansive Soils" - Preface to Set of Papers. Proc. 3rd Int. Conf. Expansive Soils, Haifa, Israel, vol. 2, pp. 79-82.
5. Alonso, E. E., Gens, A., and Hight, D. W. (1987). "Special Problem Soils", General Report, Proc. of the 9th European Conf. on Soil Mech. Found. Eng., Dublin, vol. 3, pp. 1087-1146.
6. Alonso, E.E., Gens, A., Josa A. (1990). "A Constitutive Model for Partially Saturated Soils", Geotechnique, Vol. 40(3), pp. 405-430.
7. Al-Strife, W. (1986). "Water consumption of agricultural crops in Jordan" Bulletin No. 41, Ministry of Agriculture, Amman, Jordan. 113.
8. Aubertin, M. and el. (2003). "A Model to Predict the Water Retention Curve from Basic Geotechnical Properties", Can. Geotech. Journal, Vol. 40, pp.1104–1122.
9. Australian Standards (AS 2870), (1998). "Residential Slabs and Footings Construction"
10. Biddle, P.G. (1983). "Patterns of soil drying & moisture deficit in the vicinity of trees on clay soils", Geotechnique, Vol. 83 (2), pp. 107-126
11. Biot, M. A. (1941). "General Theory of Three-Dimensional Consolidation", Appl. Phys., Vol. 12, pp. 155-164.
12. Bishop, A.W. (1959). "The Principle of Effective Stress", Lecture Delivered in Oslo,

Norway, Teknisk Ukeblad, 106(39), pp. 859-863.

13. Britto, A. M. and Gunn, M. J. (1987). "Critical State Soil Mechanics Via Finite Element", John Wiley & Sons, New York, 488 p.

14. Cameron, D. A. (2001). "The extent of soil desiccation near trees in a semi-arid environment", Geotechnical and Geological Engineering, Vol. 19, pp. 357–370.

15. Chad, K.C., Overton, D.D., and Nelson, J.D., (2006). "The Effects of Site Conditions on the Predicted Time Rate of Heave", Unsaturated Soils 2006 Conference, Carefree, AZ, ASCE.

16. Chen, F. H. (1988). "Expansive Soils What Have We Accomplished", Proceedings of International Conference on Engineering Problems of Regional Soils, Beijing, China, pp. 561– 563.

17. Chen, F. H. (1988). "Foundations on expansive soils", Elsevier, New York.

18. Childs, E.C. and Collis-George, N. (1950). "The Permeability of Porous Materials", Proc. Royal. Soc., Vol. 21 OA, pp. 392-405.

19. Corapcioglu, M. Y. (1984). "Land subsidence - A State of the Art Review. Fundamentals of Transport Phenomena in Porous Media", Nijhoff, Dordrecht, pp. 371-444.

20. Darcy, H. (1856). "Histoire des Foundataines Publique de Dijon", Dalmont, Paris, pp. 590-594.

21. Dhowian, A. W. (1990). "Heave Prediction Techniques and Design Consideration on Expansive Soils", J. King Saud Univ., Vol. 2, Eng. Sci. (2), pp. 355-377.

22. El-Garhy, B. M. (1999). “Soil suction and analysis of raft foundation resting on expansive soils”, Ph.D. Dissertation, Minufiya University, Egypt.

23. Erdal, C. (2001). "Use of C Fly Ashes for The Stabilization of An Expansive Soil", Journal of Geotechnical and Geo-environment Engineering.

24. Escario, V., Juca, J. F. T., and Coppe, M. S. (1989). "Strength and Deformation of Partly Saturated Soils", Proc. 12th Int. Conf. Soil Mech. Found. Eng., Vol. 1, pp. 43-46.

25. Fatahi, B. (2007). "Modelling of influence of matric suction induced by native vegetation on sub-soil improvement", PhD thesis, University of Wollongong, Australia.

26. Fityus, S. G., Walsh, P. F. and Kleeman, P. W. (1998). "The Influence of Climate as Expressed by the Thornthwaite Index on the Design Depth of Moisture Change of Clay Soils in the Hunter Valley", Proc. of Conference on Geotech. Eng. And Eng. Geology, Hunter Valley, Australia, pp. 251-265.

27. Footings Group (SA) (1996). "Special Provisions for the Design of Residential Slabs and Footings for South Australian Conditions", Inst. Engrs. Aust. S.A. Div.

28. Foundation Performance Association-Structural Committee, (2004). "Foundation Design Options for Residential and Other Low-Rise Buildings on Expansive Soils", Document No. FPA-SC-01-0, Houston, Texas, 41p.

29. Fredlund, D. G., and Hung, V. Q. (2001). "Prediction of Volume Change in an Expansive Soil as a Result of Vegetation and Environmental Changes", Geotechnical Special Publication No. 115, ASCE, Reston, pp. 24–43.

30. Fredlund, D. G., Hasan, and Filson, H. L. (1980). "The Prediction of Total Heave", Fourth International Conference on Expansive Soils, Sponsored by the American Society of Civil Engineers, Denver, Vol. 1, 16–18 June, pp. 1–17.

31. Fredlund, D. G., Xing, A., and Huang, S. (1994). 'Predicting the Permeability Function for Unsaturated Soils Using the Soil-water Characteristic Curve", Canadian Geotechnical Journal, Vol. 31, pp. 533–546.

32. Fredlund, D.G. (1981). Discussion: "Consolidation of Unsaturated Soils including Swelling and Collapse Behaviour" by Lioret and Alonso, 1981, Geotechnique, Vol. 30(4), pp. 449-477, Discussion in Geotechnique.

33. Fredlund, D.G. (1983). “Prediction of Ground Movements in Swelling Clays”, 31st Annual Soil Mechanics and Foundation Engineering Conference. University of Minnesota, MN. February.

34. Fredlund, D.G. (2000). "The 1999 R.M. Hardy lecture: the implementation of unsaturated soil mechanics into geotechnical engineering", R.M. Hardy Address, Canadian Geotechnical Journal, Vol. 37(5), pp. 963-986.

35. Fredlund, D.G. and Rahardjo, H. (1993). "Soil Mechanics for Unsaturated Soils", John Wiley & Sons, New York, 560 p.

36. Fredlund, D.G., and Hasan J. (1979). "One-dimensional Consolidation Theory: Unsaturated Soils", Can. Geotech. J., Vol. 16(2), pp. 521-531.

37. Fredlund, D.G., and Xing, A. (1994). "Equations for the soil-water characteristic curve", Canadian Geotechnical Journal, Vol. 31(3), pp. 521-532.

38. Fredlund, M. D., Fredlund, D. G., and Wilson, G. W. (2000). "Estimation of Volume Change Functions for Unsaturated Soils", Proceedings of the Asian Conference on Unsaturated Soils, 18–19 May, pp. 663–668.

39. Fredlund, M.D. (1999). "The role of unsaturated soil property functions in the practice of unsaturated soil mechanics", Ph.D. Dissertation, University of Saskatchewan, Saskatoon, SK., Canada.

40. Freeze, R. A. and Cherry, J. A, (1979). "Ground water", Englewood Cliffs, Prentice-Hall, New York, 604 p.

41. Gens, A. and Alonso, E. (1992). "A framework for the behaviour of unsaturated expansive clays", Can. Geotech. Journal, Vol. 29, pp.1013-1032.

42. Geo-Slope International Ltd. (2007). "SEEP/W user's guide", Geo-Slope International Ltd., Calgary, AB.

43. Gitirana Jr., G.F.N. (2005). "Weather-Related Geo-Hazard Assessment Model for Railway Embankment Stability", Ph.D. Dissertation, University of Saskatchewan, Saskatoon, SK, Canada, 411p.

44. Hamilton J. J. (1977). "Foundations on Swelling or Shrinking Sub-Soils", Can. Building Digest, CBD 184, Div. of Building Research, Nat. Res. Council, Ottawa, 4p.

45. Harold, D. and el. (1961). "Expansion of Soils Containing Sodium Sulphate" Proc. 5th International Conference on Soil Mechanics and Foundations Engineering, Paris pp.13-16.

46. Hillel, D. (1971). "Soil and water physical principals and processes", Academic, New York

47. Holtz, W. G. (1959). "Expansive Clays – Properties and Problems", Quarterly, Colorado School of Mines, Vol. 54, No. 4, PP. 89-125.

48. Holtz, W.G. and Gibbs H J. (1956). "Engineering Properties of Expansive Clays", Trans. ASCE, vol. 121, pp. 64-663.

49. Hudak, P. F., Sadler B. and Hunter B. A. (1998). "Analyzing Underground Water-Pipe Breaks in Residual Soils", Water/Engineering Management, pp.15-20.

50. Hung Q., Fredlund D. G., and Lee Barbour, S. (2005). "A study of hysteresis models for soil-water characteristic curves", Can. Geotech. Journal, Vol. 42, pp.1548–1568.

51. Hung, Q. and Fredlund, D. G. (2004). "Prediction of one-, two-, and three-dimensional heave in expansive soils", Canadian Geotechnical Journal, Vol. (41), pp.713-737.

52. Hung, V. Q. (2000). "Finite Element Method for the Prediction of Volume Change in Expansive Soils", M. Sc. thesis, University of Saskatchewan, Saskatoon, 314 p.

53. Hung, V. Q. (2003). "Uncoupled and coupled solutions of volume change problems in expansive soils", Ph.D. thesis, Department of Civil Engineering, University of Saskatchewan, Saskatoon, Sask.

54. Hung, V. Q., and Fredlund, D.G. (2003). "Uncoupled and coupled solutions of two-dimensional swelling in expansive soils", Proc. of the 2nd Asian Conference on Unsaturated Soils (UNSAT-ASIA 2003), Osaka, Japan, pp. 10-12.

55. Hung, V.Q. and Fredlund, D.G. (2000). "Volume Change Predictions in Expansive Soils using a Two-dimensional Finite Element Method", Proc. of the Asian Conf. on Unsaturated Soils, Singapore, pp. 231-235.

56. Jennings J. (1989). "Expansive Soils Moisture Movements in Partly Saturated Soils", Proc. 5th International Conference on Soil Mechanics and Foundations Engineering, Mexico pp. 423-425.

57. Jennings, J. E. (1961). "A Revised Effective Stress Law for Use in the Prediction of the Behaviour of Unsaturated Soils", Pore Pressure and Suction in Soils Conf., London, England, pp. 26-30.

58. Jennings, J. E. and Knight, K. (1957). "The Prediction of Total Heave from the Double Oedometer Test", Proc. Symp. Expansive Clays, South African Inst. of Civil Engineers, Johannesburg, 7(9): pp. 13-19.

59. Johnson, L. D. (1978), "Predicting Potential Heave and Heave with Time in Swelling Foundation Soils", Technical Reports S-78-7, U.S Army Engineer Waterways Experiment Station, Vicksburg, Mississippi.

60. Johnson, L.D. (1979). "Overview for Design of Foundation on Expansive Soils", Paper GL-79-21, U.S Army Engineer Waterways Experiment Station, Vicksburg, Mississippi.

61. Johnson, L.D. and Snethen, D. R. (1978). "Prediction of Potential Heave of Swelling Soil", Geotechnical Testing Journal, Vol. 1, No. 3

62. Johnson, W. and el. (1973). "The Consolidation and swell Characteristics of Accra Molted Clay" Proc. 3rd International Research and Engineering Conference on Expansive soils, Heifa, pp. 75-80.

63. Jones, D. E. and Holtz, W.G. (1973). "Expansive Soils-The Hidden Disaster", Civil Eng., ASCE, New York, NY, pp. 87-89.

64. Kariukia, p. c. and van der Meer, F. (2004). "A Unified Swelling Potential Index for Expansive Soils", Engineering Geology Journal, Vol. 72 , pp.1–8.

65. Komornik, A. and el. (1971). "Strength Characteristics of Expansive Clays Containing Granular Constituents" Proc. 4th Asian Regional Conference on Soil Mechanics and foundation Engineering, Bangkok, pp. 129-134.

66. Krahn, J. and Fredlund, D.G. (1972). "On total, matric and osmotic suction", Soil Sci., Vol. 114(5), pp. 339-348.

67. Lawson, M. and O'Callaghan D. (1995). "A Critical Analysis of The Role of Trees in Damage to Low Rise Buildings", Journal of Arboriculture, Vol. 21(2), pp. 90-97

68. Leong, E. C. and Rahardjo, H. (1997). "Permeability Functions for Unsaturated Soils", Journal of Geotechnical and Geoenvironmental Engineering, ASCE, pp. 1118-1126.

69. Likos, W. J. and el. (2003). "Measured and Estimated Suction Indices for Swelling Potential Classification", Journal of Geotechnical and Geoenvironmental Engineering, Vol. 129, No. 7, July 1, 2003., pp. 665-668.

70. Lioret, A., and Alonso E. E. (1980). "Consolidation of Unsaturated Soils including Swelling and Collapse Behaviour", Geotechnique, Vol. 18(4), pp. 449-477.

71. Lytton, R. L. (1994). "Prediction of movement in expansive clay", Geotechnical Special Publication (Vertical and Horizontal Deformations of Foundations and Embankments), Proc. of Settlement 94, College Station, Tex., ASCE, 40, pp. 1827-1845.

72. Lytton, R. L. (1995). "Foundations on expansive soils", Class notes, CVEN 646, Texas A&M University.

73. McKeen, R. G. (1992). "A Model for Predicting Expansive Soil Behaviour", Proc. 7th

Int. Conf. Expansive Soils, pp. 1-6.

74. Michel, J., Beaumont, A. and Tessier, D. (2000). "A Laboratory Method for Measuring the Isotropic Character of Soil Swelling", European Journal of Soil Science, Vol. 51, pp.689-697.

75. Mitchell, J. K. (1976). "Fundamentals of Soil Behavior", John Wiley, New York.

76. Mitchell, P. W. (1979). "The structural analysis of footings on expansive soil", Kenneth W.G. Smith and Associates Research Report No. 1, pp. 1-159, Newton, South Australia.

77. National House Building Council (NHBC) (1985). "Building near trees", NHBC Practice Note 3, NHBC Build mark House, Amersham, Bucks HP6 5AP.

78. National House Building Council (NHBC) (1992). "NHBC Standards, Chapter 4.2. Building near trees'" NHBC Build mark House, Amersham, Bucks HP6 5AP.

79. Nayak, N. V. and Christensen, R. W. (1974). "Swelling Characteristics of Compacted Expansive Soils", Clays and Minerals, Vol. 19, No. 4, pp.251-261.

80. Nelson, J.D. and Miller, D.J. (1992). "Expansive Soils: Problems and Practice in Foundation and Pavement Engineering", John Wiley & Sons, Inc., New York.

81. Nelson, J.D., Overton, D.D., and Durkee, D.B. (2001). "Depth of wetting and the Active Zone", Proceedings of the Geo-Institute Shallow Foundation and Soil Properties Committee Sessions at the ASCE 2001 Civil Engineering Conference, Houston, Texas, October.

82. Ng, C. W. and Pang, Y. W. (2000). "Influence of stress state on soil-water characteristics and slope stability", J. Geotech. and Geoenviron. Eng., Vol. 126(2), pp. 157-166.

83. O'Malley, A. P. K. and Cameron, D. A. (2002) "The Influence of Tress on Soil Moisture Dwellings and Pavements in an Urban Environment", Uni. of South Australia, School of Geoscience, Minerals and Civil Engineering, 90p.

84. PDE Solutions Inc. (2004). "FlexPDE 4.1 Reference Manual", PDE Solutions Inc., Antioch, CA.

85. Pereira, J. H. (1996). "Numerical Analysis of the Mechanical Behavior of Collapsing Earth Dams During First Reservoir Filling", Ph.D. Thesis, University of Saskatchewan,

Saskatoon, Canada, 449 p

86. Pereira, J. H. F. (1996). "Numerical Analysis of the Mechanical Behavior of Collapsing Earth Dams during First Reservoir Filling", Ph.D. dissertation, University of Saskatchewan, Saskatoon, 449 p.

87. Pereira, J. H. F., and Fredlund, D.G. (1997). "Constitutive Modelling of a Metastable-structured Compacted Soil", Proc. Int. Symposium on Recent Developments in Soil and Pavement Mechanics, Rio de Janeiro, Brazil, pp. 317-326.

88. Perko, H. A., Thompson R.W., and Nelson J. D. (2000). "Suction Compression Index based on CLOD Test Results", GeoDenver 2000: Advances in Unsaturated Geotechnics, ASCE, pp. 393-408.

89. Perpich, W. M., Lukas, R. G., and Baker, C. N. (1965). "Desiccation of soil by trees related to foundation settlement", Can. Geotech. J., Vol. 2(1), pp. 23-39.

90. Pham H.Q. (2005) "A volume-mass constitutive model for unsaturated soils", Ph.D. Dissertation, University of Saskatchewan, Saskatoon, SK., Canada, 404p.

91. Post-Tensioning Institute (1996). "Design and construction of post-tensioned slabs-on-ground", Second Edition, 101 p.

92. Potts, D. M. and Zdravkovic, L. (1999). "Finite element analysis in geotechnical engineering: theory", Thomas Telford, London.

93. Potts, D. M. and Zdravkovic, L. (2001). "Finite element analysis in geotechnical engineering: application", Thomas Telford, London.

94. Raman, V. (1967). “Identifications of Expansive Soils from the Plasticity Index and the Shrinkage Index Data”, The Indian Engineer, Calcutta, Vol. 11 (1), pp.17–22.

95. Rees, S. W. and Thomas, H. R. (1993). "Simulating Seasonal Ground Movement in Unsaturated Clay", Journal of Geotechnical Engineering, ASCE, Vol. 119(7), pp. 1127-1143.

96. Richards, B.G. (1967). "Moisture Flow and Equilibria in Unsaturated Soils for Shallow Foundation", Symp. on Permeability and Capillary in Soils, ASTM Spec. Tech. Pub., 47(7), pp. 185-191.

97. Richards, L. A. (1931). "Capillary Conduction of Liquids through Porous Medium", J. Physics, Vol. l, pp.318-333.

98. Roberts, B. R. and Schnipke, V. M. (1994), "The Relative Water Demand of Five Urban Tree Species", Journal of Arboriculture, Vol. 20(3), pp. 156-159

99. ROSCOE, K. H. and BURLAND, J. B. (1968). "On the generalised stress-strain behaviour 'wet' clay", Eng. plasticity, Cambridge Univ. Press, pp. 535-609.

100. Sankaran, K. and el. (1973). "A Microscopic Model of Expansive Clay" Proc. 3rd International Research and Engineering Conference on Expansive soils, Heifa pp.65-71.

101. Satyanarayana, B. (1969). "Behaviour of Expansive Soil Treated or Cushioned with Sand", Proceedings of 2nd International Conference on Expansive Soils, Texas, pp. 308–316.

102. Schneider, G. L. and Poor, A. P. (1974). "The Prediction of Soil Heave and Swell Pressures Developed by an Expansive Clay", Research Rep. TR-9-74, Construction Research Center, Univ. of Texas, Arlington.

103. Schofield, A. and Wroth, P., (1968). "Critical Soil Mechanics", Mc-Graw-Hill, London.

104. SCHOFIELD, A. N. and WROTH, C. P. (1968). "Critical state soil mechanics", McGraw Hill, London.

105. Seed, H. and el. (1964). "Clay Mineralogical Aspects of the Atterberg Limits", J. Soil Mech., Found. Div., Am. Soc. Civ. Eng., Vol. 90 (SM4), pp. 107-131.

106. Seed, H. B., Woodard, R. J., and Lundgren, R. (1962). "Prediction of Swelling Potential for Compacted Clays" J. Soil Mech., Found. Div., Am. Soc. Civ. Eng., Vol. 88 (SM3), pp.53–87.

107. Sheng, D. and el. (2003). "Finite element Formulation and Algorithms for unsaturated soils. Part I: Theory", Int. J. Numer. Anal. Math. Geomech, Vol. 27, pp. 745-765.

108. Shuai, F. (1996). "Simulation of swelling pressure measurements on expansive soils", Ph.D. dissertation, University of Saskatchewan, Saskatoon, Sask.

109. Skempton, A. W. (1953). "The Colloidal Activity of Clays", Proc. 3rd Int. Conf. Soil Mech. Found. Eng., Switzerland, Vol. 1, pp. 57-61.

110. Snethen D. R. (1986). "Expansive Soils: Where Are We?", Nat. Res. Council, Comm. On Ground Failure Hazards, Vol. 3, pp. 12-16.

111. Snethen, D. R. et al. (1975). "A Review of Engineering Experiences with Expansive Soils in Highway Subgrades", Report No. FHWA-RD-75-48, Federal Highway Administration.

112. Snethen, D. R. et al. (1979). "An Evaluation of Methodology for Prediction and Minimization of Detrimental Volume Change of Expansive Soils in Highway Sub–grades", Research Report, Vol. (1), Federal Highway Administration, Washington.

113. TM 5-818-7, "Foundations in Expansive Soils"

114. Toll, D. G. (1990). "A Framework for Unsaturated Soil Behaviour", Geotechnique, Vol. 40(1), pp. 34-44.

115. Tucker, R. L. and Poor, A. R. (1978). "Field study of moisture effects on slab movements", ASCE, Journal of Geotechnical Engineering. Vol. 104(4), pp.403-415.

116. U.S. Army, (1983), "Foundations in Expansive Soil", Technical Manual, Headquarters, Department of the Army.

117. Uppal, H. (1969). "The Laboratory Testing of Expansive Soil" Proc. 2nd International Research and Engineering Conference on Expansive soils, Texas, pp. 121-131.

118. Uppal, H., (1969)., "Measurement of Swelling Pressure of Expansive Soils", Proc. 2nd International Research and Engineering Conference on Expansive soils, Texas, pp.250-255.

119. US Navy (1986). "Design Manual-Soil mechanics, foundations and earth structures", No: NAVFAC DM-7, U.S. Naval Publications and Forms Centre.

120. Van Der Merw, D. H., (1964). “The Prediction of Heave from the Plasticity Index and Percentage Fraction of soils”, Civil Engineer in South Africa, Vol. 6, No. 6.

121. Vanapalli, S.K. and Fredlund, D.G. (2000). "Comparison of different procedures to predict unsaturated soil shear strength", Proceedings of the GeoDenver Conference, Denver, CO., August 3-8, pp. 3-8.

122. Vijayvergiya, V. and el. (1973). "Prediction of Swelling Potential for Natural Clays" Proc. 3rd International Research and Engineering Conference on Expansive soils, Heifa, pp. 227-235.

123. Wong, T. T., Fredlund, D.G., and Krahn, J. (1998). "A Numerical Study of Coupled Consolidation in Unsaturated Soils", Can. Geotech. J., Vol. 35, pp. 926-937.

124. Xiaodong Wang and el. (1995). "Infiltration and Saturated Hydraulic Conductivity of Compacted Clay". Vol. 121."Journal of Geotechnical Engineering.

125. Yoshida, R. T., Fredlund, D. G., and Hamilton, J. J. (1983). "The prediction of total heave of a slab-on-grade floor on Regina clay", Canadian Geotechnical Journal, Vol. 20, pp. 69-81.

126. Zeitlen, J. and el. (1961). "Deformations and Moisture Movements in Expansive Clays" Proc. 5th International Conference on Soil Mechanics and Foundations Engineering, Paris, pp. 873-878.

127. Zeitlen, J. G. (1969). Some Approaches to Foundation Design for Structures in an Expansive Soil Area", Proceedings of 2nd International Research and Engineering Conference on Expansive Clay Soils, Texas, pp. 148-156.

128. Zhang, L. L., Fredlund, D. G., Zhang, L.M. and Tang, W.H. (2004). "Numerical study of soil conditions under which matric suction can be maintained", Can. Geotech. J., Vol. 41, pp. 569-582.

129. Bozozuk, M. and Burn, K. N. (1960). "Vertical ground movement near elm trees", Geotechnique, Vol. 10, pp. 19-32.

130. Tucker, R. L. and Poor, A. R. (1978). "Field study of moisture effects on slab movements", ASCE, Journal of Geotechnical Engineering, Vol. 104(4), pp. 403-415.

131. Ward, W. H. (1953). "Soil movements and weather", Proc. 3rd Int. Conf. Soil Mech., Zurich 1953, 2, 477 – 481.

132. Wesseldine, M. A. (1982)."House foundation failures due to clay shrinkage caused by gum trees", Transactions, Institution of Professional Engineers, N.Z., CE9 (1).

133. Bozozuk, M. (1962). "Soil shrinking damages shallow foundations at Ottawa, Canada", Res. Paper 163, Div. Building Research, NRCC, Canada.

134. Lytton, R.L. (1995). "Foundations and Pavements on Unsaturated Soils", Proc. of the 1st International Conference on Unsaturated Soils, Paris, France, Vol. 3, pp. 1201-1220.

135. Rogers, J. D., Crane, K. M. and Snyder, D. L. (1993). "Damage to foundations from expansive soils", Claims People, vol. 3, no. 4 (April), pp. 1-4.

136. Pryke, J. F. K. (1975). "Differential foundation movement of domestic buildings in

South-East England Settlement of structures" Proc. of Conference organised by the British Geotechnical Society, The Lady Mitchell Hall, Cambridge, Pentech Press, London.

137. Li, J. (2006). "Two dimensional simulation of a stiffened slab on expansive soil subject to a leaking underground water pipe" Proc. of the 4th International Conference on Unsaturated Soils, Arizona, ASCE, pp. 2098-2109.